UNIVERSITÀ DI PARMA

UNIVERSITÀ DEGLI STUDI DI PARMA

DOTTORATO DI RICERCA IN
INGEGNERIA INDUSTRIALE
CICLO XXXI

Design and development of an additive manufacturing prototype

Coordinatore

Chiar.mo Prof. Gianni Royer Carfagni

Tutore

Chiar.mo Prof. Marco Silvestri

Dottorando: Luca Sbaglia

Anni 2015/2018

To my family

Acknowledgments

Ringrazio la mia famiglia e tutte le persone che mi hanno aiutato e sostenuto durante questo percorso durato tre anni. Non è stato sempre facile, ci sono stati momenti difficili e a chi mi dato senza mai voler niente in cambio non posso che dire grazie. È stata un'esperienza importante che senza dubbio mi ha formato e dato diverse soddisfazioni, rimarrà con me per il resto della mia vita. La soddisfazione maggiore l'ho avuta nel risolvere i continui problemi che mi sono trovato davanti, nel mettere in pratica quello che prima era solo su carta. Ho apprezzato più di tutto l'ambiente universitario, inteso come ambiente di condivisione e divulgazione della conoscenza, con il suo continuo relazionarsi con persone di formazione e cultura diversa. Ora non mi resta che decidere come utilizzare la conoscenza acquisita.

Luca Sbaglia, Milano, Ottobre 2018

...Toda la tarde se ha estado ablando del desarrollo sustentable...
el modelo de desarrollo y de consumo es el actual de la sociedades ricas?...
la gran crisis no es ecológica es política...
no podemos indefinidamente continuar gobernados por el mercado...
los viejos pensadores definían... pobre no es el que tiene poco sino que
verdaderamente pobre es el que necesita infinitamente mucho...
esta es una clave de carácter cultural...
la crisis de la agresión al medio ambiente no es una causa
la causa es el modelo de civilización que hemos montado
y lo que tenemos de revisar es nuestra forma de vivir...
El desarrollo non puede ser en contra de la felicidad
tiene que ser a favor de la felicidad humana
del amor arriba de la tierra, de las relaciones humanas
de cuidar a los hijos, de tener amigos
de tener lo elemental...

José Mujica
ONU speech, 20 June 2012

How to read the thesis

This thesis work has been developed in order to be read both integrally than partially through its chapters; every chapter has its own bibliography and a little introduction. This kind of structure allows the reader to exploit this opera as he pleases without the constraint of totally read the text. Anyway it is suggested the read of the initial introduction to the entire work as the last paragraph of the chapter 1 which introduce the project Efesto, common thread of this work. The introduction of the book gives a comprehensive vision of the work done, its starting point and the topics touched inside it. The introductions of each chapter are a foreword to the arguments exposed inside the chapters themselves with a focus on the issues treated. At the end of the book are presented two appendixes for the reader; one aimed to the reader with some missing knowledge of robotics and its terms, and one aimed to the ones interested to deepen some part of the work done during the design of the Efesto machine that have been omitted from the main text. In the conclusions of this work are listed the scientific publications effectuated during the three years of this doctoral thesis period.

INDEX

LIST OF FIGURES

LIST OF TABLES

Introduction

Starting from the '80s there's been an increasing development and interest by the industrial and scientific community for the technology labelled under the name Additive Manufacturing(AM), with a constant growth in the number of printing processes, in the utilize of different materials and with the use in many applications. The advantages of this technology have been several in different industrial sectors and in the everyday life through the realization of applications previously not possible with traditional production technologies, that is why its development has been strongly promoted in the latest years. Among the various AM processes, those dedicated to printing metallic/ceramic components are of great interest even though their use is still limited. This thesis work is born within a project for the development of a new process of AM based on the extrusion of a metallic/ceramic feedstock according to the production processes based on the use of powders. This process promises to lower the barriers for the production of metal and ceramic parts as compared to other AM processes based on the use of powders. During the design and development of an AM prototype it has been faced various topics all linked by the common belonging to the development of the AM and its affirmation in the industrial field. The entire design process is carried out with the aim of obtaining a machine capable of insert itself in an industrial environment which is rapidly evolving with a series of changes often collected under the name of industry 4.0. Divided by chapters the work here presented contains the following topics.

The thesis starts with the introduction of AM technology, its history, applications and with its bonds with the industrial field and in particular industry 4.0 as representative of the industrial development. It is presented the impact of this new technology at an industrial and social level by highlighting the production concepts of a customized, decentralized and digital production. It is analysed the technological steps necessary for the production of one component, several processes belonging to this technology and the general architecture of an AM machine. It is finally presented the Efesto project, father of this work, with the introduction of a new technology which aims to face the problems of the metal and ceramic parts production comparing it other AM processes based on the use of powders.

Starting from the machine technical specifications, in particularly from

the printing volume and speed,it has been accomplished a mechatronic design which has lead to the prototype here presented, based on a linear delta robot and an extrusion system. A kinematic analysis, an optimization of the robot geometrical parameters together to a dynamic study have lead to the sizing of the mechanical structure and the choice of the actuation systems. A specific control architecture has been choice and customized considering the necessities of a 3D printing machine including its communication skills. The architecture proposed is a tailored solution for the technological process here developed.

With the goal of guarantee the correct execution of the AM process it is accomplished a calibration study of the robotic system. Too often the calibration processes are carried out without considering the technological needs of the application where the robot is used. It is developed a stochastic method, based on the mechanical tolerances of the robot, which arrives to evaluate the success probability of the calibration process through the generation of success maps. The entire process is simulated in order to foresee the goodness of the solution proposed.

The development of an AM machine requires the development of a trajectories generator in order to accomplish the printing process. In the case of extrusion-based processes, as the Efesto, two main problems arise known as overfill and underfill. Starting from the passages necessary for the correct generation of 3D printing trajectories, digital chain, it is developed a trajectory generation algorithm pointed to allow a constant extrusion rate during the printing process. The algorithm is based on the use of Bézier curve. This solution aims to minimize the overfill/underfill problems.

AM is considered one of the main technology in the new industrial framework of which industry 4.0 is considered the main representative. In order to integrate the digital chain of AM machines, meant as the data flow from a CAD file to the final printed object, inside the evolving industrial environments it is carried out a critical analysis on the industry 4.0 concepts and the changes brought; particularly it's the focus on the role of cyber-physical systems which are considered at the basis of the new industry. A theoretical example is given on the Efesto machine in order to demonstrate the importance of the AM integration according to a proposed scheme inside the industrial environments.

This work is ended by highlighting the results obtained and its contribution in the field of the scientific research. A tailored solution through a mechatronic approach to the design of an innovative AM machine for the production of metallic/ceramic parts. A stochastic method for the evaluation of a calibration process for AM machines based on extrusion systems. A trajectory generation algorithm dedicated to a printing process with constant extrusion rate. An analysis of the industry 4.0 concepts aimed to integrate the AM data flow inside the digital world proposed by this new paradigm. All along this work has been deepen the knowledge about AM

machines, for their design and implementation. Some objects printed with the Efesto prototype are proposed in a photo book at the end of the work.

Chapter 1

Additive Manufacturing

introduction

Additive manufacturing, AM, technology is entered in the industrial world from the 80's and it has gained a relevant position in the production systems such as it is recognized as one of the main technologies for the development of the future industry. The changes brought by this technology are many at the industrial level and not only, by pushing for a customized, decentralized and digital production, perfectly in common with the concepts of industry 4.0, one of the main holistic vision for the future of the industry and one of the main sponsor of AM. Here, starting from its history, it is introduced this technology pointing out its benefits, impacts and the great interest gathered around it and demonstrated by many government initiatives. It is described the main steps of this technology and the related passages to obtain a 3D object, furthermore some specific processes labelled under the name of AM are discussed and it is shown the general design of an AM machine. At the end is presented the Efesto project which is the common thread of this thesis work all around the topic of AM. The project aims to lower the barriers for the production of metal/ceramic components as regards other AM technologies based on the use of powders, as SLS, SLM, EBM and 3DP.

1.1 History

Additive manufacturing enters in the industrial history in the 80's when the first machines were realized with their related patents, fig.1.1. The attribution of the title of AM inventor is not unique, first of all because there are many processes which go under the name of AM and so we should define one inventor for each of them. Interesting is the historical analysis done in [10] and derived from a research among the united states patents. From this analysis it comes out that the concept behind the AM, overlap-

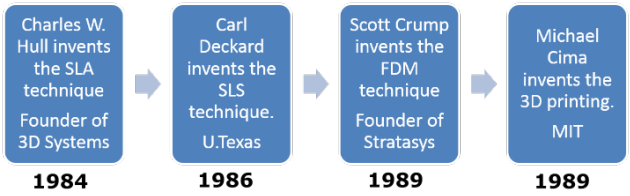

Figure 1.1: Additive Manufacturing begins

ping of material for the creation of three dimensional objects, derives from two technical fields such as topography and photosculpture. In the 1890 Blanther patented a method to create three dimensional maps starting from moulds created from the overlap of wax dishes properly shaped. In the 1902 Baese patented a method based on the use of a photosensitive jelly to create sculptures, this was an attempt to automatize the photosculptures job which should reproduce three dimensional statues starting from pictures. The development of this two fields kept going during the years until fifty years later we find the first applications similar to the current concept of AM. In the 1967 Swainson applied a patent for the creation of 3D objects obtained through the use of two laser and one photopolymer [72]. In [10, 72] it is possible to find reference to other developments obtained in the AM field, mainly in the USA, Europe and Japan, but if we focus our attention to the first commercial success of this technology the name Charles Hull is the first one coming out. Hull started the use of AM in industrial applications through the commercialization of stereolithography in the 1984. Others people and processes followed him; today the evolution of AM processes is still going on [18].

The first AM applications are in the prototyping field, in fact this technology was initially called rapid prototyping [21]. The possibility to produce a part in 3D decreased the designing times and it allowed to anticipate possible problems related to the manufacturing of the part itself [45]. A other field where AM was very important from the beginning is the foundry [70]; we can find applications in investment casting, where the AM was used to create wax objects, for the creation of ceramic moulds for metal components [57] and in the creation of inserts for die casting [70]. Here the AM could stand out thanks to the decrease in production times and costs [70]. After that the AM has been used more and more in the direct production of final parts, products or semi-products, so starting a phase of rapid manufacturing(RM). The commercial sectors which has most than others promoted for the use of the additive production are the automotive one, aeronautic and medical sector [26, 45]. In the automotive sector the entrance of AM

Figure 1.2: Plan of the italian ministry for the economic development, MISE, for industry 4.0

has free the designers from many constraints imposed by traditional manufacturing technologies so allowing the customization of some car areas by fulfilling some of the clients requests. In the aeronautic field the AM had particular interest since the low volume production of high complex parts. In the medical field the AM allowed the production of tailored components for the single person with a cost that would be unreachable by other means. Main applications are the production of prosthesis and artificial limbs, construction of dental implants, scaffolds for the development of organic tissues and the production of patient models to use before surgical operations.

1.1.1 Industrial interest

Among the biggest supporters of the AM development we find many governmental initiatives from several countries aimed to the development of the manufacturing sector of their own nation, starting from the most famous, the German plan industry 4.0. The additive manufacturing is not directly mentioned in the starting document of industry 4.0 [3], but it has become one of the main pillar of this paradigm thanks to the concepts of customization, decentralized and digital production which are perfectly embraced by this technology. We can find trace of what it is stated for instance in the plan of the Italian government for its industry [28] where the AM is directly named as one of the main points to invest in for the development of the industry itself, fig.1.2; the United Kingdom lists the additive manufacturing among the technologies of the Catapult-High value manufacturing project [67]which is related to an initiative for the development of future manufacturing technologies; similar initiatives can be found in the most of EU governments, how it is proved by a study for the European commission [31], which have

planned several funds for the development of the manufacturing industry, and inside most of these plans the AM is directly mentioned. Inside the platform industry 4.0 is possible to find applicative examples related to the use of AM [53]. We can find examples in the literature of the AM importance inside industry 4.0 where it is highlighted the connection on the topics of mass customization which is one the goal of this new industrial paradigm; Dilberoglu et al. [16] points out the use of this technology in the future industry where even though it is not suitable for high volume production it can be very important for the production of customized products, for the production of different materials and for the decentralization of production; Gaub [19] describes a pratical example of AM use inside an industry 4.0 system in the attempt to overcome the above mentioned problem to join custom products with high volume productions.

The technology evolution has lead to several techniques inside that area called additive manufacturing by bringing a growth in the number of possible processes, applications and use of different materials. At the time of industry 4.0 born, 2011, AM was in expansion and evolution; it was natural to incorporate what is considered the technology of the future in the industry of the future. The bond AM-industry 4.0 results to be circumstantial due to a contemporary historical evolution; with that it is not wanted to diminish the importance of AM in that context but only to point out a parallel development , as for the majority of industry 4.0 technologies, which have merged due to a natural convergence of concepts. Who has depicted the framework of industry 4.0 has used the available technology and among them the AM had sure a strong appeal. AM reflects a research for a more and more customized production with an increasing connection between digital and real.

1.2 AM impacts

The advent of AM has brought and it is bringing different changes inside the industrial worlds, introducing new production techniques and not only [42, 61]. In [61] the changes brought by AM are analysed and classified in four categories accordingly to the resulting impact, starting from the level incremental changes until arriving to what are defined industrial revolutions. In some sectors and for particular applications the AM has brought significant savings of time and money respect to traditional technologies as in the aeronautic sector, incremental change. In other sectors the AM has integrally modified the way of doing business, radical change; for instance in the medical sector the mock-up production before surgical operations has changed the manner how the operations themselves are carried out, and in the production of prosthesis the cost has fallen thanks to the entrance in the market of new producers without no experience in a medical field since the

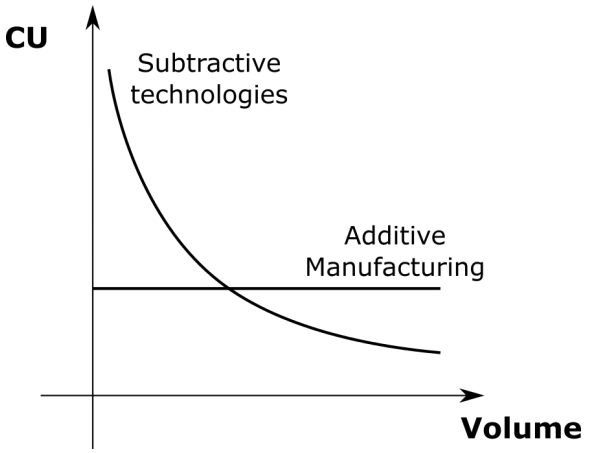

Figure 1.3: Qualitative behavior of AM unit cost compared to standard technologies

automatic production of AM machines. The AM introduction in the industrial sector has a disruptive effect in the moment it put in crisis industries which use other technologies for the production of the same good; in the casting field of complex components with a low volume production the AM has shown itself far more convenient than traditional casting techniques. In the end AM can arrive to start an industrial revolution in the moment it leads to social changes and not only industrial ones; the arising number of people which have started to print directly at home their consume goods shows a change from a production organized and centralized to a distributed one; this gives to the AM the right to claim itself as part of a social change in the labour world.

The importance of AM is confirmed by the increasing interest of the governments with initiatives pointed to support the development of this technology as America Makes in the USA or AMAZE in the EU [42], which are born to fight the trend that has brought many factories outside of their native countries [61]. The tendency of the last decade in the industrial world has been the one to point to a mass customized production, so a production of high customized products. This goal has been mainly reached trough a make-to-stock production based on the forecast demand of standard components, which are assembled in a customized solution only consequently to a customer order [14]. This kind of customization is different from the one offered by AM which directly from raw materials produces highly complex final goods [9]. It is not easy to say in which markets the AM can make the difference but the first graph you have to look at if you wonder that question it's the one reported in fig.1.3 which is shown several times in the literature regarding specific examples of AM [41, 61]. The AM is indifferent to the effect of economy of scale, no matter the production volumes are the cost

per unit will not change. This makes the technology interesting in primis for all that sectors where there are low production volumes and high costs due to complex products.

The decision to invest in AM from a company rely very much upon the product and industrial sector [41]; in [41] is analysed an industrial case related to a company which decided to invest in 3D printing of metal components by having as main client the aeronautic sector; here the possibility to produce ultra-light metal components thanks to reticular structure, impossible to produce with other means, has given to the AM an immense advantage. In [12] is proposed a quality classification of manufacturing products based on a three dimensional scale composed by production volume, customization and product complexity; the classification of a product according to this scale help to understand if the AM is a suitable solution for the production of that good or not. Generally the AM techniques are suitable for products with low production volumes and high customization and/or complexity. It is possible to find anyway some cases outside these conditions where the AM can be a competitive solution, for instance in the production of that components, as fixturing or tools, with low production volumes but with low complexity too that would discourage the use of AM. In some sectors the AM is changingthe way of doing business; an example is the supply chain of spare parts. This sector is in a constant search for a decrease in the operative costs by maintaining at the same time the same level of service quality ti the final client [30]. Main problems are related to the warehouse costs of these components which must be necessarily produced before the actual client request in order to have satisfying lead times, and to the necessity of a technician presence accordingly to the spare part to produce. In [30] is executed an analysis which shows how thus of AM can bring to the elimination of storages of spare parts thanks to a centralized production on request and a consequent distribution of the spare part, or through a distributed production thanks to AM machines dislocated directly in the geographical regions of the final clients. Today the first solution, centralized production of spare parts through AM, seems to be still more convenient than the second one because of high costs of AM machines which requires the attention of a specialised technician. In the near future, with the development of AM technology, the spare parts will be produced directly on the site on customer request reducing lead times and bringing to null storages.

The AM promotes new form of business based on a decentralized production by bringing the manufacturing of the final product directly in the client house [55]. In this way the figure of producer and consumer arrive to merge; it is born the figure of prosumer [56]. With the increasing number of 3D printers in private houses the companies will sell no longer the product but the way of produce it. The toys company Hasbro has declared the intention to use 3D printers to bring its products directly at its client houses. It is no longer sold the toy, but the file to print it directly at home [24].

This phenomenon is in counter trend respect to what happened with the first industrial revolution which has brought the workers and the means of production to gather in the shop floors [61]; AM assumes a change in the industrial value chains pushing for a local production more close to the final client until to reach a domestic production [35].

AM is a digital technology. It allows the direct production of any component without intermediate passages, with a direct connection between the computer design, CAD, to the final object. Off course not everything is reproducible and some process can be required before and after printing, but the nature of this technology makes it suitable for the production of very different objects. This inclination to digital is perfect inside the manufacturing sector which is trying to more and more a continuity between the digital world of designing and the manufacturing production [42]. An example of digital production can be found in the hobbyist field and in websites like 3DHubs [2], here hundreds of 3D printers are connected to this platform and put at disposal the possibility to produce parts from anywhere and delivering them everywhere in the world. Here the concepts of digital production and customization of the product reach their extreme.

AM does not touch only industrial topics but it raises issues in other fields among which we care to remember the ones related to intellectual property, safety and regulations [42]. The AM techniques combined with the emergent technologies of digital scanning can arrive to copy and reproduce objects protected by patents and whose production would be excluded to the ones not having the rights; if the digital scanning of a patented object is lightly modified is its production acceptable? To them we can add all the objects covered by design trademark and so under counterfeiting risk. The AM can bring to the production of very dangerous components which once was impossible to produce without the specific knowledge and tools; the most clear example is the weapons market. A 3D printer capable to produce these objects and sold in countries where the legal possess of guns is admitted, as in the USA, is it marketable in different countries with a different law? Another issue is related the the environmental impact of this technology which is not clear even though it is seems to be promising in terms of sustainability, saving of materials and energy [52].

The importance of AM is sustained by all the changes is bringing; limited to the industrial world this technology promotes a customized, decentralized and digital production.

1.3 The Technology

An additive manufacturing process is different from most of the other manufacturing technology for the fact that it adds material instead that removing it. The ASTM, American Society for Testing and Materials, defines the AM

Table 1.1: AM technological steps

Pre-printing	1-CAD design 2-File format 3-Machine input file
Printing	4-machine setup 5-Build 6-post-processing
Post-printing	7-application

as the *process of joining materials to make objects from three-dimensional (3D) model data, usually layer upon layer, as opposed to subtractive manufacturing methodologies.* To develop an AM technique is important to understand its main steps.

Even though there are many different AM processes, everyone with its peculiarities, they all have in common some phases listed in table1.1, [21]. Below:

Conceptualization and CAD

The starting point for the design of a AM component is equal to the most of any other manufacturing objects, it starts from a concept design and it arrives to the technical design with all the necessary details of the final object. Nowadays this is done through the use of CAD software, Computer Aided Design, which are used to create a digital representation, a 3D drawing, of the object to produce. A main difference between an AM process and other manufacturing technologies is that the passages between the CAD file of the object and its actual production is very short, and that is why this is considered a technology bringing together real and digital world. The CAD file can be expressed in different file formats; different choices can be done since every file format has his own advantages and disadvantages.

File format

The CAD file must be expressed in a format which is the most suitable for the representation of the piece since the file contains all the informations about the geometrical parameters of the part; it is evident how if the file contains some errors the part can not be produced in the correct way. The de facto standard of CAD file format for the additive manufacturing is the STL, StereoLiThography or Standard Tessellation Language, which represents the object through an approximation made of several triangles. Being an approximation this format is not error free on the dimensional tolerances of the object, furthermore this kind of format is basically a cloud of points

which represent the object, it does not contain any other information related to the object itself. This is why we can find alternatives to this CAD format which are able to describe the object in a more complete way as the AMF, Additive Manufacturing File Format. This format beyond the geometrical dimension of the object, which can be described not only with simple triangles, contains informations about its material, colours and topology of the part

AM machine input file

The CAD format must be in the end traduced in a language understandable by the AM machine who will actually carry out the production process. The standard usually used in this case is the g-code. This file format contains all the passages that the machine must execute to print the object; this format is tailored on the particular machine which executes the printing since every AM process has its own characteristics. This phase is the one usually carried out by CAM software, Computer Aided Manufacturing, that in the AM field are usually called slicing software. As in the case of CAD format, where there is a constant research for a more and more suitable representation of the object, there is a research pointed to the development of different CAM format. For instance in the latest years the STEP-NC format has been introduced as a good alternative to the g-code. This format substitutes the logic How-To-Do with of g-code with the one What-To-Do. This means to instruct the machine on what must be the result of its operations and not how to carry them out.

Machine setup

The machine setup consists in th preparation of the machine for the printing phase. This means preparation of the material to use and setting the parameters to use for the printing. On the same AM machine can be used different materials and according to the specific 3D object to print the best setting for the machine parameters can be different. According to the peculiar AM process the setup can be a phase more or less time consuming and costly, in any case it is fundamental for a good printing.

Build

The actual printing phase is the core of any AM process which take place through a continuous deposition of material, one layer after the other. The discrete nature of this technology leads to what is one of its main problems in the manufacturing of finite goods, the staircase effect which is the impossibility to exactly recreate a continuous geometric figure designed on a CAD software through a layer approximation. There is a constant search

Table 1.2: List of AM companies by revenue for AM machines sold

Company	Revenue[USD]
Stratasys (US)	405.5M
EOS (DE)	240.4M
GE Additive (US)	145.9M
3D Systems (US)	123.3M
HP (US)	97.3M
Ex-One (DE)	-
Arcam AB (SE)	-
Ranishaw (GB)	-

for a compromise between printing quality and production time. To minimize the staircase effect, and so improve the surface finishing of the object, thin layers are required but in the other hand this would lead to increasing production times. The discrete production furthermore leads to structural anisotropy which are in general undesired.

Post-processing

The AM techniques require a post-processing phase starting from the removal of the 3D printed object from the machine and the removal of support material, material used to build the object but which is not part of it, if there is any. It is common the use of operations pointed to improve the finishing surface of the piece or heat treatments; this phase can vary a lot according to the material and AM process used.

Application

Finally the product is used in its reference application. Today AM has several application fields thanks to the possibility to use practically any kind of material, from plastic ones to metals and ceramics; nevertheless still today its major field of application at an industrial level remains the one of prototyping due to production times and costs which are usually not competitive in other sectors.

1.4 AM processes

Additive manufacturing includes a long varieties of processes united by the common idea of manufacturing objects by a selective and iterative add of material. The general list of all these processes is very long and it is under a constant change; here we decide to proceeded by clustering these processes according to the material state utilized to print. It is included not only the

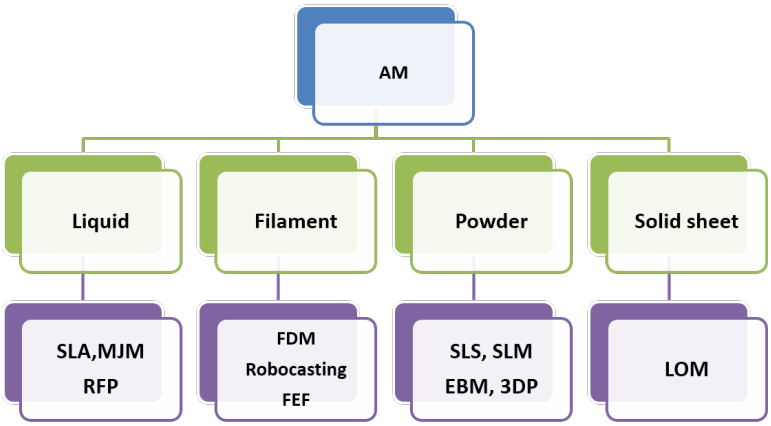

Figure 1.4: Additive Manufacturing processes

physical state but even the shape, for instance powder or wire. Below we describe more in detail some of these processes by showing how the single steps of AM technology change from one process to another. Looking at fig.1.4 it is possible to see how we have four major groups of AM based on liquids, solid sheets, powders and wires. Some of the acronyms of the known processes are listed in the respective fields. For descriptive completeness we cite another reference way of clustering AM processes which is possible to find in the literature and which is the one provided by the ASTM which divides the AM processes in 7 groups [18]:

- material extrusion
- powder bed fusion
- vat photopolymerization
- material jetting
- binder jetting
- sheet lamination
- directed energy deposition

In the industrial field these technological solutions are provided by different vendors. In tab.1.2 is visible a list of the first five companies by 2017 revenues in the AM sector [73]. Other companies have been added to the list whose revenue, which is referred only on the sold of AM machines, was not available, anyway they can be considered important vendors of AM industrial machines. Beside the company name is indicated their country of

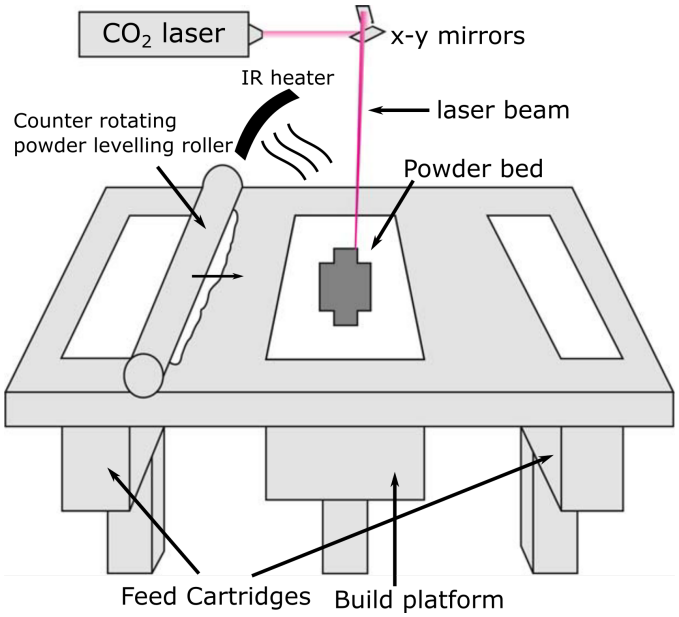

Figure 1.5: Selective Laser Sintering

origin. In [46] is indicated for the AM market a total value of about 6 billions of US dollars in a constant growth, and [7] highlights how the sold of AM systems for the production of metal parts is grown from 983 systems in 2016 to 1,768 in 2017.

SLS

The process of Selective Laser Sintering has been patented by Carl Deckard in the 1986 at the Texas University in Austin [48]; with this invention Deckard became the co-founder of the company Desk Top Manufacturing acquired in the 2001 by 3D Systems [68].

The SLS process sinters thin beds of powder, usually with a thickness of $0.1[mm]$, lied down and flattened by a rotating roll, fig.1.5. A first layer of powder is deposited in a printing area; later a laser source, usually CO_2, is used to sinter a region of interest until a 2D solid layer is created. The system comprises a laser source, a laser focus system based on lens and the use of galvanometric mirrors to control the laser direction in the printing plane. The laser control system is based on a numeric control through a g-code generate by the CAD of the object that is printed. Different trajectories can be applied to generate the 2D figure of one layer; for instance one possibility is to move the laser along the entire printing area, raster pattern, and turn on and off the laser according to the zones that must be sintered or not. Once a printing plane is completed the platform supporting the powder is lowered of quantity equal to the thickness of the powder bed, a new layer of

powder is laid down overlapping the previous one and the sintering process is repeated. The sintering process, for the layers following the first, not only guarantees the solidification of the powder but it must bond one layer with the previous in order to create a three dimensional object. The entire process is held in controlled environment. Nitrogen is used to avoid the oxidation of the piece during the printing and the temperature is kept to a value slightly lower than the melting point and/or glass transition of the material, according to the material used. The controlled temperature is needed to minimize the energy required to the laser to sinter the powder and to avoid a rapid cooling of the component with consequent deformations and thermal stresses. The temperature is kept constant through infrared lamps and the use of resistors in apposite plces of the machine. The material not sintered is used as support material during the printing of the following layers. Once the printing phase is over it is necessary a cool-down period in order to avoid thermal deformations. Later the piece is removed, freed by the excess powder and polished if required.

Among the process parameters are relevant the particle-size and the density of the powder, the laser power, the pulse frequency, the spot size and the printing temperature [34]. Furthermore it is important the trajectory used to print according to the parameters as can speed, scan spacing, and scan pattern [21]. These parameters are related one to the other and they are often dependent on the material utilized [21].

Every kind of material that can be melted and after that cured is theoretically suited to be printed through this process. Mainly it can be used thermoplastic materials, waxes, metallic and ceramic powders [22]. Inside the plastic materials often it is possible to find adds of glass fibers to increase the mechanical characteristics of the final component [21]. The metallic and ceramic powders are blended with a polymer used as binder; a post-processing operation is required to remove the binder [22] and often thermal processes are required to obtain the desired mechanical properties [4].

At the beginning this process was used in the field of prototyping for audio-visual help and fit-to-form tests, but with the introduction metal materials it began to be used for the production of functional prototypes and for rapid tooling [34]. Today it is used in several application fields as the biomedical through the development of tissue scaffolds [22].

SLA

The StereoLithography is born in the 1986 from the invention of Charles Hull [47] who founded after that the company 3D systems, one of the major actor in the 3D printing market.

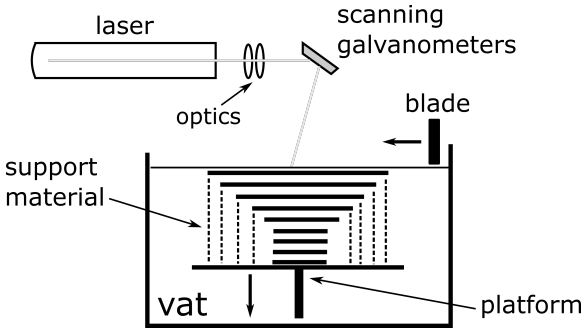

- Recoating system
- Platform System
- Vat System
- Laser & Optic System
- Control System

Figure 1.6: StereoLithography

The SLA technique requires the selective curing of liquid material through the iterative creation of 2D layers until the three dimensional object is printed [27]. The materials utilized are radiation curable resins or photopolymers that under the effect of an irradiation source, as a laser, they undergo a chemical reaction which lead them to curing. The laser is not the only irradiation source possible, even though it is one of the most used, but it can be varied according to the material used. For the good result of this technique is very important the knowledge about the polymeric structure of the material and of the chemical reactions that they have under the effect of an irradiation exposition. In fig.1.6 is shown a structure of a typical SLA machine with aside the list of its main components; here we refer mainly to the 3D system machines taken as example [21]. A laser system together with an optical system, containing galvanometric mirrors, are used to cure the first liquid layer. Once the bidimensional section is cured the platform is lowered so that the cured part is covered by new liquid. A blade is used to make the surface flat and homogeneous before to start the curing of a new layer [51]. The process is repeated until the final object is created. A post-processing phase can be required to remove the eventual support material and to polish the component surface, furthermore it can be necessary a chemical bath and a treatment in a oven [1]. There can be some changes to system here presented, particularly at the scanning system. It is possible to find two lasers instead of one, two-photon approach, which cure the material by the intersection of the two laser spots on the liquid surface; it is possible to have a system which cures the entire layer simultaneously thanks to a 2D image projected on the liquid surface, an example is the use of Digital Micro-mirror Devices, DMDs. With time this technique has been developed mainly in the scanning techniques for the systems with one or two lasers, in the use of different materials and in the designing and control of the machine [15]. The scanning technique specifies the path used by the laser to cure one layer above the other. This part of the process is very important to avoid that one layer does not bond with the underneath material or to avoid the presence of thermal stresses which can lead to the deformation of the component during the printing phase.

This technology can lead to the production of components with a resolution in the order of 0.05[mm] and with an accuracy of the same magnitude [1]. This process has been from the first moments of great interest in the field of prototyping [44] and for the development of new components in the foundry field, in particularly for the creation of models for investment casting [15]. Later developments there have been in other fields as the biomedical one where several possibilities have been created as the production of customized devices for patients, the print of resorbable scaffolding structure for tissues or the creation of cellular structures through the use of specific hydrogels [40]. With respect to other AM techniques the stereolithography allows to print a limited number of materials [44], and the scarce number of commercial resins available is often considered the main limit of this process [40]. The first resins were polyacrylate or epoxy macromers; today the majority of available resins are a mix of epoxides with some acrylate content. The stereolithography allows today the printing of ceramic materials too, thanks to the dispersion of particles inside curable resins. In this case is required a pyrolysis phase to eliminate the polymer and one of sintering to obtain the final ceramic object.

3DP

The three dimensional printing, 3DP, is born at the Massachusetts Institute of Technology in the 1989 [50] to be right after that granted to several companies. Among them there was the Z-corporation [43] which has been acquired from the bigger and most famous 3D-Systems. This technique based on the use of a movable printing head over a powder bed is visibly very resembling of the traditional ink printing machines so recalling the name three dimensional printing [1]. This process is also known by the name binder-jetting.

The 3DP technique is base on the use of powder material. Starting from an initial layer a printing head is actuated in order to selective lay down a binder, material used to bond the powder particles, and create a 2D solid layer. After that this process is repeated in a recursive way by depositing new powder layers and binder. The union of several bidimensional layers brings to the realization of the final object. In fig.1.7 there is a representation of the main components of a 3DP printer. For every printing layer the roller is used to lay down a new powder bed, right after the platform lowering, that must be flat and uniformly distributed. The powder particle size is in the order of tenth of microns and the layer height must be greater that the maximum size of the powder, usually al least three times bigger [69]. The powder is deposited at a dry state even though some

[1] It is pointed out to the reader how the term 3D printing is used commonly to indicate every AM process but in a technical field it indicates one and only one specific process. The two terms, AM and 3DP, are not to be confused.

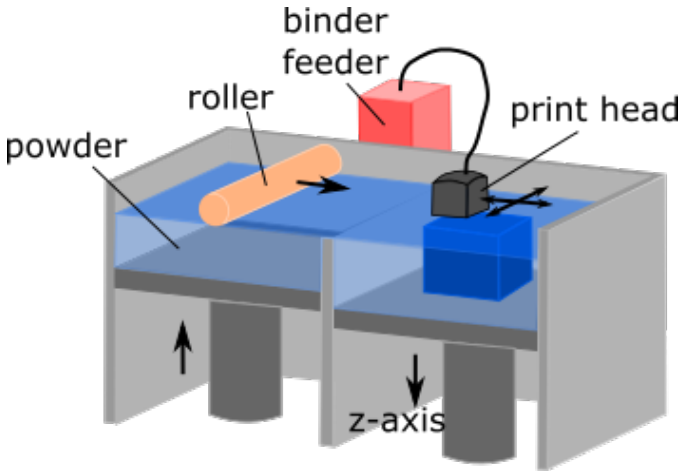

Figure 1.7: Three dimensional printing, 3DP

systems use a semi-liquid substance to carry the powder, slurry, which is dried after the deposition; this method helps to increase the powder density but it slow downs the deposition times. By moving in the printing plane the printing head deposits the binder in that points where the solidification is desired. Different kinds of binder can be used; the binder is chosen in combination with the powder used and according to the post-processing treatments required [69]. According to the materials used there are different post-processing treatments. Some treatments are carried out when the piece is still inside the powder; these operations are mainly aimed to harden the material before extracting it from the machine. Usually the piece is leaved in a resting phase to guarantee the curing of the binder and after that an operator paints with a hardener solution the surface of the object. In [36] to avoid these operations is used as binder a photosensitive resin that combined with the use of an UV rays source, system added to the classical 3DP machines, allows to obtain a printed object more compact and harder than the ones obtainable with other binders. Once the piece has been freed by the surrounding powder the operations executed are mainly two; one thermal aimed to increase the compactness and density of the piece or one of infiltrations where the component porosities are filled with a material at a liquid state which solidifies after the operation itself. The porosity of the components and the necessity of more than one post-processing phase are the main limitations of this technique.

The 3DP can ideally print any kind of material that can be reduced to a powder state, with the choice of the right binder and post-processing phases. It can be used to print metal and ceramic materials [50], or polymers and composites [58]. If we look among the applications proposed by two of the bigger producer of these machines, ExOne e 3D-Systems, we see how the major industrial sectors of interest are the production of sand core

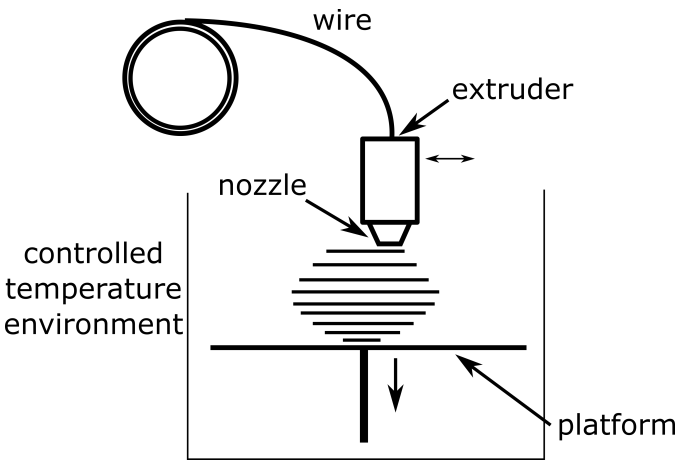

Figure 1.8: Fusion Deposition Modeling

and moulds in the foundry or prototyping. More limited seems to be the applications of metal functional components. Some applications of interest can be found in the biomedical sector [58] for the creation of tissues and scaffolds.

FDM

The Fusion Deposition Modeling is born from the invention of Scott Crump in the 1989 [49], commercialized through the foundation of the company Stratasys which holds today the property of the trademark FDM® [62], also known as FFF, used filament fabrication [13].

The FDM is an AM technique based on the extrusion of material at a fused state by starting from a wire of the same material [5], fig.1.8. The material, held in specific spools, is passed to the extrusion system where it is melted to a temperature slightly above the melting point. The extruder, capable to move in the printing plane, lay down the fused material by forming a component layer. Here resides one of the limit of this process which suffers with the masses and inertias of the extrusion system which are not present in processes like the SLS or SLA [21]. When one layer is finished the platform of the machine is lowered and the process is repeated until the object is finished. In the industrial printers usually the entire printing volume is held at a controlled temperature to avoid residual stresses and deformations of the printed part. During the post-processing can be required the removal of the support material and the surface finishing. It is possible to have FDM machines with multiple extruders in order to print one object with multiple materials.

Among the main process parameters for this technique we cite the layer thickness, the nozzle diameter and the printing temperature [60], and to

them we add the deposition pattern which influence the quality of the final results [54]. The layer thickness puts in contrast the printing quality, in particular the geometrical precision of a printed object and its surface finish, with the printing time. More thin a layer is more high is the printing quality due to a lower staircase effect; on the other hand the printing times rises. A compromise must be found to optimize this parameter. This parameter, which is common to all AM processes, for the FDM is in the order of some tenth of millimeter. The nozzle diameter defines the smallest feature printable by the machine; nothing below that dimension can be printed. For this parameter too the order of magnitude is usually the tenth of millimeter. The printing temperature, meant not only as the extruder one but the one of the printing chamber too, is strongly related to the material used, which is usually a polymer. The orientation of the piece, so the printing direction, and the deposition pattern influence both the geometrical accuracy than the mechanical properties of the final component.

The main material for the FDM are of plastic nature, especially PLA, polylactic acid, and ABS, acrylonitrile butadiene styrene [23]. These materials, whose variants are many, the extrusion temperature is around $200°C$. With time several researches have been carried out in order to print different materials and objects with good mechanical properties. Composite materials have been developed as for instance a polymeric matrix and glass fibres or a polymeric binder with metallic or ceramic powders [39]. An another important development for this technology has been the possibility to print biological material and hydrogel [21]. Given the ability of these machines to print different materials simultaneously the FDM is suited to print functionally graded materials, FGMs [59], that materials where the mechanical properties change in a gradual way inside the component.

The main FDM applications are prototyping for the developments of new components and the creation of casting patterns [22], particularly for the investment casting field [33]. A sector of great interest is the one related to the extrusion of bio-materials for the creation of scaffolds and for the generation of organic tissues [21]. To these applications we can add several, among them we cite as example the attempt to print low cost houses from straw and clay of Wasp project [71] or applications for food printing [65].

1.5 AM architecture

Regardless of the specific process applied every AM machine has a basic architecture which is followed during its designing phase. During their historical development these machines have taken many features from the CNC machines, Computer Numerical Control, with whom they necessarily share part of their DNA [21]. From [64] is possible to extract three main features from the composition of these machines as visible from fig.1.9. To the op-

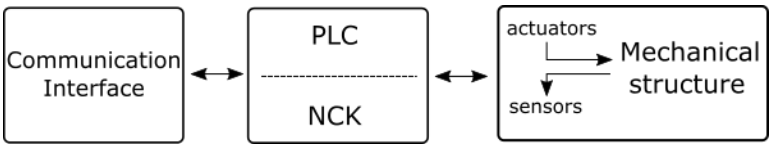

Figure 1.9: Main blocks of an AM machine

posite of this scheme we have the interface with the user, represented by a block which manage all the communications in and out the machine, and on the other the physical system with its mechanical structure, actuators and sensors. In the middle we have the core of the system; in this representation we have chosen two classical denominations that are used in the CNC field, the PLC, Programmable Logic Controller and the NCK, Numerical Control Kernel [64]. The PLC handles all that operations of soft real time which are necessary to the execution of the printing phase, whereas the numeric control takes care of all the hard real time operations, in primis of the mechanical system axes coordination. The communication interface is needed to guarantee the interaction functionalities which are today fundamental in an industrial environment; typically all the industrial machines, and not only the additive manufacturing ones, are capable to communicate through some sort of human machine interface, HMI, from a simple touch-screen to system more complex as the haptic ones. Other forms of communication can be predisposed as machine to machine, M2M, based on several types of communication protocols. Inside the control system of these machines there are two main fundamental software components; the interpreter and the interpolator. The first one has the duty to interpret the commands which arrive to the machine and translate them in executable tasks for the machine; this for CNC machines means to read an input file, the g-code, and translate it into movements to effectuate by the machine, into management commands for the system I/O, input-output, for instance as turning on or off an heating system or a milling tool and so on. The second one handles the trajectory generation for every single axis of the machine; such duty is fundamental to guarantee the correct movement of the machine tool, for instance the movement of the extruder in a FDM machine.

In order to realize an additive manufacturing machine there can be many and different engineering solutions which embody the blocks explained above; here it is described as example one particular solution which covers the conceptual scheme of fig.1.9 in order to better understand it. In fig.1.10 is possible to observe an FDM machine actually available in the market. The mechanical part of the system consists of a cartesian robot with three axis $x - y - z$ capable to guarantee the relative motion between printing plate and extruder. The system is moved by 3 stepper motors to whom is added a fourth which push the material wire inside the extruder. The control system is entirely inside the micro controller which is the core of the machine,

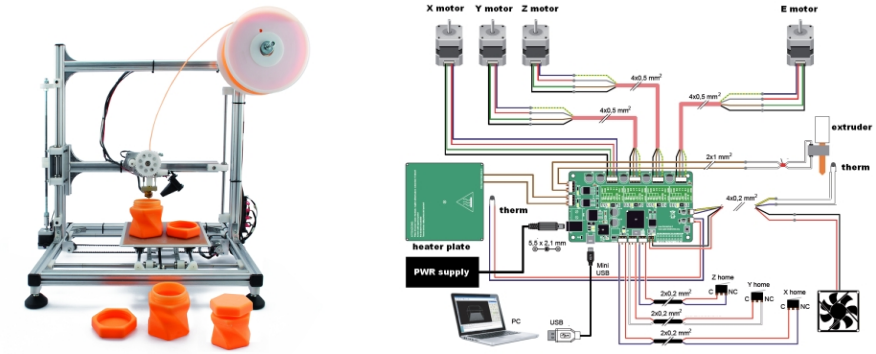

(a) 3DRag **(b)** Scheme

Figure 1.10: FDM printer

fig.1.10b. Here is where all the duties listed above are executed. From the trajectory generation for the machine motors to the control of the I/O as the fan, the extruder and plate resistors; it takes care of the communication part too, which can happen through an USB connection with a PC or through a little user-screen which is not visible in the pictures. The software used to control this machine is open source and so it is freely available to anyone, [38]. The software is capable of reading a g-code and extract from that all the necessary informations for a the correct execution of a 3D printing. Here we point out how even though from a conceptual point of view the machine here described can be perfectly used as example of an AM machine architecture, it is obvious that its performances are greatly limited by its components which are not comparable with the one used in an industrial machine.

1.6 Efesto project

The project *Efesto*, extrusion of feedstock for tiny sintered objects, is born from the idea to develop a new AM process for the manufacturing of metal and ceramic components [2], [20]. Today the main processes for the 3D printing of these materials are based on the use of laser, SLS-SLM processes, on the utilise of high power electron beam, EBM process(electron beam melting) or on the utilise of a binder over a powder, 3DP process [22, 25]; in Efesto has been decided to exploit the MIM technology [3], metal injection moulding, already largely diffused for the production of metal and ceramic components, and reapply it in the field of additive manufacturing. In fig.1.11

[2]The project has been self financed by the mechanical department of the Politecnico di Milano where it is currently located the Efesto machine. Here we recall the names of the people who started this initiative, professor Annoni M., Giberti H. and Strano M.

[3]Sometimes refered in a more general expression as PIM, powder injection moulding.

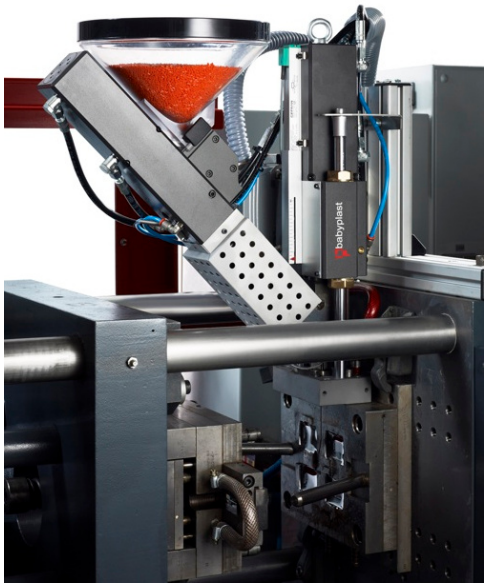

Figure 1.11: MIM extruder

is visible an extruder used for the production of plastic components through injection moulding; the same extruder of the same company, Babyplast® [8], has been bought and utilised for the Efesto project. The system, as represented in the figure, is characterized by two hydraulic actuators and a series of resistors capable of heating the material and extrude it through a nozzle. The transposition of this machine from an injection moulding application to an AM one is based on the idea to extrude a feedstock in order to realize a three dimensional object; from this point of view this technique is very similar to the FDM. Later the phases of this process will be examined in depth.

The motivations that leads to test this new process are of two kind; one economic and the other technical.

Economic The printing system of Efesto based on an extruder as the FDM acquires simplicity and so low costs.

Tecnical The use of a MIM process can lead to obtain printed parts with mechanical properties different from the ones obtained by the aforementioned processes for metal/ceramic pieces.

Tecnical The technique proposed allows to print a great variety of materials contrary to many AM processes that are limited on a very specific typology of materials.

The Efesto project aims to test several kind of materials in the additive manufacturing field through the use of a MIM process which allows the

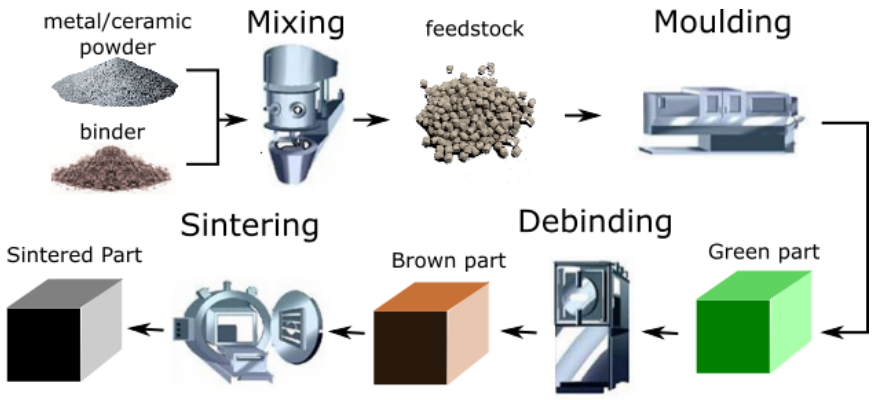

Figure 1.12: Metal injection moulding process

production of metal and ceramic components by having an impact on costs and applications currently sustained for these materials [6].

1.6.1 Metal injection moulding

The process of metal injection moulding enters in the industrial environments starting from the '70s as a valid alternative to the production of small objects of metallic or ceramic material [29]. Today many are the applications for this technology which is obviously tied to the applications of the powder market [17]. The phases that bring to the production of a MIM component are summarized in fig.1.12. Starting from metallic/ceramic powders with a powder size in the order of tenth of μm it is created the feedstock through a mixing process with another material, the binder. The purpose of the binder is to act as a glue for the powder particles during the following moulding phase. The binder is usually of polymeric nature and its composition can be based on more than only one polymer. The feedstock through an hot extrusion process is injected in a mould so obtaining the geometrical shape of the desired part; at the end of this operation we have the green part. At this point it is necessary a debinding process where the material used as binder is removed; this phase is strongly binder dependent and it takes to obtain the brown part. The final manufacturing process is the sintering phase where in high temperatures oven the powder particles are sintered together by obtaining the final object; the object can undergoes to some finishing operations if required. The project Efesto put itself in the middle of this manufacturing chain by substituting the moulding phase with an AM process based on the use of feedstock and a printing by extrusion. This means that the AM process of Efesto inherits, for better or for worse, the phases of feedstock preparation, debinding and sintering. The MIM technology is limited in the maximum widths , in the order of 10[mm] [29], or in the maximum density achievable in the components produced.

A different process

Being the printing phase of Efesto based on the same idea of FDM, which has been already described, we want here to describe the sintering phase in order to better understand the entire manufacturing process of this project and compare it with the other AM processes for the production of metal/ceramic parts. The sintering phase has been widely studied in the powder field and it consists of a thermal process, with or without an external pressure, applied to a part initially porous in order to obtain a final object solid, stable and without porosity [66]. This process, divided in three phases, starts first with the creation of contact zones among the several powder particles, after with the growth of crystal grains and in the last phase with a continuous diminishing of object porosity; to all this follows a reduction in the object volume. The physical phenomenon, whose in depth explanation can be found in [66], interests the entire part simultaneously; the object is dived in a controlled temperature environment, batch or continuous ovens [29]. The final result of this process on the object is defined by the time-temperature curve which is applied to the object itself inside the oven. The piece porosity, after the sintering phase, can reach a final value of 94%.

The physical phenomenon of binding, here meant as the bonding of powder particles, of MIM technology is part of the category Solid State Sintering as described in [32]. In SLS, SLM and EBM processes the thermal treatment of the material is different. First of all the thermal treatment is local and not global. In the MIM technology the object is entirely dived in the oven reaching the same temperature everywhere at almost the same time, depending on the time-temperature curve. In the SLS, SLM and EBM is used a power source to locally treat the material during the printing phase point by point; in the Efesto project the thermal process is separated from the printing. The material binding in these other processes takes place through Liquid Phase Sintering(LPS), in the SLS, and by Full Melting, in the SLM and EBM [32]. The processes based on LPS utilise powders made of two or more materials with different melting points. The material with the lowest melting point, binder, is the one who actually melts under the effect of the laser ray and it goes to surround the particles of the material remained solid, structural material, to solidify after that. In the full melting the powder is completely melted by creating a liquid phase which solidify and it remains a solid part virtually without no porosity. The reason why the AM processes as SLS, SLM and EBM utilise these methods is because of printing times. The binding process of SSS used by MIM is based on the physical phenomenon of atoms diffusion, it is very slow and it is unacceptable in the AM field; there has been some attempts to apply the SSS phenomenon in the SLS process but the interaction time laser-powder required was in the order of 5[s] against the typical 0.1-0.3[ms]. In all these AM processes is often required a thermal treatment after printing, in the case of LPS binding

in order to reduce the object porosity still present, in the case of full melting in order to relieve the internal stresses of the object. The Efesto project by separating the printing phase from the thermal treatment, which is most of time anyway required in the others AM processes, has two advantages: one given by the easy of print since the control parameters for a laser or electron beam system are more complex than an the ones of an FDM process and the other one given by the full control of the sintering process that according to the specific time-temperature curve used it can lead to objects with different mechanical results. Furthermore the AM processes based on laser are intrinsically not able to treat every kind of material, instead an hot extrusion of feedstock is suitable to be used with any kind of material that can be used as powder mixed with a binder.

The only AM process which presents a post-processing treatment as the one of MIM is the 3DP which also imposes the use of powders and binder, par.1.4. In this case the main difference is in the way how binder and powder are mixed. In the MIM process this phase is before the extrusion of the material, the feedstock is created and after used for printing. In 3DP the binder is locally added to the powder during the printing phase. The deposition system of 3DP is of two types; a drop-on-demand where the printing head deposits selectively binder drops or in a continuous-jet where the drops are injected in a continuous way and deviated in a gutter when it must not reach the powder [69]. In this last case the binder jet must be inductively chargeable. Very important is the impact of the binder drops on the powder. If the drop is laid down with too much energy it is possible that the powder is eroded and moved in an undesired way. In Efesto being the two operations separated, mixture of binder-powder and printing, they results simplified improving the control of the process. The FDM deposition is taken over by the Efesto project which extrudes a feedstock wire which is laid down on a printing plane1.4.

Cost

The project Efesto aims to lower the costs for the printing of metal/ceramic components compared with the AM processes strictly related. The costs study for AM technologies is a topic faced in the literature and Busachi et al. [11] list the cost models more used in this sector and they review the last twenty years literature in the field; the conclusion of such analysis is that the model cost more used is the Activity Based Costing [4], ACB, but still today these models are not complete of the entire AM chain process, so it is difficult to compare two different AM processes. By exploiting a methodology based on an analogous comparison [5] among the processes of

[4]Estimation of the total cost based on the evaluation of the single activity cost inside the entire process

[5]Cost analysis based on similarities and differences between two processes

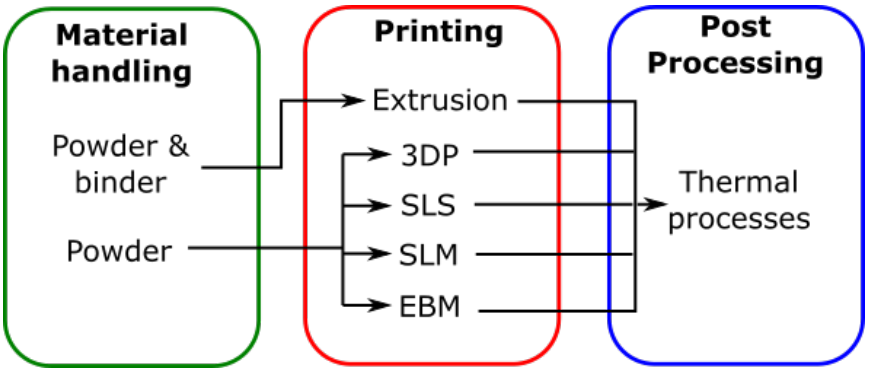

Figure 1.13: Flow of the AM processes based on powder

SLS-SLM-EBM-3DP, and by using the literature cited in [11] we can make a quality analysis on why it is reasonable to expect the project Efesto have an impact on the costs of AM processes for the production of metal/ceramic components.

In fig.1.13 are represented the AM processes based on the use of powder, included the Efesto project labelled as an extrusion system. The entire processes have been divided in three parts, the printing phase and other two phases. One prior to it, the material handling, and one after that, post-processing. We can see how all these processes use the same kind of materials and they all need thermal post-processing. In fig.1.13 is made a distinction between simple powder and powder plus binder. This differentiate the Efesto project from the other AM processes. The two raw materials both require a manufacturing process; the powder used with laser or electron beam is a complex material which requires a preparation as for the feedstock. The thermal post-processing are of different nature but they both requires similar times and equipments so it is reasonable to expect similar costs as for the material utilised. The real difference is in the printing process and the machine cost. Lindemann et al. [37] states how in the production of parts through AM techniques the main costs derive from the machine cost followed by the materials.

The FDM systems, which are based on machines very close to the Efesto project system, have machine costs very low compared to the ones based on laser [11]. This is mainly related to the difference in the equipment required; in the SLS, SLM and EBM a laser or electron source is required, furthermore the printing environment must be controlled, both in terms of temperature than atmosphere, par.1.4. In the printers based on laser is often required the use of inert gases to avoid oxidation reactions whereas in the EBM systems is necessary a vacuum environment to avoid undesired collisions of the electrons. In the FDM printers none of this is required, even though in the most modern solutions the temperature control of the printing

environment is more and more used in order to obtain a better printing quality [63]. In the case of 3DP systems the main instrument required is the printing head for the binder deposition; in this case is more difficult to have an analogous comparison between the FDM and 3DP costs since the lack of sources about the relative costs of these two systems.

Comparing the production processes of the techniques here analysed with the process proposed by the Efesto project we conclude that the main cost differences all plays in favour of the system here presented with a question mark about the 3DP technique. The materials utilised and the post-processing phases are comparable but the machine cost is in favour of the systems based on the extrusion of material respect to the AM processes for the pinting of powders.

1.7 Thesis objectives

Inside the framework of a developing technology for the production of metal and ceramic parts is born this thesis work. The development of a new manufacturing process requires the design and development of a machine capable to guarantee the productive process described, par.1.3, by taking into account the typical architecture of AM machines, par.1.5.

With the main thread of designing a new AM prototype several issues related to the AM technology will be touched and discussed in different chapters. The work hereafter presented push the development of a still growing technology whose industrial and social benefits have been largely promoted.

bibliography

[1] 3d system website. https://it.3dsystems.com/3d-printers. Accessed: 2018-05-05.

[2] 3d hubs. https://www.3dhubs.com. Accessed: 2018-09-04.

[3] Working Group Industry 4.0. Final report of the industrie 4.0 working group. securing the future of german manufacturing industry recommendations for implementing the strategic initiative industrie 4.0, 2013.

[4] M. Agarwala, D. Bourell, J. Beaman, and J. Marcus, H.and Barlow. Post-processing of selective laser sintered metal parts. *Rapid Prototyping Journal*, 1995.

[5] Sung-Hoon Ahn, Michael Montero, Dan Odell, Shad Roundy, and Paul K. Wright. Anisotropic material properties of fused deposition modeling abs. *Rapid Prototyping Journal*, 2002.

[6] M. Annoni, H. Giberti, and M. Strano. Feasibility study of an extrusion-based direct metal additive manufacturing technique. *Procedia Manufacturing*, 2016.

[7] Whoelers associates. Wohlers report 2018. 3d printing and additive manufacturing state of the industry, 2018.

[8] Babyplast website. http://www.babyplast.com/. Accessed: 2018-23-07.

[9] B. Berman. 3-d printing: The new industrial revolution. *Business Horizons*, 2012.

[10] D.L. Bourella, J.J.Jr. Beaman, M.C. Leub, and D.W. Rosen. A brief history of additive manufacturing and the 2009 roadmap for additive manufacturing: Looking back and looking ahead. *US-Turkey workshop on rapid technologies*, 2009.

[11] A. Busachi, J. Erkoyuncu, P. Colegrove, F. Martina, C. Watts, and R. Drake. A review of additive manufacturing technology and cost estimation techniques for the defence sector. *CIRP Journal of Manufacturing Science and Technology*, 2017.

[12] B.P. Conner, G.P. Manogharan, A.N. Martof, L.M. Rodomsky, C.M. Rodomsky, D.C. Jordan, and J.W. Limperos. Making sense of 3-d printing: Creating a map of additive manufacturing products and services. *Additive Manufacturing*, 2014.

[13] G. Cwikla, C. Grabowik, K. Kalinowski, I. Paprocka, and P. Ociepka. The influence of printing parameters on selected mechanical properties of fdm/fff 3d-printed parts. *IOP Conference Series: Materials Science and Engineering*, 2017.

[14] G. Da Silveira, D. Borenstein, and F.S. Fogliatto. Mass customization: Literature review and research directions. *Int. J. Production Economics*, 2001.

[15] P.M. Dickens. Research developments in rapid prototyping. *Proceedings of the Institution of Mechanical Engineers, Part B: Journal of Engineering Manufacture*, 1995.

[16] U.M. Dilberoglua, B. Gharehpapagha, U. Yamana, and M. Dolena. The role of additive manufacturing in the era of industry 4.0. *27th International Conference on Flexible Automation and Intelligent Manufacturing*, 2017.

[17] Metal Powder Industries Federation. 2017 pm industry road map - technology update for the powder metallurgy industry, 2017.

[18] W. Gao, Y. Zhang, D. Ramanujan, K. Ramani, Y. Chen, C.B. Williams, C.C.L. Wang, Y.C. Shin, S. Zhang, and P.D. Zavattieri. The status, challenges, and future of additive manufacturing in engineering. *Computer-Aided Design*, 2015.

[19] H. Gaub. Customization of mass-produced parts by combining injection molding and additive manufacturing with industry 4.0 technologies. *Reinforced Plastics*, 2016.

[20] H. Giberti, M. Strano, and M. Annoni. An innovative machine for fused deposition modeling of metals and advanced ceramics. *MATEC Web of Conferences*, 2016.

[21] I. Gibson, D.W. Rosen, and B. Stucker. *Additive Manufacturing Technologies. Rapid Prototyping to direct digital manufacturing.* Springer, 2010.

[22] N. Guo and M.C. Leu. Additive manufacturing: technology, applications and research needs. *Frontiers of Mechanical Engineering*, 2013.

[23] M.N. Hafsa, M. Ibrahim, M.S. Wahab, and M.S. Zahid. Evaluation of fdm pattern with abs and pla material. *Applied Mechanics and Materials*, 2013.

[24] Hasbro. https://www.theguardian.com/technology/2014/feb/17/hasbro-3d-printing-children-kids. Accessed: 2018-09-04.

[25] D. Herzog, V. Seyda, E. Wycisk, and C. Emmelmann. Additive manufacturing of metals. *Acta Materialia*, 2016.

[26] N. Hopkinson, R.J.M. Hague, and P.M. Dickens. *Rapid Manufacturing-An Industrial Revolution for the Digital Age.* John Wiley & Sons, 2006.

[27] C. Hull. Stereolithography: Plastic prototypes from cad data without tooling. *Modern Casting*, 1988.

[28] Piano nazionale industria 4.0. http://www.sviluppoeconomico.gov.it/index.php/it/industria40. Accessed: 2018-06-02.

[29] Merhar J.R. Overview of metal injection moulding. *Metal Powder Report*, 1990.

[30] S.H. Khajavi, J. Partanen, and J. Holmstrom. Additive manufacturing in the spare parts supply chain. *Computers in Industry*, 2014.

[31] D. Klitou, J. Conrads, and M. Rasmussen. Key lessons from national industry 4.0 policy initiatives in europe. https://ec.europa.eu/growth/tools-databases/dem/monitor/category/national-initiatives, 2017. Accessed: 2018-23-07.

[32] J.P. Kruth, G. Levy, F. Klocke, and T.H.C. Childs. Consolidation phenomena in laser and powder-bed based layered manufacturing. *Annals of the CIRP*, 2007.

[33] P. Kumar and I.P.S. Ahuja. Application of fusion deposition modelling for rapid investment casting – a review. *Int. J. Materials Engineering Innovation*, 2012.

[34] S. Kumar. Selective laser sintering: A qualitative and objective approach. *Journal of Metals*, 2003.

[35] A.O. Laplume, B. Petersen, and J.M. Pearce. Global value chains from a 3d printing perspective. *Journal of International Business Studies*, 2016.

[36] W.H. Lee, D.S. Kim, J.S. Kim, T.M. Lee, D.Y. Shin, and M.C. Lee. Strength and processing properties using a photopolymer resin in a powder-based 3dp process. *SICE-ICASE International Joint Conference*, 2006.

[37] C. Lindemann, U. Jahnke, M. Moi, and R. Koch. Analyzing product lifecycle costs for a better understanding of cost drivers in additive manufacturing. *23rd Annual International Solid Freeform Fabrication Symposium - An Additive Manufacturing Conference*, 2012.

[38] Marlin firmware. https://github.com/MarlinFirmware/Marlin. Accessed: 2018-09-02.

[39] S.H. Masood and W.Q. Song. Thermal characteristics of a new metal/polymer material for fdm rapid prototyping process. *Assembly Automation*, 2005.

[40] Ferry P.W. Melchels, J. Feijen, and D.W. Grijpma. A review on stereolithography and its applications in biomedical engineering. *Biomaterials*, 2010.

[41] S. Mellor, L. Hao, and D. Zhang. Additive manufacturing: A framework for implementation. *Int. J. Production Economics*, 2014.

[42] J.O. Milewski. Trends in am, government, industry, research, business. In *Additive Manufacturing of Metals*. Springer, 2017.

[43] Three dimensional printing. http://www.mit.edu/ tdp/whatis3dp.html. Accessed: 2018-26-07.

[44] T.D. Ngo, A. Kashani, G. Imbalzano, K.T.Q. Nguyen, and D. Hui. Additive manufacturing (3d printing): A review of materials, methods, applications and challenges. *Composites Part B*, 2018.

[45] A.P. Nyaluke, D. An, H.R. Leep, and H.R. Parsaei. Rapid prototyping: Applications in academic institutions and industry. *Computers and Industrial Engineering*, 1995.

[46] Oerlikon. Additive manufacturing. the next industrial revolution. https://www.oerlikon.com/ecoma/.../Oerlikon-AM-Factsheet$_I$$I$...., 2017. $Factsheet$.

[47] US Patent. Us4575330 - apparatus for production of three-dimensional objects by stereolithography, 1986.

[48] US Patent. Us4863538a-method and apparatus for producing parts by selective sintering, 1986.

[49] US Patent. Us5340433 - modeling apparatus for three-dimensional objects, 1989.

[50] US Patent. Us5204055-three-dimensional printing techniques, 1993.

[51] US Patent. Us5651934 - recoating of stereolithographic layers, 1997.

[52] T. Peng, K. Kellens, R. Tang, C. Chen, and G. Chen. Sustainability of additive manufacturing: An overview on its energy demandand environmental impact. *Additive Manufacturing*, 2018.

[53] Platform 4.0. http://www.plattform-i40.de/I40/Navigation/EN/InPractice/Map/map.html. Accessed: 2018-08-02.

[54] F. Rayegani and G.C. Onwubolu. used deposition modelling (fdm) process parameter prediction and optimization using group method for data handling (gmdh) and differential evolution (de). *The International Journal of Advanced Manufacturing Technology*, 2014.

[55] T. Rayna and L. Striukova. From rapid prototyping to home fabrication: How 3d printing is changing business model innovation. *Technological Forecasting & Social Change*, 2016.

[56] J. Rifkin. *The zero marginal cost society.* Palgrave macmillan, 2014.

[57] E. Sachs, M. Cima, J. Cornie, D. Brancazio, J. Bredt, T. Curodeau, A. Fan, S. Khanuja, A. Lauder, J. Lee, and S. Michaels. Three-dimensional printing : The physics and implications of additive manufacturing. *CIRP Annals - Manufacturing Technology*, 1993.

[58] S.F.S. Shirazi, S. Gharehkhani, M. Mehrali, H. Yarmand, H.S.C. Metselaar, N.A. Kadri, and N.A.A. Osman. A review on powder-based additive manufacturing for tissue engineering: selective laser sintering and inkjet 3d printing. *Science and Technology of Advanced Materials*, 2015.

[59] M. Srivastava, S. Maheshwari, and T.K. Kundra. Virtual modelling and simulation of functionally graded material component using fdm technique. *Materials Today: Proceedings*, 2015.

[60] M. Srivastava and S. Rathee. Optimisation of fdm process parameters by taguchi method for imparting customised properties to components. *Virtual and Physical Prototyping*, 2018.

[61] H.J. Steenhuis and L. Pretorius. The additive manufacturing innovation: a range of implications. *Journal of Manufacturing Technology Management*, 2017.

[62] Inc. Stratasys. Us trademark- serial number 74133656, 1991- renewed in 2011.

[63] Stratasys website.

[64] S.H. Suh, S.K. Kang, D.H. Chung, and I. Stroud. *Theory and Design of CNC Systems*. Springer, 2008.

[65] J. Sun, W. Zhou, L. Yan, D. Huang, and L. Lin. Extrusion-based food printing for digitalized food design andnutrition control. *Journal of Food Engineering*, 2018.

[66] F. Thummler and W. Thomma. The sintering process. *Metallurgical reviews*, 1967.

[67] Catapult- high value manufacturing. https://hvm.catapult.org.uk/technologies/core-technologies/additive-manufacturing-3/. Accessed: 2018-06-02.

[68] Selective laser sintering, birth of an industry. http://www.me.utexas.edu/news/news/selective-laser-sintering-birth-of-an-industry. Accessed: 2018-16-04.

[69] B. Utela, D. Storti, R. Andersonb, and M. Ganter. A review of process development steps for new material systems in three dimensional printing (3dp). *Journal of Manufacturing Processes*, 2008.

[70] S. Van De Crommert, S. Seitz, K.K. Esser, and K. McAlea. Sand, die and investment cast parts via the sls, selective laser sintering process. *Proceedings of SPIE - The International Society for Optical Engineering*, 1997.

[71] World aadvanced saving project. http://www.wasproject.it/w/stampa-3d/bigdeltawasp-12m/bigdelta-la-ricerca. Accessed: 2018-05-05.

[72] T. Wohlers and T. Gornet. History of additive manufacturing. *Wohlers Report*, 2016.

[73] Website www.engineering.com. Hp, ge additive and eos lead 3d printing revenue growth for 2017. https://www.engineering.com/AdvancedManufacturing/ArticleID/16797/, 2018. Accessed: 2018-20-10.

Chapter 2

Mechatronic Design

introduction

The design of AM machines is derived from the design of numeric control machines, CNC, whose architecture has been largely shared with the AM machines. The development of AM machines has been focused on the research of new processes, materials and applications with a minor attention to the customization of the designing solutions which have been taken from the CNC systems. The design of the Efesto machine requires a compromise between an off-the-shell solution capable to guarantee the correct functioning of the classic features needed by AM machines and a customized solution capable to adapt itself to a new AM process by allowing its study and development along the entire testing of the technology itself. Here is presented the design of an innovative AM machine whose particular characteristics have been reached through a mechatronic design approach and whose solution has been obtained and optimized by integrating several software tools and state of the art techniques. The mechatronic design, meant as an holistic solution of the entire system, starts from the technical requirements for the machine and propose a solution with a mechanical, hardware and software architecture tailored to the technological needs of the process. The different phases of the design process are faced starting from the kinematic synthesis of the machine and by ending with the architecture of the control and communication systems.

2.1 Design approach

The additive manufacturing technology is moving the attention to a different way of producing goods by forcing the machine designers to reconsider their solutions for this kind of production which has different technological needs than subtractive manufacturing. The need to improve performance in systems based on AM and to develop new technology leads us to reconsider the

approach to projecting, designing and manufacturing these machines, the control systems, sensor system and movement strategies [11]. In fact automated machine design is based not only on science and technology, but also on the art of integrating devices originally designed for other and differing purposes. For instance, if we consider cameras, communication networks, microcontrollers, operating systems, an the like, the industrial version of these objects or even the ones dedicated to automation, are often an evolution of something initially created for other purposes, forcing the designers to adapt existing systems. Frequently the reason for this is linked to the size of a market. In this scenario, one of the few exceptions is the computer numerical control (CNC), which obviously was not derived from consumer products and was developed for controlling the tool trajectory in multi-axis machines [2]. It is therefore not surprising that such controllers are designed and can be programmed according to a relatively rigid approach, which makes almost exclusive reference to machine tools and shows significant limitations when applied to other types of machines [3]. The additive manufacturing machines have a designing solution based on the industrial CNC architecture and this limits their capacity to achieve the required performances. To overcome this situation a mechatronic approach to the design of AM machine is necessary in order to take into consideration all the aspects involved in the realisation of these devices.

In order to fulfil the required standards of production environments the concept solution must be based, as much as possible, on the integration of commercial off-the-shelf components and on the proven architecture concepts currently adopted in state-of-art automated machines, leaving most of the design efforts to the integration and the correct balance of performance of all subsystems. The Efesto machine must satisfy the technological steps as described in par.1.3 while fulfilling the main functional blocks of an AM machine as described in par.1.5.

Nowadays, mechatronics-oriented design tools improve and assist the development process by simulating the interaction between mechanical and electrical subsystems, making it possible to work in parallel and cooperate on design, prototyping, and deployment. In most structured environments, this process is carried out through the following steps:

1. Including the disciplines involved in formal design reviews;

2. Formally documenting cross-disciplinary design open points and provide notification of possible issues arising from changes in inter-dependant subsystems;

3. Set design performance metrics for all engineering disciplines and formally collect, manage, and track design requirements throughout the development process;

4. Use assessment techniques, including those based on simulation, to detect weaknesses or criticalities. Usually the same simulation tools can also provide support to set the optimal trade-offs

Some typical examples of these can be listed as follows:

Architectural choices: kinematic solution; actuator type; controller type;

Sizing: mechanical component sizing; motoreducer sizing;

Design choices: sensors placement; Mechanical stiffness requirements;

Devices and components: Actuators and sensors selection; Motion controller and drive; I/O module selection;

Coding: control logic, timing and sequencing; Motion trajectory design;

This is not a comprehensive check-list but as a set of elements which illustrate the kind of inescapable cross-dependencies to be considered and solved. A typical project is expected to include these main aspects:

1. To decide the kind of kinematic architecture to use with a conceptual design of the entire machine. This choice will drive almost all the other machine aspects. Common alternatives, among others, could be e.g. linear Cartesian gantries, SCARA robots, rotary indexing tables, and conveyers.

2. To select the adequate motoreducers in order to satisfy the dynamic requirements of the system. Their calculation can be done on the basis of the requirements needed to execute the motion trajectories and to deal with the inertia of the mechanical load.

3. To define the architecture and the control logic of the machine. Their modification can have consequences on the machine behaviour, user-machine interaction, on the choice of the actuators and other machine parts.

4. To design the motion trajectory to initially approximated the shape of the tool motion providing the starting indications on the machine characteristics by evaluating how the part accelerates along the path. Consequently, one can calculates the inertia forces which in most cases represent the greater part of the resistant torque and consequently greatly affect the motor choice.

All these phases are executed in the following by starting from the design requirements of the machine and through the use of advanced tools as CAD, multibody and technical calculation software.

2.2 Design requirements

The machine design starts with the design requirements. These are:

- Printing volume of side 100[mm]
- Printing speed of up to 100 [mm/s]
- 3 translational Degree of Freedoms, Dofs, with the possibility to introduce two additional rotations
- Possibility to implement customized trajectories

After that we have to take into account the main constraint of the system given by the extrusion system already chosen.

- Extrusion system for a MIM technology of the Babyplast® company based on two hydraulic pistons and an heating system of the material, cap.1. The system has a total mass of about 25kg.

The requirements listed above derive directly from specific considerations about the AM technology here implemented, based on a MIM technique, cap.1, and onto its development necessities. The printing volume has been arbitrarily chosen by considering the typical volumes of commercial 3D printers and by considering the main goal of this machine is to print test components. In the same way, with a particular attention to the FDM machines whose process is very similar to the Efesto one, has been chosen the maximum printing speed. The system Dofs must be at least 3, translational, in order to guarantee the printing of a three dimensional component; this is the most common solution in commercial printers. To these 3 degrees is added the request to potentially implement in the future 2 rotational Dofs. This requirement, unusual for most of the AM machines, is aimed to face two typical problems of additive manufacturing, regardless of the process utilised: the staircase effect and the use of support material [1, 5, 6]. The first one derives from the layer approach of the AM and it interests mainly the surface finish and the geometrical accuracy of the final object; the second one depends on the utilise of extra material to the one actually needed to produce the object so increasing printing times and costs. By giving the possibility of a relative rotation between extrusion system and printing plate will allow the machine to face two relevant issues in the field of AM which otherwise it could not face; furthermore 2 Dofs would increase the possibility to generate more complex trajectories for the printing process. In fig.2.1a are represented schematically the problem of the staircase effects and of the support material; both issues can be faced by giving a more printing freedom through the use or rotational Dofs, fig.2.1b. As last consideration we point out the fact that he machine here proposed is a prototype and some degree

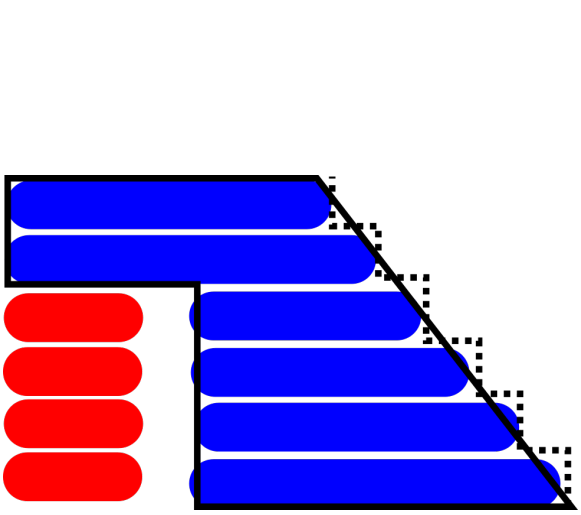

(a) Staircase effect and use of the support material

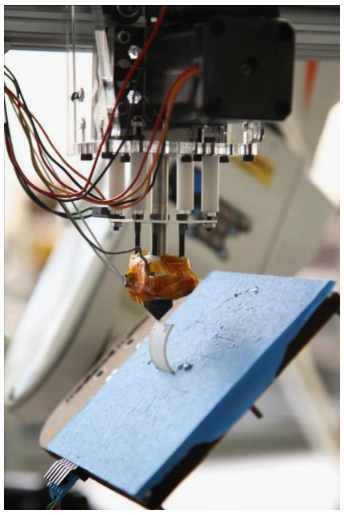

(b) 3D printing with multiple DoFs. Source: [13]

Figure 2.1: 3D printing issues and solutions

of flexibility is required during its use; the necessity to experiment could bring the necessity to change and that is why there is as requirement the request to generate customized trajectories. The architecture of the control system must be correctly tailored to allow the flexibility required.

2.3 Hybrid solution

Starting from the design requirements it has been chosen the kinematic architecture to use in order to cover the 5 Dofs required to the machine, 3 translational and 2 rotational. The first distinction must be made between the possibility to use a serial or a parallel kinematic. In the AM machines field based on extrusion systems the most common solution is the serial one with 3 Dofs, and we can find several examples of industrial machines with such a structure and the relative patents [20,21]. The serial machines has the advantage to have bigger ratio between workspace and machine dimensions; this means that the chose of a parallel robot generally would bring to obtain a bigger printer with the same printing volume. In the modern 3D printers the serial solution is consequent to the desire of a compact machine and to the fact that the extrusion head is usually little, easy to move, furthermore this solution has been largely used and so it is largely known in the industrial world. Robots with a parallel kinematic have the advantage to bear severe loads, a greater positioning accuracy thanks to a more rigid system and higher dynamic responses. Since in the Efesto project the extruder has a very big mass a solution with a moving head would lead to an over sizing

of the system actuators and of the mechanical structure which should bear very high inertial loads during the printing phase. It has been decided to keep the extruder fixed and the Dofs required to the system are entirely given to a printing plate where the material extruded is laid down. A serial system with 5 Dofs would lead to the choice of very big actuators at the base of the kinematic chain and dynamic performances not very high. At the same time even though there are some existing solutions with 5 parallel Dofs as required by the project [16], such solutions are rarely used in an industrial environment for two main reasons:

- workspace too limited
- joints with too wide movement required

As already mentioned the ratio workspace-dimension of the robot is usually against the parallel kinematic solutions; this disadvantage became worst when the number of Dofs required increase. This is because of an interference among the kinematic chains which have a greater possibility to enter in contact during the robot movements. Furthermore the search of a greater robot mobility brings the necessity of passive and active joints capable of bigger translations and rotations and that implies a complication in the constructive phase. For these reasons and the consequent designing complexity today it does not exist in the market a *full parallel robot*, a parallel robot with the same number of kinematic chains and Dofs, capable of three translations and two rotations [22].

Taking into account the disadvantages of a fully parallel or serial solution, and the fact that of the 5 Dofs required two can be implemented in a later development of the machine, it has been chosen a modular or hybrid solution. The proposal here made is constitute of two parallel kinematic robots put in series, the first robot capable of three translations and the second of two rotations, yaw and pitch. This solution, derived from the above considerations, brings with it a series of advantages:

- possibility to have a 3 Dofs system that can be expand with other 2
- compromise between parallel and serial solution
- design simplicity with respect to a fully parallel solution

The modular solution allows to have a robot with 3 Dofs to whom will be possible to add a 2 Dofs robot in the future development of the project; the total printing volume of the design requirements, the cube of side 100[mm], must be the result of the two robots workspaces. With two robots in series we can limit the disadvantages of parallel solutions about the total workspace reachable, furthermore by having a two-piece solution we can design separately the two robots. On the other hand the two parallel solutions allow to

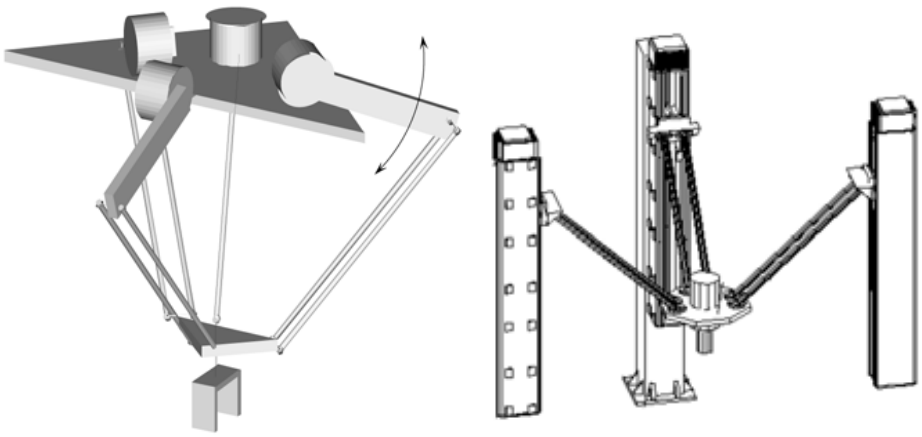

(a) *Delta* robot **(b)** *Linear Delta*

Figure 2.2: Parallel robots with 3 Dofs

exploit high dynamic and stiffness of these systems by pointing to a precise and fast printing.

At this point we have to choose the right architecture for the translations and rotations desired. The approach used is based on the research of already existing technical solutions, [16], and among them it is chosen the most suitable robot in order to comply the design requirements. The parallel robots capable to accomplish three translations are based mostly on the *Delta* robot structure, fig.2.2a. This robot is made of three kinematic chains of the type RRP_aR, Revolute-Revolute-Parallelogram-Revolute, capable to give three translational Dofs to the robot end-effector. From the same family we have the *Star* robot with the difference that this robot has redundant constraints, differently from the delta. From the delta is possible to obtain the *Linear Delta*, fig.2.2b, by replacing the first revolute joint with a prismatic one. In the parallel robot family with 3 translational Dofs we can finally list the *Orthoglide* robot, which is another derivation of the delta and which is characterized by a good isotropy inside its workspace, and the *Tricept*.

The robotic solution must guarantee:

- good ratio workspace/dimension
- isotropy

Even though it is not a feature in favour of parallel machines it is worthy to search among the possible choices one that leads to obtain a printer with a relative small size in order to cover the workspace required. The isotropy, meant as the robot capacity to have the same kinematic/dynamic properties inside its workspace, is another feature that is not in favour of parallel robots. To limit this problem is convenient to choose a kinematic architecture with

the greatest grade of symmetry as possible since a symmetrical geometry leads to the same behaviour of the machine in every points and planes of symmetry. The kinematic architecture more suitable to face these issues result to be the linear delta. This robot has high dynamic performances and it has the advantage of a preferential move along one direction, usually the vertical one, since the use of prismatic joints as visible in fig.2.2b. This fact has a series of positive consequences:

1. the vertical development of the machine allows to respect the request of a non excessive size by limiting the lateral dimensions of the machine;
2. the presence of a preferential direction of movement is in line with the printing process which proceeds layer by layer;
3. the vertical development gives to the machine an ergonomic solution for the operator who must work on it, with a zone of work not too low or to high;
4. along the direction of the prismatic joints the only limit to the translations is given by the stroke of such constraints, this will make easy to cover the workspace along this direction;
5. the robot develops around a central axis by having a certain degree of symmetry and so the isotropy researched.

For the choice of the robots with 2 rotational Dofs we proceed in an analogous way than for the linear delta, by listing the existing choice and by picking one by taking into account the main constraint that the second robot must be integrated with the linear delta. In fig.2.3 it is possible to see three different kinematic solutions. Each of theme has three rotational Dofs instead of two, but it is possible to change these solutions in order to obtain only two Dofs. Among these robots the one which is best suited to be integrate wit the linear delta is the spheric wrist of Gosselin, fig.2.3b, also said *Agile Eye*. The agile eye offers a solution that from the points of view of size and weight is fare more attractive than the other two solutions, where there is the necessity of heavy linear actuators, fig.2.3a, or the use of longer kinematic chains, fig.2.3c.

At the end of this study the two kinematic architectures chosen are the linear delta for the trnaslations and the agile eye for the rotations. The two robots are in series by forming an hybrid solution capbable to guarantee the total 5 Dofs required. The agile eye must be properly modified in order to have only the 2 Dofs required. Since the add of the 2 rotational Dofs is a future development of this project hereafter the design of the system is focused on the linear delta. Of the agile eye are of interest only the weight and size in order to correctly design the linear delta. In the appendix B are shown the consideration and work made about the agile eye.

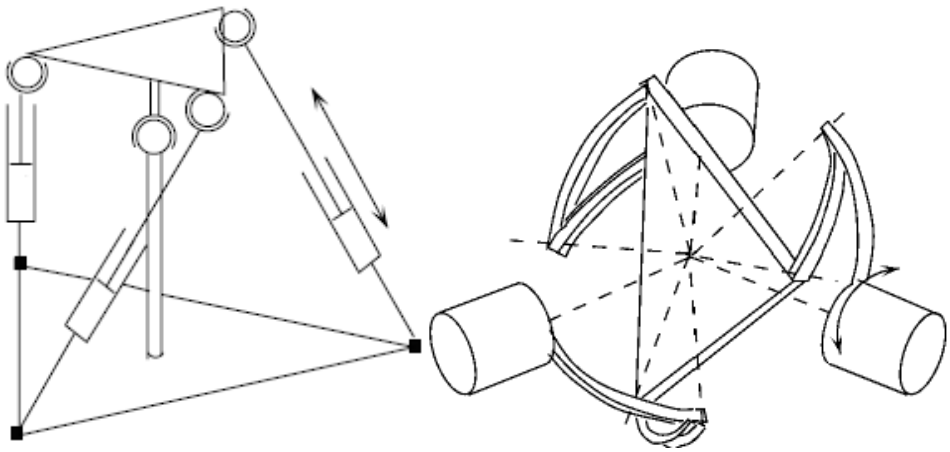

(a) Parallel wrist **(b)** Gosselin spherical wrist

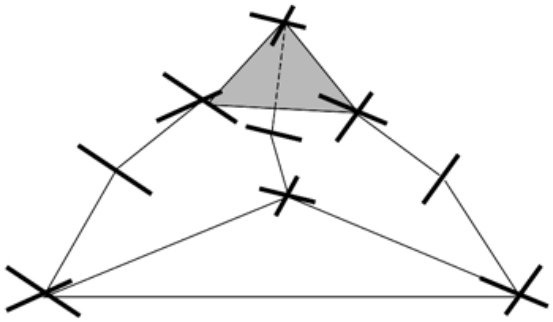

(c) *Dymo* mechanism

Figure 2.3: Parallel solutions with rotational Dofs

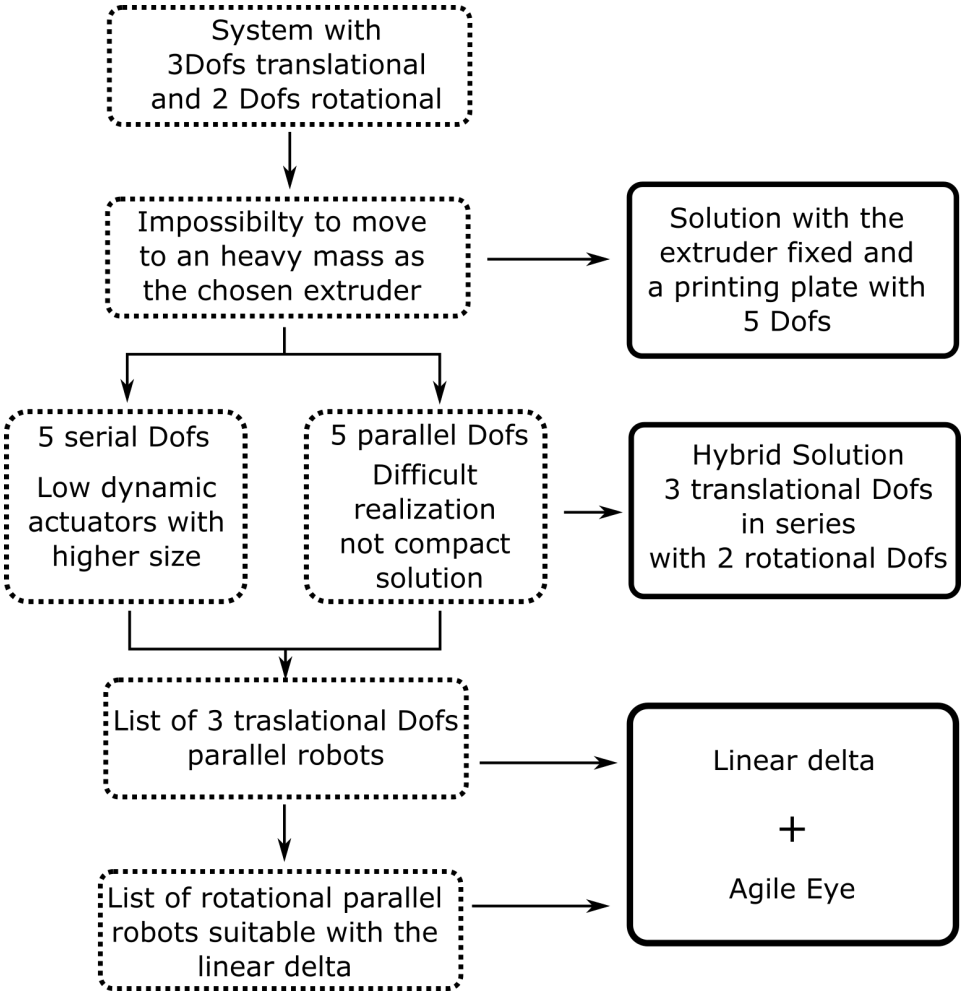

Figure 2.4: Choice of the kinematic solution

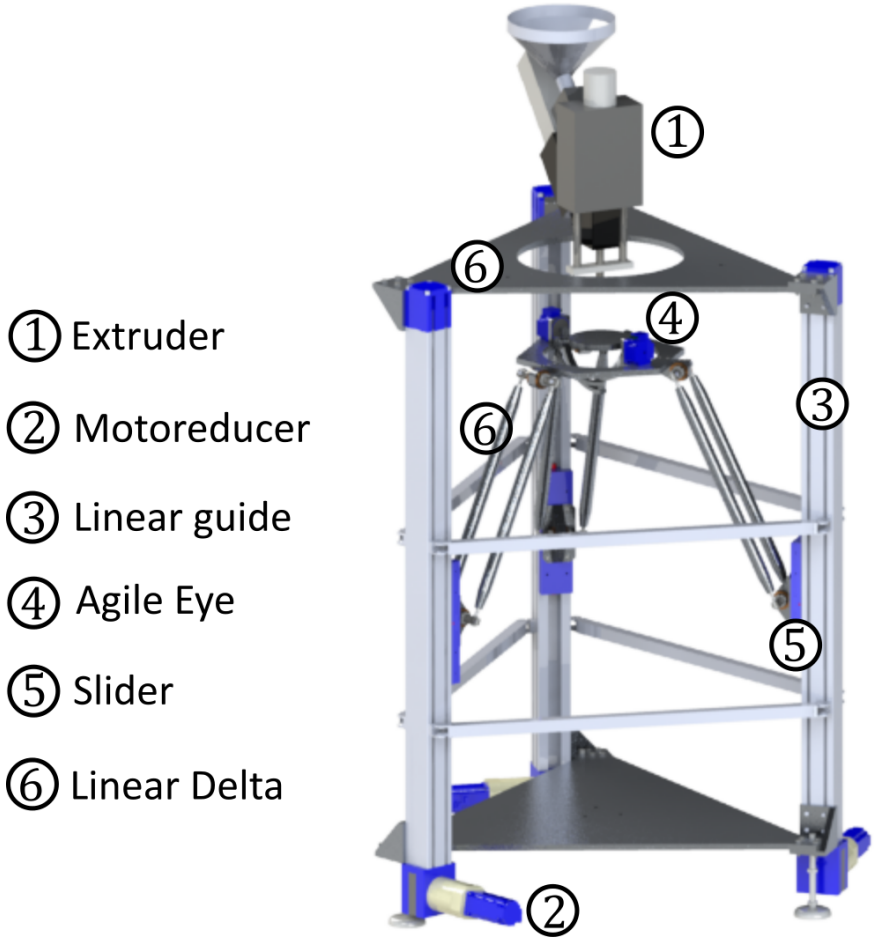

Figure 2.5: Concept design of the Efesto Machine

2.4 Kinematic analysis of the linear delta

The linear delta is parallel kinematic robot capable of three translations. The robot is composed by three identical kinematic chains of the type PUU(Prismatic-Universal-Universal). It is possible to refer at fig.2.5, where it is depicted the concept design of the Efesto machine, to understand the basic scheme of this robot. The linear delta structure is based on three sliders moving along three linear guides, each of them is connected through a link to the robot end-effector. In the figure over the platform moved by the linear delta is represented the agile eye. The sliders are the prismatic constraints of the robot which are the active joints of the system thanks to the motoreducers at the base of the printer. The links are realized through a parallelogram structure which realizes the two universal joints, passive joints, of the single kinematic chain. It is possible to find in the literature references to the kinematic of this robot [19]. For the development of the project is required the resolution of the forward and inverse kinematic equations, so we must be able to evaluate the sliders position by imposing the end-effector position and vice versa.

2.4.1 Forward and inverse kinematic

For the inverse kinematic we start by imposing the position of the machine tool centre point, TCP, which in this case it is arbitrarily chosen to be the centre of the platform moved by the linear delta. The three coordinates of this point are sufficient to describe the platform in the space since it can only translate. From now on to better understand the vectorial equations used to arrive at the mathematical solution of the problem the reader can refer to the notation given in table 2.1 which refers to fig.2.6.

Defined the TCP position are perfectly known the vectors $\underline{p}$, $\underline{b}_i$ and $\underline{s}_i$, which express respectively the TCP position, the position of the universal joints on the platform and of the sliders initial position. From these vectors is possible to obtain the vector $\underline{d}_i$ which connects the initial position of the $i-$th slider to the $i-$th joint on the platform. At this point the TCP position is compatible with the system if it exists a slider movement q_i such that the link of a fixed length l_i is capable to connect the slider and the platform; this must be true for all the three kinematic chains. all this is expressed by the following equations:

$$\underline{d}_i = \underline{p} + \underline{b}_i - \underline{s}_i \tag{2.1}$$

$$\underline{l}_i = \underline{d}_i - q_i \hat{u}_i \tag{2.2}$$

$$l_i^2 = \underline{l}_i^T \underline{l}_i = (\underline{d}_i - q_i \hat{u}_i)^T (\underline{d}_i - q_i \hat{u}_i) = \underline{d}_i^T \underline{d}_i - 2\underline{d}_i^T \hat{u}_i q_i + q_i^2 \tag{2.3}$$

Symbol	Meaning
O-xyz	Global frame
$\hat{x}$, $\hat{y}$, $\hat{z}$	Unit vectors of the global frame
TCP-xyz	Local frame fixed to the platform
$\hat{x}'$, $\hat{y}'$, $\hat{z}'$	Unit vectors of the local frame
TCP	tool center point
A_i	i-th center of the universal joints
B_i	i-th center of the universal joints on the platform
$\underline{p} = \{x_p, y_p, z_p\}^T$	Coordinates of TCP
$\underline{b}_i$	Vector of the i-th platform joint
$\underline{l}_i = l_i \hat{n}_i$	Vector of the i-th link (module and unit vector)
$\underline{s}_i = \{s_{i,x}, s_{i,y}, 0\}^T$	Position vector of the i-th guide
q_i	Coordinates of the i-th slider
$\hat{u}_i$	Unit vector of the i-th guide
$[J]$	Jacobian matrix

Table 2.1: Symbols used in the resolution of the kinematic problem.

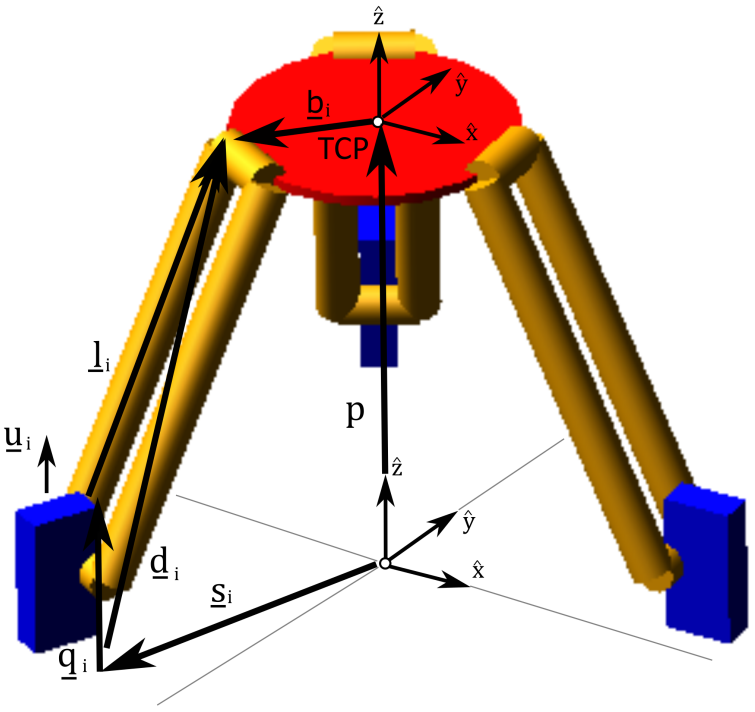

Figure 2.6: Linear delta model

$$q_i = \underline{d}_i^T \hat{u}_i - \sqrt{\underline{d}_i^T (\hat{u}_i \hat{u}_i^T - [I]) \underline{d}_i + l_i^2} \qquad i = 1, 2, 3 \tag{2.4}$$

The eq.2.4 does not have a solution when term under the square root is negative. This case express the impossibility of the link to connect the slider and the platform.

For the forward kinematic the mathematical problem is imposed in an opposite way. Known the sliders position we want to evaluate the platform position. This problem is notoriously more difficult to solve for parallel kinematic robot; in fact while in serial robot for any given set of displacements and rotations is defined a position of its end-effector, the same in sot guaranteed in parallel robots. In any case for the linear delta is possible to reach a closed form solution for the forward kinematic.

The equations are the following:

$$\underline{d}_i = \underline{p} + \underline{b}_i - \underline{s}_i \tag{2.5}$$

$$\underline{d^T}_i \underline{d}_i = \underline{p^T p} + \underline{b^T}_i \underline{b}_i + \underline{s^T}_i \underline{s}_i + 2\underline{p^T} \underline{b}_i + -2\underline{p^T} \underline{s}_i - 2\underline{b^T}_i \underline{s}_i \tag{2.6}$$

$$l_i^2 = \underline{d}_i^T \underline{d}_i - 2\underline{d}_i^T \hat{u}_i q_i + q_i^2 \tag{2.7}$$

By replacing 2.6 in 2.7 we have:

$$\underline{p}^T \underline{p} + \underline{b}_i^T \underline{b}_i + \underline{s}_i^T \underline{s}_i + 2\underline{p}^T \underline{b}_i - 2\underline{p}^T \underline{s}_i - 2\underline{b}_i^T \underline{s}_i - 2q_i p_z + q_i^2 - l_i^2 = 0 \tag{2.8}$$

By considering a linear guides disposition at 120° [1] and taking into account that R_p and s are respectively the modules of $\underline{b}_i$ and $\underline{s}_i$ it is possible to rewrite:

$$\begin{cases} \underline{p}^T \underline{b}_i = p_x R_p \, cos\left(\frac{2(i-1)\pi}{3}\right) + p_y R_p \, sin\left(\frac{2(i-1)\pi}{3}\right) \\ \underline{p}^T \underline{s}_i = p_x s \, cos\left(\frac{2(i-1)\pi}{3}\right) + p_y s \, sin\left(\frac{2(i-1)\pi}{3}\right) \end{cases} \tag{2.9}$$

If we evaluate all the scalar products of eq.2.8 we obtain:

$$p_x^2 + p_y^2 + p_z^2 + 2(R_p - s) cos\left(\frac{2(i-1)\pi}{3}\right) p_x + 2(R_p - s) sin\left(\frac{2(i-1)\pi}{3}\right) p_y - \\ -2q_i p_z + (R_p - s)^2 + q_i^2 - l^2 = 0 \tag{2.10}$$

[1] Here is proposed a solution specifically evaluated for a relative disposition of the linear guides with a relative angle of 120°, which is the final solution adopted for the Efesto machine. During the kinematic optimization of the robot the meaning of this disposition will be more clear to the reader. iN any case the procedure and the equations described do not lose generality and they can be utilised for different liner delta configurations

By multiplying by two this equation with $i = 1$ and subtracting the same equation with $i = 2$ and $i = 3$ we have:

$$6(R_p - s)p_x - 2(2q_1 - q_2 - q_3)p_z + 2q_1^2 - q_2^2 - q_3^2 = 0 \tag{2.11}$$

By subtracting to eq.2.10 with $i = 3$ the same equation with $i = 2$:

$$2\sqrt{3}(R_p - s)p_y - 2(q_2 - q_3)p_z + q_2^2 - q_3^2 = 0 \tag{2.12}$$

These equations defines a linear relationship between p_x and p_z and between p_y and p_z. If the expressions of p_x and p_y as function of p_z are substitute in the eq.2.10 with $i = 5$ we obtain a second degree equation in p_z:

$$k_1 p_z^2 + k_2 p_z + k_3 = 0 \tag{2.13}$$

Where the terms k_1, $k - 2$ and k_3 are:

$$\begin{aligned} k_1 &= \frac{(2q_1 - q_2 - q_3)^2 + 3(q_2 - q_3)^2}{9(R_p - s)^2} + 1 \\ k_2 &= \frac{3(q_2 - q_3)(q_3^2 - q_2^2) - (2q_1 - q_2 - q_3)(2q_1^2 - q_2^2 - q_3^2)}{9(R_p - s)^2} + \frac{2(2q_1 - q_2 - q_3)}{3} - 2q_1 \\ k_3 &= \frac{3(q_2^2 - q_3^2)^2 + (2q_1^2 - q_2^2 - q_3^2)^2}{36(R_p - s)^2} - \frac{(2q_1^2 - q_2^2 - q_3^2)}{3} + (R_b - s)^2 + q_1^2 - l^2 \end{aligned} \tag{2.14}$$

From eq.2.13 we obtain two solutions, which are equivalent to two possibility of mounting of the linear delta. The p_z final value is:

$$p_z = \frac{-k_2 \pm \sqrt{k_2^2 - 4k_1 k_3}}{2k_1} \tag{2.15}$$

The values of p_x and p_y can be finally obtained by eq.2.11 and eq.2.12.

2.4.2 Velocity analysis

For the robot analysis is not only important to know the kinematic equations of the system but the relationships which relate the end-effector velocity to the velocity of the actuators. In this case the following equations will related the end-effector to the sliders, which are moved by the electrical motors of the system, which are the real actuators of the robot. These equations are fundamental in order to evaluate during the designing phase the transmission factors between and end-effector and actuators. High transmission factors would force to chose big size motors.

The relationships between end-effector and sliders velocities can be obtained through the time derivative of the kinematic equations. By deriving eq.2.3 we can obtain the following expression:

$$2\underline{d}_i^T \dot{\underline{d}}_i - 2\underline{d}_i^T \hat{u}_i \dot{q}_i - 2q_i \hat{u}_i^T \dot{d}_i + 2\dot{q}_i q_i = 0 \tag{2.16}$$

That can be rewritten as :

$$(\underline{d}_i - \hat{u}_i q_i)^T (\dot{\underline{d}}_i - \hat{u}_i \dot{q}_i) = 0 \tag{2.17}$$

Where it is possible to recognize the first term as the $i-$th link vector:

$$\underline{l}_i^T (\dot{\underline{d}}_i - \hat{u}_i \dot{q}_i) = 0 \tag{2.18}$$

The term $\dot{\underline{d}}_i$ is equal to $\dot{\underline{p}}$, being $\underline{b}_i$ and $\underline{s}_i$ constant. We get:

$$\underline{l}_i^T (\hat{u}_i \dot{q}_i - \dot{\underline{p}}) = 0 \tag{2.19}$$

and by expressing $\underline{l}_i$ as $l_i \hat{n}_i$ by dividing the equation by the module l_i:

$$\hat{n}_i^T \hat{u}_i \dot{q}_i - \hat{n}_i^T \dot{\underline{p}} = 0 \tag{2.20}$$

If we consider all the three kinematic chains is possible to express these equations in a matrix form:

$$diag(\hat{n}_1^T \hat{u}_1, \ldots, \hat{n}_3^T \hat{u}_3)\dot{\underline{q}} - [J_{gs}]^{-1} \dot{\underline{p}} = \underline{0} \tag{2.21}$$

where:

$$[J_{gs}]^{-1} = \begin{bmatrix} \hat{n}_1^T \\ \hat{n}_2^T \\ \hat{n}_3^T \end{bmatrix} \tag{2.22}$$

and so we can explicit the Jacobian inverse matrix:

$$[J]^{-1} = diag(\hat{n}_1^T \hat{u}_1, \ldots, \hat{n}_3^T \hat{u}_3)^{-1} [J_{gs}]^{-1} \tag{2.23}$$

In an extended form:

$$[J]^{-1} = [J_q]^{-1}[J_{gs}]^{-1} = diag(1/n_{i,z}) \begin{bmatrix} \hat{n}_1^T \\ \hat{n}_2^T \\ \hat{n}_3^T \end{bmatrix} \tag{2.24}$$

The Jacobian matrix express the link between the platform velocity $\mathbf{W} = \{\dot{p_x}, \dot{p_y}, \dot{p_z}\}^T$ and the sliders velocities $\dot{\mathbf{q}} = \{\dot{q}_1, \dot{q}_2, \dot{q}_3\}^T$. For the inverse an forward kinematic the following relationships apply:

$$\begin{aligned} \dot{\mathbf{q}} &= [J]^{-1}\mathbf{W} \\ \mathbf{W} &= [J]\dot{\mathbf{q}} \end{aligned} \tag{2.25}$$

2.5 Kinematic optimization

To define the geometrical parameters of the linear delta it is decided to proceed through a kinematic optimization of the parameters itself. We start by defining the linear delta workspace that must take into account the future introduction of the agile eye: the geometrical parameters are optimized in two consecutive phases, one dimensionless and one dimensional, through the use of a mono-objective genetic algorithm in order to cover the linear delta workspace. We point out how the kinematic synthesis is related to the dynamic study but for the fluency of the work the two designing phases are presented separately.

2.5.1 Workspace

For workspace is intended the volume inside the robot is able to work, or more precisely the volume inside which the robot can position its end-effector with the required pose. In the Efesto project the final workspace required is:

- printing volume 100x100x100[mm]
- rotations $\pm 45°$, yaw and pitch

The hybrid solution proposed allows to develop only the linear delta in a first phase of the project by taking into account the rotations that will be introduced by the agile eye. If we consider the final robot with 5 Dofs and the fact that the printing volume moves together with the robot itself we can notice how any rotations of the agile eye would bring a rotation of the printing part. The movements induced by the agile eye must be compensate by the linear delta in order to position every ideal points of the cubic printing volume under the extruder nozzle. In fig.2.7 shows how an α rotation of the printing platform around the robot TCP, considered as the centre of any possible rotations, brings a displacement of a generic A point of the ideal printing volume over the platform itself. In order to continue to extrude material on the point A the linear delta must compensate the displacements due to the agile eye rotations. If the final machine would have only three translational Dofs the linear delta would need a workspace equal to the printing volume. By considering the agile eye rotations we can evaluate the necessary linear delta workspace in order to guarantee a cubic printing volume of side 100[mm] and with the possibility to reach in each point a $\pm 45°$ of rotations, pitch and yaw. After this evaluation will be possible to optimize the linear delta parameters on the workspace evaluated.

To evaluate the linear delta workspace a discrete set of points of the printing volume is used and at each point different values of rotations α and β are assigned. It is considered the points on the external surface

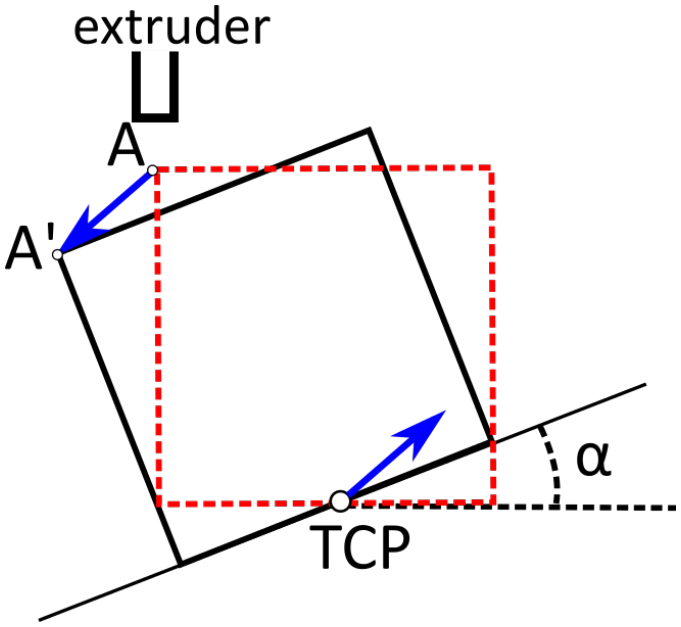

Figure 2.7: Compensation of the translations effect of the rotations by the agile eye

Table 2.2: Equivalent workspaces

	$x[mm]$	$y[mm]$	$z[mm]$
30°	186.6	198.4	169.1
45°	210.8	227.2	182.1
60°	223.2	243.6	187.4
90°	223.6	245	187.4

of the cube, its vertices and the middle points of each cube side. Each point of the printing volume is positioned under the extruder nozzle with a specific set of angles α and β, and the position of the linear delta TCP is evaluated. At the end of the process, after testing each points, are taken the maximum displacements along the three direction x, y and z. This displacements are the displacements that the linear delta must effectuate in order to compensate the agile eye rotations. In tab.2.2 are listed these displacements with different values of rotations, taken equal for α and β. From the table it is possible to notice how the volumes obtained are not cubes but parallelepipeds, each value indicates the length of the side. Even though the design requirements are of $\pm 45°$ it has been studied the possibility to reach until $\pm 90°$.

Given the kinematic of the linear delta, whose translation along the z axis can be easily extended to any length by correctly sizing the linear guides

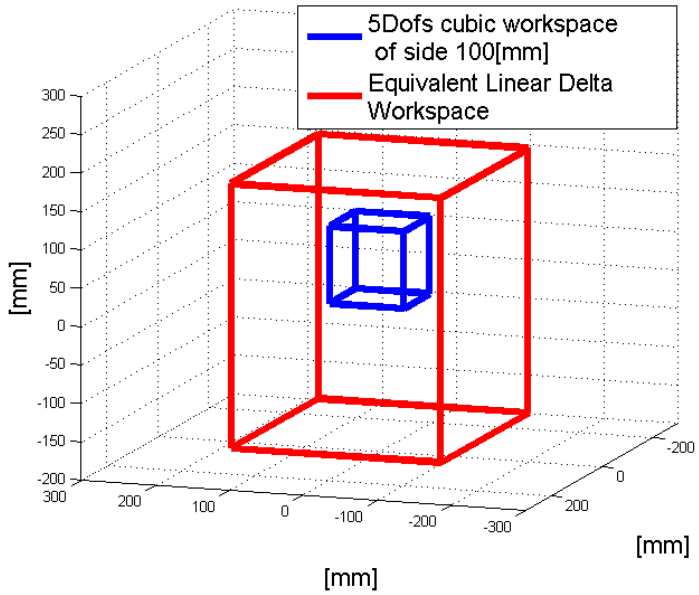

Figure 2.8: New workspace

where the sliders moves, the problem to cover a three dimensional workspace for a linear delta can be translated in a planar problem in the $x-y$ plane. Differently stated, if the linear delta is able to cover a plane figure in the $x-y$ plane, its final workspace will be the projection of this figure along the z axis and this is why in our kinematic study we will take care only of the $x-y$ dimensions. From tab.2.2 we see how the minimum area to cover by the linear delta in the plane $x-y$ is $210.8x227.2[mm]$. Starting from these values and considering that the Efesto machine will not be equipped by the agile eye immediately, and so the linear delta workspace will be the Efesto machine workspace we decide to optimize a the linear delta on:

- square workspace of side 230[mm]

In fig.2.8 is possible to see the transformation of the 5 Dofs cubic workspace in an equivalent 3 Dofs linear delta workspace.

2.5.2 Linear delta optimization

Parameters choice

The linear delta optimization is meant as its geometrical parameters evaluation in order to cover the desired workspace, which in this case in a square of side $230[mm]$. First of all we must define which are the geometrical parameters to optimize; these are the parameters which defines the linear delta

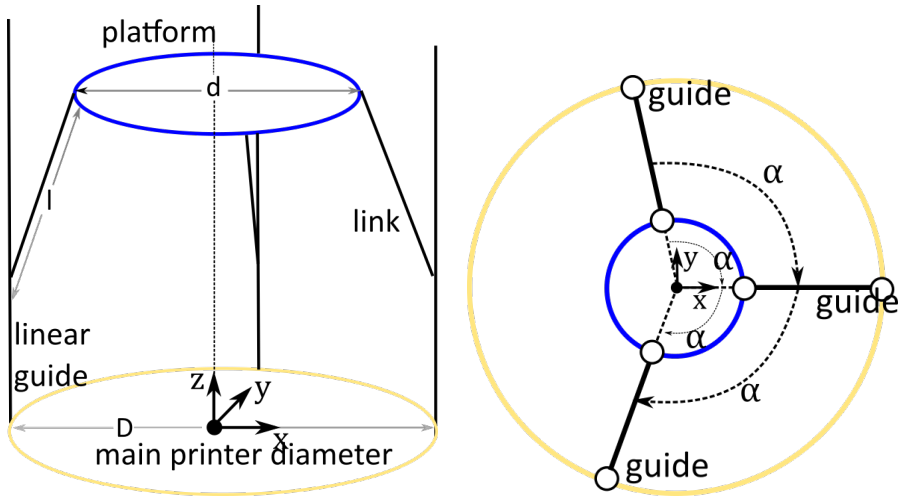

(a) Linear delta **(b)** Angle α

Figure 2.9: Linear delta geometrical parameters

structure and mobility. It has been chosen 4 parameters retained fundamentals:

- l link length
- d platform diameter
- D printer diameter
- α relative positions among the linear guides

To better understand the meaning of such parameters it is possible to refer to fig.2.9. The parameters l and d defines the size of the main bodies of the robot whereas the diameter D defines the general size of the printer since the linear guides are positioned on it. Once a linear guide is positioned on this circle the other two are placed in a $\pm\alpha$ position on the same circle. It is pointed out how the choice of these parameters has been arbitrary but based on the idea to respect the geometrical symmetry of the machine; links with different lengths or linear guides positioned to a different distance from the machine centre would lead to change the initial symmetry of the machine.

Genetic algorithm

The genetic algorithm is method utilised for the optimization study for the 4 linear delta parameters. The genetic algorithm will be used in order to minimize a cost function and evaluate the best value for the 4 parameters. The genetic algorithms are generally divided in multi-objective or mono-objective; in this study it is used a mono-objective genetic algorithm through

the use of the MatLab function *ga*. Two types of studies will be performed; one dimensionless and one dimensional. The first one to understand how the parameters chosen influence the machine workspace and how the parameters are influenced by the constraints of the optimization study, the second to obtain the real values of the geometrical parameters. In the first study the parameters are made dimensionless by dividing each parameter for the diameter D and the genetic algorithm is used to maximize the linear delta workspace. In the second study the genetic algorithm try to cover the square are required for the linear delta by optimizing the geometrical parameters inside specific ranges.

A genetic algorithm mono-objective as the one of the *ga* function proceeds in the following way:

1. A first population is created by the genetic algorithm. A population is a set of individual and each individuals are nothing else than a specific set of values of the parameters to optimize, in this case an individual is the four values of l,d, D and α. The values are called genes.

2. For each individual is evaluated the cost function which express the goal to reach. In this way is possible to list a ranking of the population.

3. According to the ranking a limited number of individuals with the best rank, the elitè, are used unchanged in the generation of the next populations;

4. The new populations are created thanks to the elitè and the creation of new individuals. This can be done by casual combination of the genes of the previous generation, *crossover*, or by changing the values of the genes, *mutation*. The fraction of individuals deriving from elitè, crossover or mutation can be imposed to the algorithm;

5. The algorithm keeps running creating new populations until a stop condition is reached. There are different kind of stop conditions and they can be customized by the user. A typical stop condition is to set a threshold for the cost function, or a stall condition based on the best value obtained for the cost function. The aim of the algorithm is to find the individual which minimize or maximize, according to the necessities, the cost function.

In the study effectuated are created populations constitute by 300 individuals and it is imposed a stop conditions based on a stall condition of 50 consecutive generations. The genetic algorithm is set in order to minimize the cost function.

Cost function

The genetic algorithm is based on the evaluation of a cost function. Both in the dimensionless optimization than in the dimensional one this function corresponds to the evaluation of an area not covered by the linear delta, so in both cases minimize the cost function means to maximize the linear delta workspace. In the dimensionless study this area correspond to the difference between the area defined by the circle of diameter D and the linear delta workspace. The linear delta could reach some positions outside the circle but these positions are of no interest, by considering that the nozzle of the printer is fixed in the centre of machine which is the centre of the linear delta too, and so such positions are excluded from the study.

$$f_{ad} = \frac{\pi D^2}{4} - W_{ld} \tag{2.26}$$

The cost function is f_{ad} whereas W_{ld} is the workspace of the linear delta. In the dimensional study the cost function is given by the difference between the desired workspace and the intersection between the actual linear delta workspace and the desired workspace. It could happen that the linear delta has a workspace sufficiently big but it is not able to cover the desired square shape centred in the machine.

$$f_d = W_d - (W_d \cap W_{ld}) \tag{2.27}$$

The dimensional cost function is f_d and W_d is the objective workspace. The function 2.10a guarantees that the minimum of the function itself is zero, value too which the genetic algorithm will converge. Same consideration can be done for the function 2.10b where the intersection between the two workspace has as maximum value W_d and so the function minimum is the null value.

Regardless of the study effectuated, dimensionless or not, the evaluation of the linear delta workspace is done according to the following steps:

1. Defined the 4 robot parameters the linear delta platform is positioned in its central position; position where the centre of the platform is equal the the machine centre defined by the circle of diameter D, fig.2.9a;

2. The robot is moved along the x axis by a discrete displacement of the TCP and every time is checked if the position reached respects the inverse kinematic equations and the constraints of the system, fig.2.10a;

3. when the conditions are not respected the workspace border has been reached;

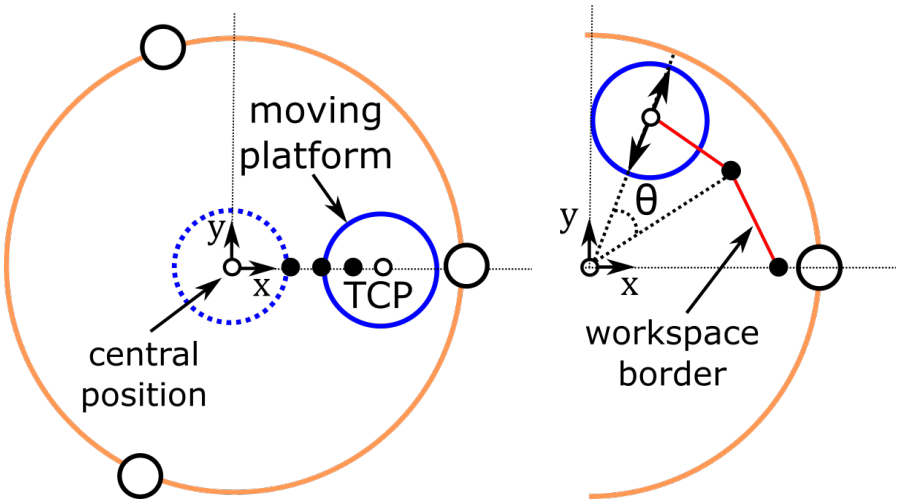

(a) Linear displacement **(b)** Rotation

Figure 2.10: Evaluation of the linear delta workspace

4. the platform is moved counter-clockwise according to a rotation angle θ and along the new radial direction is newly searched the workspace border, fig.2.10b;

5. Once a complete rotation of 360° around the machine central axis is effectuated the linear delta workspace in the plane $x - y$ is completely defined.

Constraints

In the evaluation of the cost function and so in the evaluation of the linear delta workspace we introduce some constraints which takes into account the feasibility and the quality of the solution found in terms of robot performances. These constraints are:

Kinematic The solution must respect the inverse kinematic of eq.2.4.

Universal joints The solution must be compatible with physical limits of the universal joints which have limited rotations.

Force and velocity transmission factors The linear delta must have a kinematic structure which allows to use the actuators of the lowest size as not generate excessive stresses on the mechanical components.

Singularities The robot must not fall in singularities positions.

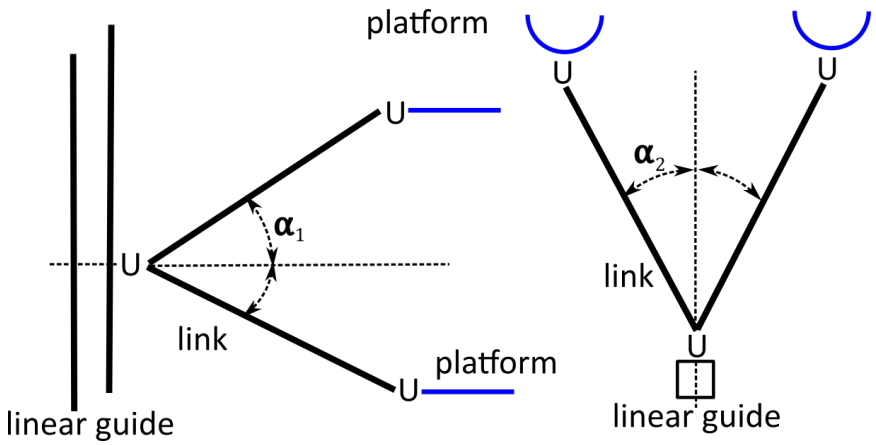

Figure 2.11: Rotations of the universal joints

Being the condition on the kinematic pretty obvious here we focus on the other three constraints.

The linear delta has three kinematic chains of type PUU, Prismatic-Universal-Universal. The universal joints aloes two relative rotations but these rotations are not unlimited and they depend on the mechanical design of the component. In fig.2.11 are schematically represented the relative rotations α_1 and α_2. The rotation α_1 indicates the angle between the link and its projection on the $x-y$ plane, instead the rotation α_2 indicates the angle between the link and its projection on plane orthogonal to the $x-y$ plane and passing through the centre of the linear guide and of the machine. Since the use of a parallelogram structure for the linear delta links the rotations of the universal joint on the slider side are the same than the rotations of the universal joint on the platform side. If one of the two joints goes over the limits the same happens for the other. The limits given by these rotations are fundamental fro the mobility of the robot. Bigger are the admissible rotations bigger will be the linear delta workspace. The universal joint has basically no limits on the rotation α_1 but a value of 90° is introduced to avoid collision between the platform and the linear guide. For α_2 is used a value of 60° for the dimensionless optimization and it is varied during the dimensional optimization. These values are taken from the mechanical design of the universal joint which is faced in a later part of this chapter. During the evaluation of the cost function every position which exceeds the joint limits is considered not feasible and excluded.

In the synthesis of a robot we want to verify the performances reached. There are different parameters used in the literature to measure different aspects of the robot performances, some of that already used on a linear delta [14]. Some of these parameters are:

- Dexterity index $\sqrt{det(J^{-T}J^{-1})}$, which indicates the ability of the end-

effector to move in different directions in a specific robot pose;

- Conditioning number $\frac{\sigma_{max}(J^{-1})}{\sigma_{min}(J^{-1})}$, which can assume values between 1 and ∞ and it is an indicator of kinematic isotropy of the robot
- Stiffness matrix $(JJ^T)^{-1}$, the eigenvalues of this matrix are an index of the system stiffness under the assumption that all the bodies of the robot are rigid

Here it is possible to notice how all these indexes depends on the robot Jacobian which is fundamental to define the robot performances. In order to measure the linear delta performances it has been decided to use to other indexes not listed above, based on the Jacobian matrix and which takes into account two important factors for the design of the machine. These two parameters are the force and velocity transmission factors, τ_f and τ_v.

$$\tau_f = ||J^T||_\infty \qquad \tau_v = ||J^{-1}||_\infty \tag{2.28}$$

These two parameters are evaluated through the infinity norm of the transpose of the inverse Jacobian matrix. These expressions derives from considering a unitary force and velocity applied on the TCP; the consequent forces and velocities on the actuators can be evaluated.By imposing a limit on τ_f and τ_v is possible to constrain the linear delta to respect them. If in a linear delta position these limits are exceeded the position is considered not feasible. It is pointed out how in the eq.2.28 the τ are scalar values, they are the transmission factor for one of the three actuators. If sufficient that only one actuator exceed the limits to consider the position not feasible. The choice of the infinite norm has been arbitrary; it has been choice because it takes into account the worst case when all the forces, or velocities, on the TCP have a unitary value. This would not be possible with the euclidean norm for instance. In fig.2.12 is shown an example of relationship between the velocity and force applied on the platform and the response of the actuators. With small transmission factors is possible to have actuators with a small size.

The last constraint is the one on the robot singularities. A robot is defined in a singular position when it is in a pose where it verifies the nullify of the Jacobian determinant of its inverse.

$$det([J]) = 0 \Leftrightarrow det([J^{-1}]) = \infty \tag{2.29}$$

$$det([J]^{-1}) = 0 \Leftrightarrow det([J]) = \infty \tag{2.30}$$

This means that the robot is in a configuration where or it has lose the control of the mechanical system or it is not able to move anymore. In the

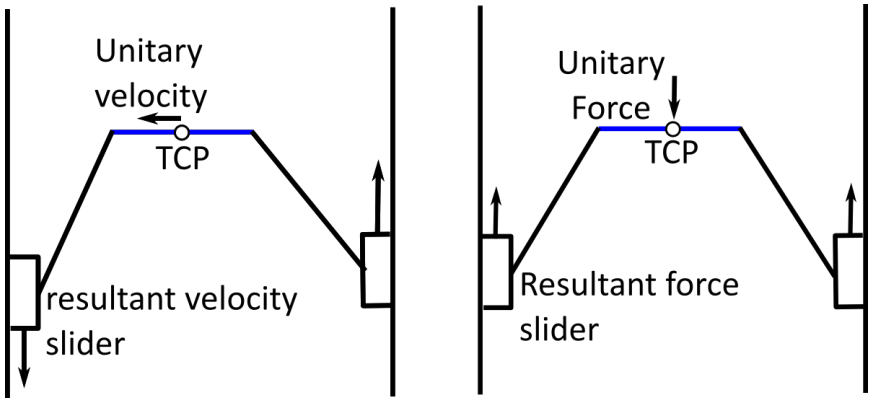

Figure 2.12: Force and velocity transmission

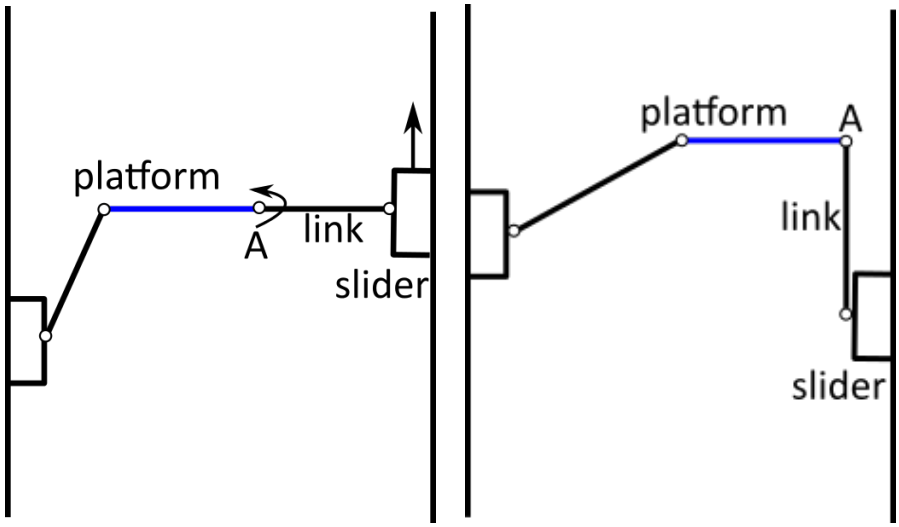

Figure 2.13: Singularities of the linear delta

case of the linear delta it easy to find at least two singular configurations as shown in fig.2.13. In fig.2.13a is shown a configuration where a link is completely horizontal. Here for any displacements of the slider the platform remains still, lose of control. This due to the particular kinematic configuration reached among the bodies platform-link-slider and their respective kinematic constraints. In fig.2.13b we have another critical situation where the robot can remain blocked. Here we have a perfectly vertical link and its respective slider can not move in any direction. In the study of the robot workspace we want avoid this positions. Since the singular configurations are defined by the Jacobian matrix we can use the transmission factors to find this positions. Close to the singular positions the transmission factors increase their values or they goes to zero. That is why in these configurations the robot along a specific direction is able to transmit infinite forces and no velocity or vice versa. By taking into account the two transmission factors at the same time it is possible to avoid the singular configurations of the system.

It is pointed out how the use of the transmission factors as constraints on the system and not as goals of the genetic algorithm has allowed the possibility to use a mono-objective function instead of a multi-objective one.

Dimensionless optimization

In the dimensionless optimization we want to understand how the robot geometrical parameters chosen have an influence on the robot workspace with different values of the constraints. Since the final goal is to cover a specific area, square of side 230[mm], the genetic algorithm is reasonably expected to find an infinite set of solutions capable to achieve that goal. With a pure dimensional optimization would be impossible to differentiate between two different solutions of the genetic algorithm. Through a dimensionless optimization we search for an optimum ratio among the 4 parameters and use it to guide the solution of the genetic algorithm in the search of the final sizes of the 4 parameters.

In order to effectuate the dimensionless study each parameters is divided by D, so the diameter of the structure will have always a unitary dimension, instead l and d will be expressed as function of D. The angle α, which is dimensionless by definition, has been leaved as it is. In tab.2.3 we can see the ranges inside which the genetic algorithm can vary the parameters value.

The choice of such ranges is dictate by some pragmatical considerations. The internal platform of the linear delta can assume a maximum value of 1, this means to reach a diameter equal to the size of the entire printer. Such a ratio in not feasible since it would impossible for the linear delta to move the platform, and this is because 1 is set as maximum value acceptable. The inferior limit has been chose by considering that the platform must

Table 2.3: Parameter range of the dimensionless study

Parameter	Range
d	$0.2 - 1$
l	$0.4 - 2$
α	$10° - 170°$

contain the general design the agile eye, furthermore it must be considered that the minimum size of the platform depends on the minimum size of the links. The size of the links and platform must be at least sufficient to mount the robot in the central position of the printer. The maximum limit for the links has been set very high, twice the printer diameter given to the genetic algorithm the possibility to explore different solutions. The linear guides position defined by the α angle has been left free to vary in almost the entire circle with a little margin which avoids the physical interference among the linear guides.

The dimensionless study is carried out through the MatLab function ga. The function takes the upper bounds and lower bounds defined for the parameters ranges and try to minimize the cost function of the eq.2.26. The result produced by the genetic algorithm is highly influenced by the constraints used; here it is executed a campaign of trials by varying the three constraints α_2, τ_f e τ_v which represents the mechanical limits of the system and the robot performances. Off course the respect of the kinematic equations will be always considered. During the trials α_2 has been varied between 30° to 75° with a discrete step of 15°, whereas τ_f and τ_v assume the values 3 or 5.

In tab.2.4 are shown the results obtained by the dimensionless optimization. In the first part are shown the results and the average os some tests effectuated with different values of α_2 and with $\tau_{f,max}$ and $\tau_{v,max}$ equals to 3. In the bottom part of table with can see the results with the transmission factors equals to 5. The index cp indicates the percentage of area covered by the linear delta workspace in respect of the area defined by the circle of diameter D. Higher the cp higher is the linear delta workspace in respect of its dimensions. Since the linear delta workspace is evaluated from the TCP displacements, par.2.5.2, and the universal joints have limited rotations, par.2.5.2, the cp can never reach the 100% value. From the table data it is possible to notice how the diameter d converges to the ratio 0.2. With a smaller platform the TCP has a bigger mobility by allowing the linear delta to cover a bigger space. The values of l have a small variation and they are comprised between the values 0.9 and 1.1. The links length must be of the same size of D. No converge is achieved for the parameter *alpha* where we have very different values during the tests, from 120° to 60°. It is possible to notice how there is a tendency of the algorithm to set α equal to about 60°

Table 2.4: results of the dimensionless optimization

	1	2	3	Average	cp	
l	0.893	0.894	0.9	0.896		$\tau_{f,max} = \tau_{v,max} = 3$
d	0.2	0.2	0.2	0.2	25.3%	$\alpha_2 = 30°$
α	120.14	120.18	119.91	120.08		
l	0.928	0.925	0.957	0.937		$\tau_{f,max} = \tau_{v,max} = 3$
d	0.2	0.2	0.2	0.2	39.3%	$\alpha_2 = 45°$
α	88.24	90.13	90.57	89.65		
l	1.013	1.024	1.007	1.015		$\tau_{f,max} = \tau_{v,max} = 3$
d	0.2	0.2	0.204	0.2	54.8%	$\alpha_2 = 60°$
α	95.34	97.02	95.96	96.11		
l	1.08	1.02	1.02	1.04		$\tau_{f,max} = \tau_{v,max} = 3$
d	0.2	0.2	0.2	0.2	69.5%	$\alpha_2 = 75°$
α	108.93	95.59	100.0	101.51		
α_2	30°	45°	60°	75°		
l	0.906	0.984	0.967	0.991		
d	0.2	0.2	0.2	0.2		
α	119.37	63.8	63.45	64.34		$\tau_{f,max} = \tau_{v,max} = 5$
cp	25.2%	42.9%	63.6%	74.5%		

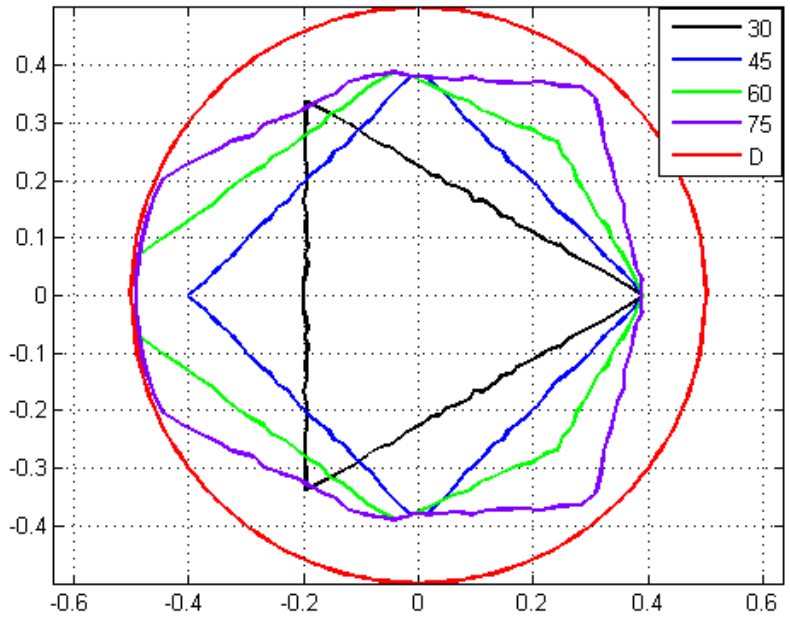

(a) Workspaces with different values of α_2, $\tau_{f,max} = \tau_{v,max} = 3$

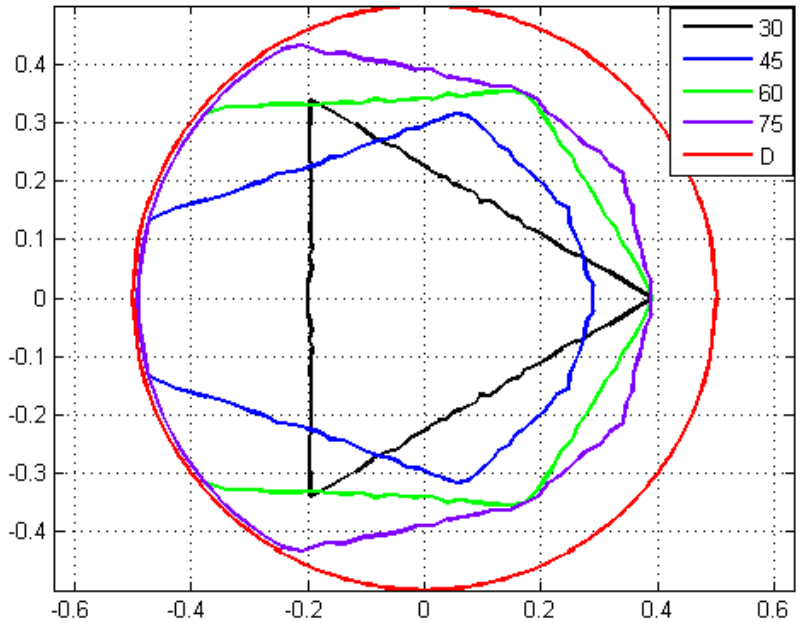

(b) Workspaces with different values of α_2, $\tau_{f,max} = \tau_{v,max} = 5$

Figure 2.14: Workspaces with different values of α_2 and τ

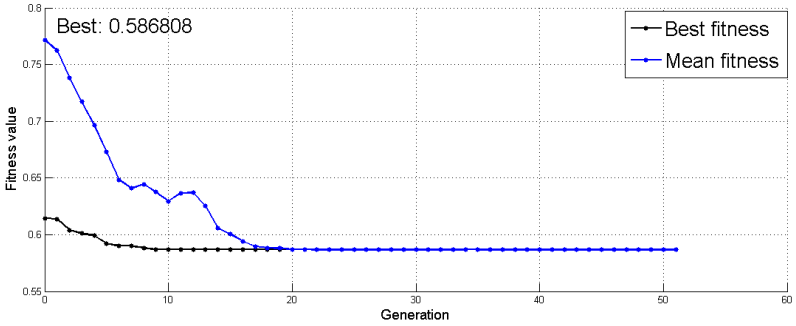

(a) Dimensionless optimization $\alpha_2 = 30$

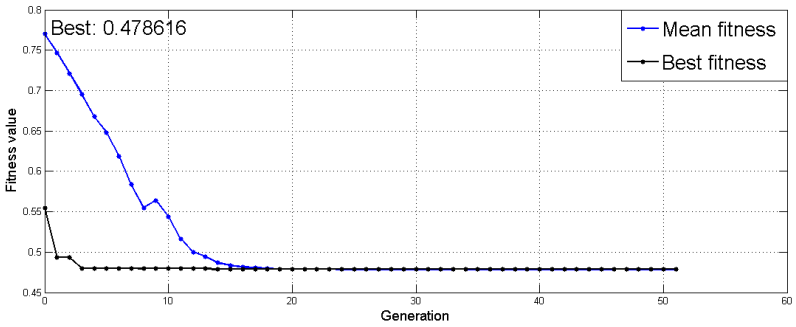

(b) Dimensionless optimization $\alpha_2 = 45$

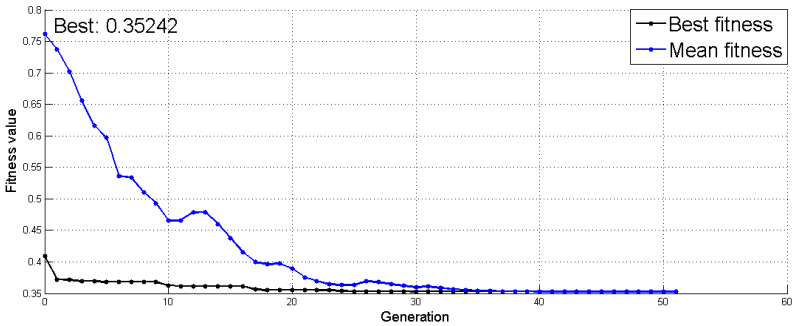

(c) Dimensionless optimization $\alpha_2 = 60$

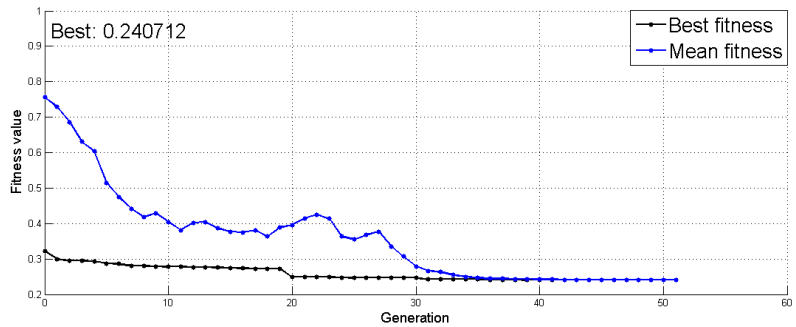

(d) Dimensionless optimization $\alpha_2 = 75$

Figure 2.15: Convergence of the genetic algorithm with different α_2 and $\tau_{f,max} = \tau_{v,max} = 3$ values

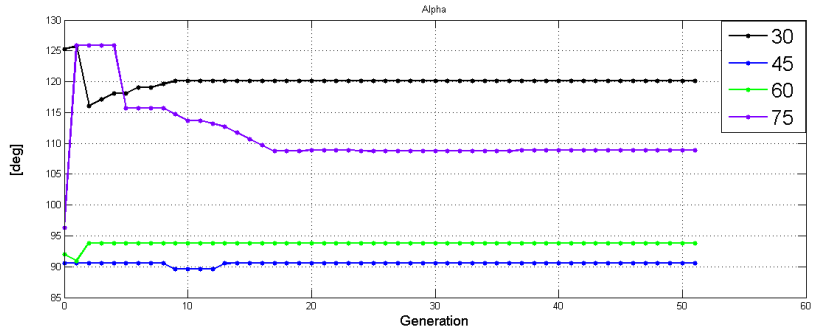

(a) Convergence α

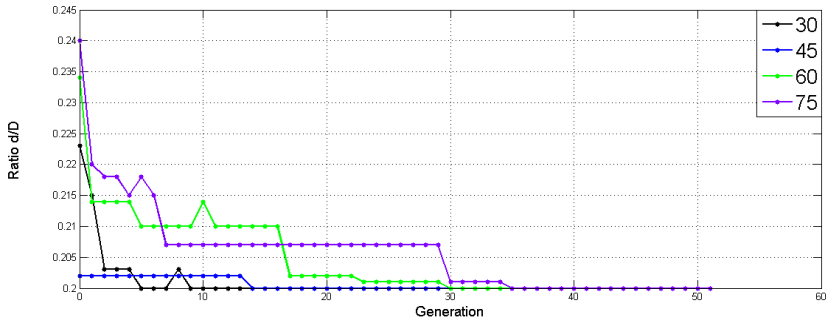

(b) Convergence d

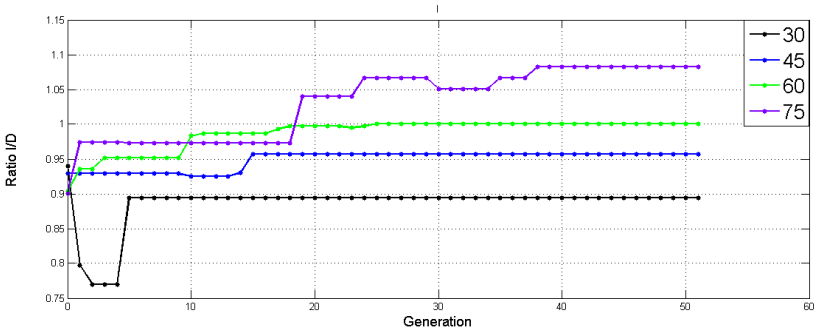

(c) Convergence l

Figure 2.16: Parameters dimensionless optimization α, d and l with different α_2 values

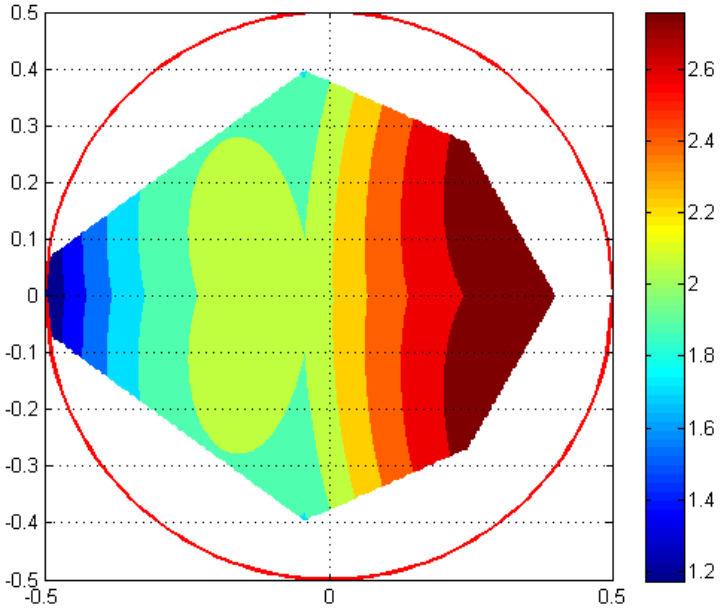

(a) $\tau_{f,max} = 3$, $\alpha = 96.11$

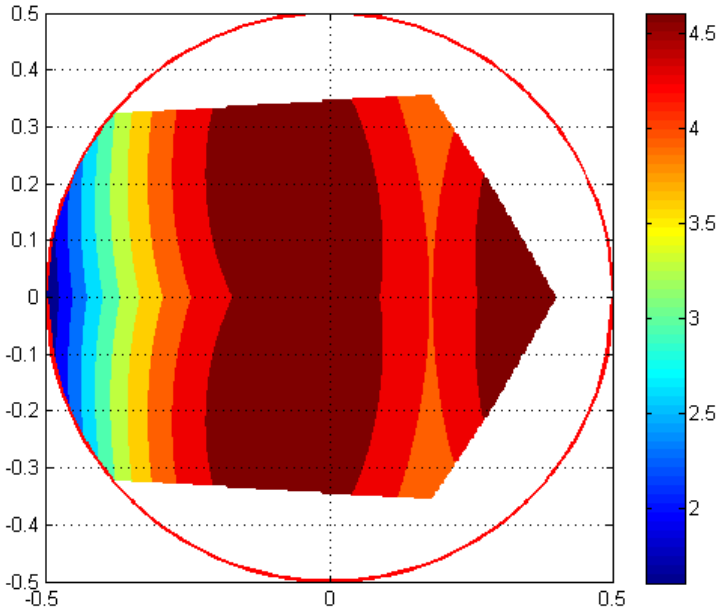

(b) $\tau_{f,max} = 5$, $\alpha = 63.45$

Figure 2.17: Force transmission factor with $\alpha_2 = 60°$

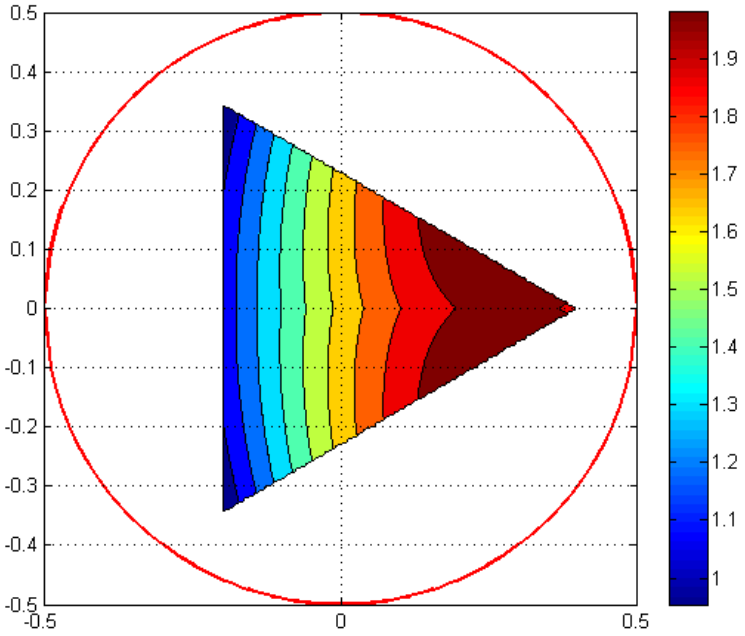

(a) Force transmission factor

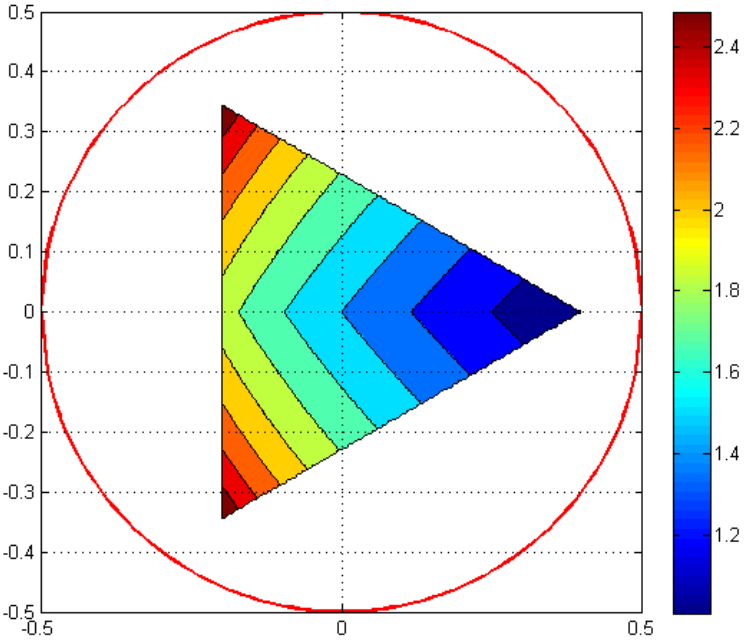

(b) Velocity transmission factor

Figure 2.18: Force and velocity transmission factor with $\alpha_2 = 30$, $\tau_{f,max} = \tau_{v,max} = 3$

when the transmission factors are higher. Closer linear guides give to the machine a better mobility but they worst the transmission factors, so this solution is feasible only when the limit on τ_f and τ_v is higher. In fig.2.17 it is possible to see for one the three kinematic chains how the force transmission factor change when its limit is increased. In fig.2.14 it is possible to see how the linear delta workspace change with different constraints values. The increase of α_2 and τ leads to an increase in the machine workspace; this is a clear consequence of the major joints mobility and the possibility to bear worse transmission factors. The workspace border is defined by the positions reachable by the linear delta TCP; as imposed the TCP can never cross the circle even if the robot is capable of doing it. The increase in the τ limits increase the workspace in every case except for $\alpha_2 = 30°$ situation. In this case the limit imposed on the joints rotations result to be predominant.

The genetic algorithm converges to the solutions found as shown in fig.2.15. In the 4 figure is possible to see 4 different tests, one for each α_2 values. In black is represented the convergence of the cost function which refers to the best individual of each generation; the best individual of the final generation corresponds to the solution which minimizes the cost function. In blue is represented the mean value of the entire population for each generation. In fig.2.16 it is possible to see the convergence of each parameters α, l and d with different α_2 values.

In the end in fig.2.18 are shown the transmission factors, force and velocity, for the case $\alpha_2 = 30°$ and $tau_{f,max} = \tau_{v,max} = 3$. It is possible to notice how in this case the transmission factors are both under the limit of 3, so the robot workspace must be limited by the joints rotations. It interesting to notice the kinetostatic duality, where the force transmission factor is high the velocity transmission factor is low and vice versa. The pictures represent the transmission factors for one of the three kinematic chains.

Dimensional optimization

In the dimensional optimization we want to cover the square area required for the robot and so specify the actual dimensions of the robot geometrical parameters to utilise in the linear delta design. As described in the par.2.5.1 of this chapter in order to obtain the desired printing volume the linear delta must cover a square area of side 230[mm]. This evaluation has been carried out by considering the agile eye rotations. We can see how by simply extended the square area of 20[mm],tab.2.7, it would be possible in the future to have by the agile eye any rotations until 90°. Even though it was not in the design requirements it has been decided to extend the area to cover by the linear delta by reaching a square area of side 250[mm]. After that this area has been increased to reach a final square area of side 300[mm]. This further increase in the workspace has been done for two reasons:

- safety margin for the machine
- help the genetic algorithm to find an optimum solution

An identical match between the desired workspace and the linear delta workspace would introduce a risk for the safety of the machine. At the minimum positioning error the machine would face some damages more or less severe; giving to the linear delta a workspace bigger than the one desired a safety margin is created for some errors that could happen during the use of the machine. The second reason depends on the multitude of solutions that the genetic algorithm could find during the minimization of the cost function. The dimensional optimization is based on the minimization of the cost function of the eq.2.27; since this equation express the covering of an area different solutions can be found for the geometrical parameters of the robot and the genetic algorithm could not be able to converge to a unique solution. If we increase the total area to cover we diminish the number of feasible solutions.

The dimensional optimization is carried out by respecting the ranges expressed in tab.2.5. During this phase the values of α_2, $\tau_{f,max}$ and $\tau_{v,max}$ are fixed to 60° for the first and 3 for the transmission factors. The value of D has been set with a maximum value of 1000[mm] in order to obtain a compact machine; the minimum value has been evaluated by considering how in the dimensionless optimization for the values of α_2 and tau_{max} here chosen the index cp was about 55%. In order to cover a square area of side 300[mm] the minimum value for the diameter D would be:

$$D = \sqrt{\frac{4A_c}{cp\pi}} = 457[mm] \tag{2.31}$$

where A_c is the area to cover. Since this is the minimum theoretical value which do not take into account the size of the platform and the space of the area to cover the minimum value for D is set to 600[mm]. Since in the dimensionless optimization the ratio between the link length and D was about 1 a similar range is set for the parameter l. From the table is possible to see how the parameter d is constant. According to the ratio of 0.2 derived from the dimensionless optimization the parameter d should have a maximum value of 200[mm] considering the maximum value of D. From the mechanical design of the linear delta platform, which must hold the agile eye, the size of the same can not be smaller than 400[mm]. Here is decided to fix the parameter d to minimum value acceptable for sizing reasons. The value of α has been left to vary between 90° and 170°.

The results of the dimensional study can be seen in tab.2.6. How it is possible to notice we do not have obtained a unique solution but several ones. This is due to the fact that inside the ranges of the geometrical parameters there are more than one combination capable to satisfy our requests.

Table 2.5: Parameters range of the dimensional optimization

	range	constraints
d	400[mm]	$\alpha_2 = 60°$
l	400-1000[mm]	
D	600-1000[mm]	$\tau_{f,max} = \tau_{v,max} = 3$
α	90°-170°	
Area to cover	300x300$[mm]$	

Table 2.6: results of the dimensional study

Parameter	set 1	set 2	set 3
l[mm]	660	610	580
D[mm]	950	920	890
α	93°	124°	117°

From fig.2.19, which represents one of the dimensional study we can see how the minimum of the cost function is zero; that means the the linear delta workspace is capable to cover entirely the desired area. By having multiple solutions we need some criteria in order to choice the parameters values. By observing fig.2.20 we can see how with a bigger value of α we obtained lower values for the transmission factors. This is in accordance with the dimensionless study where for higher limits on the τ we have obtained lower values of α. It is so decided to set α equal to 120°. This choice, besides to lower the transmission factors, will allow to better distribute the loads of the system by given to the system itself a 120° symmetry and it will permit to choice actuators of the same size.

After setting the angle α a last testis carried out to evaluate the values

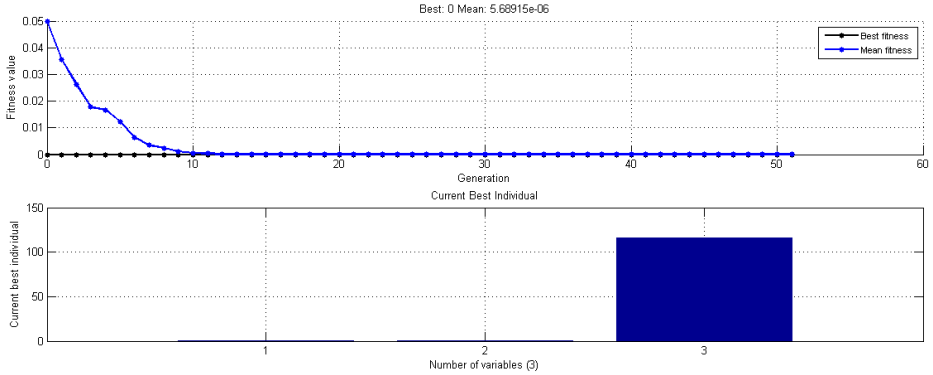

Figure 2.19: Convergence of the genetic algorithm in dimensional optimization

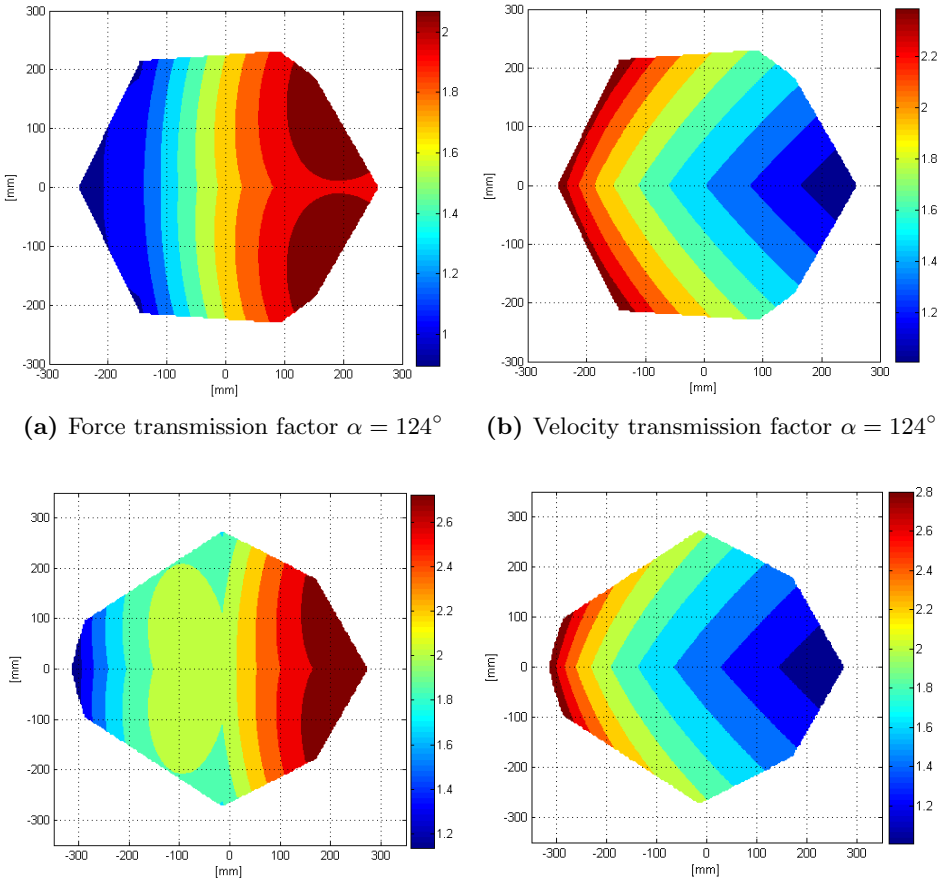

(a) Force transmission factor $\alpha = 124^\circ$ **(b)** Velocity transmission factor $\alpha = 124^\circ$

(c) Force transmission factor $\alpha = 93^\circ$ **(d)** Velocity transmission factor $\alpha = 93^\circ$

Figure 2.20: Force and velocity transmission factors with different α values

of D and l. At the end of the dimensional optimization the values of the geometrical parameters are:

$$d = 400[mm] \qquad D = 913[mm] \qquad l = 598[mm] \qquad \alpha = 120^\circ \qquad (2.32)$$

Since the kinematic optimization is not separated from the mechanical design of the robot, as we have already seen by some previous considerations, before to obtain the final workspace of the linear delta we have to correct one of the value herein considered. During the mechanical design phase it was not possible to reach a value of 60° for the angle α_2 of the universal joints but the actual value is a little more than 45°. With this difference the robot was not able to cover the square area of side 300[mm] but it was still able to cover the area of side 250[mm] which makes the linear delta capable to compensate any displacements of the printed part due the agile eye rotations. Of the final robot the cp index is very low, $cp = 18.2\%$, a value below of the 39.3% obtained in the dimensionless study. The mechanical design has strongly influenced the final result, particularly the not respect of the ratio between the diameter of the platform d and the main size of the printer D. Anyhow the constraints on the transmission factors, which will be fundamental in the dynamic study, have been respected. In fig.2.21 is visible the final linear delta workspace. The workspace covers a square area of side 250[mm]. In fig.2.22 are visible the final transmission factors of the robot, both under the limits imposed.

2.6 Dynamic analysis

Following the kinematic synthesis it has been carried out a dynamic analysis. This phase is fundamental to correctly size the motoreducers of the system and to evaluate the main forces and torques on the passive joints of the system which are necessary for the sizing of the mechanical components. During this phase has been utilised the multibody software Adams.

2.6.1 Model

To study the dynamics of the robot is developed a linear delta model. In fig.2.23 is possible to observe the model in a configuration where the platform is centred in the linear delta workspace. In red colour we have the platform, in orange the links which are formed by a parallelogram structure and the sliders are in blue. In the model is taken under consideration the development of the system with the introduction of the agile eye by adding an additional mass to the platform. In tab.2.7 are listed the bodies of the model with the data of masses and inertias and the type and number of constraint used. The pivots anf the links are the bodies which forms the parallelogram

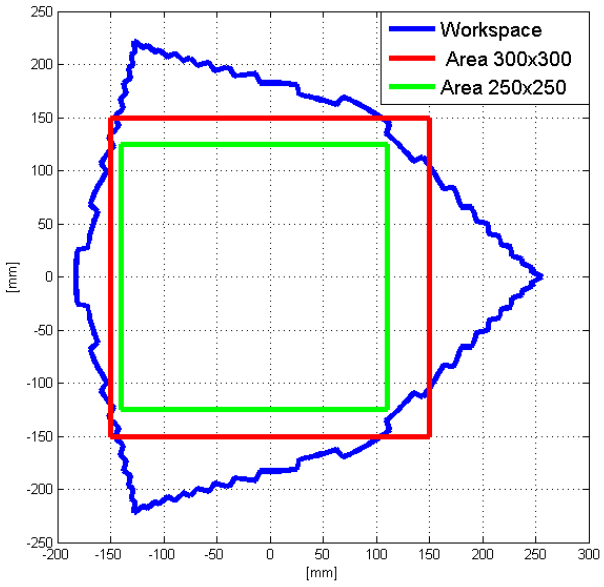

Figure 2.21: Final linear delta workspace

Table 2.7: Adams model data

Body	Mass$[kg]$	$I_z[kgmm^2]$	$I_x = I_y[kgmm^2]$	Number
platform	16	-	-	1
pivot	0.3	19.0	263.0	6
link	0.55	80.0	16002.7	6
slider	3.1	-	-	3
Constraint			Number	
Spherical			6	
Revolute			12	
Translation			3	

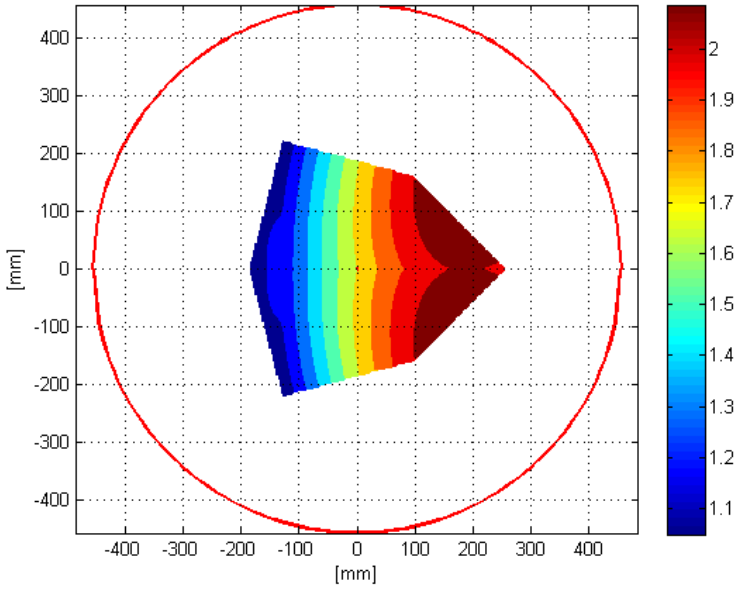

(a) Force transmission factor

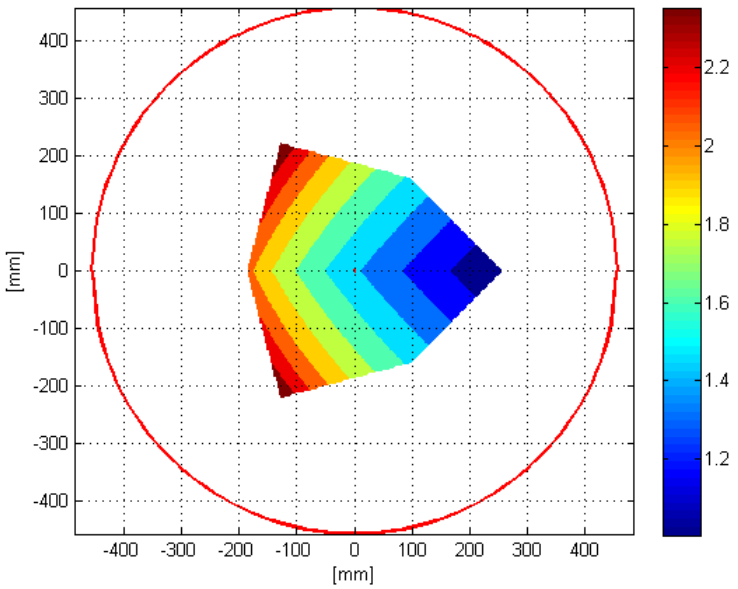

(b) Velocity transmission factor

Figure 2.22: Final values of the linear delta transmission factor

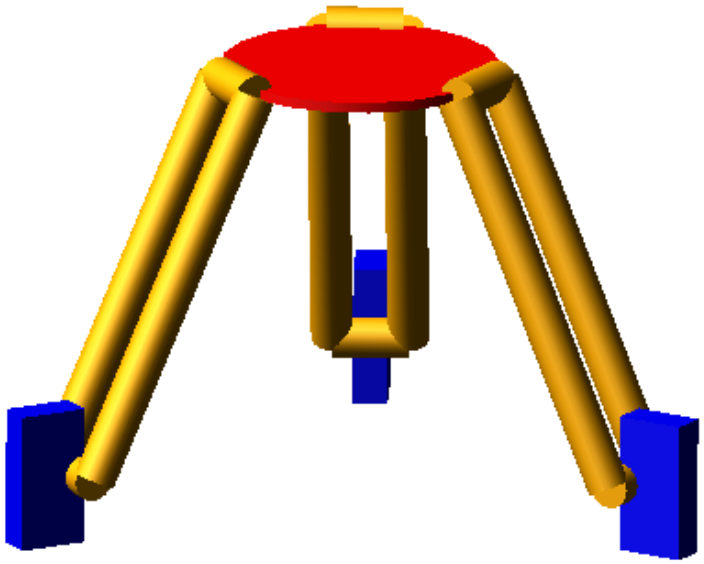

Figure 2.23: Adams model of the linear delta

system. A pivot connects the platform with two links which are connected to another pivot attached to a slider on the other side. This the kinematic chain PUU(Prismatic-Universal-Universal) as it has been used during the kinematic study of the system. The masses and inertias have been acquired from the mechanical design phase; some of the dynamic model bodies are an equivalent body, in term of mass and inertia, respect to the actual number of bodies present in the actual linear delta. The inertias I_z, I_x and I_y are expressed respect to the principal central frame of the body. For the platform and the slider, which can only translate, the inertias value is irrelevant. The total mass of 16[kg] for the platform is comprehensive of:

- agile eye, mechanical structure and actuators
- material of the printing process

The maximum volume of material printable is a cube of 100[mm] side, as expressed in the design requirements. By knowing the density of the material laid down we can suppose an additional mass given by a cube filled by the printed material. By don't be known at this time of the design phase the exact density of the materials that will be printed during the project life, we take a reference data from a study on the extrusion of powder steel with a paraffin binder [15]. In this study is declared a theoretical density of the material of 8$[g/cm^3]$ which after the sintering process reach a density of 5-6$[g/cm^3]$. For the printing phase we consider the theoretical density

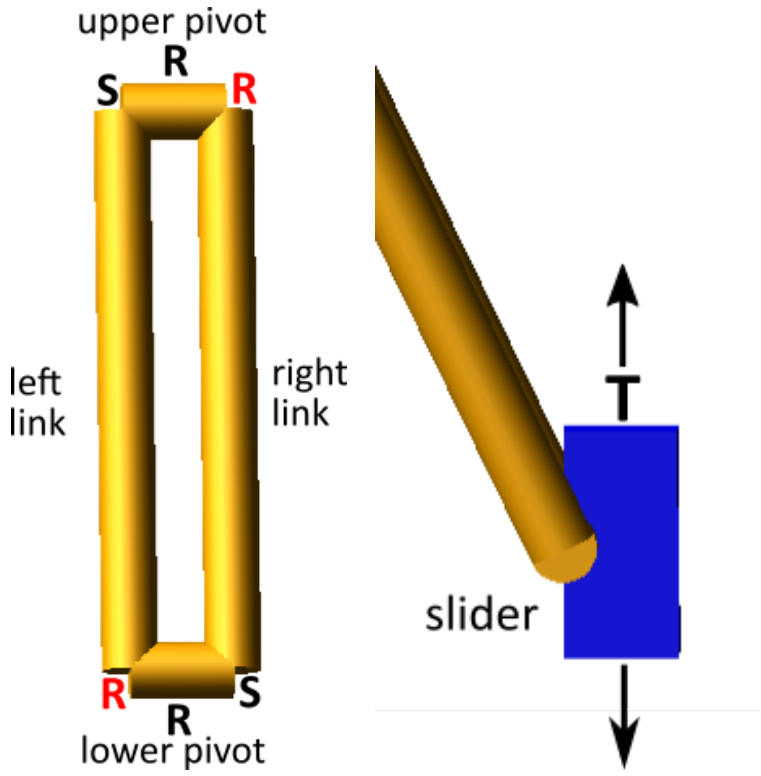

(a) Parallelogram **(b)** Slider

Figure 2.24: Constraints of the model

before the sintering process by obtaining a printed cube with a mass of $8[Kg]$. To this mass we add the weight of the agile eye motoreducers and mechanical structure that we hypothesize as other 8[kg] to obtain the final mass of 16[kg] assigned to the platform.

In fig.2.24 is represented the parallelogram structure with its constraints labelled and the slider which is free to move along the vertical direction; the linear guides which are fixed in the printer are not graphically represented. The use of two spherical joints and two revolute joints in the model allows to recreate the kinematic behaviour of the parallelogram structure. The revolute joint between platform and pivot, and the revolute joint between slider and pivot represent the α_1 angle used as constraint in the kinematic optimization; the relative rotation between pivot and link corresponds to the α_2 angle.

2.6.2 Sizing of the motor reducer

Fundamental part of the dynamic analysis is the sizing of the motoreducers. The three sliders of the linear delta will be actuated along the linear guides by means of these electromechanical systems. The three actuators, since the 120° symmetry of the linear delta, will be chosen identical. In order to evaluate the correct size a series of trials are effectuated during which the robot is moved inside the desired workspace and the torques and angular acceleration on the reducer side are measured. By considering the worst case scenario among the trials we proceed to the sizing.

Method

The electrical motors present a characteristic curve Torque-Velocity with two main zones. One inside which the motor can work an unlimited amount of time, and another where the motor can stay only for a certain period. This distinction resides mainly in the fact that at the increase of the torque and velocity the heat generated by the motor increases. It is necessary guarantee to the motor the time to dissipate such a heat by evaluating how they work during their utilise to avoid their overheating. Furthermore it is necessary to respect the maximum torque, $C_{m,max}$, and the maximum velocity, $\omega_{m,max}$, of the motor by considering at the same time the reducer coupled with it. For every motoreducer selected we are going to check the following conditions:

- respect of the maximum torque:

$$max|C_m(t)| < C_{m,max} \tag{2.33}$$

- Root mean square below the nominal torque:

$$C_{m,rms} < C_{m,nom} \tag{2.34}$$

- respect of the maximum velocity:

$$max|\omega_m(t)| < \omega_{m,max} \tag{2.35}$$

For the reducer, which defines the mechanical transmission ratio τ such as $\omega_r = \tau\omega_m$, we verify the admissibility of the input torques and velocities, which are the $C_{m,max}$ and the $\omega_{m,max}$. The dimensions labelled with the subscript m and r are related respectively to the motor and to the reducer. Following the procedures found in the literature [9,10,12], it is presented the method used to choice the most suited motoreducer group for this application. If we apply a power balance between the motor side and the reducer side, by expressing every terms on the reducer side, we can write:

$$C_m = \tau C_r^* + J_m \frac{\dot{\omega}_r}{\tau} \tag{2.36}$$

Where the term τ is unknown and it is part of the motoreducer choice, the term C_r^* stands for the resistant torque of the system and the last term J_m is the motor inertia, which depends on the motor. If we evaluate the root mean square on both members of the eq.2.36 and by collecting the terms we obtain:

$$\alpha > \beta + [C_{r,rms}^*(\frac{\tau_{rid}}{\sqrt{J_m}}) - \dot{\omega}_{r,rms}(\frac{\sqrt{J_m}}{\tau_{rid}})]^2 \tag{2.37}$$

where α, defined *acceleration factor*, has the following expression:

$$\alpha = \frac{C_{m,nom}^2}{J_m} \tag{2.38}$$

It is evident how α is an unknown term function of the motor chosen. The term β, defined *load factor*, has the followinf expression:

$$\beta = 2[\dot{\omega}_{r,rms} C_{r,rms}^* + (\dot{\omega}_r C_r^*)_{medio}] \tag{2.39}$$

This term depends only on the accelerations and torques imposed to the mechanical system. The rms terms are so defined:

$$C_{r,rms}^* = \sqrt{\frac{1}{T}\int_0^T [C_r^*(t)]^2 dt} \qquad \dot{\omega}_{r,rms} = \sqrt{\frac{1}{T}\int_0^T [\dot{\omega}_r(t)]^2 dt} \tag{2.40}$$

The respect of the inequality 2.37 guarantees that the motor works on average under its nominal torque by avoiding overheating problems. To be the inequality verified the term α must be bugger than β or at least equal. Such eventuality it is verified when there is a specific value of the transmission ratio called optimum ratio, τ_{opt}, which can be obtained by nullifying the quadratic term.

$$\tau_{opt} = \sqrt{J_m \frac{\dot{\omega}_{r,rms}}{C_{r,rms}^*}} \tag{2.41}$$

If we chose a reducer with $\tau = \tau_{opt}$ in the choice of the motor we must guarantee that $\alpha > \beta$. The ratio τ_{opt} could not be available in the market, so by expressing the inequality 2.37 respect to $\tau/\sqrt{J_m}$ it is possible to define an interval inside which every value of τ satisfy the inequality.

$$\tau_{min,max} = \sqrt{J_m} \frac{\sqrt{\alpha - \beta + C_{r,rms}^* \dot{\omega}_{r,rms}} \pm \sqrt{\alpha - \beta}}{2C_{r,rms}^*} \tag{2.42}$$

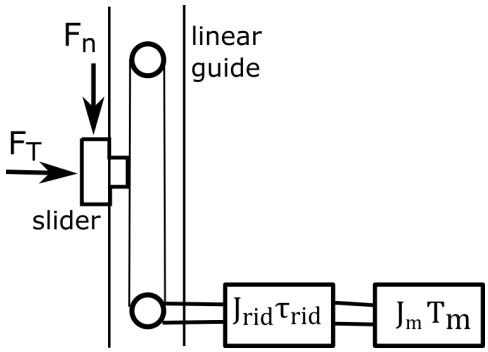

Figure 2.25: System motor-reducer-linear guide-slider

The value of τ chosen must guarantee that the velocity required from the reducer side must be inside the limits of the motor. We define a τ such that the maximum velocity of the motor corresponds to the maximum velocity of the load:

$$\tau_p = \frac{\omega_{r,max}}{\omega_{m,max}} \tag{2.43}$$

The procedure followed in order to choice the motoreducer is comprehensive of the following steps:

1. a motion law is imposed to the system and the terms $C_r^*(t)$ and $\dot{\omega}_r(t)$ are evaluated so defining β

2. A motor is chosen so defining $C_{m,nom}$, J_m and α which must be bigger than β

3. The values τ_{min}, τ_{max} and τ_p are evaluated. If $\tau_p > \tau_{max}$ we need to chose a motor with a bigger α. If $\tau_{min} < \tau_p < \tau_{max}$ we need to choice a reducer with $\tau_p < \tau < \tau_{max}$. If $\tau_p < \tau_{min}$ all the interval between τ_{min} and τ_{max} is acceptable.

4. once τ is chosen it is necessary to verify that the maximum torque required can be supplied by the motor.

5. it is necessary to verify the compatibility between motor and reducer

Resistant torque

The term C_r^* is evaluated through the dynamic model. In fig.2.25 is shown the scheme of the system with the motoreducer connected to the slider. The actuator is directly connected on a pulley which is inside the liner guide, through that and a belt is possible to move the slider. In the dynamic model is measured the force parallel to the slider displacement which is the

force needed to impose on the body the desired motion law. This force can be easily translated in the torque on the reducer side by knowing the diameter of the pulley d_p. The resistant torque here is:

$$C_r^*(t) = F_N(t)d_p/2\eta_s \tag{2.44}$$

The term η_s evaluates the efficiency of the system by considering the internal frictions of the system, in particular the linear guide ones. For the linear guides chosen the vendor does not tell any data about their friction. The value $\eta_s = 0.9$ has been chosen to take into account the imperfections of the model here proposed. After the motoreducer has been chosen it is possible to add at the system the contribute of the reducer inertia J_{rid} and take into account its mechanical efficiency. This efficiency, usually very high, it is considered only after the actual choice of the motoreducer.

In the same manner of the torque it is possible to measure the acceleration of the slider, a_s, and translate it in an angular acceleration of the pulley.

$$\dot{\omega_r} = \frac{2a_s}{d_p} \tag{2.45}$$

Motion law

To evaluate the torque on the load side of the system we have to choose a motion law for the linear delta. In the dynamic model it is assigned a motion law to the platform, it is measured the motion law on the sliders and the same one it is assigned to the slider to move the linear delta. This procedure has been preferred to the direct evaluation of the sliders motion through the use of the kinematic equations. The choice of the motion law it's very important because on it depends the choice of the motoreducer groups. We have to determine:

- trajectory of the platform
- velocity of the platform

It is clear how with increasing velocities on the same trajectory there will be an increase in the accelerations required. The inertial forces and torques become bigger and this would lead to the design of mechanical components which must bear bigger loads and to the choice of motors with a bigger size. Since it is not specified in the design requirements the trajectories for the printer we chose to impose on the linear delta sinusoidal motion laws which cover the entire workspace. The workspace considered is the same used in the kinematic optimization with a square of side $300[mm]$. In fig.2.26 is represented in red the workspace on which it is effectuated the dynamic study. It has been initially chosen 9 points of study signed on the workspace.

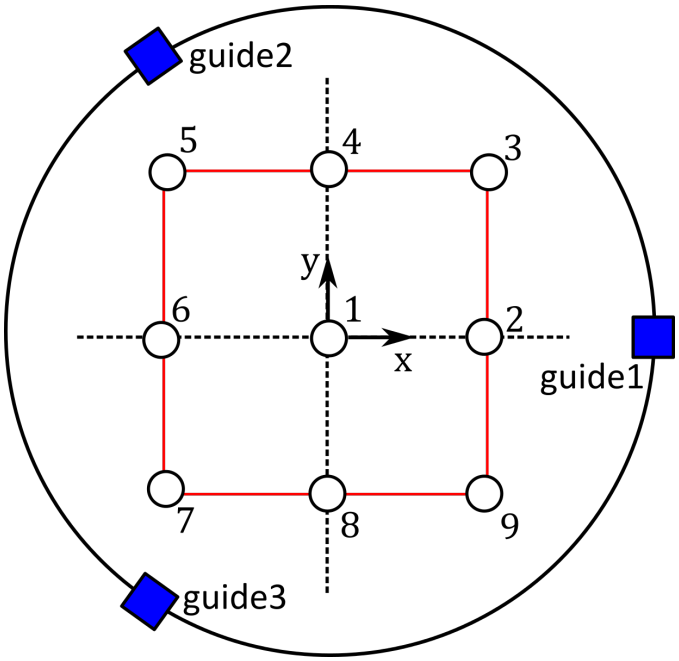

Figure 2.26: Points chosen for the dynamic study

Since the symmetry of the system along the x axis only 6 points are actually considered, from 1 to 6, since for the points 7, 8 and 9 would give the same results than the points 1, 2 and 3 for the linear guide 1, and specular results for the linear guides 5 and 6. We would not get additional informations.

The dynamic trials are executed according to the following steps:

- The TCP of the linear delta is positioned in one of the six points of study
- it is imposed a sinusoidal motion law along one direction per time $x(t)$, $y(t)$ or $z(t)$, which cover the entire workspace

$$x(t) = 150 * sin(2\pi t) \tag{2.46}$$

- In the points along the border the sinusoidal movements are chosen without making the liner delta cross the border of the square workspace and by avoiding to repeat similar movements

The last step takes into account that in some points as 5and 6 a movement along the y will give the some results even though the starting point is different. At the end we have done 11 trials; three in point $1(x, y, z)$, two in the points 2, $6(y, z)$ and $4(x, z)$ and one in the points 3 and 5 along z. The sinusoidal movement has an amplitude of $150[mm]$,so as example if the TCP of the linear delta starts from point 1 and it moves along x it will reach the

point 2 before going back to point 6 and return back where it started; since the argument of the sine is $2\pi t$) the all movement is accomplished in 1[s]. By considering the maximum printing velocity required, 100[mm/s], the tests here proposed are suited to correctly size the motors. It is pointing out how during the printing face, since the printed object moves along with platform, it is not ensured that it could stands the accelerations generated. Even if the velocity of 100[mm/s] is feasible for the robot it could be undesirable to achieve it to avoid any deformations or damages on the printed object.

Choice of the motor reducer groups

By executing the dynamic trials we obtain the results of table 2.9. In the table the results are classified according to the three linear guides, G1, G2, G3, according to the point of study in the printing area, from 1 to 6, and according to the direction of the motion law imposed, x, y or z. The maximum value for β, factor dependent only from the structure load and the motion law, is of 2797 and it has been obtained in the point 5 along the direction z. In the table is shown the biggest β value per each study point and direction among the three linear guides. The maximum angular velocity obtained is $31.42[rad/s]$, which is about $300[rpm]$. Taking as reference the worst case we proceed in the choice of the motoreducer group. For the choice of the motor we turn our attention to products family of the vendor *Mitsubishi Eletric* and in particular we refer to the ac brushless motors. In tab.2.10 are listed all the motors inspected, each belonging to a specific motor series and with their main technical data. Every motor is associated with a number in the right side of the table that can be used to find it in the graphs with the results of the dynamic study, graph 2.27 and 2.28. In this two graphs are evaluated the α value per each motor respect to β_{max} obtained from the dynamic simulations, and the ranges τ_{max} and τ_{min} respect to τ_p. It has been utilised the value of $C^*_{r,rms}$ and $\dot{\omega}_{r,rms}$ of the same simulation of β_{max}. It can be notice that almost the entire motor series is able to carry out the required job. By having several possible solutions we used two choice criteria:

- smaller size motor
- most suitable motor series

With a determined work to do it is preferable to chose a motor with the smallest size as possible. A motor with a bigger size than the required one would be oversized an it will have bigger costs that it's better to avoid if it is possible. We immediately exclude the motors from the 11 to the 25 which have a nominal power starting from $0.5[KW]$. The remaining motors belong to the series HG-MR and HG-KR which are very similar with differences only in the inertia values. Excluding the motors which do not have a suitable

Table 2.8: Motor Mitshubishi HG-KR 43(B), reducer Bonfiglioli TR 080 1_10

HG-KR 43(B)	$T_n[Nm]$	$T_{max}[Nm]$	$\omega_n[r/min]$
	1.3	4.5	3000
	$\omega_{max}[r/min]$	$J_m[Kgm^2 * 10^{-4}]$	$P_n[Kw]$
	6000	0.393	0.4
TR 080 1_10	$M_{n2}[Nm]$	$M_{a2}[Nm]$	$n_1[min^{-1}]$
	40	80	6000
	$J_{rid}[Kgm^2 * 10^{-4}]$	τ	η_{rid}
	0.29	0.1	97%

transmission ratio, motors 1, 2, 6 and 7 all the others could be a suitable solution. It is here decided to pick the motor number 9 with a transmission ratio of 0.1. In tab.2.8 are listed the main data of the chosen motor. For the reducer we have referred to the the *Bonfiglioli* vendor; some of its technical data are listed in the same table. It is a planetary gear reducer with only of stadium of reduction and reduced backlash; in the table are indicated its nominal and maximum output torque, the admissible input velocity, inertia, transmission ratio and efficiency.

We can use the motor and reducer data to run a final simulation of the dynamic model and verify the respect of the inequality 2.37 and the respect of the maximum torque limit.

$$C_r^*(t) = \frac{F_N(t)d_p}{2\eta_s} + J_{rid}\dot{\omega}_r \qquad \alpha = \frac{(C_n\eta_{rid})^2}{J_m} \tag{2.47}$$

$$\alpha = 40461.1 > 2798 + [7.24\frac{0.1}{\sqrt{0.393 * 10^{-4}}} - 138.88\frac{\sqrt{0.393 * 10^{-4}}}{0.1}]^2 \tag{2.48}$$

The inequality is verified and the maximum torque required, $10.68[Nm]$ on the reducer, is under the motor limit. The motoreducer group fits the application.

2.6.3 Linear guides

The linear delta movements are controlled through the displacements of the sliders along the linear guides. Two typical transmission systems we can find in a linear guide:

1. belt
2. ball screw

Table 2.9: Torque, acceleration, velocity results and β_{max}

	$T^*_{r,rms}[Nm]$	$\dot{\omega}_{r,rms}[rad/s^2]$	$(T^*_r\dot{\omega}_r)_{average}[Nm/s^2]$	$\omega_{r,max}[rad/s]$	β_{max}	
G1	6.28	85.05	357.13	18.06		x displacement
G2	4.12	54.37	100.57	10.72	1782.5	Point 1
G3	4.12	54.37	100.57	10.72		
G1	3.1	39.62	14.5	4.42		y displacement
G2	5.65	75.82	271.16	16.01	1399.1	Point 1
G3	5.65	75.82	271.16	16.01		
G1	3.59	138.88	195.46	31.42		z displacement
G2	3.59	138.88	195.46	31.42	1388.1	Point 1
G3	3.59	138.88	195.46	31.42		
G1	5.1	36.46	-21.31	4.04		y displacement
G2	5.19	88.13	371.58	18.34	1657.9	Point 2
G3	5.19	88.13	371.58	18.34		
G1	6.42	138.88	348.43	31.42		z displacement
G2	2.19	138.88	118.97	31.42	2480.1	Point 2
G3	2.19	138.88	118.97	31.42		
G1	1.07	49.45	8.83	5.48		y displacement
G2	6.48	73.6	282.68	15.54	1519.2	Point 6
G3	6.48	73.6	282.68	15.54		
G1	1.12	138.88	60.56	31.42		z displacement
G2	4.84	138.88	262.91	31.42	1870.2	Point 6
G3	4.84	138.88	262.91	31.42		
G1	5.98	89.49	354.2	18.93		x displacement
G2	5.86	50.24	109.18	9.92	1780.5	Point 4
G3	2.53	67.24	92.38	13.18		
G1	3.44	138.88	186.8	31.42		z displacement
G2	5.97	138.88	324.43	31.42	2307.1	Point 4
G3	1.38	138.88	75.14	31.42		
G1	6.03	138.88	327.29	31.42		z displacement
G2	4.21	138.88	228.69	31.42	2329.5	Point 3
G3	0.56	138.88	30.4	31.42		
G1	1.14	138.88	61.95	31.42		z displacement
G2	7.24	138.88	393.01	31.42	2797	Point 5
G3	2.42	138.88	131.43	31.42		

Table 2.10: Brushless motors Mitsubishi Electric

Motor series	$T_n[Nm]$	$T_{max}[Nm]$	$\omega_{max}[r/min]$	$J_m[Kgm^2 * 10^{-4}]$	$P_n[KW]$	Number
HG-MR	0.16	0.48	6000	0.0224	0.05	1
	0.32	0.95	6000	0.0362	0.1	2
	0.64	1.9	6000	0.109	0.2	3
	1.3	3.8	6000	0.164	0.4	4
	2.4	7.2	6000	0.694	0.75	5
HG-KR	0.16	0.56	6000	0.0472	0.05	6
	0.32	1.1	6000	0.0837	0.1	7
	0.64	2.2	6000	0.243	0.2	8
	1.3	4.5	6000	0.393	0.4	9
	2.4	8.4	6000	1.37	0.75	10
HG-SR	2.4	7.2	3000	9.48	0.5	11
	4.8	14.3	3000	13.8	1.0	12
	7.2	21.5	3000	18.2	1.5	13
	9.5	28.6	3000	56.5	2.0	14
	16.7	50.1	3000	88.2	3.5	15
HG-RR	3.2	8.0	4500	1.85	1.0	16
	4.8	11.9	4500	2.25	1.5	17
	6.4	15.9	4500	2.65	2.0	18
	11.1	27.9	4500	11.8	3.5	19
	15.9	39.8	4500	15.5	5.0	20
HG-JR	1.6	4.8	6000	1.85	0.5	21
	2.4	7.2	6000	2.25	0.75	22
	3.2	9.6	6000	2.65	1.0	23
	4.8	14.3	6000	11.8	1.5	24
	6.4	19.1	6000	15.5	2.0	25

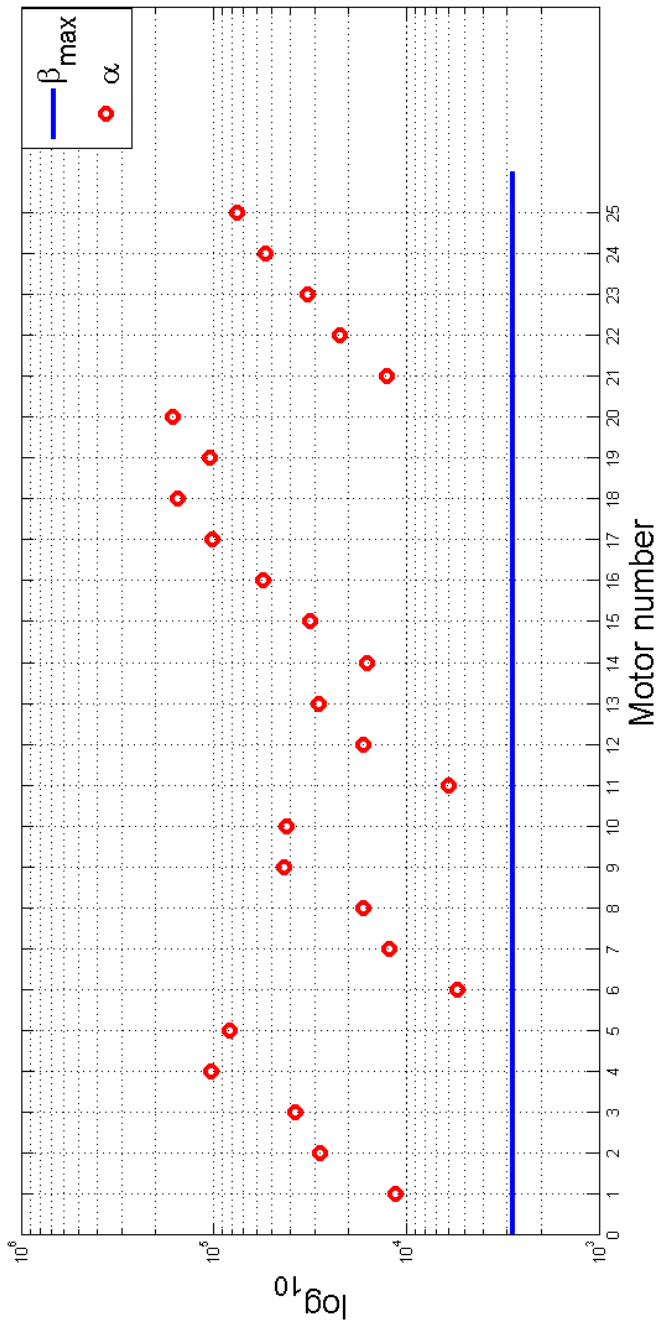

Figure 2.27: α for the different motors respect to β_{max}

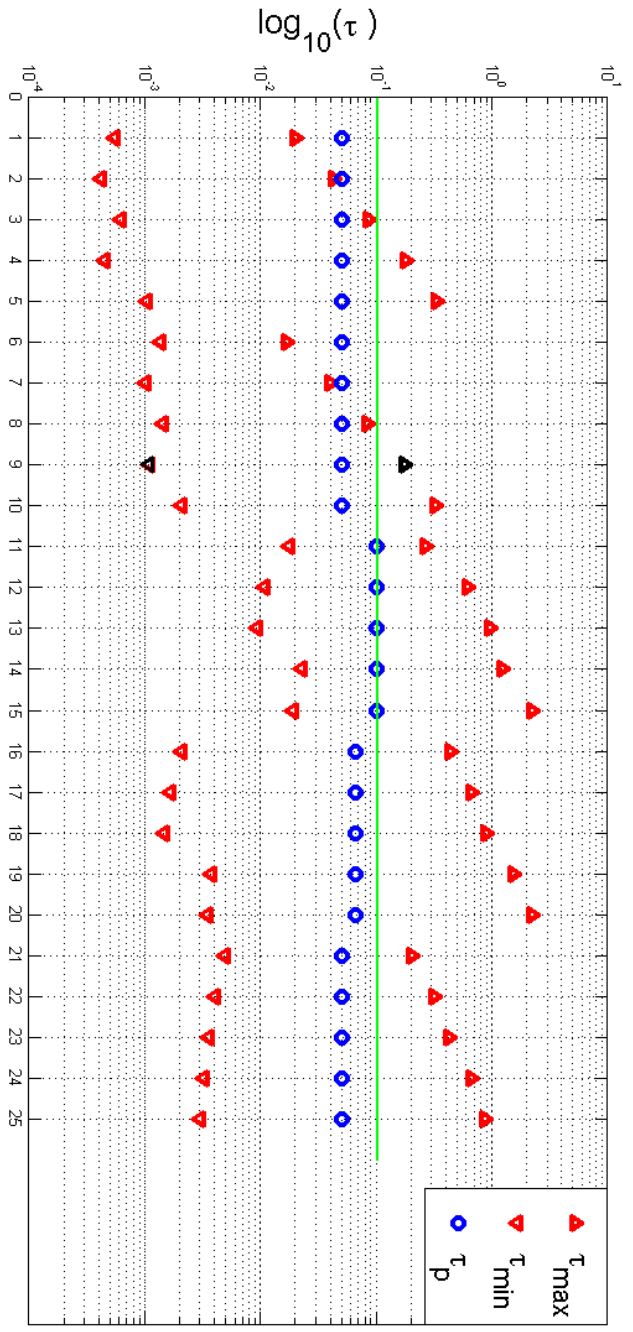

Figure 2.28: Admissible transmission rates for the motors

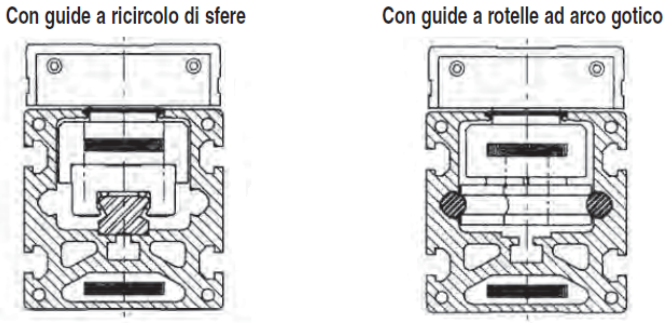

Figure 2.29: Guide Rollon Series SP and CL

The linear guides driven by belt generally are generally cheaper and less energy consuming than the linear guides based on ball screw which, on the other hand, have a greater stiffness and precision. Since from the dynamic study the acceleration measured were not very high, we decide to choose a linear guide driven by belt.

For the choice of the linear guide we refer to the vendor *Rollon* which has two kind of belt driven linear guide:

Series SP The slider is mounted above two preloaded ball recirculating carriages moved by the belt.

Series CL The slider is mounted on four wheels with two lines spheres with oblique contact and with an external shape that allows the sliding on two steel bars.

In fig.2.29 are visible two sections of the series SP and CL. For the choice of the linear guide is fundamental to take into account the accelerations and velocities admissible, the loads that can withstand, an it must be evaluated the total stroke necessary for the sliders.

The sliders stroke can be evaluated through the use of the inverse kinematic. If we consider the linear delta workspace of fig.2.21 and we measure the total stroke of each slider needed to move the linear delta we obtain a maximum value of 197[mm], whose 137 are in an higher position respect to the starting position of the slider when the linear delta platform is centred in the workspace. This stroke is the one needed to move the linear delta in a plane. We add the stroke necessary to move the linear delta along the z direction. It is taken the value 187[mm] from the data of the tab.2.2 and it is obtained a final stroke of 384[mm]. This minimum stroke is increased by a specific design choice. If The fig.2.31 shows how the linear guides contains the entire structure of the linear delta. The linear guides are used not only to guarantee the stroke of the sliders but to support the extruder on top of the machine, fig.2.5, by giving an ergonomic solution for the operator who

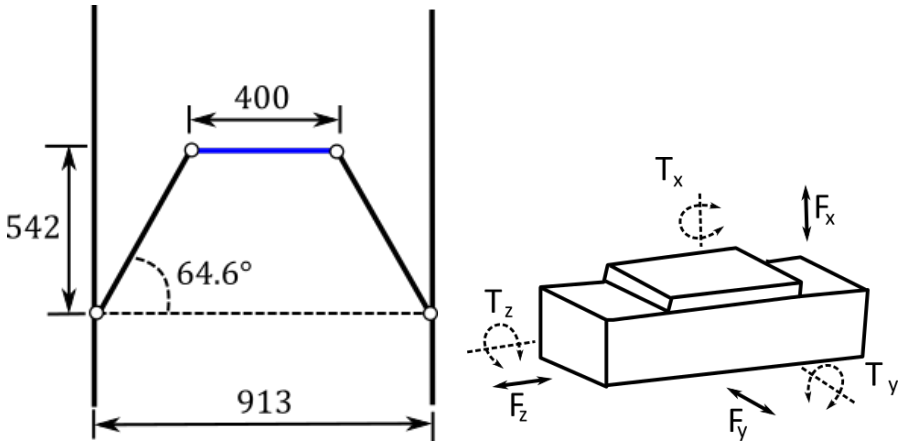

(a) Size of the linear delta **(b)** Forces and torques on the slider

Figure 2.30: Linea delta, main dimensions and forces-torques on the sliders

will use it. The entire height of the printer, without the extruder, is about 1.5[m]. By considering the size of the linear delta we define a final stroke of 1000$[mm]$ and a total length for the linear guides of 1540$[mm]$. The two extremities of the linear guide are not usable by the sliders.

The maximum accelerations and velocities can be retrieved from the dynamic simulations and their values are 5910$[mm/s^2]$ and 942.5$[mm/s]$. The forces and torques exercised on the linear guide have been measured too on the sliders. The critical values for the choice of the linear guides is the torque T_z which has the lower value among the datasheet of this component. In fig.2.30b are represented the forces and torques which acts on the sliders and by consequence on the linear guides. We point out here that during the dynamic study has been executed a measuring campaign in some key points of the linear delta structure in order to measure the forces and torques necessary fro the mechanical design of the system. In fig.2.26 are defined those points which are settled in three constraints of the system; the translational constraint for the slider, T, and the revolute joints on the pivot and links, S1, S2 and S3. For the choice of the linear guide we have used the torque measured on the T points of the sliders. In tab.2.12 are shown the results obtained. The maximum torques measured are:

$$M_x = 48.3[Nm] \qquad M_y = 24.7[Nm] \qquad M_z = 38.2[Nm] \tag{2.49}$$

Since the data obtained it has been chosen the linear guide ELM 80 SP whose main technical data are reported in tab.2.11, where it is expressed the maximum dynamic loads admissible and where it is reported the diameter of the pulley d_p.

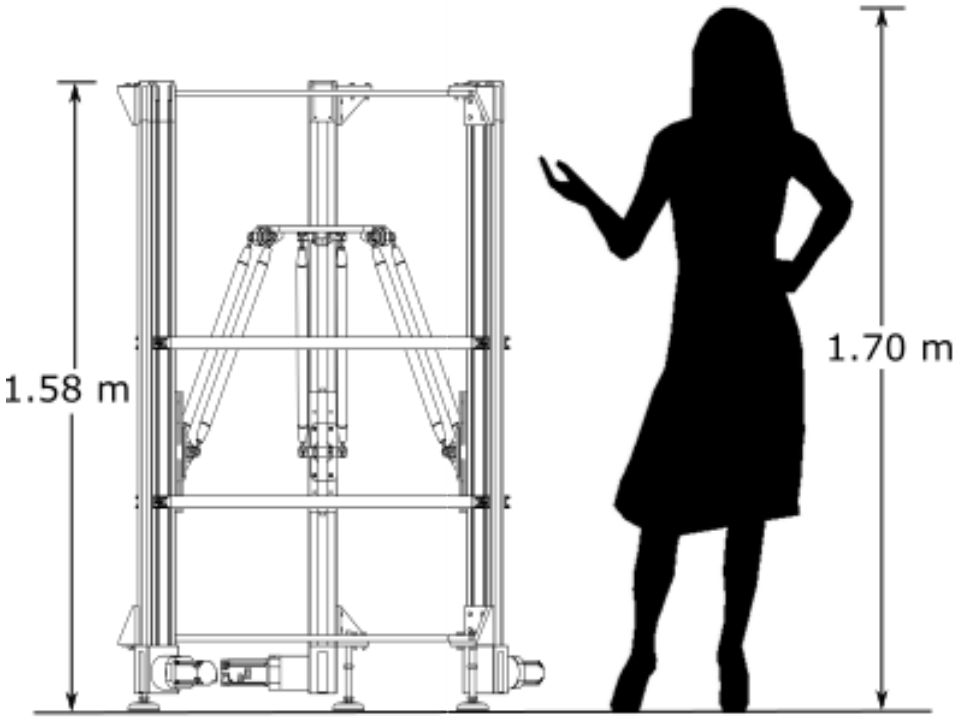

Figure 2.31: Human scale solution

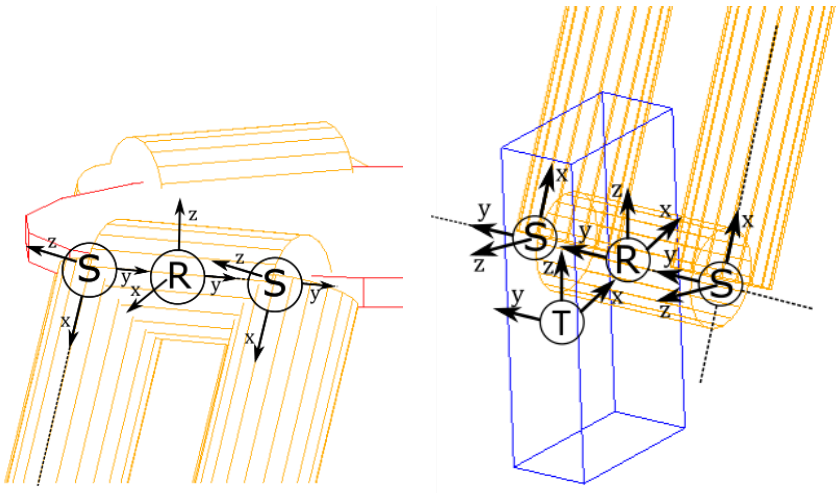

(a) **(b)**

Figure 2.32: Points for the study of the constraint reactions

Table 2.11: Rollon guide ELM 80 SP, maximum dynamic loads admissible

$v_{max}[m/s]$	$a_{max}[m/s^2]$	$F_x[N]$	$F_y[N]$
5	50	4180	4180
$T_x[Nm]$	$T_y[Nm]$	$T_z[Nm]$	$d_p[mm]$
300	300	58	60

2.6.4 Results of the dynamic study

At the end of the dynamic study section it is listed the results of the measuring campaign obtained in other points of the machine and that they have been utilised during the mechanical design. The points are labelled according to the system used in fig.2.32 and we show the results in the points S1, S2 and S3. In the S1 point has been measured the radial force on the pivot, F_t, the axial force, F_a, and the total torque on the constraint C_p. In the points S2 and S3 have been evaluated the forces along the three direction x, y and z and the angular velocity of the pivot ω_p. In tab.2.13 are shown the maximum values obtained. In the table the term G1, G2 and G3 refers to the three different linear guides. For the forces F_x, F_y and F_z is indicated only the maximum value between the two points S1 and S3.

2.7 Extruder

The extruder chosen for the Efesto printer has been acquired by an external company, Babyplast®, where it was used mainly for the injection moulding of plastic components. Such a mechanism , represented in fig.2.33, is characterized by:

1. a hopper for the material insertion as pellet
2. two pistons with an hydraulic system
3. three resistors and four thermocouples for the heating and control of the extruder temperature

The material introduced inside the machine through the hopper is preheated in a first zone of the machine. Here a first piston, the plasticizer, push the material in a collecting chamber of volume about $9000[mm^3]$. The material before of reaching the chamber pass through a canal full of spheres; this phases is needed in order to plasticize the material and obtain a better extrusion process. The material, once arrived in the collecting chamber, is pushed by a second piston, the extruder, for the real extrusion through a nozzle. The entire system is kept to a desired temperature through the use of the resistors and thermocouples. The temperature of the pre.-heated

Table 2.12: Forces and torques on the linear guides

	$T_x[Nm]$	$T_y[Nm]$	$T_z[Nm]$	$F_x[N]$	$F_y[N]$	
G1	0	14.4	0	119.5	0	x displacement
G2	37.6	8.1	25.1	51.11	35	Point 1
G3	37.6	8.1	25.1	51.11	35	
G1	42.6	3.5	21.6	28.9	12.2	y displacement
G2	20.6	12.6	16.6	93.7	30.7	Point 1
G3	20.6	12.6	16.6	93.7	30.7	
G1	0	5.5	0	46	0	z displacement
G2	0	5.5	0	46	0	Point 1
G3	0	5.5	0	46	0	
G1	48.3	7.2	12.6	25.4	22.5	y displacement
G2	21.6	24.7	22.1	124.8	95	Point 2
G3	21.6	24.7	22.1	124.8	95	
G1	0	17.8	0	40.2	0	z displacement
G2	20.2	6	15.3	24	9.4	Point 2
G3	20.2	6	15.3	24	9.4	
G1	39.1	0	38.2	7.3	3.3	y displacement
G2	33.5	15.4	22.7	61.9	40.6	Point 6
G3	33.5	15.4	22.7	61.9	40.6	
G1	0	1.7	0	11.7	0	z displacement
G2	13.7	15.7	8	49.7	35.5	Point 6
G3	13.7	15.7	8	49.7	35.5	
G1	16.5	16	10.9	119.3	68.7	x displacement
G2	44.9	11.3	17.1	29	18.6	Point 4
G3	39.7	5.8	29.1	87.4	37.3	
G1	20.7	11.8	13.4	44.1	25.9	z displacement
G2	6	17.4	3.3	44.4	26.1	Point 4
G3	11.8	0.5	10.1	0.5	0	
G1	10.3	16.6	5.8	38.3	53.7	z displacement
G2	23	14	14	47.7	48.3	Point 3
G3	7.8	8	8.3	45.4	5.4	
G1	22.9	1.6	21.6	11.4	4.2	z displacement
G2	2.7	17	1.6	22.6	23.8	Point 5
G3	30.5	7.4	23.2	29.9	19.6	

Table 2.13: Results of the dynamic study in the points S1, S2 and S3 of the three parallelograms

	$F_t[N]$	$F_a[N]$	$T_p[Nm]$	$\omega_p[deg/s]$	$F_x[N]$	$F_y[N]$	$F_z[N]$	
G1	291.7	0	0	144.2	112	0	2	x displacement
G2	170.6	35	45.6	51	453.9	1	2	Point 1
G3	170.6	35	45.6	51	453.9	1	2	
G1	76.2	12.2	47.5	5.5	474.4	1.2	1.3	y displacement
G2	257.6	30.7	27	87	318.6	0.7	1.8	Point 1
G3	257.6	30.7	27	87	318.6	0.7	1.8	
G1	119.7	0	0	0	57.7	0	2	z displacement
G2	119.7	0	0	0	57.7	0	2	Point 1
G3	119.7	0	0	0	57.7	0	2	
G1	145.9	22.5	50	19.5	516.3	1.5	1	y displacement
G2	308.7	95	28.9	90.2	343.3	1.4	2.5	Point 2
G3	308.7	95	28.9	90.2	343.3	1.4	2.5	
G1	238.6	0	0	0	117	0	0.8	z displacement
G2	53.8	9.4	26.2	0	269.1	0.77	2.5	Point 2
G3	53.8	9.4	26.2	0	269.1	0.77	2.5	
G1	7.5	3.3	54.8	11	513.6	1	2	y displacement
G2	290.3	40.6	44.4	88.5	482.7	1	1.5	Point 6
G3	290.3	40.6	44.4	88.5	482.7	1	1.5	
G1	11.8	0	0	0	5.5	0	2.9	z displacement
G2	172.8	35.5	20	0	272.5	1	1.3	Point 6
G3	172.8	35.5	20	0	272.5	1	1.3	
G1	275.4	68.7	19.8	104	252.6	1	2	x displacement
G2	222.5	18.6	48.4	88.5	471.6	1	1	Point 4
G3	112.6	37.3	48.4	88.5	526.3	1	2	
G1	112.6	25.9	27.4	0	313.2	1	2	z displacement
G2	220.1	26.1	9.6	0	196.3	1	2	Point 4
G3	12.5	0	15.5	0	144.9	0.5	3	
G1	221.3	53.7	16.7	0	268.1	1	1	z displacement
G2	145.6	48.3	32.4	0	387.5	1	1.5	Point 3
G3	51.3	5.4	11	0	127.5	3.5	3.5	
G1	11.5	4.2	31.2	0	298.3	1	3	z displacement
G2	272.4	23.8	4.2	0	172.9	0.5	0.5	Point 5
G3	66.5	16	27.8	0	420.7	1	2.5	

Figure 2.33: Babyplast® extruder

chamber, the central chamber and the nozzle can be set separately and to different values. The system, in its commercial version, has its own control which allows to regulate the temperatures and to actuate the hydraulic pistons; a pump system is needed fro the actuation system. In the original application the use of an hydraulic system is far more than adequate, but the utilise of this extruder for an AM application makes it inadequate. Foe the design solution here proposed we need two fundamental things:

- Integration between the robot control system and the extruder
- Control of the extrusion rate

In order to obtain a correct printing procedure in the project Efesto, as in all the processes based on the extrusion of material like the FDM, it is fundamental to coordinate the material extrusion with the movement of the printer in order to obtain the desired object shape with te correct quantity of material deposited in the correct points. The Babyplast® control system is no capable to integrate the electrical motors chosen for the linear delta; we could chose two different control systems, one for the robot and one for the extruder, or we could use a unique controller to command the motors and the hydraulic pistons. Both the solutions as presented have their issues. The first one presents the problem to coordinate two different control systems with the uncertainty of a perfect synchronism among the two. The second is inadequate for the use of the hydraulic pistons. In order to control correctly the printing process we need to precisely control the material extrusion rate exiting the nozzle and so we need to control the piston velocity which push the material. The hydraulic systems, and this in particular, are not well suited to have a velocity control. In its original application the piston duty was to exercise as much pressure as possible in order to fill a mould with

the material; the entire system was thought to exercise a precise pressure, not to have a precise velocity. The use of an electric motor with its encoder, in exchange of the hydraulic system, would allow to overcome this problem. We decide to substitute the original actuation system with two electrical motors; to facilitate the integration of these two motors with the linear delta one we will refer to the same vendor. With this solution we can easily have a unique control system for the entire printer by reaching a compact solution.

2.7.1 Sizing of the motors

To correctly size the electrical motors an experimental test has been carried out at the company Rambaldi + Co.I.T. srl in Molteno, associated of the Babyplast group. The test has been carried out with specific measuring systems, a temperature of $180°C$, material 17-4PH(stainless steel) and a nozzle with a $0.6[mm]$ diameter. It has been measured an extrusion pressure of $11[MPa]$ and a plasticizer pressure of about $18[MPa]$; such results have been supported in some laboratory tests effectuated in another work [4]. If to this values we add the diameters of the piston extruder, $14[mm]$, and piston plasticizer, $20[mm]$, we have all the data to correctly size the motors. The forces required on each piston can be easily evaluated as:

$$F_e = \frac{11[MPa]\pi 14[mm]^2/4}{C_f} = 1881N \quad F_e = \frac{18[MPa]\pi 20[mm]^2/4}{C_f} = 5585N \tag{2.50}$$

Where C_f, equal to $0,9$, is a friction coefficient which takes into account the insert in the system of a ball screw which allows the transmission between the motor and the piston. Before to proceed we need the acceleration and velocity required during the utilise of the extruder. In the case of FDM machines typical printing velocities are in the order of tenth of $[mm/s]$. In this case the maximum printing velocity required is $100[mm/s]$, if we consider a $0,6[mm]$ nozzle diameter wit is possible to obtain from a mass balance the velocity required for the extrusion piston.

$$v_p = 100\frac{0.6^2}{14^2} = 0.184[mm/s] \tag{2.51}$$

The maximum piston velocity is very low; and this was perceivable by being the velocity function of the nozzle and piston diameters ratio. If we suppose an acceleration time of $0.1[s]$, starting from null velocity it would be necessary an acceleration of $1,84[mm/s^2]$ to reach such a velocity. This low values allow us to study the extrusion system in a static way. The plasticizer would require different considerations. Here the piston duty is to load the material in the central chamber and at hte same time plasticizing it.

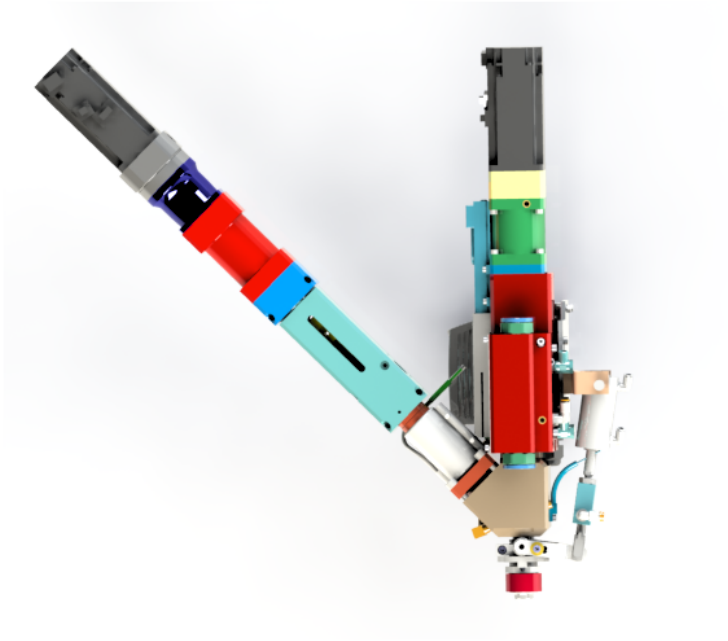

(a)

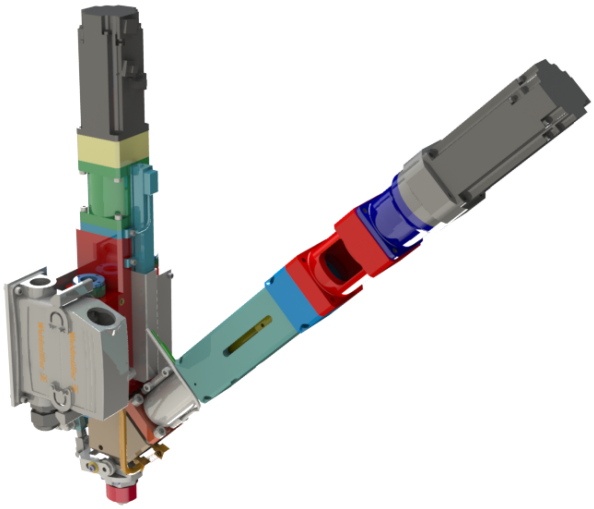

(b)

Figure 2.34: Extruder modified with two electrical motors

From a process point of view it would be desirable that have this phase the most short in time as possible but it would requires great accelerations and torques. In this application, a 3D printing, the loading of the material si not required very often. If we consider an average printing speed of $25[mm/s]$, we suppose this velocity under the maximum velocity required, to empty the central chamber of volume $9000[mm^3]$ would be required about 21 minutes. On a printing of 3-4 hours it would be necessary to reload the system about ten times; a few seconds more in the loading phase are marginal to the total printing time. This part of the system too will be evaluated in a static way by accepting a slow down in the loading phase.

For each of the two branches in the extrusion system we evaluate the torque required by taking into account the forces on the extruder and plasticizer by considering the use of two ball screws.

$$T = \frac{F.p}{2\pi} \quad T_e = 0.6[Nm] \quad T_p = 4.45[Nm] \tag{2.52}$$

The equation expresses the power balance between the torque required and the force applied on the material. The screw steps are respectively $5[mm]$ fro the plasticizer and $2[mm]$ for the extruder. With this value and by considering as valid options the same motors listed in the dynamic study it is chosen the same type and size of the motors chosen for the linear delta. These motors has a nominal torque of 1,3[Nm] and a maximum one of 4,5[Nm] and they are suited to execute the work here required. In the case of the plasticizer where the torque required to the motor is near its limits is introduced a reducer with a transmission ratio 1:4.

In the end we obtain the final configuration of the extruder which has been specifically modified, as shown in fig.fig.2.34, in order to be integrated in final system of the printer. The extruder has been tested in an initial phase separately from the machine, fig.2.35. In tab.2.14 are listed the main data used for the two extruder branches.

2.8 Mechanical design

It is now possible to proceed with the mechanical design of the linear delta components, to their manufacturing and to final assembling of the printer. Here it is utilised as input the data coming from the kinematic and dynamic study. Many of the work done has been supported by the use of the software *SolidWorks*.

2.8.1 Linear Delta

During this phase of the design process every components of the linear delta is defined. From the kinematic optimization we take the values of l, which

Table 2.14: Data of plasticizer and extruder

Data		Plasticizer	Extruder
Piston diameter [mm]		20	14
Piston stroke [mm]		74	60
Force required[N]		5585	1881
Torque required[Nm]		4.45	0.6
Motor	Mitsubushi Electric model	HG-KR43(B)	HG-KR43(B)
	Nominal torque[Nm]	1.3	1.3
Reducer	Wittenstein model	SP+	–
	transmission ratio	4	–
Ball screw	Bosch Rexroth model	ZEV-E-S	FEM-E-B
	step[mm]	5	2

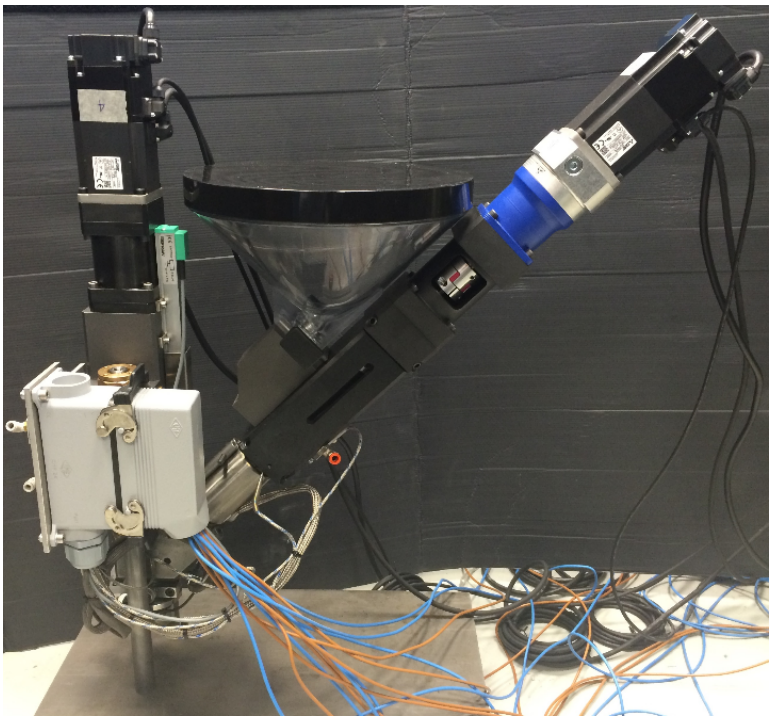

Figure 2.35: Bench test for the extrusion system

Table 2.15: Aluminium Anticorodal 6012

$\sigma_R[MPa]$	$\sigma_{Rp0,2}[MPa]$	$E[GPa]$	$A\%^1$	$\rho[g/cm^3]$	HB [2]	$T_f[°C]$
350	320	69	10	2,75	105	580-650

[1] Cylindrical sample with diameter 12,5 mm;
[2] 10mm sphere with applied load of 500 kg for 30 seconds;

defines the links length, d, which defines the platform diameter, α and D which together specify the linear guides position. From the dynamic study are taken the values of forces and torques to be used for the correct sizing of the components. The design of the components has been carried out with the aim to obtain low mechanical stresses and so low deformations; this is important in order to not have positioning errors of the robot.

Material

For the construction of the robot has been chosen an aluminium alloy 6012, also known as anticorodal. The choice of this material depends on:

- light weight
- low loads to bear
- resistance to corrosion

The linear delta structure must be as light as possible; extra weight would limit the dynamic performances of the system and the maximum bearable load. The aluminium with its low density, $2.7[g/cm^3]$, is ideal for this purpose. Furthermore the forces and torques obtained from the dynamic study are not very high, this allows to use the aluminium without having excessive deformations and size of the components. The use of aluminium avoids corrosion issues allowing to have maintenance of the machine parts, and it allows to avoid the use of stainless steel, more expensive and heavier. In tab.2.15 are reported the technical characteristics of the material.

Link

In fig.2.36 is shown the link component which is composed by three parts. A central tube with two extremities where are tight two rod ends. The rod ends, which are spherical joints, realize that mobility grade that during the kinematic study has been called α_2. The extremities of the central tube are two separated bodies with a thread hole needed to host the rod ends. The two extremities are attached to the central tube through a cyanoacrylate glue. The links during the dynamic study have shown principally a compression or tensile stress. In tab.2.13 is possible to notice how the measured

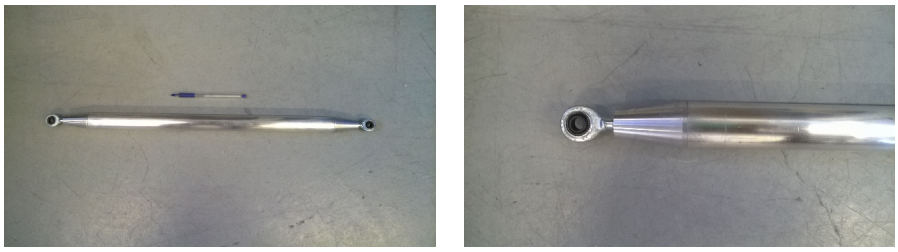

(a) **(b)**

Figure 2.36: Link

force are mainly along the x direction, which is this case the link axis. This is the result that we expected given the use of the spherical joints. Here we take care of the central tube sizing by checking that its critical section could withstand the maximum load without having excessive deformations. The maximum value measured during the dynamic study is:

$$F_{x,max} = 526.3[N] \tag{2.53}$$

The minimum area, A_m, of a section by considering the yield strength, σ_s, must be:

$$\frac{F_{x,max}}{A_m} = \sigma_s \qquad A_m = \frac{\pi}{4}(D^2 - d^2) \qquad A_m = 1.64[mm^2] \tag{2.54}$$

Where D and d are the external and internal diameter of the tube. The minimum area si very little since the low load. The use of a tube, instead of a bar, for the realization of link helps to host the rod ends without increasing the link weight. The final link has a 30[mm] diameter and a 3,5[mm] width. The tube section is bigger than the minimum required. The total maximum stain of the link $\delta L_{x,max}$ is:

$$\epsilon_{x,max} = \frac{\sigma_x}{E} = 0.258 \cdot 10^{-4} \qquad \delta L_{x,max} = L \cdot \epsilon_{x,max} = 0.015[mm] \tag{2.55}$$

Such an aspect is important taking into account that the control system of the linear delta, which is described later in this chapter, is based on the encoders of the motors; since there is no direct measurement of the robot end-effector any deformations of its bodies will lead to an incorrect positioning of the robot itself. By minimizing the deformations during the mechanical design we minimize the effect of this error. The check on the minimum area is executed on the tube extremities too; the sizing of this component is mainly guided by the necessity to host the rod ends on one side and the tube on the other. Here too the stresses evaluated are very low.

Table 2.16: Spherical node SKF SA8E

Roll angle[deg]	Load coefficient[kN]		Friction coefficient
	static	dynamic	
α	C_0	C	μ_{max}
15	12.9	5.5	0.2

The rod end has been selected from the SKF catalogue "*spherical plain bearings and rod ends*", and it has been chosen the rod end SA 8 whose technical characteristics are listed in tab.2.16. The coefficient μ_{max} refers to the maximum radial friction of the bearing inside the rod end; the roll angle is half of the total mobility capacity of the rod end around the bearing. On the rod end is effectuated one static and one dynamic evaluation. For both we have referred to the SKF catalogue. For the static evaluation must apply:

$$P_{perm} = C_0 b_2 b_6 \qquad F_a < 0.1 C_0 \qquad b_6 = 0.5 \qquad b_2 = 1 \tag{2.56}$$

The coefficients b_6 and b_2 take into account the type of load, alternate in this application, and the exercise temperature. The force F_a is the axial force of internal bearing of the rod end. In this application the bearing is subject of almost pure radial force, the low axial forces measured during the dynamic study are neglected. Aa result we have a permissible load of $6.25[kN]$, far more big than the required. The dynamic evaluation must apply:

$$\frac{C}{P} > 1.25 \qquad\qquad P = yF_r \tag{2.57}$$

Where P the equivalent dynamic load which depends on the radial load of the bearing, F_r, and from a coefficient y function of the radial and axial load ratio. Even this condition is verified. Furthermore the dynamic evaluation requires that the rod ends work conditions must be checked by considering the actual work pressure, p, and a sliding speed, v, between the bearings parts. They can be verified through the following equations:

$$p = K\frac{P}{C} \qquad v = 5.82 \cdot 10^{-7} d_k \frac{4\beta}{t} \qquad \beta = 14.4^\circ \tag{2.58}$$

$$t = 1[s] \qquad d_k = 10[mm] \qquad K = 50[N/mm^2] \tag{2.59}$$

Where β is the half angle of the total oscillation during the rod end movements and t is the time required for a total oscillation. It is considered

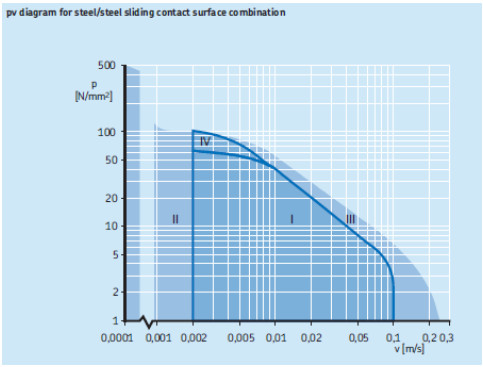

Figure 2.37: Graph pv

the maximum oscillation and sliding velocity measured during the dynamic study. The term d_k takes into account the bearing size whereas the coefficient K takes into account the bearing type and its contact surface; the bearing chosen has a type of contact steel/steel. Evaluated p and v is possible to use a graph pv, fig.2.37, to verify the field of applicability of the solution. In this case the values $p = 4.78[N/mm^2]$ and $v = 0.3 \cdot 10{-}3[m/s]$ satisfy the dynamic evaluation.

It is possible to notice how both static and dynamic evaluation suggest that the rod end is oversized in respect to the loads measured. Here too the physical dimensions of the component has been influenced by its connection with the link on one side and the pivot of the universal joint on the other.

Universal joint

For the design of the linear delta is fundamental the design of the universal joint which connects the links to the sliders and to the platform by allowing two degree of freedom, the rotations α_1 and α_2.

In fig.2.38 and 2.39 are presented the two constraints on the slider and platform sides. The two constraints are identical in their kinematic even though they have been adapted to fit into two different parts of the machine. By referring to fig.2.41 it is possible to see how the realization of the universal joint is made through the use of two bronze bushings which allow the rotation of a pivot. This is one of the two rotations allowed by the constraint and it is the one called α_1. This rotation has the only limit imposed by the interferences among links, platform and linear guides. The rod ends are connected to the pivot and they are free to rotate around their bearing axis. This relative rotation between rod end and pivot is α_2. In fig.2.42 is possible to see how this angle is limited by the interference between the link and the universal joint itself. The maximum value of α_2 obtained during the mechanical design of the universal joint has been a little more of 45°. The lock nuts are needed to tight the pivot in a centred position among the

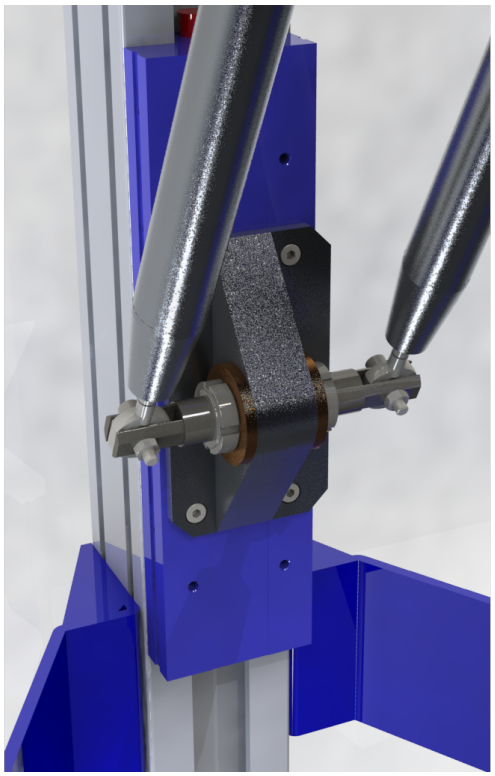

Figure 2.38: Universal joint on the slider

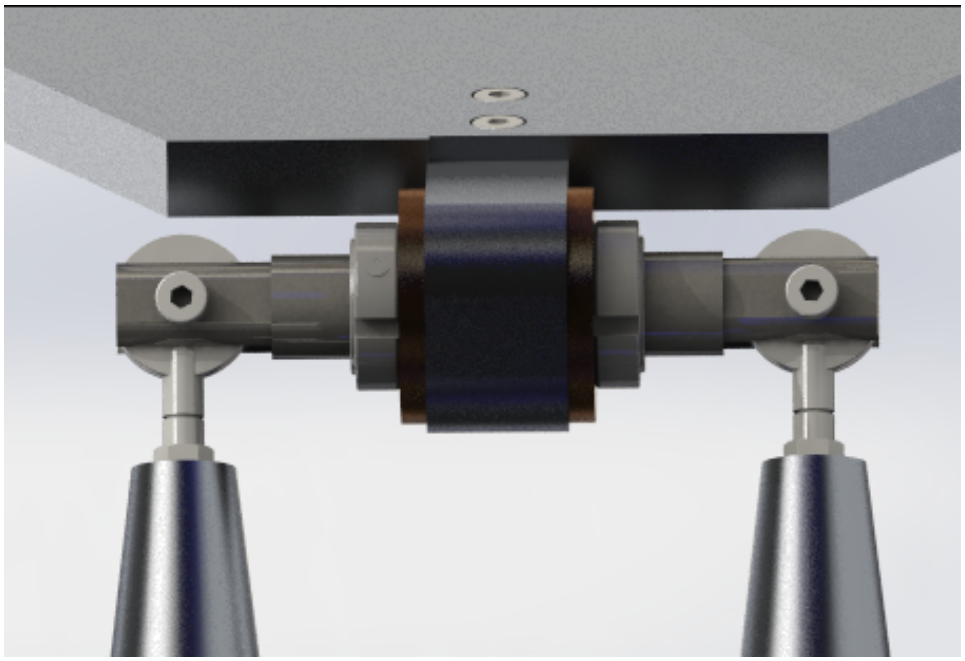

Figure 2.39: Universal joint on the platform

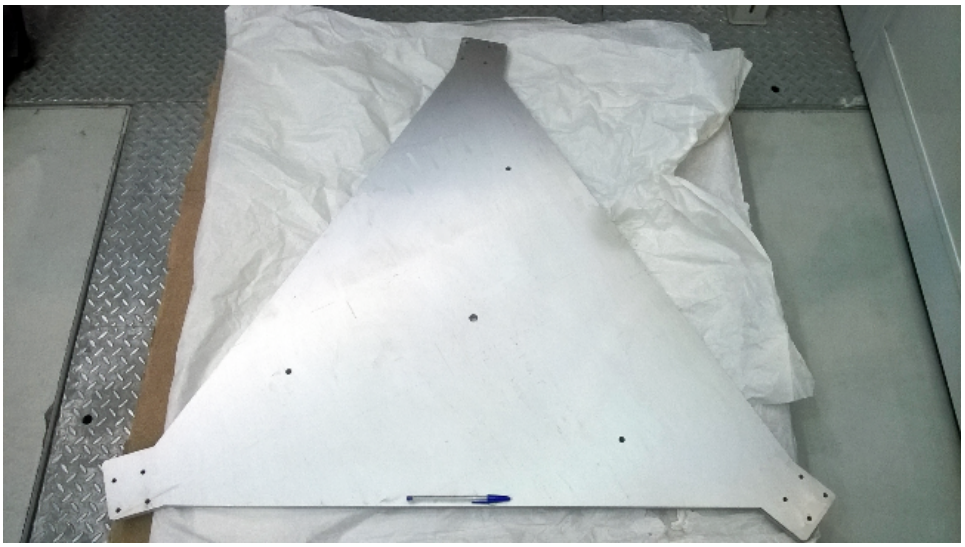

Figure 2.40: Moving platform of the linear delta

Table 2.17: Bushing SKF PBMF 253516 M1G1

Material	Admissible load[MPa] static	dynamic	Creep speed[m/s] max	μ
Solid bronze	45	25	0.5	0.15

two bushings.

For the choice of the bushings we have referred to the SKF catalogue *bushings, thrust washers and strips*, and it has been chosen the flanged bushing PBMF 253516 M1G1. In tab.2.17 are reported its technical data. The bushings has the duty to bear the torques and radial forces transmitted by the pivot to the linear guide and that have been measured during the dynamic simulations. The maximum forces and torques measured are:

$$F_{t,max} = 308.7[N] \qquad T_{p,max} = 54.8[Nm] \tag{2.60}$$

The bushing can exercise a radial force in respect of their own axis. Looking at fig.2.43 is possible to see how the bushing choice is function of their distance d between the centres of application of their respective forces; this distance is fundamental to allow the bushing to withstand the pivot torques. As application centre for the forces we chose the midpoints of the bushings. The force exercised by the single bushing is:

$$F = \frac{C_{p,max}}{d} + F_{t,max} = 3048.7[N] \qquad d = 20[mm] \tag{2.61}$$

108

Figure 2.41: Exploded view of the universal joint on the platform

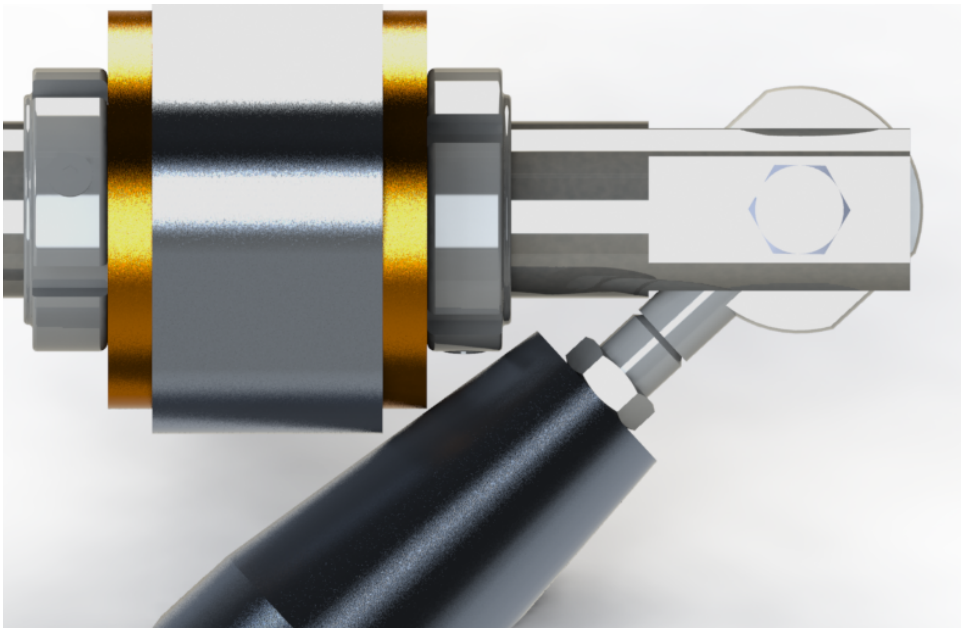

Figure 2.42: Limit of α_2

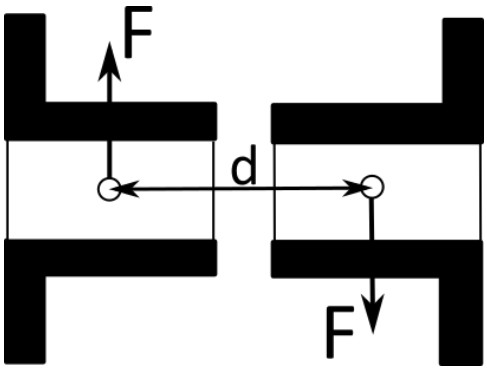

Figure 2.43: Forces exercised on the bushings

The final value of d derives from a series of trials on the dynamic and static load evaluation among several bushings taking into account their size that must fit with the pivot diameter and other parts of the universal joints. The technical verification on the single bushing consists of verify that the specific load p do not cross the upper limit of the dynamic load and that the sliding velocity does not exceed the value 0.5[m/s].

$$p = \frac{F}{d_b \cdot b} = 7.62[MPa] \tag{2.62}$$

The terms d_b and b of the eq.2.62 are respectively th internal diameter of the bushing and its length. The check on the dynamic load is succeeded. To evaluate the sliding velocity between pivot and bushing we use the maximum angular velocity of the pivot obtained during the dynamic simulations, $\omega_{p,max} = 104[deg/s]$, and here too the limits are respected.

$$v_{s,max} = \omega_{p,max} \cdot \frac{d_b}{2} = 0.023[m/s] \tag{2.63}$$

The pivot of the constraint is realized in steel, only component in the linear delta. This mainly because the use of the bronze bushings force to have a pivot with an high superficial hardness with a value between 165 and 400 HB; this in order to avoid a wear of the pivot itself. This hardness values are very difficult to reach for an aluminium and that is why a steel has been chosen. At its extremities the pivot has been machined in order to host the rod ends and to let one of their rotations free to move. The central part of the pivot has a bigger diameter than its extremities in order to create a mechanical stop for the lock nuts.

For the pivot have been verified that the stresses during exercise were not too high in order to limit the strains. By considering the maximum force on the link, $F_{x,max} = 526.3[N]$, applied in the worst case orthogonal to the pivot axis, and it is evaluated the maximum stress in two critical sections of the pivot, outlined in fig.2.44. In this two sections we obtain the torques:

$$M_1 = 8947.1[Nmm] \qquad M_2 = 20788.9[Nmm] \tag{2.64}$$

For the section 1 we consider the inertia of two rectangular sections outlined in blue in fig.2.44 and whose area is comprised inside the total area of the section. This choice, which diminishes the total area of the section, increase the safety margin. For the section 2 we use the exact inertia of the section and we use a notch factor of $K_t = 2.5$. The maximum stresses obtained here are:

$$\sigma_{x1,max} = 46.6[MPa] \quad \sigma_{x2,max} = 33[MPa] \quad \epsilon_{x1,max} = \frac{\sigma_{x1,max}}{E} = 0.218 \cdot 10^{-3} \tag{2.65}$$

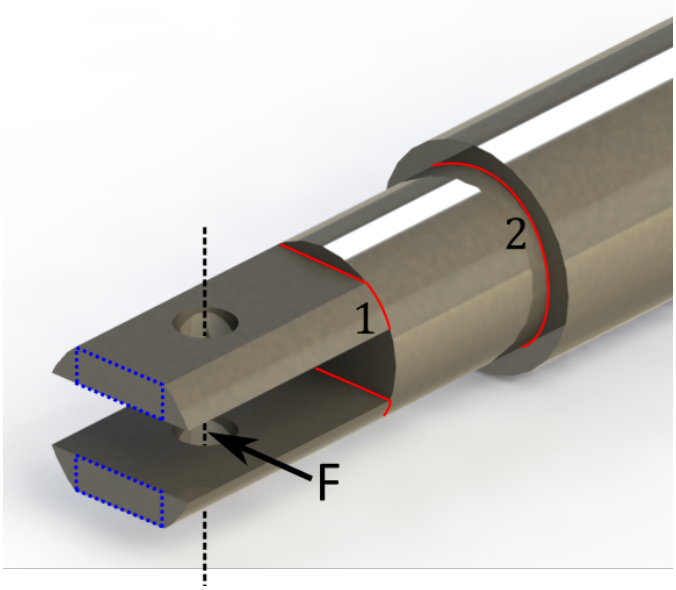

Figure 2.44: Pivot critical sections

Table 2.18: Steel C40

$R_{p0,2}[MPa]$	$R[MPa]$	$E[GPa]$	HB
460	750	220	180

For the typology of steel to use for the pivot we must take into account the maximum stresses, which are pretty low, and of the superficial hardness for a good coupling with the bushings. It is chosen a C40 steel whose mechanical characteristics are shown in tab.2.18.

In regard of the universal joint design we conclude with choice of the lock nuts which is basically driven by the pivot diameter. The lock nuts must fix the pivot position and bear its axial load; the maximum load measured is 68.7[N]. It has been selected a lock nut SKF KMK 4 capable to stand loads far more severe.

2.8.2 Support structure

After the design of the linear delta mechanical components we proceed with that components that take part of the supporting structure of the entire printer; besides to bear the weight of the printer some of this components are used to increase the stiffness of the structure in order to avoid undesired vibrations. For the latter reason this components are largely oversized in respect of the extruder weight, positioned on top of the printer, and of the low dynamic loads. In fig.2.46 is shown a plate positioned at the printer base;

(a) Lock nut

(b) Rod end

Figure 2.45: Components of the universal joint

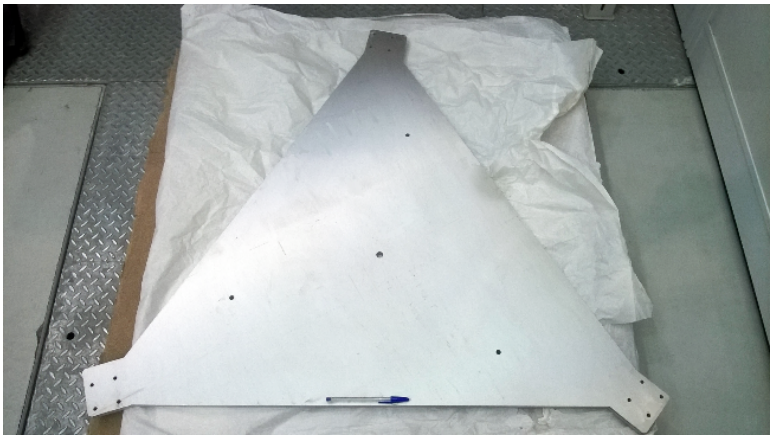

Figure 2.46: Plate at 3D printer basis

this component have been extracted from an aluminium sheet of 15[mm]. The duty of this component is fundamental, not as a structural part, but in order to correctly mount the linear guides on the ideal circle of diameter D and with a relative angle of α; both evaluated during the kinematic optimization. This concept is more understandable taking a look at fig.2.47 where it is shown on of the three attaching points between the plate and the linear guides. It is possible to notice how a mounting foot is used to lean the structure to the ground.

Laterally on the printer are mounted three structures used to increase the stiffness of the system, fig.2.48a. The linear guides chosen are not designed to have an high bending stiffness and so there is the risk to obtain undesired vibrations due to the presence of the extruder on top of the machine and to linear guides too much long. Steel sheets of 6[mm] width have been shaped and used to constraint the linear guides and without limiting the linear delta workspace. A support structure was needed to mount the extruder on top of the entire machine, fig.2.48b. The extruder is fixed while the linear delta moves its platform under its nozzle.

At the end of the mechanical phase we obtain the result of this design process, the complete printer, fig.2.49 and fig2.50.

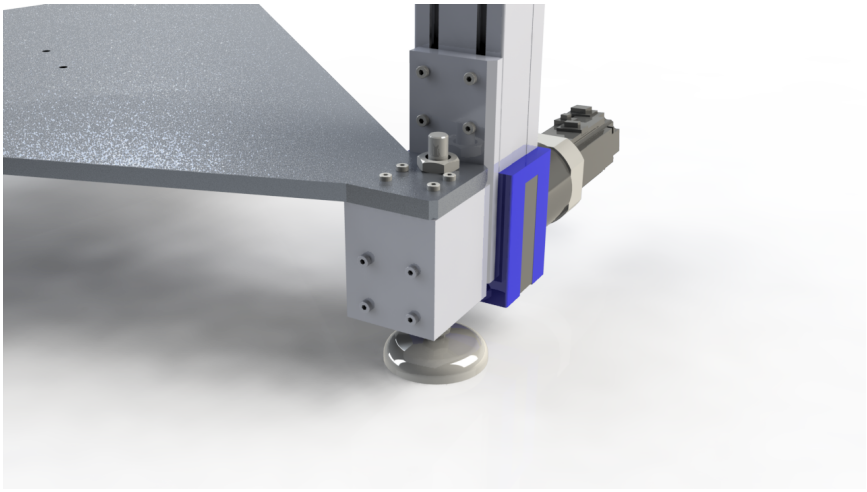

(a) Basis support

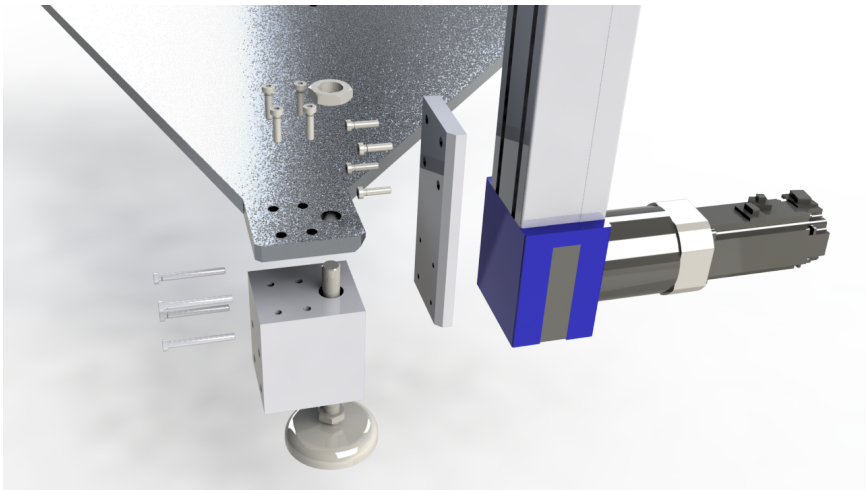

(b) Explode drawing

Figure 2.47: Basis support of Efesto printer

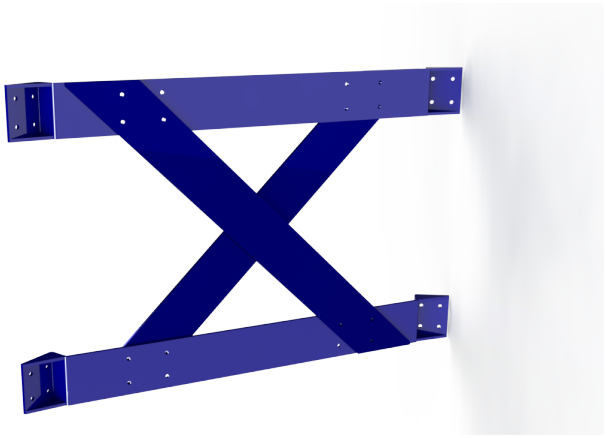

(a) Lateral suppport

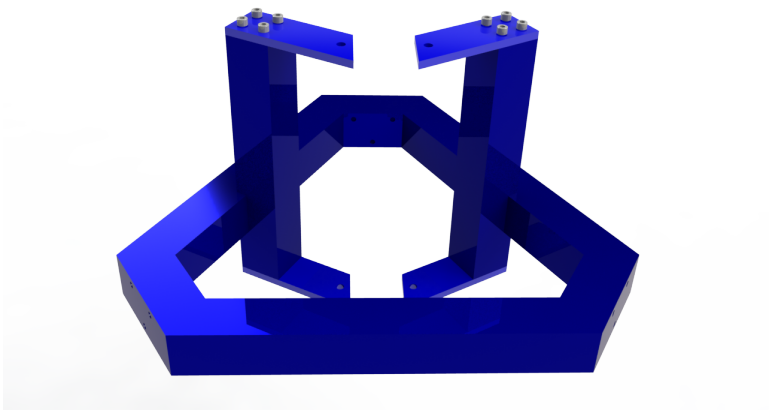

(b) Extruder suppport

Figure 2.48: Lateral and extruder support of Efesto printer

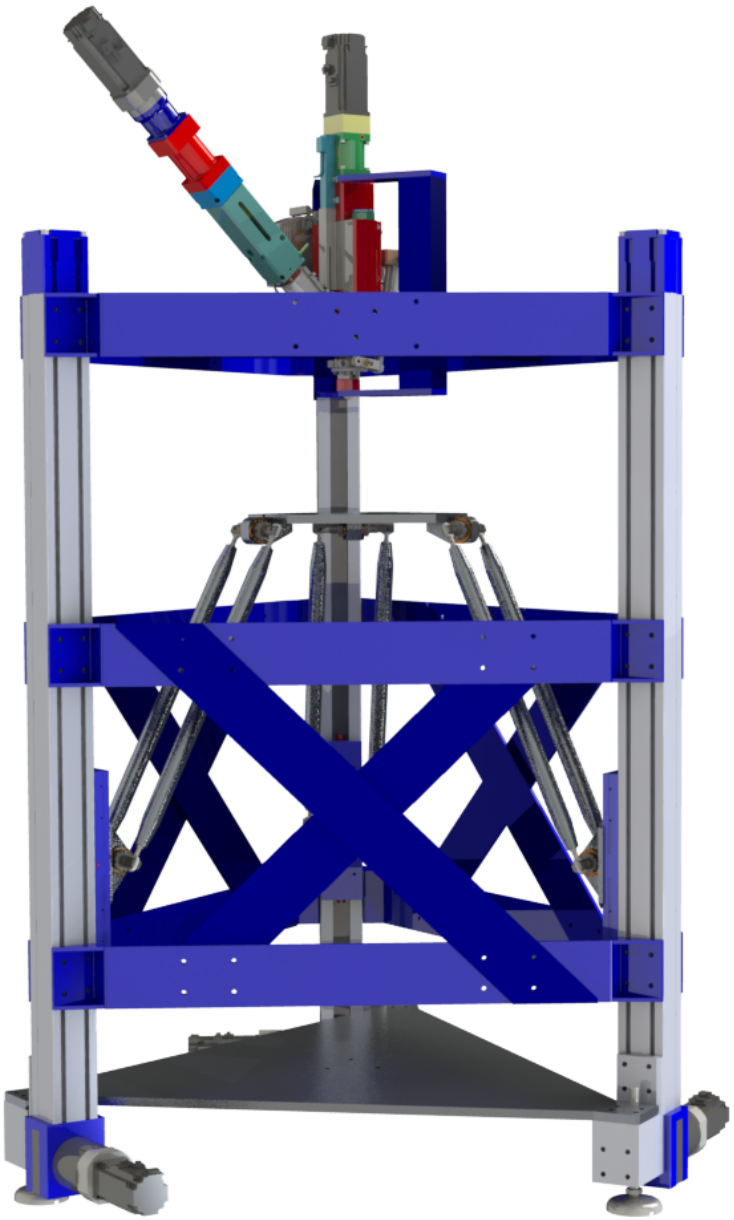

Figure 2.49: Efesto rendering

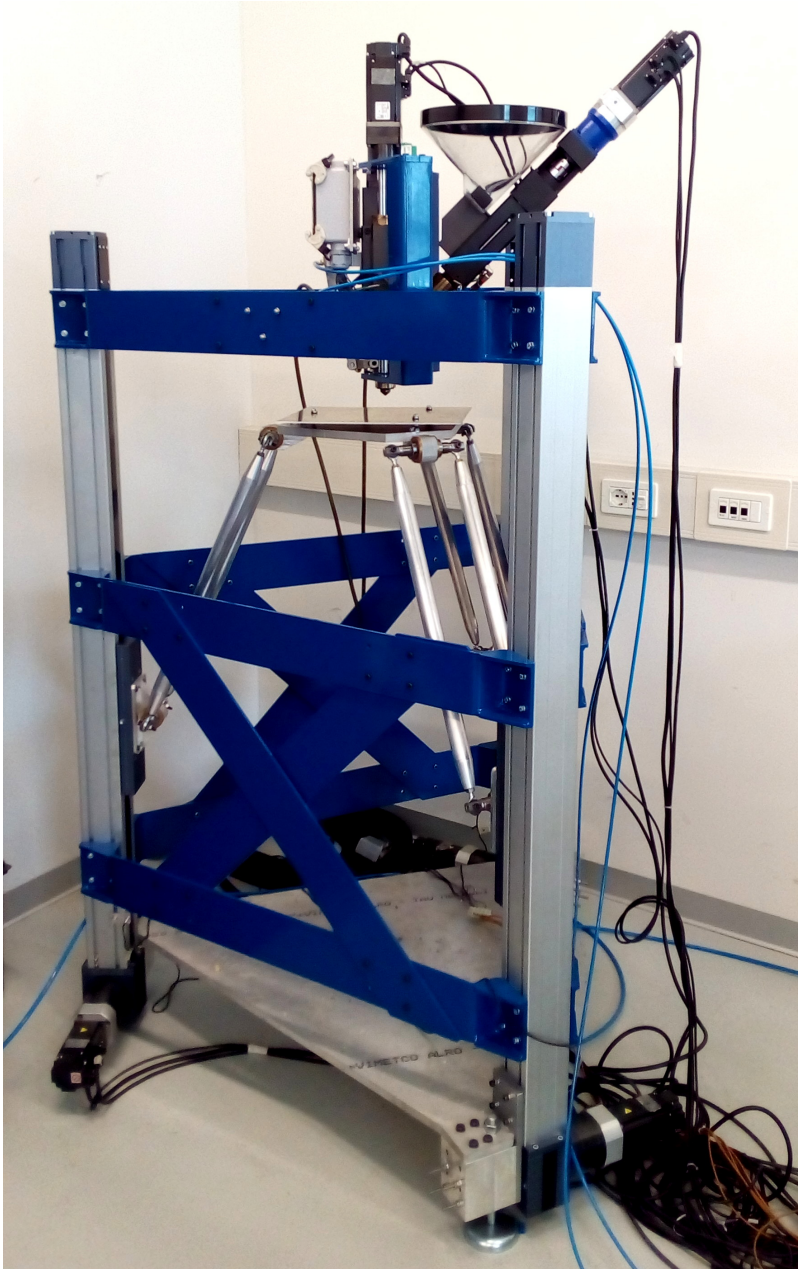

Figure 2.50: Efesto 3D printer

2.9 Control System and Communication

The printer control system is chosen among some off-the-shell solutions by taking into account that the system architecture must allow the manufacturing of components according to the production chain of AM as described in cap1, by starting from an STL file and by ending with the printing of the component. At the same time must considered the prototyping nature of the Efesto machine; the single phases of the production chain must be customizable in order to allow their improvement for the AM process here proposed and to study their influence on the overall chain. During the development of a prototype can be necessary to customize the general AM production chain to the specific process of the Efesto machine. For instance the standard phases for a 3D printing requires the use of a g-code in order to correctly instruct the machine on how to carry on the manufacturing process; the g-code is a language which contains specific commands tied the the machine utilised, for instance *turn on a fan* or *turn off the mill* or other commands referred to specific machine parts. There is no commercial slicing software, software dedicated to the creation of a g-code for AM machines, capable to generate a g-code for the Efesto machine; just the fact that the extruder has 3 resistors, which is unusual respect to many AM printers, lead to the necessity of some tailored solution.

In the market it is possible to find different systems which allow to obtain a customized solution. Many of these are in the field of multi-axis control and CNC systems; an example is the one offered by the company Delta Tau with the controller Power PMac [7] which with the use of a linux real-time operating system allows to control a multi-axis system, based on a generic kinematic solution, and the control of several I/O, input-output. A solution like this would be oversized for the necessity of the Efesto machine and in the end it is decided to chose on an architecture more similar to the one of a CNC machine with a PLC for the soft real-time operations and a motion unit for the control of the actuators.

To facilitate the integration of the control system with electric motors it has been decided to take it from the same automation vendor. In tab.2.19 are listed the components chosen and the relative code and where it is presented the software used to program it. It is possible to notice that other the PLC and Motion have been taken I or O systems digital, D, and analogous, A, and a temperature control module, T. A screen is used as HMI, human-machine-interface, with the operator of the machine. The all components have been integrated inside an electrical cabinet dedicated to the machine, fig.2.51. It is possible to notice how a personal computer, PC, is used together with the control system. The PC is directly connected through USB to the PLC and it completes the series of components used to control the printer. The choice of such a system on one side allows to fulfil all the necessary steps for the management of the printing process, minimum goal for the control

(a)

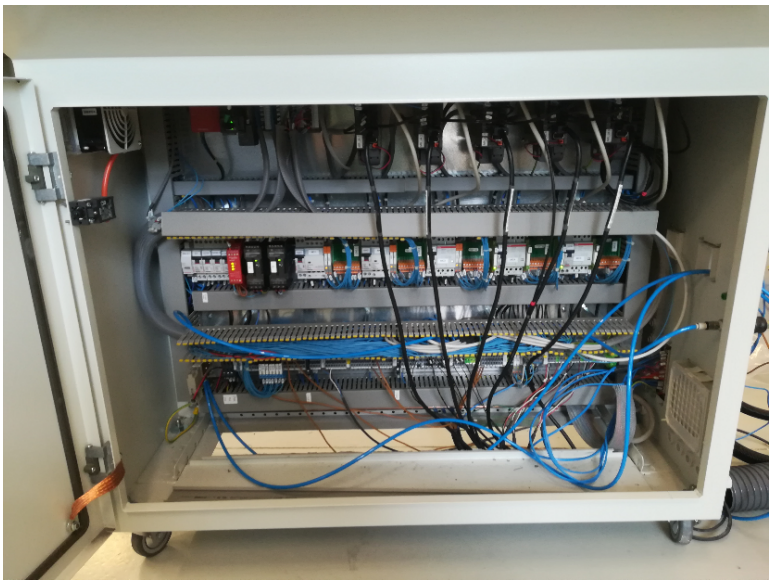

(b)

Figure 2.51: Electrical cabinet

Table 2.19: Control system Mitsubishi Electric, hardware and programming software

Component	Hardware	software
PLC	Q03UDVCPU	GX-Works2
Motion	Q172DSCPU	MT Developer2
D/O	QX80	–
D/I	QY80	–
A/I	Q64AD	–
T	Q64TCTTN	–
HMI	GS2107	GTD3
Servo	MR-J4-40B	MR Configurator

system, on the other to customize the several phases of the printing process. These phases with the control system here presented are the following:

1. A CAD file is created of the object ot print in an STL format.
2. The file is processed and a g-code is generated for the machine.
3. The g-code data are passed from the computer to the internal memory devices of the control system
4. The data are processed by the PLC and Motion in order to execute the printing process

These four passages can be all implemented in different ways according to the necessities; in this work we will focus on the last two steps which will be programmed on the exact necessities of the printer. Specifically the system is used in the following way:

- the g-code for the printer is generated from an open source software, as Slic3r, or it can be created in a customized way with other software as MatLab.
- The g-code data are pre-processed and send to the control system through a desktop application for Windows OS developed in C#. Such application has been developed integrating some Mitsubishi libraries which allow the serial communication with PLC and Motion.
- Inside the PLC and Motion are developed the functions needed to handle the system I/O, as the extruder temperatures, and the logics required for the trajectories generation for the axis.

The system developed in this way allows a wide freedom in the management of the printing process and at the same time it compensates an

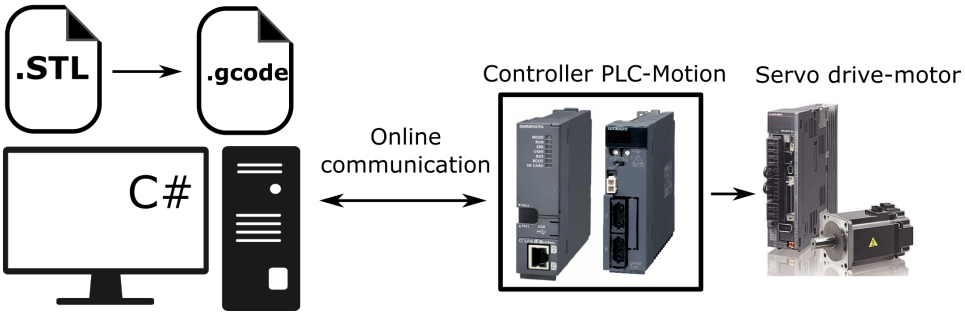

Figure 2.52: Architecture of the control system

intrinsic problem of the equipment chosen, which is the limited memory available. The PLC and Motion are systems developed to work under defined cycle times, this means that they must be able to process a specific amount of programming instructions in a specific amount of time. In order to do that the access to the data stored in the memory devices must be very fast, and that is why it is necessary the use of memories whose cost is not negligible and that in this system are limited to few megabytes. This amount of memory is relatively small for the needs of a 3D print. The amount of data coming from a g-code is too big to be stored entirely in the internal memories of the control system(PLC-Motion). We can work around the problem through the use of a desktop application which is not only used to pre-process the g-code and send the data to the controller, but it is used to maintain an interactive communication with it. The data relative to the print of a specific object are stored in the PC and they are passed iteratively to the controller in an amount that it can handle. The solution so presented allows to use a control system which was not fitted for the 3D printing. We present a:

Tailored solution which allows maximum flexibility in its use with respect to AM technology starting from generally rigid automatic systems such as PLCs and Motion units.

In fig.2.52 is shown the system architecture, starting from the computer where are elaborated the stl and g-code files, the control system made of the PLC and the Motion unit and ultimately the servo drives with their motors. In this architecture the Motion units deals with the hrad real-time operations as the coordination of the servo drive, instead the PLC takes care of the soft real-time operations as the extruder temperatures control, the management of the cooling system(it is present a little water cooling system to protect from excessive heat the motors on the extruder), and to handle the request of the operators coming from the HMI.

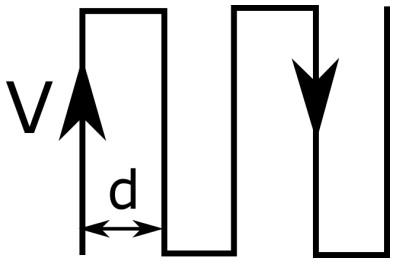

Figure 2.53: Path of the experiment

Table 2.20: Parametes of the experiment

V	printing speed
Q	flow rate of the extruder
d	two adjacent wires distance

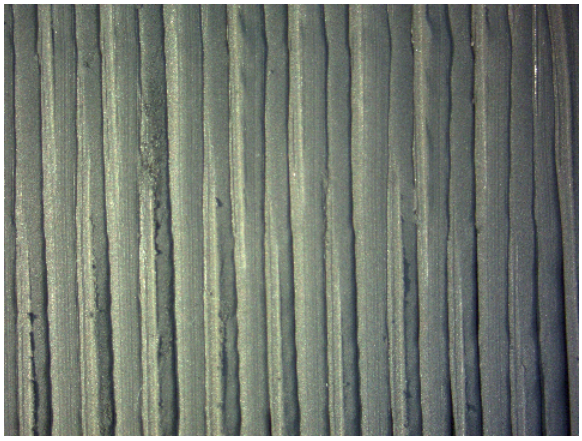

Figure 2.54: Zoom of a test sample

2.9.1 Open system example

To clarify the concept of open system and the possibilities of customization given by the proposed architecture we show an example whre the Efesto machine has been utilised [2]. During the experimentation phase of the Efesto machine it has been tested the influence of the parameters printing speed, material flow rate and wires overlapping. In order to do that an experimental campaign it has been executed where several samples have been printed by varying the parameters listed in tab.2.20. The printing path is very simple and it is shown as example in fig.2.53 and one of the samples obtained is shown in fig.2.54. The parameters control have been possible thanks to a customized g-code created in MatLab where it has been defined the path points in the linear delta workspace, the linear delta velocity and the velocity of the extrusion piston which is related to the material flow rate. An experiment like this, which is needed to test the process parameters of the machine on the printing quality result, would be difficult, if not impossible, to carry on with slicing software not dedicated to the machine where such parameters or do not exist, as the extrusion piston velocity, or they are not directly expressible, as the distance d between two material wires. The

[2]We thanks here the ing.Castelli author of the study here described.

concept of customized solution will be taken up later in this work during the study on the trajectories generation of the machine.

2.9.2 Communication

The machine Efesto is conceived as an industrial machine and as such its communication capabilities are fundamental. In the latter of this work, in the cap.5, it is shown and discussed the importance of communication for the industrial machines integrated in an industrial environment. It desirable that the Efesto machine has the possibility to be integrate in such environment. In order to do so we define for the machine a communication interface which allows to share the internal data of the machine itself and to receive orders if necessary. The complete development of such a structure, meant as a reliable IT system, bugs free and which fulfil the requirements of an industrial environment is beyond the scope of this prototype, but we want to show how the architecture proposed could make possible such a development.

In fig.2.55 is shown the final result of the communication capabilities given to the machine, three web pages visualized on-line through a google chrome browser with an http communication with the printer itself. It is possible to see how the printer communicates through a server-client system, through what is basically a website. It is possible to notice how in the address bar has been typed directly the printer IP address and its communication port. The images refers to a communication happened on a LAN, local area network, between a desktop computer and the PC used on the printer. Of the three opened pages the first one introduces the Efesto project, the second allows to log-in through a username and password and enter in the last page where they are gathered in real-time the temperatures data of the machine.

This structure has been developed by starting from a web application template in ASP.net where it has been developed both the client side n(HTML-JS-CSS) and the server side(C#) of the application. Inside the application have been integrated the functions developed in C# which allow the communication with PLC and Motion. The web application has been released on the PC through the use of the application IIS 7.5, internet information services, of Microsoft. The solution so proposed use the PC of the control system as ingress point of the machine by allowing the data sharing through an http communication.

The example here shown is limited on gathering real-time the 4 temperatures of the extruder; at the same time with the same architecture we can imagine several applications based on the availability of an active machine connection where it is possible to retrieve any kind of data from the machine itself. Today there are industrial examples which show the importance of this concepts. General Electric has launched the platform Predix [8]; this platform allows to connect a GE machine to a remote assistance service

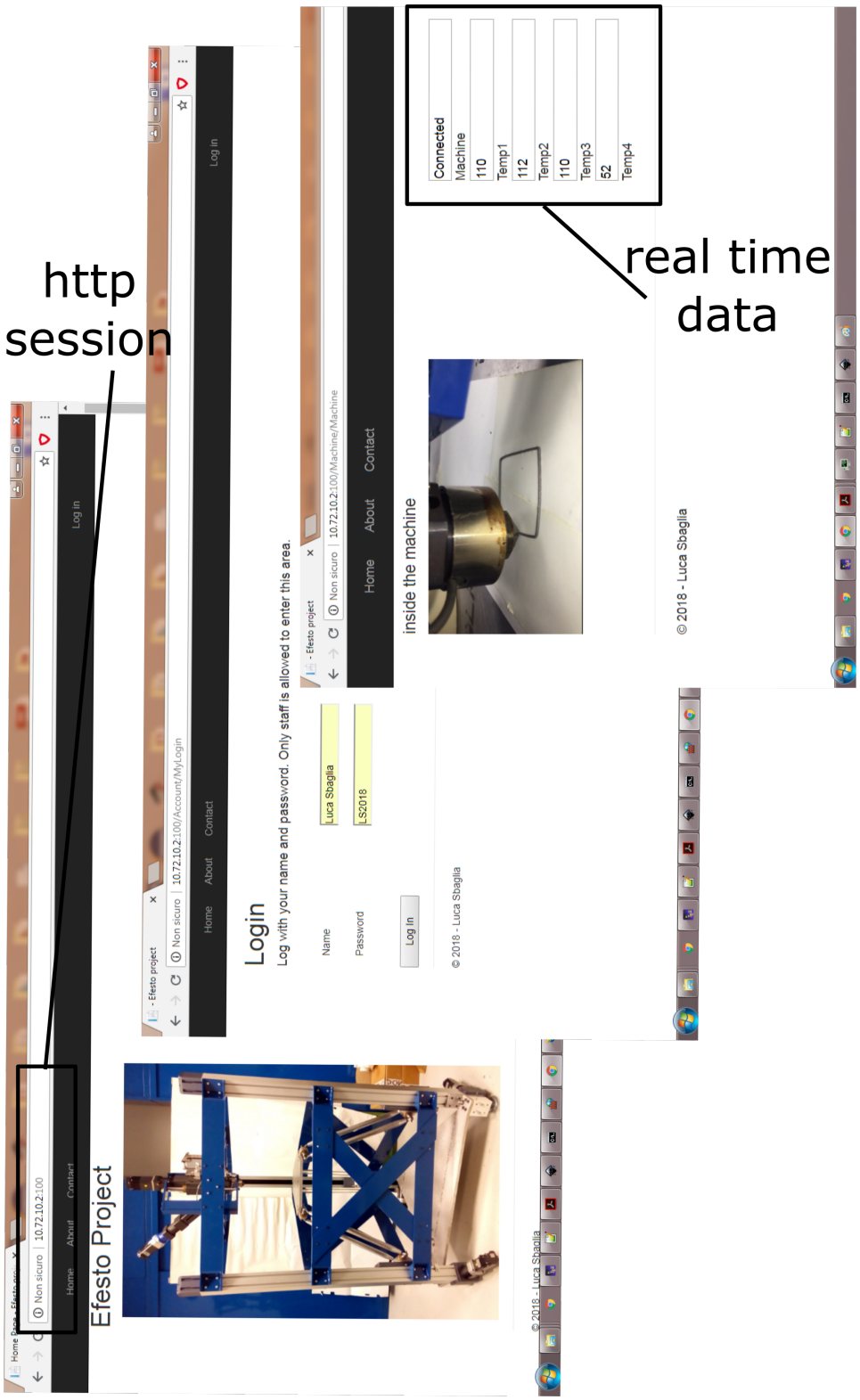

Figure 2.55: Web connection through Google Chrome

where the machine is monitored constantly. From one side is offered a service to a client allowing to anticipate undesired idle times and to schedule maintenances when required, on the other GE can gather a continuous flow of data and informations for a continuous improvement of their machines. These services are based on a digital version of the real world. Siemens has launched its platform digital enterprise suite [18]. In this case is proposed a service based on the complete digitalization of an industry and so to the connection of every manufacturing machine to its digital version. The purpose of this solution is not only the connection of the machines with software as MES or ERP but the possibility to simulate in advance a production process; in an industrial world aiming to the production of customized and unique components with reduced lead times the products must be produced well the first time they are put into production [17].

These real examples show where the industrial production is going and how the machine communication abilities are fundamental for this evolution. In the Efesto machine we take under consideration this necessity by predisposing the system to the sharing of its internal data. We have given a little demonstration by exampling the architecture of the communication process.

2.10 Conclusions

AM machines have always had an architecture taken from CNC machines with minimal flexibility compared to the needs of this technology and its individual processes. On the other hand, the design of industrial machinery has increasingly exploited holistic solutions that take into account the mechanical, electrical and control parts consistently through mechatronic approaches and through the use of increasingly advanced design tools. Here we propose a specific and tailor-made solution for a specific additive manufacturing process based on an extrusion system and a linear delta; the solution has been optimized through the use of state-of-the-art software tools. The conceived machine has been equipped with a flexible control architecture in its various parts in order to meet the needs of development and customization of the machine itself, at the same time ensuring the execution of those steps necessary for an AM process. The machine was designed to live within an industrial environment and it has been predisposed to have communication interfaces.

bibliography

[1] M.K. Agarwala, V.R. Jamalabad, N.A. Langrana, A. Safari, P.J. Whalen, and S.C. Danforth. Structural quality of parts processed by fused deposition. *Rapid Prototyping Journal*, 1996.

[2] Y. Altintas. *Manufacturing Automation: Metal Cutting Mechanics, Machine Tool Vibrations, and CNC Design.* Cambridge University Press, 2012.

[3] O.L. Asato, E.R.R. Kato, R.Y. Inamasu, and A.J.V. Porto. Analysis of open cnc architecture for machine tools. *Additive Manufacturing*, 2002.

[4] S. Bertozzi. Design di un ugello per stampaggio tridimensionale di materiali per fused deposition modeling of metals (fdmm). Master's thesis, Politecnico di Milano, 2015.

[5] A. Boschetto and L. Bottini. Accuracy prediction in fused deposition modeling. *International Journal Advanced Manufacturing Technology*, 2014.

[6] A. Boschetto, V. Giordano, and F. Veniali. Modelling micro geometrical profiles in fused deposition process. *International Journal Advanced Manufacturing Technology*, 2014.

[7] Delta tau website. http://www.deltatau.com. accessed september 2018.

[8] General electric website. https://www.ge.com/digital/. accessed september 2018.

[9] H. Giberti, S. Cinquemani, and G. Legnani. Effects of transmission mechanical characteristics on the choice of a motor-reducer. *Mechatronics*, 2010.

[10] H. Giberti, S. Cinquemani, and G. Legnani. A practical approach to the selection of the motor-reducer unit in electric drive systems. *Mechanics Based Design of Structures and Machines*, 2011.

[11] J. Go, S.N. Schiffres, A.G. Stevens, and A.J. Hart. Rate limits of additive manufacturing by fused filament fabrication and guidelines for high-throughput system design. *Additive Manufacturing*, 2017.

[12] Giberti H., Clerici A., and Cinquemani S. Specific accelerating factor: One more tool in motor sizing projects. *Mechatronics*, 2014.

[13] S.J. Keating. *Renaissance Robotics: Novel Applications of Multipurpose Robotic Arms spanning Design Fabrication, Utility, and Art.* PhD thesis, Massachusetts Institute of Technology, 2012.

[14] R. Kelaiaia, O. Company, and A. Zaatri. Multiobjective optimization of a linear delta parallel robot. *Mechanism and Machine Theory*, 2012.

[15] J. Lia, Z. Xieb, X. Zhangc, Q. Zengd, and H. Liue. Study of metal powder extrusion and accumulating rapid prototyping. *Key Engineering Materials*, 2010.

[16] J.P. Merlet. *Parallel Robots-second edition.* Springer, 2006.

[17] Driving the digital enterprise. https://www.youtube.com/, 2016. accessed september 2018.

[18] Siemens website. https://www.siemens.com/global/en/home/company/topic-areas/future-of-manufacturing/digital-enterprise.html. accessed september 2018.

[19] M.J. Uddin, S. Refaat, S. Nahavandi, and H. Trinh. Kinematic and dynamic modeling of a robotic head with linear motors. *School of Engineering and Technology - Deakin University*, 2003.

[20] Modeling apparatus for three-dimensional objects. 1994 -assignee Stratasys Inc.

[21] Us patent 8951033 - construction box for a rapid prototyping system. 2010 - assignee ExOne GmbH.

[22] L. Xinjun, W. Jinsong, L. Tiemin, and D. Guanghong. Parallel mechanisms with two or three degrees of freedom. *Tsinghua science and technology*, 2003.

Chapter 3

Calibration

introduction

The Additive Manufacturing processes based on the use of extrusion method are in a constant growth. The studies, aimed to the quality improvement of these processes, are focused or on the optimization of the process parameters or on the calibration of the robotic system used on support of these processes. The calibration of the robotic systems are often aimed to reach high level performances on the accuracy and precision of the robot itself and by consequence they aim to satisfy the technological process where the robots are applied. Such robot performances are often oversized in respect of the true requirements of the technological processes, in particular as regards the AM extrusion processes where a specific calibration can reduce the necessary efforts to make the robotic system suitable for the printing phase. In this chapter is studied the calibration of AM extrusion processes inside which the Efesto project is comprised. We start from the technological limits which characterize this family of processes by ending with the evaluation of success maps of the robotic system calibration. Applying this study to the linear delta are shown the several phases of a robotic calibration; starting from the mechanical tolerances and from the technological limits of the application we apply a stochastic method in order to evaluate the goodness of the calibration procedure and of its phases. The entire process is simulated in order to foresee the success probability of the process itself.

In the following we start by pointing out the concept of a calibration focused on the process. Right after we show some examples in the literature of robot calibration to give a better understanding to the reader of this field. After these parts which describe the framework, the study starts with the description of the limits of the AM extrusion processes and the definition of a yardstick for the evaluation of the robotic systems applied to these applications.

3.1 Calibration of AM extrusion processes

Many researches are going on trying to improve the quality of the AM processes, in particular as regards the ones based on the extrusion of material for the printing phase [28]. The improvements of these processes can be faced in two ways; or through the optimization of the process parameters as the layer thickness, raster angle, nozzle diameters or others [20, 25], or through the robotic calibration of the mechanical system applied to the 3D printing process. The calibration process of a robot has been largely studied in the literature and we can find several description on how to execute it, both on serial than on parallel robotic architecture [10, 21]. In the field of robotic the calibration goal has always been the improvement of the accuracy and precision of the system regardless of the application field of the robot itself.

The AM extrusion processes are based on the selective deposition of material on printing planes, usually denoted on $x - y$, along a printing direction, usually indicated with z, until is created the 3D object. If we take as representative of the AM extrusion processes the FDM, fusion deposition modelling, we can see how the typical precision of the printed parts with these systems is in the order of $\pm 100 \mu m$ in the plane $x - y$ [27]. Along the printing direction, z, the precision is dictated by the process parameter layer thickness and it is in the order of few tenth of millimetre [5]. Lower is the the single layer height better is the surface finish of the printed part, on the other hand the printing time increase. It is usually searched for a compromise by considering that the minimum height possible is limited by the system itself [27].

In the project Efesto has been chosen a parallel kinematic architecture based on the use of a linear delta; this choice is not very common in the AM field even though in the last years there is been an increase in the use of this robotic solution [3]; this robot by having an high dynamic and a prevalent direction of displacement , its vertical axis or z axis, is suitable to be used in the AM field. The linear delta belongs to a robot family coming from the delta robot. In the literature the calibration effectuated on this robot family are aimed to reach a precision level which is beyond of the necessities shown by the FDM numbers, for example in [23, 29] is reached a precision in the order of the μm, much lower than the tenth of millimetre. In [2, 8] the precision required is in the order of the tenth of millimetre, but in the first it is not specified the application field of the robot, making impossible to evaluate its suitability to the application, in the second the application is surgical operation but the limits required by such application are not explained. In general a bigger precision is more suitable to any kind of application but it requires mechanical components with high manufacturing precision and more complex and onerous measurements; a calibration aimed to a specific application can minimize the required efforts

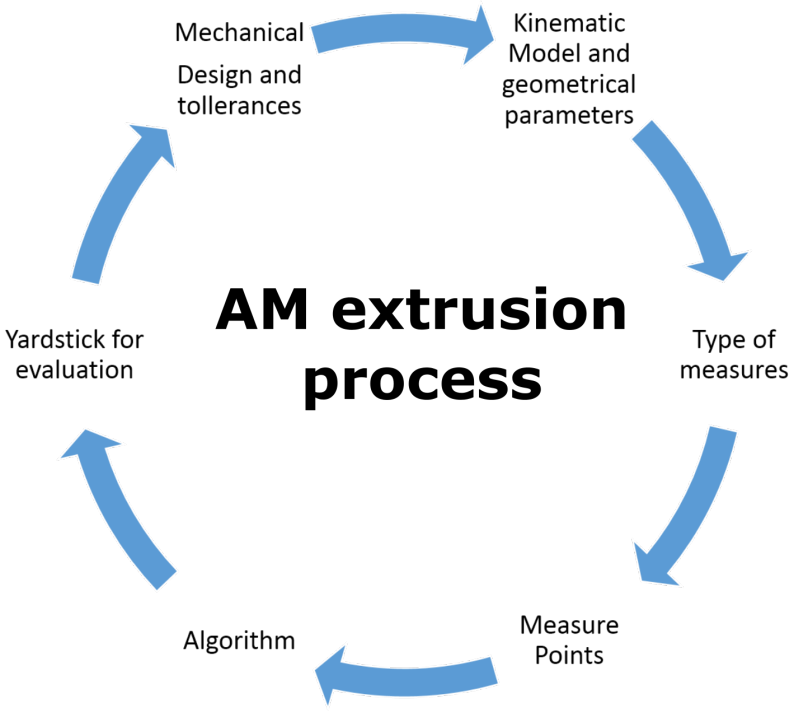

Figure 3.1: Phases for the evaluation of an AM extrussion process

to comply the operations to follow.

In any industrial process the final goal is not the precision of the robotic system but the quality of the piece produced. In many calibration process of mechanical systems it is not taken under consideration the application field and the calibration procedures are evaluated according to the concepts of precision and accuracy and not according to the quality of the process obtained. If we consider the limits of an AM extrusion process, whose maximum representative today is the FDM, and the method according which it is executed we can establish a yardstick for the evaluation of a mechanical system suitability for such application. Starting from the mechanical tolerances of the robot, which are at the basis of its kinematic errors, we propose a stochastic method which connects them to the success of the calibration process for an AM extrusion process application.

In fig.3.1 it is possible to see all the phases here considered central parts of a robotic system calibration with the goal to obtain a 3D printing extrusion process. The phases comprehend the choice of the mechanical system, its kinematic architecture and geometrical parameters and its constructive tolerances. For the calibration process if fundamental the type o measures effectuated, which and how much measure points are taken and the algorithm used to evaluate the actual values of the geometrical parameters. The

entire calibration chain is evaluated through a yardstick defined on the AM extrusion process and not on the robot. This work is represented in a circular way since it can be iterated several times or some of its phases can be changed in order to change the final result. In this study are done specific choices for each of the phases here shown and a series of simulations are carried out to obtain a success map which shows the result obtained.

3.2 Literature on robotic calibration

For a better understanding of the robotic calibration and to have a reference to the state of the art, here we describe the fundamental passages of a geometrical calibration and after we describe and discuss some works applied to the robot delta family by ending with the description of the robotic calibration here applied.

The calibration process, meant as the effort to improve the precision and the accuracy of a robot pose, is from a long time considered very important in all fields where automated machines are used [30]. The main causes of these inaccuracies are designing mechanical tolerances and mounting of the system, elastic deformations due to contact forces for instance and thermal deformations [10]. It is common to define as geometrical calibration the one which focus its efforts on minimizing the errors generated by mechanical tolerances by researching the values of the robot geometrical parameters. Generally a robot calibration is composed by a phase where a kinematic model of the system is defined based on the geometrical parameters to estimate, a measuring phase and a phase where an algorithm is used to extract from the measures the parameters researched [30]. In the field of PKM, parallel kinematic machines, a distinction is made depending on the measures type. Measures effectuated on the passive joints of the system, internal calibration, or measures of the robot pose, meant as the position and orientation of the end-effector, external calibration [21]. It is possible furthermore make a distinction between measures effectuated respect to an absolute frame, coordinate-based approach, or relative to the distance between two points, distance-based approach [2].

In the literature of robotic is not easy to find direct study on the calibration of the linear delta robot type rather on its kinematic synthesis [26]. It is easier to find studies on the calibration of the Delta robot, which is the father of the linear delta. The two solutions belong to the same robot family of 3 translational Dofs, degrees of freedom, furthermore they derive from the study of the same author [6], in fact it can be obtained a Delta robot by changing the first joint P of each chain of the linear delta with a revolute joint, R. In [29]is proposed a geometrical calibration study of the Delta robot based on two kinematic models, one with 54 parameters and one with 24. It has been taken 74 measure points uniformly distributed in the

robot workspace of $300x300x120[mm]$. As measuring system has been utilized a CMM, coordinate-measuring machine, able to measure position and orientation on the entire robot workspace. Two methods are presented for the geometrical parameters research, one based on a least-squares estimation with the use of the Levenberg-Marquardt algorithm, and one defined by the authors as a semi-parametric calibration based on a linearization of the system. It has been achieved an improvement of factor 15.2 in positioning and 3.7 in the robot orientation, meant as a ratio between the error before and after the calibration. In [8] is proposed a calibration of a Delta for neurosurgical applications based on a kinematic model with 18 parameters, relative measures and a workspace of $900x550x300[mm]$. Three dial gauges and a reference jig are used to effectuate the measures. It is proposed two least-squares estimation methods based on a linear and a non-linear model of the positioning error. The use of 40 measures has brought to an improvement of the robot position of the 90%. In [2] are utilized two kinematic models with 18 and 32 parameters for the realization of a real-time linear compensator for a Delta robot control system. It is effectuated an external calibration with relative measures taken trough a laser tracker. It is considered 7 and 9 poses for the calibration of the two models. The calibration is effectuated on a cylindrical volume of radius $250[mm]$ and height $500[mm]$; it is reported some improvements on the major distance error and on the volumetric error of the robot. In [23] we found a study on a linear delta applied in the FDM field where the extruder of the system is moved by the linear delta itself. Here is proposed a calibration method which starts by considering the relationships among the position errors of the robot inside the printing plate and the geometrical parameters. It is considered only 6 type of possible errors and of these only three are studied; the one causing a positioning error along the vertical axis. This choice leads to consider a kinematic model with 9 geometrical parameters to evaluate. Nineteen measures are executed on the printing plate of the printer and it is claimed a final precision along the z axis of $\pm 3\mu m$. It is not directly specified how the measures are taken; a switch is used to detect the contact between the linear delta end-effector and the printing plate but no direct measure of the robot displacements are taken. In all these examples of robotic calibration either is not specified the robotic requirements of the application or it si not specified the application itself at all.

In this study is proposed a linear delta model with 24 parameters.In the following it will be explained the kinematic model chosen and the geometrical parameters considered. It will be explained which and how much measuring points are considered in the printing volume and it is proposed a measuring system based on the use of dial gauges with the resolution of $0.01[mm]$.

3.3 Precision of AM extrusion processes

The AM extrusion processes are based on the material deposition of fused material on a printing plane $x - y$; the material is heated, melted and deposited by a specific extrusion system and through the iterative deposition of a layer above the other, and through their curing, it is obtained a three dimensional object [12]. To make competitive these techniques in the market is important to maximize their building rate, which today is usually around $10 - 100 cm^3/h$ [13], by keeping the same grade in the final product quality. Several studies have been done to model the physic of these processes in order to optimize the process parameters [27,28]. If we focus on the geometry obtainable the final quality of these processes can be tied to two fundamental parameters, the nozzle diameter D, and the layer thickness, h [1]. The first one influences strongly the minimum feature achievable, no printed feature could ever have a dimension smaller than such a length, furthermore if we consider the die-swelling effect, which states how the material tends to enlarge after the nozzle exit, the minimum feature achievable is even bigger than D [27]. The second one defines the resolution used to recreate the three dimensional object and so it is directly connected to the dimensional tolerances achievable and to the surface roughness of the piece. To improve the process quality from this point of view means to minimize D and h by trying to keep constant the material flow rate, Q, to not diminish the building rate. The amount of material extruded is evaluated through the use of a mass balance [1]; given the width, w, and the layer height, the distance between the nozzle and the deposition plane, and defined the printing speed it is possible to evaluate the material flow rate to extrude.

$$Q = whv \tag{3.1}$$

In fig.3.2a the layer height and the width of the material deposited are expressed as function of the nozzle diameter and usual coefficients of these processes. If we diminish h by keeping Q constant we need to increase the printing speed; the first physical limit of this systems is given by the maximum velocities, and accelerations, reachable by the mechanical system. Furthermore it must be considered that it exists some threshold velocities, depending on the flow rate and on the layer thickness, that can not be passed otherwise there is a risk to break the wire of material deposited during the printing phase [7]. If we diminish D we will have a double effect; one identical to the one previously considered due to the fact that the dimension w is tied to the dimension D, and one related to the increase of pressure required to maintain constant the material flow rate with a smaller nozzle. In [4] is modelled the behaviour of a fluid inside an extrusion system by describing the pressure drop as function of the extruder geometry, temperature of the nozzle and of the physical properties of the material. A decrease in the noz-

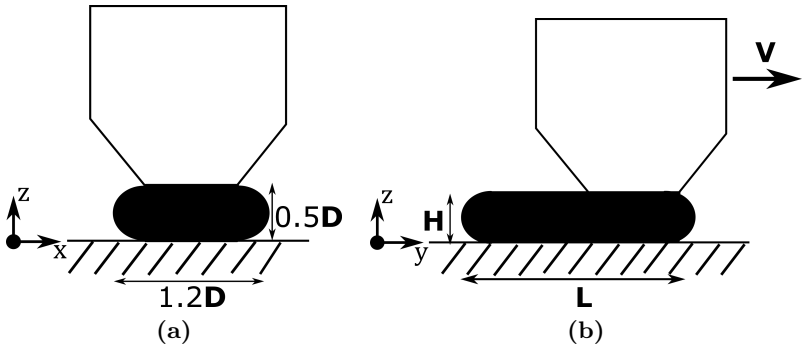

Figure 3.2: Relantionship between the nozzle diameter and machine precision

zle diameter leads to an increase in the pressure drop required by keeping constant the flow rate; to have an idea of the pressure incremental required it can be considered that the flow rate is inversely proportional to the fourth power of the nozzle diameter [9]. A direct consequence of this fact is that diameters too small require very high forces to push the material through the extrusion system; in the typical FDM systems this can lead to the break of the material wire before to be melted in the extruder. In [13] has been maximized the flow rate of an FDM machine by improving the system capacity to reach high speeds and to exert high forces on the material pushed in the extrusion system. An increase in the flow rate, above the $100cm^3/h$, requires bigger amount of heat per unit of time in order to correctly melt the material. In [13] the problem has been faced by introducing a laser before of the extruder nozzle. By considering a constant building rate, and so by keeping constant the production times which are fundamental for the competitiveness of these systems, the main limits of this process lie in the maximum printing speeds achievable, in the maximum pressure obtainable in the extruder and in the necessity to guarantee the correct melting of the material. The limits here discussed are the ones which bring these processes to have limits in the geometrical tolerances achievable in the final products.

If we take under consideration the precisions of the robotic systems used for these applications we see how very important the relative displacement between extruder nozzle and printing plane in order to guarantee the correct deposition of the right amount of material. An error in the relative position between nozzle and printing plate leads to a printing error due to an excess or to a deficiency, according to the case, of material extruded. If we consider a material wire deposited as the one in fig.3.2 a position error of the machine in the plane $x-y$ leads to a variation in the length of the material extruded, L, whereas an error along z leads to a variation in the desired height h. We need to make a distinction between the errors committed in the plane $x-y$ and the ones committed along the printing direction z. In this process a rule of thumb is to have a layer height almost equal to half the diameter length D;

Table 3.1: AM extrussion process performances

direction	magnitude[mm]
$x-y$	± 0.1
z	± 0.01

an example is given by the commercial 3D printer mojo of Stratasys, which is a leader company in the FDM field, which has a nozzle diameter of $0.35[mm]$ and it allows to print with only one layer height equal to $0.178[mm]$ [13]. By being the height h for these processes in the order of $0.1 - 0.5[mm]$, depending on the nozzle [24], the position error along z has a much severe consequence on the process than a positioning error along the plane $x-y$. If we consider the deposition of a wire of length $20[mm]$ with a fixed height of $0.2[mm]$ it is clear how a variation of the tenth of millimetre on L has a very different impact than the same variation of h. All this leads to state that during the calibration process of AM machines based on extrusion systems the maximum precision required is dictated by the printing direction, z, which today must be in the order of the hundredth of millimetre.

3.3.1 Precision of robot for AM extrusion processes

In order to define if a calibration procedure is successfully we need an evaluation criteria. According to the norm ISO-9283 [19] for industrial manipulators a series of standard tests are defined to measure and compare a robot performances. Among them the firsts are the ones aimed to measure the accuracy and precision in the robot pose, which are the capacity of the robot to reach a specific pose in a repetitively way with a certain degree of error. This kind of procedure is the one followed in [2, 8, 23, 29] to evaluate the results of the calibration effectuated. It is evident how this method is effective and suitable for the evaluation of a robot performances, and how bigger is the accuracy and precision of a machine and bigger is its capacity to execute any kind of work; it is possible to wonder if in the case of a specific application would be possible to follow a different procedure, a procedure focused on the application by allowing to diminish the calibration efforts to reach the good execution of the application itself. In particular as regard costs and production times in the construction of the robot itself through:

- Increase in the mechanical tolerances of the robot mechanical components.
- Decrease in the number of measures effectuated and in the resolution required

The AM extrusion processes start the printing procedure on an initial printing plane, z_0, where the material is deposited until the first layer of the

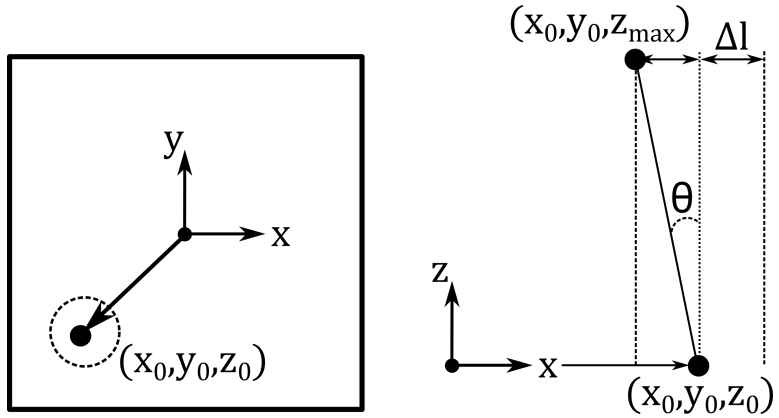

(a) Measure of errors in the $x - y$ planes

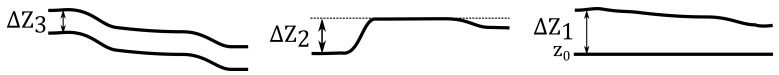

(b) Measure of errors in the along the z axis

Figure 3.3: Measure of errors for robot testing

component is created. After that is executed a displacement along z equal to the layer thickness and the machine starts over by moving in the plane $x - y$ to deposit a new layer. These displacements are the only one required to the machine during the printing phase and is in respect of them that we measure the accuracy of the system. In fig.3.3 are represented the measures effectuated during the calibration process to verify that the geometrical parameters evaluated by the algorithm chosen are a solution capable to satisfy the AM extrusion process limits. The errors are divided in errors in the plane $x - y$ and errors along z. This division is a direct consequence of how the machine carry out the process as described previously.

On the initial plane is measured the distance between the desired point $\begin{pmatrix} x_0 & y_0 & z_0 \end{pmatrix}$, and centre of the plane, $\begin{pmatrix} 0 & 0 & z_0 \end{pmatrix}$, by evaluating a positioning error on the starting plane $\Delta l(z_0)$. For all the planes after the first, the positioning error in the plane Δl is measured as distance between the point actually reached by the robot , x_0, y_0, and the vertical line traced starting from the point with the same theoretical coordinates in the initial plane. The positioning errors of the robot are acceptable if they fall all inside a cylinder of radius Δl, axis parallel to the z axis and centred in the point $x_0 - y_0$ of the starting plane. The choice of measure the errors in the plane by using as reference point the projection of the point in the plane z_0 depends on the fact that for the AM process is very important the relative distances among points, in this case the points with the same couple $x - y$ must be one in top of the other as much as possible in order to correctly deposit one layer over the other. Along z are considered three types of er-

Table 3.2: Tolerances for linear dimensions

Tolerance class		Tolerance range[mm]				
Designation	Description	0.5 up to 3	over 3 up to 6	over 6 up to 30	over 30 up to 120	over 120 up to 400
f	fine	±0.05	±0.05	±0.1	±0.15	±0.2
m	medium	±0.1	±0.1	±0.2	±0.3	±0.5
c	coarse	±0.2	±0.3	±0.5	±0.8	±1.2
vc	very coarse	-	±0.5	±1.0	±1.5	±2.5

rors, represented side by side in fig.3.3b and indicated with ΔZ_1, ΔZ_2 and ΔZ_3. ΔZ_1 is an absolute error in respect of the starting plane z_0, ΔZ_2 is a relative error in respect of a reference z value for the plane and ΔZ_3 is a relative error between two consecutive planes. With these measures is kept constant the distance between two planes by respecting the process parameter layer thickness, which is fundamental in these processes, the respect of the nominal distance from the plane z_0 in order to respect the dimensional tolerances of the printed object. The relative measure ΔZ_2 verifies a flatness condition on each plane.

Defined the measures to effectuate it must be established a yardstick for the evaluation of the robot positioning errors and decide when they are acceptable or not. The norm ISO-52902 proposes the print of some standard artefacts to evaluate and compare the AM processes [18]. The goal of this norm is to allow a qualitative and quantitative evaluation of an AM system in terms of accuracy, resolution, surface texturing and labelling. The norm does not give any specifications about the tolerances that should be respected during the manufacturing of the artefacts, that is because it is duty of who apply the norm on a specific AM machine, usually the vendor of the machine, to compile a report where are specified the tolerances obtained. The aim of the norm is not to specify a tolerance for the AM processes but a way to compare them in order to better chose the right AM process according to the necessities. Since the lack of a norm which specifies the tolerances for an AM process it seems reasonable to apply to the final object the tolerances usually applied on the mechanical components and expressed in the norm ISO-2768-1 [16]. This norm defines a tolerance range, for linear and angular dimensions, inside which the normed components must fall in order to consider the manufacturing process executed from a quality point of view, from fine(the best) to very coarse(the worst). The principle applied here is the one that bigger is a dimension bigger is the admissible tolerance. In tab.3.2 and tab.3.3 are shown the tolerances values for linear and angular dimensions until 400[mm], [16]. Starting from these values is possible to set up a gradual evaluation of the robot performances where bigger are the

Table 3.3: Tolerances for angular dimensions

Tolerance class		Tolerance range based on the shorter side[mm] of the angle			
Designation	Description	up to 10	over 10 up to 50	over 50 up to 120	over 120 up to 400
f m	fine medium	$\pm 1^o$	$\pm 0^o 30'$	$\pm 0^o 20'$	$\pm 0^o 10'$
c	coarse	$\pm 1^o 30'$	$\pm 1^o$	$\pm 0^o 30'$	$\pm 0^o 15'$
vc	very coarse	$\pm 3^o$	$\pm 2^o$	$\pm 1^o$	$\pm 0^o 30'$

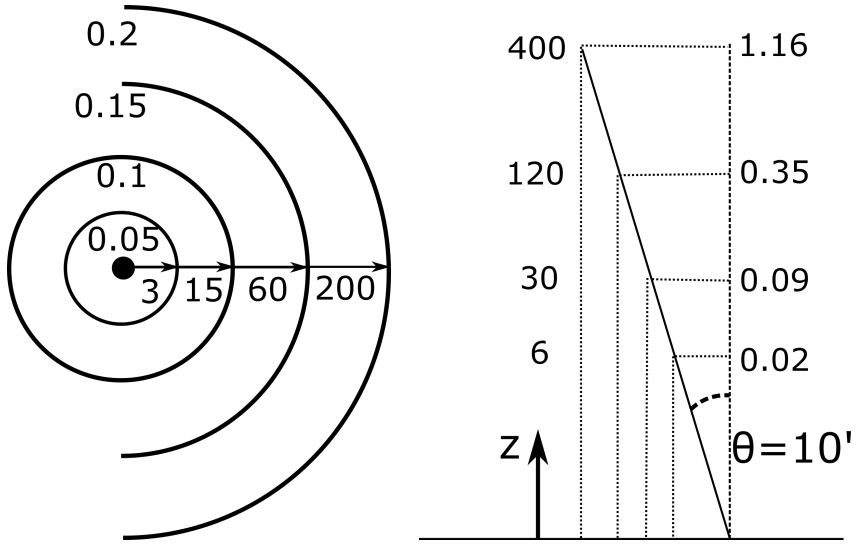

(a) Evaluation of Δl in the starting plane z_0

(b) Evaluation of Δl at the increase of z value

Figure 3.4: Gradual evaluation of the Δl errors

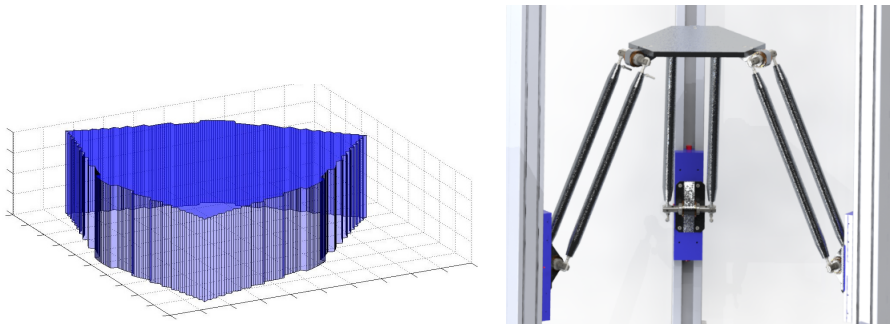

(a) Workspace **(b)** Configuration at 120^0

Figure 3.5: Vertical linear delta

printed object dimensions bigger are the admissible errors. The admissible errors in the printing plane will be function of their distance from the centre $l = \sqrt{(x - x_0)^2 + (y - y_0)^2}$ as shown in fig.3.4a in the starting plane, and they will be function of angle θ and of the absolute height z for the others planes, fig.3.4b. The tolerances values and the length utilised in the figure are taken from the fine class of tab.3.2; for the angle θ has been taken the most restrictive value of the considered class, tab.3.3. The error ΔZ_1 follows the same behaviour of the error $\Delta l(z_0)$ since it is an error on a linear dimension, but it will be function of z; the error ΔZ_2, flatness condition, is function of l and it si possible to refer at the norm on the geometrical tolerances ISO-2768-2 [17]. So given a point of coordinate $\begin{pmatrix} x & y & z \end{pmatrix}$ the statical positioning error of the robot is considered admissible if the following conditions apply:

$$\Delta l(z_0) <= f(l) \tag{3.2}$$
$$\Delta l(z) <= z_{ref} sin\theta \tag{3.3}$$
$$\Delta Z_1 = \|z - z_0\| <= f(z) \tag{3.4}$$
$$\Delta Z_2 = \|z - z_{ref}\| <= f(l) \tag{3.5}$$
$$\Delta Z_3 = \|z - z_u\| <= 0.01 \tag{3.6}$$

where z_u is the value in z reached by the robot in the plane below to the one considered with the same $x - y$ coordinates, and where z_{ref} is the value in z reached by the robot in the central point of the plane considered. The error ΔZ_3 is the only constant and it is imposed by considering the usual values of the parameter layer thickness in the AM extrusion processes. All the errors are evaluated through their module.

3.4 Linear delta model

The linear delta is a parallel kinematic robot which derives from the Delta robot invented by Clavèl among the years '80-90 [6]. Clavèl has arrived to the synthesis of this robot through the study of some possible solutions in the attempt, achieved, to obtain a robot with great dynamic properties for pick and place operations in the industrial field. Clavèl in the synthesis process did not follow one of the procedures usually used in the field of robotics, listed for instance by Merlet [22], but he has examined a series of solutions according to a logic defined by Hervé *a group-theory-independent way* [14]. Hervé himself explains better the kinematic principle of this robot. The Delta kinematic, three translations in the space, is based on the use of 3 identical kinematic chains whose motion is included in that which is defined Schoenflies motion $X(w)$, eq.3.7. This group defines a set of motions which are a translation in a reference frame, $\mathbf{u}-\mathbf{v}-\mathbf{w}$, and a rotation around one of these three axis, $\mathbf{w}$, as expressed by the exponential term of the equation. A chain of this type has 4 Dofs expressed in the equation by the parameters a, b, c and h. This motions, together with others, have been extensively studied by Hèrve which states as the union of three Schoenflies chains leads to a pure translational motion on the robot end-effector [15].

$$X(\mathbf{w}) \quad a\mathbf{u} + b\mathbf{v} + c\mathbf{w} + exp(h\mathbf{w}\Lambda)(NM) \tag{3.7}$$

$$X(w) \cap X(w') \cap X(w'') = T \qquad w \neq w' \neq w'' \tag{3.8}$$

To obtain this motion group, $X(w)$, Clavèl has utilized a mechanical solution often defined as spatial parallelogram; in this solution lies the innovation of Clavèl and not in the kinematic principle of which there was an historical precedent [22]. In fig.3.6a is possible to see one of the chains which form the delta robot, often indicated with the acronym RRP_aR which indicates the three revolute joints of the system and the parallelogram joint which constraints the parallelism between two axis. In the figure are indicated the three rotations axis of the arm. In order to generate a Schoenflies motion it is needed that the three axis, indicated by the letter w, remain perfectly parallel among them during all the possible motions of the system; in order to guarantee to the end-effector a translational motion in the three-dimensional space it is needed of three Schoenflies chains whose w axes are not parallel among them, as expressed by the eq.3.8. The linear delta, variation of the Delta robot supposed by Clavèl himself, is based on the same kinematic principle with the difference that the first rotation axis w, the one in the upper part of fig.3.6a, is not present and it is substitute by a prismatic joint. We have a kinematic chain of type PRP_aR, where the first letter indicates a prismatic joint. In this case, in order to guarantee a translational motion to the end-effector, is needed to preserve the parallelism of the two

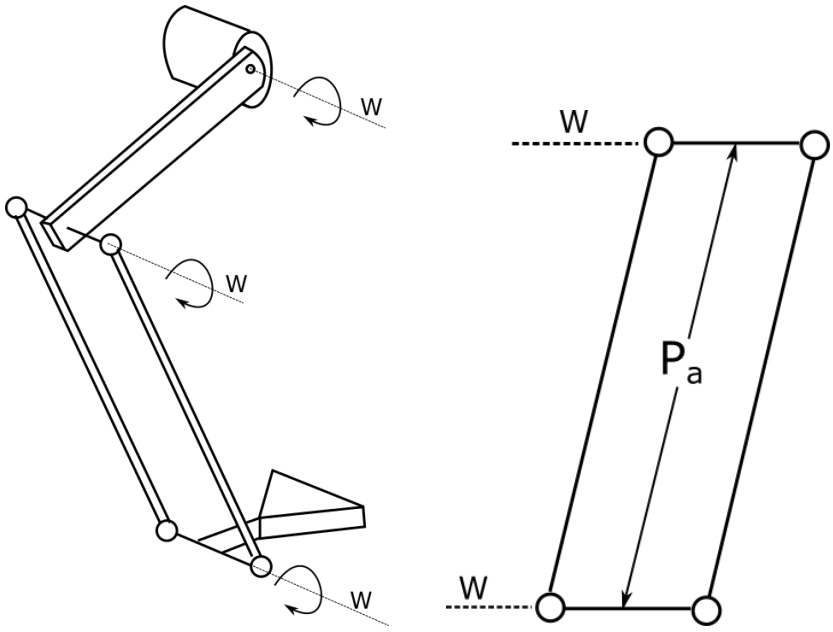

(a) Delta arm. source [15] **(b)** Parallelogram

Figure 3.6: Clavel solution for a Schoenflies motion

rotation axis left for each kinematic chain; the usual mechanical solution is even here the parallelogram, fig.3.6b. These considerations bring us to claim that in the attempt to calibrate a linear delta the perfection of the joint P_a is fundamental to the goal of avoiding unwanted motions, so the rotations of the end-effector. In [29] Clavèl in the calibration of a Delta robot with a model with 54 geometric parameters considers the geometric errors of the parallelogram and therefore the resulting rotations. In a robot with 3 Dofs these rotations are anyway unavoidable and as claimed by Clavèl the only thing that can be obtained is a *better prediction of the end effector's orientation*. In this calibration study it is considered:

- A vertical linear delta whose three kinematic chains of type PRP_aR have a P_a joint whose geometrical errors are negligible and so any kind of end-effector rotations are neglected too.

This consideration, beside to be mandatory for the understanding of the kinematic model that is going to be proposed, is important to anyone who wants to design a linear delta. Being any kind of rotations impossible to correct it is of great importance the design of the P_a joint or equivalent. In the AM field any rotations would lead to an increasing or decreasing of the relative distance between print plane and the extruder nozzle by affecting the final result. In fig.3.5b is shown the vertical linear delta of the Efesto project with the prismatic axis settled in a 120^o position, one respect to

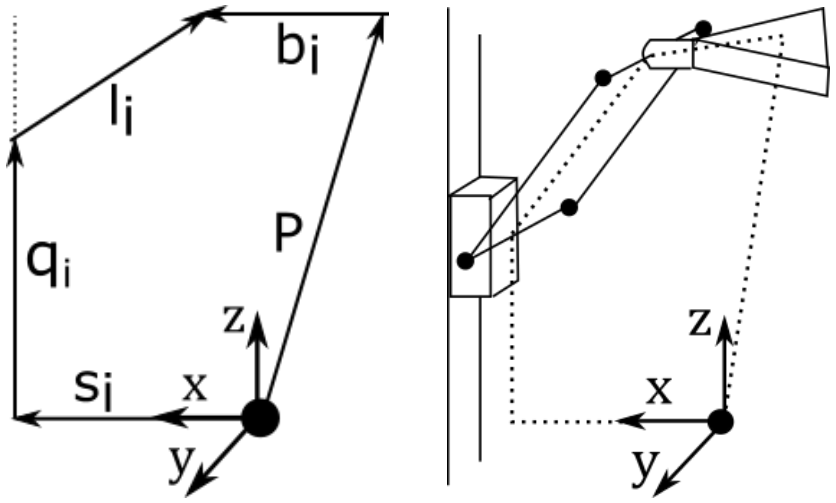

(a) Vectorial scheme of the linear delta kinematic chain

(b) Linear delta arm with parallelogram

Figure 3.7: Linear delta kinematic

the other. Next to it there is a quality representation of the workspace of this type of robot. It is important to notice how the space covered is the projection along the vertical axis, z, of a plane figure. In a theoretical perfect vertical linear delta there is no variations at the vary of z axis.

3.4.1 Kinematic equations and choice of the geometrical parameters

In the following it is specified the kinematic equations of the linear delta and the choice made for the geometrical parameters of the robot. For a deeper insight on the kinematic equations the reader can refer to cap.2 of this work.

The linear delta is composed by three kinematic chains of type PUU, prismatic-universal-universal, that can be rewritten as PRP_aR when it is chosen, as it often happens in the practice, the parallelogram as a mechanical solution for its constructing. The vector equation which relates the robot workspace to the joints space is:

$$s_i + q_i + l_i = p + b_i \qquad i = 1, 2, 3 \tag{3.9}$$

The equation is valid for all the three kinematic chains like the one represented in fig.3.7a. Starting from this equation is possible to find the solutions for the inverse and forward kinematic problems, [11]. In fig.3.7b there is a schematic representation of a linear delta kinematic chain realized through the utilize of a parallelogram which connects the robot end-effector with a prismatic joint. If we make explicit the scalar values of the vectors

in eq.3.9 it is possible to write:

$$\underline{p} = \begin{pmatrix} p_x \\ p_y \\ p_z \end{pmatrix} \quad \underline{s_i} = \begin{pmatrix} s_{ix} \\ s_{iy} \\ 0 \end{pmatrix} \qquad \underline{b_i} = \begin{pmatrix} b_{ix} \\ b_{iy} \\ b_{iz} \end{pmatrix} \quad \underline{l_i} = |l_i|\hat{u}_i \qquad \underline{q_i} = q_i \begin{pmatrix} q_{ix} \\ q_{iy} \\ q_{iz} \end{pmatrix} \tag{3.10}$$

$\underline{P}$ is the position vector of the end-effector, $\underline{q_i}$ is the i-th actuated joint of the system, $\underline{s_i}$, $\underline{b_i}$ and $\underline{l_i}$ the vectors which describe the robot geometry, where the module of the latter $\left|\underline{l_i}\right|$ is the fixed distance imposed by the parallelogram previously indicated by P_a, fig.3.6b. Of the scalar values listed above the unknown variables for each kinematic chain are 8, s_{ix},s_{iy},b_{ix},b_{iy},b_{iz},$\left|\underline{l_i}\right|$ and two values among q_{ix},q_{iy} and q_{iz} which are the components of the unit vector which defines the prismatic joint. We have a total of 24 variables which form the geometrical parameters set Λ which describe completely the robot. It can be noticed that if we keep generalized all the scalar values of each vector it would be obtained 11 variables for each kinematic chain, 3 scalar values for the vectors $\underline{s_i}$,$\underline{b_i}$,$\underline{l_i}$ and 2 for the vector $\underline{q_i}$. For q_i it has to be find only the unit vector of the prismatic axis and not the module. The choices made are explained as follow:

- Of the vector $\underline{l_i}$ is of interest only the module. This can be seen from the fact that only the module is needed to solve the kinematic equations, as shown in the latter, eq.3.13-3.16. This fact matches the choice of a perfect parallelogram which set the distance $\left|\underline{l_i}\right|$.
- The vector $\underline{s_i}$ is imposed to lie on the plane $x - y$, thus removing one variable. This choice matches the fact that it is not imposed any constraint on the position of the reference frame and that the prismatic axis are considered parallel to the z axis. This choice will result in the necessity to obtain an offset position from the machine as shown in the later.

The above considerations lead us to a total set of 24 parameters which will be used to calibrate the linear delta. The geometrical parameters has been chosen starting from the closure equations of the robot. It is possible to compare this result with others methods used in the robotic field which are usually based on the number and type of joints present in the system. In [21] is given the following equation for the evaluation of the parameters number to choose in a PKM:

$$N = 3R + P + 2C + SI + E + 6L + 6(F - 1) \tag{3.11}$$

where we have the joints R, revolute, P, prismatic, C, cylindrical, ed SI which are defined as singular links. These are passive joints of the system.

Further we have the number of actuated joints E, the number of independent loops L and the number of frames freely chosen, F. For an in depth analysis of this equation and its parameters refer to [10,21]. In the linear delta case, by considering the statements of the previous sections, some adjustments have to be done.

- The term $6(F-1)$ becomes $3(F-1)$ by considering that no rotations are allowed
- In the chain PRP_aR the last revolute constraint is not independent from the first one. The absence of rotations impose the perfect parallelism between the two. The two revolute joints are the one that in a Schoenflies group it has been indicated as w.

Considering that the terms C, SI and P are not present in our system, it must be remind that for P are meant only the passive prismatic joints, the equations can be rewritten as:

$$\begin{gathered} N = 3R_1 + R_2 + E + 6L + 3(F-1) \\ R_1 = 3 \quad R_2 = 3 \quad E = 3 \quad L = 2 \quad F = 0 \end{gathered} \tag{3.12}$$

where with R_1 and R_2 it is done a distinction between the first and second revolute joint of each kinematic chain. We have two independent loops, $L = 2$, given the three kinematic chains of the linear delta and it is not not add any additional frame to the absolute one, $F = 0$. We obtain 24 parameters to estimate. It is worthy to notice that eq.3.11 gives the number of parameters to chose but not which, so it has been decided to start directly from the closure equations of the system.

Even though we refer to cap.2 for the complete development of the inverse and forward kinematic equations [11], in the following it is written the first:

$$\begin{gathered} q_i = \underline{d_i}^T \hat{u}_i - \sqrt{\underline{d_i}^T(\hat{u}_i\hat{u}_i^T - [I]) + l_i^2} \\ \underline{d_i} = \underline{p} + \underline{b_i} - \underline{s_i} \end{gathered} \tag{3.13}$$

where $\hat{u}_i$ is the unit vector of $\underline{l_i}$. And the second:

$$\underline{d}_i = \underline{p} + \underline{b}_i - \underline{s}_i \tag{3.14}$$

$$\underline{d^T}_i\underline{d}_i = \underline{p^T p} + \underline{b^T}_i\underline{b}_i + \underline{s^T}_i\underline{s}_i + 2\underline{p^T}\underline{b}_i - 2\underline{p^T}\underline{s}_i - 2\underline{b^T}_i\underline{s}_i \tag{3.15}$$

$$l_i^2 = \underline{d}_i^T\underline{d}_i - 2\underline{d}_i^T\hat{u}_i q_i + q_i^2 \tag{3.16}$$

By substituting the eq.3.14 and 3.16 in 3.15 it is obtained a vectorial equation that can be written in the form:

$$[ones]\underline{P}^2 + [A]\underline{P} + \underline{B} = 0 \tag{3.17}$$

where the geometrical parameters, Λ, and the actuated joints, q, are nested inside the matrix $[A]$ and the vector $\underline{B}$. The system can be solved numerically through the utilization of the Jacobian matrix $[J]$.

$$\underline{P}_{i+1} = \underline{P}_i - [J]^{-1}([I]\underline{P}_i^2 + [A]\underline{P}_i + \underline{B}) \tag{3.18}$$

We will indicate in the following with $f(\Lambda, q)$ the forward kinematic equations and with $g(\Lambda, P)$ the inverse kinematic equations.

3.4.2 Mechanical tolerances and stochastic method

In the robotic calibration the research of the geometrical parameters starts from the nominal values of the mechanical components. It is reasonable to expect that the values estimated from the calibration procedure fall into the range defined by the mechanical design of the components, which take into account the manufacturing tolerances for the single part and the mounting tolerances for the assembly. Since the non linearity of the kinematic equations in respect of the geometrical parameters there could be more than one solutions which satisfy the equations themselves. Different values of the geometrical parameters could lead to the same identical positioning errors of the robot during the measuring phase of the calibration process; it would be impossible to distinguish two different set of geometrical parameters with the same positioning errors. In order to simplify the calibration it is sometimes possible to use a minor set of parameters in the calibration process respect to the number of parameters derived from the kinematic equations of the robot. For instance in [23] is used a minor number of parameters to describe the linear delta in respect of the number here used. This is a simplification of the kinematic problem since the complete model of the linear delta contains far more geometrical parameters [29], but this choice does not exclude the possibility to calibrate the machine inside the tolerances required from the printing process. Anyway by reducing the number of geometrical parameters in [23] are considered perfectly parallel the linear guides of the linear delta so excluding the geometrical parameters related; this implies very strong tolerances on the mounting of the linear guides of the robot as for any other parameter omitted.

It is possible to reduce the parameters number by attributing the positioning errors to a limited number of independent parameters as show in [10]. Let's consider the positioning error of the robot end-effector, $\begin{pmatrix}\Delta x & \Delta y & \Delta z\end{pmatrix}^T$, for small variations of the geometrical parameters it is possible to write:

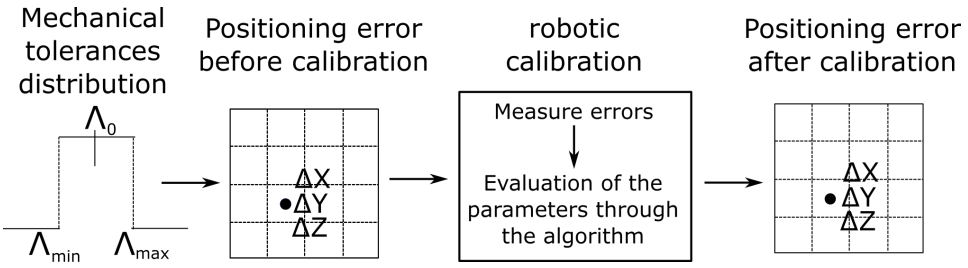

Figure 3.8: From the mechanical tollerances to the positioning error after the calibration process

$$\begin{pmatrix}\Delta x\\ \Delta y\\ \Delta z\end{pmatrix} = \left[J_\Lambda\right]\Delta\Lambda = \begin{pmatrix}\frac{\delta f_x}{\delta\Lambda_1}\\ \frac{\delta f_y}{\delta\Lambda_1}\\ \frac{\delta f_z}{\delta\Lambda_1}\end{pmatrix}\delta\Lambda_1 + ... + \begin{pmatrix}\frac{\delta f_x}{\delta\Lambda_n}\\ \frac{\delta f_y}{\delta\Lambda_n}\\ \frac{\delta f_z}{\delta\Lambda_n}\end{pmatrix}\delta\Lambda_n \tag{3.19}$$

where the matrix $\left[J_\Lambda\right]$ is the geometrical Jacobian of the robot, the derivatives of the direct kinematic equations, f in respect of the single geometrical parameters, Λ. In a situation like this is evident where only one measurement point would be needed to evaluate 3 independent geometrical parameters. This reconstruction applies only in one point x, y, z, the one where the measure is taken.

$$\begin{pmatrix}\Delta x_1\\ \Delta y_1\\ \Delta z_1\end{pmatrix} = \begin{bmatrix}\frac{\delta f_x}{\delta\Lambda_1} & \frac{\delta f_x}{\delta\Lambda_2} & \frac{\delta f_x}{\delta\Lambda_3}\\ \frac{\delta f_y}{\delta\Lambda_1} & \frac{\delta f_y}{\delta\Lambda_2} & \frac{\delta f_y}{\delta\Lambda_3}\\ \frac{\delta f_z}{\delta\Lambda_1} & \frac{\delta f_z}{\delta\Lambda_2} & \frac{\delta f_z}{\delta\Lambda_3}\end{bmatrix}\begin{pmatrix}\delta\Lambda_1\\ \delta\Lambda_2\\ \delta\Lambda_3\end{pmatrix} \tag{3.20}$$

Since the non linear equations is impossible to construct a linear system which can guarantee the validity of the solution in every point of robot workspace; when the geometrical parameters errors are big this linearization is not even valid. It is not possible in general to exclude a geometrical parameter without losing in the solution precision; it would be necessary to demonstrate the identity of two kinematic equations with two different set of kinematic parameters:

$$f(\Lambda, q) = f(\widetilde{\Lambda}, q) \qquad \forall q \tag{3.21}$$

where the q the coordinates of the actuated joints of the system.

Independently from the kinematic model and the number of geometrical parameters chosen is possible to take into account during the development of the calibration method of the actual variations from their nominal values of the parameters themselves. Here we point out how the following method is used during the simulation process explained in the later of this chapter. By varying the parameters chosen for the kinematic model inside a tolerance range, the range around the nominal value of the parameter, is possible to

test the reliability of the calibration method. In fig.3.8 is shown the idea behind the stochastic method of this study. For each of the 24 geometrical parameters is defined a range, $\Lambda_{Min} - \Lambda_{Max}$ around the nominal value Λ_0, inside which the parameters are free to vary. A uniform probability distribution is chosen, a parameter has the same probability to assume any values inside the range. Defined the values, which means to have defined the linear delta structure, specific positioning errors values will be obtained, Δx Δy Δz. Using the a robotic calibration, measuring the errors and evaluating the geometrical parameters, we obtain a new error, hopefully smaller than the one at the start. Using the yardstick defined for the robot for AM extrusion processes it will be decided the success or not of the calibration executed. The stochastic method iterates this procedure a sufficient number of times in order to have a statical evaluation of the results. Even though in this study the number of parameters used to reconstruct the robot geometrical errors is the same of the number of parameters used in the kinematic model it would be possible to reduce them and try to reconstruct the errors with fewer parameters than the ones modelling the robot. It is pointed out that when a lower number of parameters are used to reconstruct the robot errors which have been modelled with a greater number, the values of the parameter chosen can not be searched only inside their mechanical tolerances; in order to compensate the errors given by the parameters excluded from the study the ranges of the remaining parameters must be enlarged. It would be possible too, and this has be done, to vary the mechanical tolerances of the parameters to evaluate the influence of the precision of the mechanical components on the final results.

3.5 The robotic calibration

The goal of the robotic calibration is the research of the robot geometrical parameters values in order to improve the precision and accuracy of the robot itself. The parameters are fundamental for the use of the inverse, g, and forward, f, kinematic equations which ties the robot workspace to the joints workspace. The geometrical calibration methods are divided mainly in two groups; pose measuring and pose matching [10]. In the first one for a specific value of q, the actuated joints, an error is measured between the expected pose of the robot, P, and the actual one. In the second the end-effector is placed in a specific pose P and an error is measured between the expected value of q and the actual one. From the analysis of the measured errors, different algorithm can be used, are estimated the geometrical parameters.

The method here proposed is based on a pose measuring method with measures of relative errors in the robot pose. Let's consider the kinematic equations which link the robot pose P and the actuated joints q. For a variation of the actuated joints Δq it is get a variation of the robot pose ΔP.

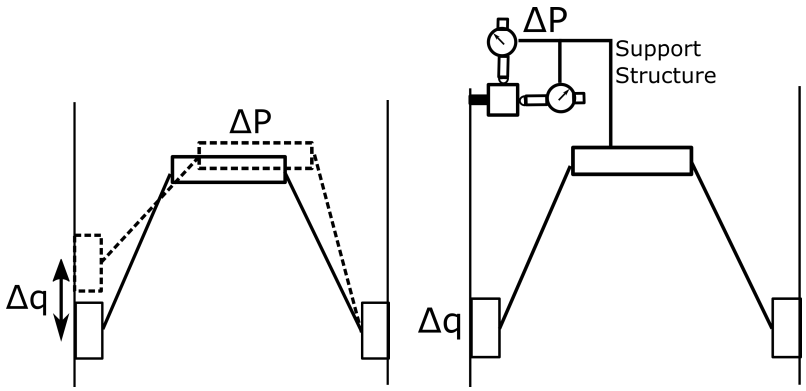

(a) ΔP of the linear delta for a given Δq

(b) Measuring system with dial gauges

Figure 3.9: Measuring system

If this operation is repeated n times is possible to set up an interpolation problem where the goal is to find a function f to relate the variations imposed to the actuated joints q to the variations measured on pose P. From a mathematical point of view this could be done with a generic function with enough parameters to simulate the behaviour measured empirically. In a calibration process are utilized the kinematic equations of the system with an adequate number of geometrical parameters since they are obviously the functions which better reflects the real behaviour of the system. The goal of the method is to find a set of parameters $\widetilde{\Lambda}$ such that:

$$P = f(\Lambda, q) \simeq f(\widetilde{\Lambda}, q) \qquad q = g(\Lambda, P) \simeq g(\widetilde{\Lambda}, P) \tag{3.22}$$

The procedure to obtain the robot measures are:

- Position the actuated joints q in a known position, so to positioned the three prismatic joints of the linear delta.
- Vary the value of a q by a specific Δq one at a time.
- Measure the relative ΔP obtained on the linear delta.
- Repeat the same operations starting from a different initial value of q according to the number of measure to get

In the case of the linear delta we have 3 q and the pose consist in the x,y,z values. For each variation of one q it is obtained 3 error measures Δx,Δy,Δz, so in each point we can achieve until 9 error measures by moving the prismatic joints one at the time. To repeat the operations listed above for different initial values of q means to evaluate the robot behaviour

in different workspace points. In fig.3.9 is possible to see how the linear joints are actuated to obtain an end-effector displacement. We suggest the use of a measuring system based on three dial gauges mounted on a supporting structure fixed on the linear delta in order to measure the three displacements $x - y - z$. The three dial gauges can measure the relative displacements of a reference object, a calibrate cube for instance, put in the robot workspace. Such a system is used in [8] for the measures effectuated on a delta robot. This procedure for the evaluation of the measures in the robot workspace is suitable for any PKM. Being this method based on relative measures and not on an absolute frame, it will be needed a starting offset for the initial robot position as we will see in the testing of the method.

3.5.1 Algorithm

Starting from n measures ΔP we want to find a set of values $\widetilde{\Lambda}$ such that:

$$\left| f(\widetilde{\Lambda}, q) - f(\Lambda, q) \right| < \epsilon \tag{3.23}$$

We want to approximate the kinematic function of the system. This approximation must be valid in the entire workspace and not only in the measure points. With Λ are indicated the real parameters of the robot, with $\widetilde{\Lambda}$ the parameters estimated, ΔP the errors measured and with $\Delta \widetilde{P}$ the estimation of the errors measured. By referencing to section 3.5 the values ΔP are obtained as follow:

$$\begin{gathered} \Delta P = f(\Lambda, q_p) - f(\Lambda, q_m) = \begin{pmatrix} \Delta x & \Delta y & \Delta z \end{pmatrix}^T \\ \underline{q_p} = \begin{pmatrix} |\underline{q_1}| \\ |\underline{q_2}| \\ |\underline{q_3}| \end{pmatrix} + \begin{pmatrix} \Delta q \\ 0 \\ 0 \end{pmatrix} \quad \underline{q_m} = \begin{pmatrix} |\underline{q_1}| \\ |\underline{q_2}| \\ |\underline{q_3}| \end{pmatrix} - \begin{pmatrix} \Delta q \\ 0 \\ 0 \end{pmatrix} \end{gathered} \tag{3.24}$$

Specified an initial set $q = \begin{pmatrix} |\underline{q_1}| & |\underline{q_2}| & |\underline{q_3}| \end{pmatrix}^T$ and applying a variation on the i-th joints we obtain three measure given by $\begin{pmatrix} \Delta x & \Delta y & \Delta z \end{pmatrix}^T$. For each point P in the robot workspace we can obtain until 9 error measures by varying the three joints q_i one at the time. We want to find a set of values $\widetilde{\Lambda}$ which minimize the difference between measured and estimated values by using the same q used during the measuring phase.

It is used for this purpose a genetic algorithm through the function *lsqnonlin* of *MatLab*, so it is a least square minimization for non linear equations. The objective function is the average square error given by:

$$\epsilon = \frac{\sum_{i=1}^{N} (\Delta \widetilde{P}_i - \Delta P_i)^2}{N} \tag{3.25}$$

where N is the number of measure errors. The parameters to find are the 24 geometrical robot parameters; for each of them the algorithm goes

to search their values between a minimum and a maximum specified at the beginning of the minimization of the objective function. These values are given by the mechanical tolerances of the geometrical parameters; for example the length l_i, representative of the parallelogram, could change between the values $l_i \pm \Delta l_i$ which depend on the designing and mounting tolerances.

3.5.2 Measure points

In order to effectuate a robot calibration it must be decided which and how many measure points to utilize. In [29] the measure points are *about uniformly distributed within the workspace* and the same is in [8] where the measure points are *distributed in a* $900x550x300[mm]$ *volume*. In [2] the measuring points are spaced along the external surface of the robot workspace. Spacing the measuring points evenly in the working space on which we want to calibrate the robot is a reasonable choice, but before to proceed in this direction we want to examine the possibility to differentiate a measuring point from another. The least squares algorithm works utilising the derivatives of the objective function that we want to minimize and which is based on the kinematic equations of the linear delta. If we evaluate the derivative of the robot position respect to the 24 parameters we get:

$$\frac{\Delta p}{\Delta \Lambda} = \sum_{i=1}^{24} \frac{\delta f(\Lambda, q)}{\delta \Lambda_i}|_{\bar{q}} \tag{3.26}$$

where the i-th derivative of the geometrical parameter is evaluated in the position defined by $\bar{q}$. A null value of the derivative is equal to state the non influence of that parameter on the robot pose in that specific point of the workspace. In these points the least square algorithm could not differentiate among different parameter values not being any difference in the robot position. Evaluating the eq.3.26 in a dense discretization of the workspace it is obtained a map relating the global influence of the geometrical parameters on the robot pose. In fig.3.10 are represented 6 maps obtained starting from a nominal set Λ_0 on a square workspace $200x200[mm]$, so in the plane $x-y$. The shapes of these maps do not have great variation by moving along the z axis. The derivatives are evaluated numerically from the ratio $\delta p/\delta \Lambda_i$. The maps 3.10a, 3.10c and 3.10e represent the variation $\Delta p = \begin{pmatrix} \Delta x & \Delta y & \Delta z \end{pmatrix}$ for a unitary variation of each geometrical parameters. From fig.3.10a and 3.10c is possible to see how there is a zone with a null value. The interpretation is that here a variation of the geometrical parameters could result in a null change in the robot position; off course that is not necessarily true but it depends on the specific variations $\delta \Lambda_i$. In the maps 3.10b, 3.10d and 3.10f are represented the number of parameters which cause a robot displacement greater or equal to the hundredth of millimetre. The zones with the colour

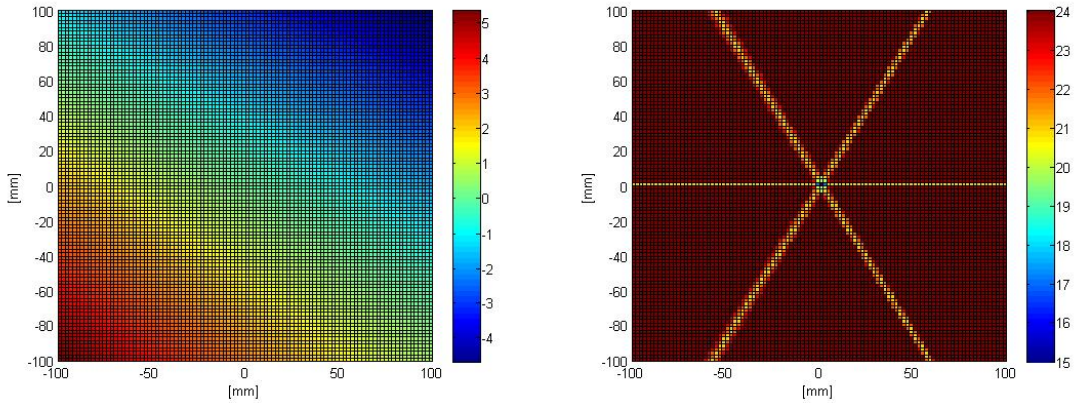

(a) Δx **(b)** Threshlod 0.01mm Δx

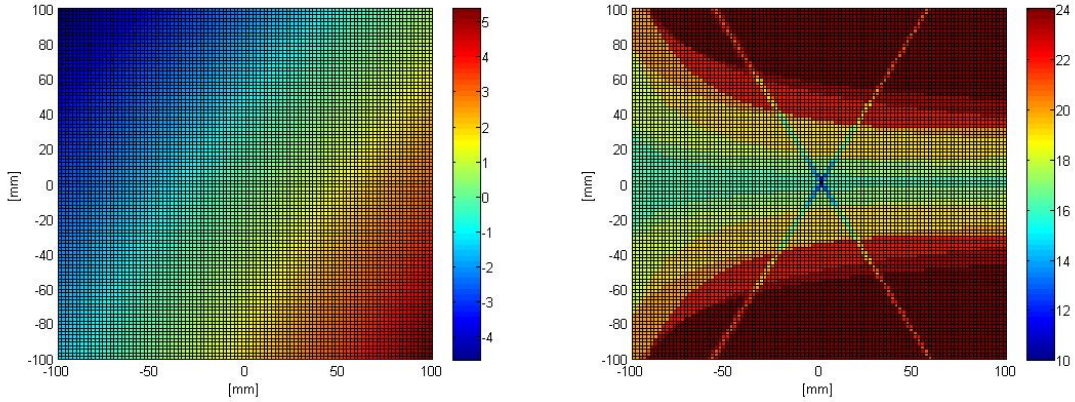

(c) Δy **(d)** Threshlod 0.01mm Δy

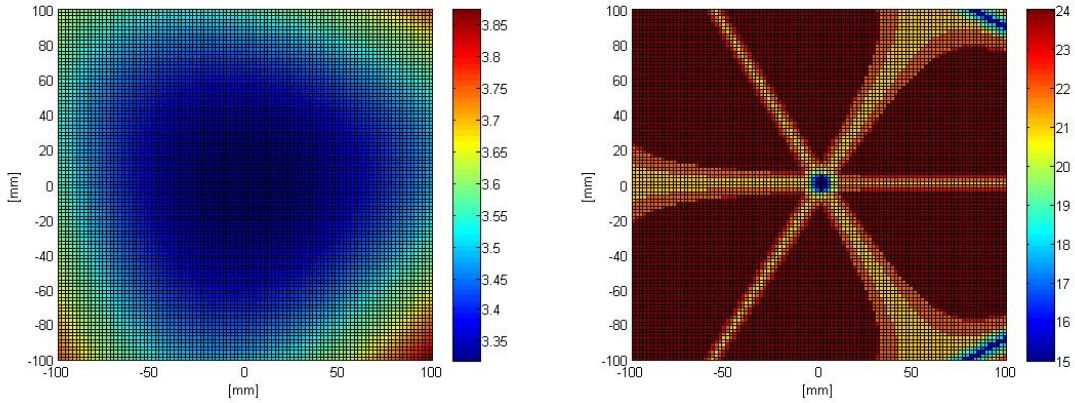

(e) Δz **(f)** Threshlod 0.01mm Δz

Figure 3.10: Relationship between geometrical parameters and robot position

corresponded to 24 parameters are zones where every geometrical parameters affect the robot position at least of $0.01[mm]$. This threshold has been chosen by considering the resolution of the proposed measuring system. It is possible to notice in the cases Δx, Δy and Δz how not every parameter has an important influence in every points of the robot workspace. In all the maps is possible to notice the presence of three predominant directions which reflect the symmetry of the 120^0 configuration of the linear delta.

From the maps obtained it is not possible to extract areas better than others where to take the measurement points. In the end the measuring points are taken along the border of the robot workspace in starting and final plane of the printing volume. We point out how the number of scalar measures should be at least equal to the number of parameters to evaluate, in this case 24. Since for every measuring point we have 3 scalar measures we should need at least 8 measuring points.

3.6 Simulation process

To validate the calibration method it is proposed a procedure focused on testing its effectiveness. A linear delta is completely defined once we have chosen the values of its geometrical parameters. Let's consider a linear delta with nominal parameter values Λ_0, a linear delta affected by geometrical errors Λ, and a linear delta estimated by the genetic algorithm $\widetilde{\Lambda}$. The test is composed by the following passages:

- It is chosen a set of points in the working space of the robot, $P_i = \begin{pmatrix} x & y & z \end{pmatrix}^T$
- A random set Λ is created in order to simulate the geometrical errors of the linear delta. The 24 values of the geometrical parameters are chosen between their minimum and maximum values defined by the tolerances of the mechanical components.
- The set Λ is used to generate the error measures ΔP. By utilizing the nominal values Λ_0 and the inverse kinematic equations for each point P_i in the workspace we obtain the three value q_i. Once at the time the value q_i are varied of fixed value Δq. With the use of the forward kinematics and the set Λ we obtain 9 error measures, three for each i-th joint, given by $\Delta P = \begin{pmatrix} \Delta x & \Delta y & \Delta z \end{pmatrix}^T$. Repeating the operation N times for each measure points it is obtained the errors vector ΔP made of N measures.
- To the error vector is added a measure error due to the measuring system.

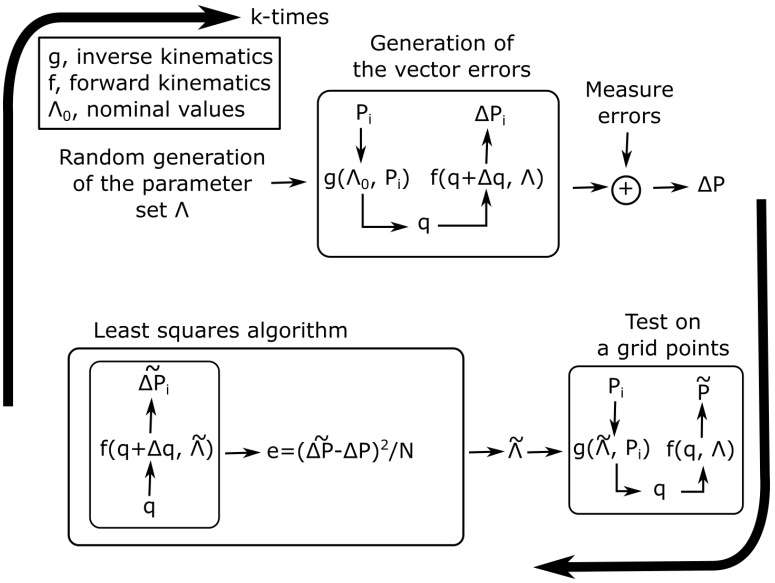

Figure 3.11: Scheme of the validation process of the method for a chosen set of points in the robot workspace

- It is utilized the least squares algorithm, based on the measures ΔP, to estimate the parameter set $\widetilde{\Lambda}$ which minimize the objective function expressed by eq.3.25.
- The set $\widetilde{\Lambda}$ is tested on a grid points in the robot printing volume. The set $\widetilde{\Lambda}$ for the inverse kinematics and the set Λ for the forward kinematics are used to evaluate the position error of the robot. By considering that the calibration is made on relative measures an initial offset is needed. It is considered as reference point the robot position for the values $q = \begin{pmatrix} 0 & 0 & 0 \end{pmatrix}^T$.
- To test the method when the initial parameters Λ change the entire process is iterated k times. At the end of the iterations is possible to evaluate as percentage the number of times the calibration method succeed, so the number of times that the set $\widetilde{\Lambda}$ estimated by the algorithm has been able to respect the limits chosen for this technology, par.3.3.1.

In fig.3.11 is possible to see a schematic representation of the validation process. The process is effectuated for a specific set of points in the robot workspace. It is worthy to notice how the set points used to test the solution of the least squares algorithm is not equal to the set of points chosen at the beginning. The number of iterations to effectuate, k a, are established empirically from the convergence of the result. In this work k has been set to 2500 iterations.

3.7 Success maps

The simulation process lead to a statistical evaluation, expressed as percentage, of the success obtained or not in the use of the linear delta for the AM extrusion processes. The percentages obtained depends on every choice done for every phase expressed in fig.3.1. If for instance we change the parameters number, the measures effectuated in number and/or position, or the mechanical tolerances expected the percentage of the positive case on the k iterations will vary. By arbitrarily varying some of the choices made during this study it is possible to obtain that maps defined at the start of this chapter success maps, which express a variation of the success rate of the calibration method as some of the parameters of the method change. Here we decide to vary two things: the number of measuring points and the mechanical tolerances. This choice is based on the fact that this two factors have a great influence on times and costs; decrease the mechanical tolerances and increase the measuring points means to have manufacturing processes longer and more expensive and a greater number of measures, so even here more time and costs.

In fig.3.7 and fig.3.7 are represented the measuring points used during this trial, the points where the positioning errors of the robot are simulated, and the planes where is verified that the parameters set found by the algorithm allow to the robot the respect of AM process limits. The measuring points are varied from a maximum of 16, the entire set of fig.3.7, to a minimum of 4; the points are taken on two planes which delimit the printing volume. The checking planes starts from the bottom of the printing volume and they are set to variable distance from each other until is reached the top of the printing volume. In tab.3.4 are listed the linear delta parameters with their nominal values and four different tolerances; for the linear dimensions the tolerances go from 0.01 until 2$[mm]$, instead the angular dimensions go from 0.5 to 2$[deg]$. In tab.3.5 are listed some of the values kept constant during this trial, the printing volume used for the calibration, the number of geometrical parameters considered or the resolution of the measuring system. In the table is specified the height, in respect of the first one, of the checking planes. The planes are chosen according to the logic of gradual precision expressed in the par.3.3.1.

In fig.3.14 is the shown the results of the simulations effectuate in a success map where on the abscissa is indicated the number of measuring points, from 4 to 12, and on the ordinate the success ratio obtained on the 2500 iterations effectuated. The four areas represented delimit the success zones of the four tolerances set utilised, from A to D, where A is the set with the finest tolerances and D is the one with the coarsest. If we take the simulation with 12 measuring points with the set D we obtain a success ratio of 50,2%; this means that if we build a linear delta according to the kinematic described and with the mechanical tolerances decided, if we effectuate the

where and how it has been chosen by evaluating the parameters through the algorithm selected, about half of these robots will respect the limits of the AM extrusion processes, the other half would to be discarded. This maps suggest use to not use this solution, 12-D, or that at least one of the phases that is possible to change, fig.3.1, must be modified. In the trial effectuated a good solution could be the combination 12-C where there is a good comprise between number of measuring points and mechanical tolerances and where the success ratio is above the 91%.

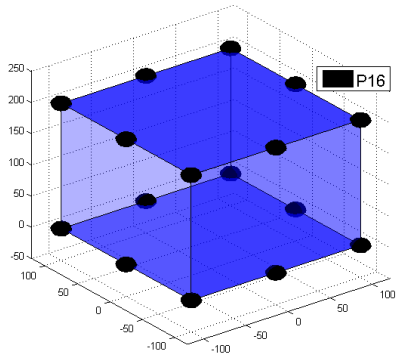

Figure 3.12: Measuring points used in the printing volume

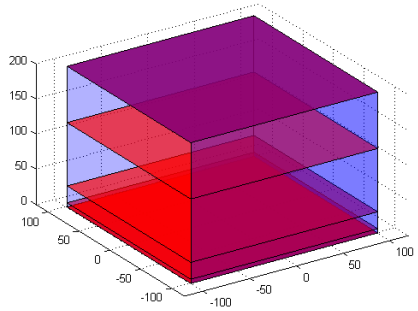

Figure 3.13: Checking planes for the evalution of the calibration success

Table 3.4: Mechanincal tollerances chosen for the study

parameter	nominal value	set A	set B	set C	Set D
$l_i[mm]$	598	± 0.01	± 0.1	± 1	± 2
$\|s_i\|[mm]$	451.5	± 0.01	± 0.1	± 1	± 2
$\|b_i\|[mm]$	200	± 0.01	± 0.1	± 1	± 2
$\theta_{s1}, \theta_{b1}, \theta_{qi}[deg]$	0	± 0.1	± 0.5	± 1	± 2
$\theta_{s2}, \theta_{b2}[deg]$	120	± 0.1	± 0.5	± 1	± 2
$\theta_{s3}, \theta_{b3}[deg]$	240	± 0.1	± 0.5	± 1	± 2
$\alpha_{bi}, \alpha_{qi}[deg]$	90	± 0.1	± 0.5	± 1	± 2

Table 3.5: Fixed parametes of the study

parameter	value
printing volume[mm]	$200x200x200$
geometrical parameters	24
algorithm	non linear least squares
measures resolution[mm]	± 0.01
height (z) of checking planes[mm]	0-6-30-120-200

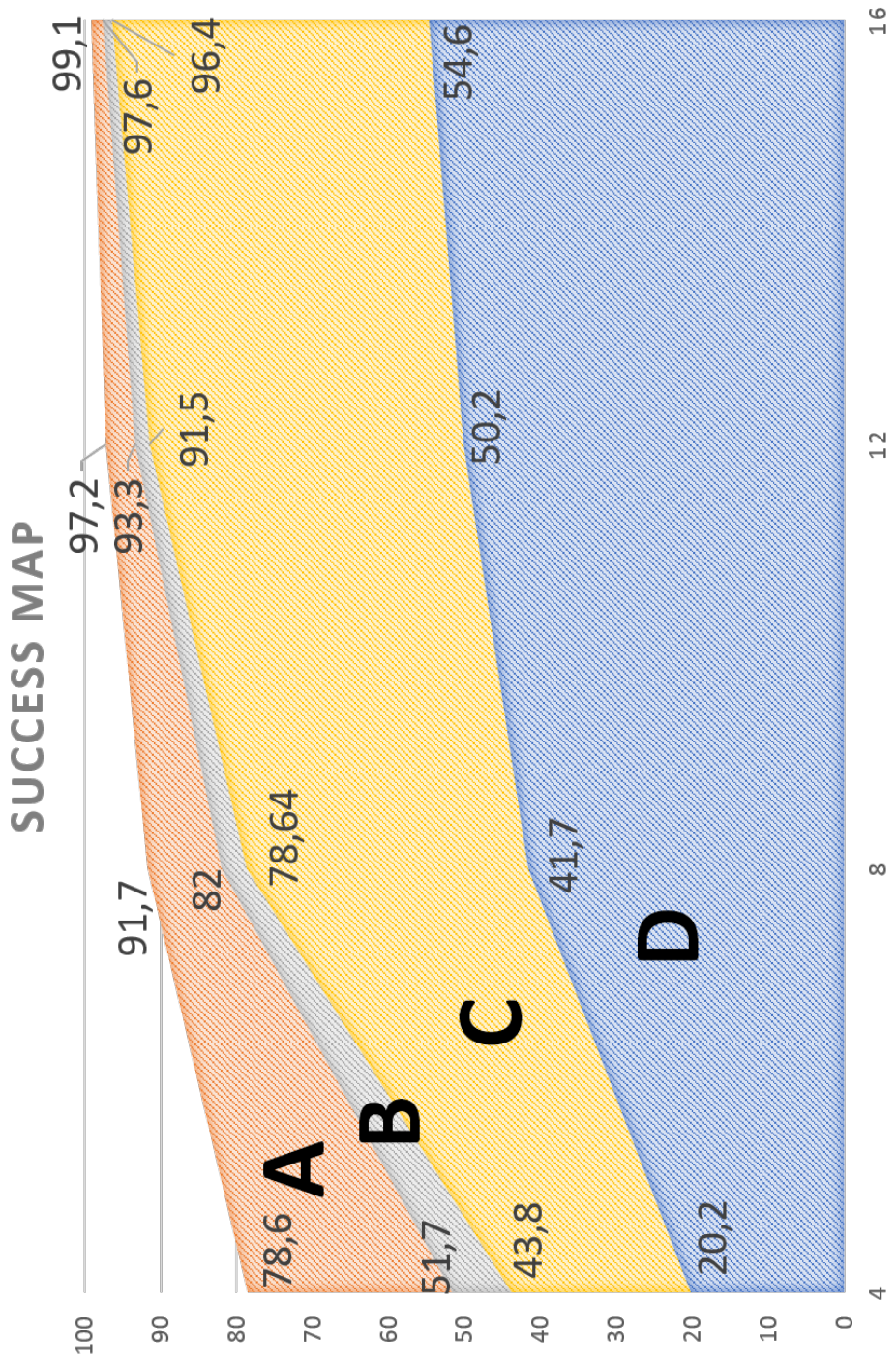

Figure 3.14: Success map

3.8 Conclusions

The generation of the maps proposed arise from the will to focus the attention on the manufacturing process and not only on the robot calibration, by optimizing the efforts in order to obtain an AM extrusion process which satisfy the final expectation on the product quality. Different maps could be obtained by varying other factors than the ones chosen here. The simulation of the entire calibration chain helps to choice in advance which is the best solution in order to carry out the manufacturing process by minimizing the efforts and avoid robotic solutions with precisions beyond the manufacturing requirements. By referring to the map we conclude with the following considerations:

- The success ratio depends on the model used to describe the robot. More is the distance of the model from the reality more the results will be inaccurate. For instance in this study has been supposed a linear delta without rotations which is true only if some conditions on the kinematic are perfectly respected as explained in par.3.4.
- The success ratio depends on the yardstick of evaluation for the technological process. In this case it has been suggested one possibility based on the same considerations usually done for the mechanical tolerances of mechanical components, par.3.3.
- The cases of the k iterations which do not respect the limits imposed are all the ones whose at least one checking points is outside the technological limits required. This means that the calibration is considered not effective even when the robot works properly in almost its entire workspace. This suggest that the robots which do not have passed the test could be only slightly over the limits and they could be taken under considerations for a production of a lower quality.

bibliography

[1] M.K. Agarwala, V.R. Jamalabad, N.A. Langrana, A. Safari, P.J. Whalen, and S.C. Danforth. Structural quality of parts processed by fused deposition. *Rapid Prototyping Journal*, 1996.

[2] P. Bai, J. Mei, T. Huang, and D.G. Chetwynd. Kinematic calibration of delta robot using distance measurements. *Journal of mechanical engineering science*, 2015.

[3] C. Bell. *3D Printing with Delta Printers*. Apress, 2015.

[4] A. Bellini, S. Guceri, and M. Bertoldi. Liquefier dynamics in fused deposition. *Journal of Manufacturing Science and Engineering*, 2004.

[5] Anna Bellini. *Fused Deposition of Ceramics: A Comprehensive Experimental, Analytical and Computational Study of Material Behavior, Fabrication Process and Equipment Design.* Phd thesis, Drexel University, 2001/2002.

[6] Raymond Clavel. *Conception d'un robot parallele rapide a 4 degree de liberte.* Phd thesis, Ecole polytechnique federale de Lausanne, 1990/1991.

[7] Robert Sinclair Crockett. *The liquid-to-solid transition in stereodeposition techniques.* Phd thesis, The University of Arizona, 1996/1997.

[8] D. Deblaise and P. Maurine. Effective geometrical calibration of a delta parallel robot used in neurosurgery. *Intelligent Robots and Systems*, 2005.

[9] L. J. L. Duddleston, K. Woznick, C. Koch, G. M. Capote, N. Rudolph, and T. A. Osswald. Extrudate mass flow rate analysis in fused filament fabrication (fff): A cursory investigation of the effects of printer parameters. In *Annual Technical Conference - ANTEC, Conference Proceedings*, volume 2017-May, pages 43–48, 2017.

[10] I. Fassi, G. Legnani, D. Tosi, and A. Omodei. Calibration of serial manipulators: Theory and applications. In *Industrial Robotics: Programming, Simulation and Applications.* Intech, 2006.

[11] E. Fiore, H. Giberti, and L. Sbaglia. Dimensional synthesis of a 5-dof parallel kinematic manipulator for a 3d printer. *16th International Conference on Research and Education in Mechatronics, REM 2015*, 2016.

[12] I. Gibson, D.W. Rosen, and B. Stucker. *Additive Manufacturing Technologies. Rapid Prototyping to direct digital manufacturing.* Springer, 2010.

[13] J. Go, S.N. Schiffres, A.G. Stevens, and A.J. Hart. Rate limits of additive manufacturing by fused filament fabrication and guidelines for high-throughput system design. *Additive Manufacturing*, 2017.

[14] J.M. Hervé. The lie group of rigid body displacements, afundamental tool for mechanism design. *Mechanism and Machine Theory*, 1999.

[15] J.M. Hervé and F. Sparacino. Structural synthesis of parallel robots generating spatial translations. *International Conference on advanced robotics*, 1991.

[16] Iso2768-1-general tolerances — part 1: Tolerances for linear and angular dimensions without individual tolerance indications. https://bsol.bsigroup.com/. 1993.

[17] Iso2768-2-general tolerances — part 2: Geometrical tolerances for features without individual tolerance indications. https://bsol.bsigroup.com/. 1993.

[18] Iso52902-additive manufacturing — test artefacts — standard guideline for geometric capability assessment of additive manufacturing systems. https://bsol.bsigroup.com/. 2018.

[19] Iso9283-manipulating industrial robots – performance criteria and related test methods. https://bsol.bsigroup.com/. 1998.

[20] F. Knoop, A. Kloke, and V. Schoeppner. Quality improvement of fdm parts by parameter optimization. *AIP Conference Proceedings*, 2017.

[21] G. Legnani, D. Tosi, R. Adamini, and I. Fassi. Calibration of parallel kinematic machines: Theory and applications. In *Industrial Robotics: Programming, Simulation and Applications*. Intech, 2006.

[22] J.P. Merlet. *Parallel Robots*. Springer, 2006.

[23] D.B. Pedersen, E.R. Eiríksson, H.N. Hansen, and J.S. Nielsen. A self-calibrating robot based upon a virtual machine model of parallel kinematics. *Virtual and physical prototyping*, 2016.

[24] A.K. Sood, R.K. Ohdar, and S.S. Mahapatra. Improving dimensional accuracy of fused deposition modelling processed part using grey taguchi method. *Materials and Design*, 2009.

[25] M. Srivastava and S. Rathee. Optimisation of fdm process parameters by taguchi method for imparting customised properties to components. *Virtual and Physical Prototyping*, 2018.

[26] M. Stock and K. Miller. Optimal kinematic design of spatial parallel manipulators:application to linear delta robot. *Journal of mechanical design*, 2003.

[27] B.N. Turner and S.A. Gold. A review of melt extrusion additive manufacturing processes: Ii. materials, dimensional accuracy, and surface roughness. *Rapid Prototyping Journal*, 2014.

[28] B.N. Turner, R. Strong, and S.A. Gold. A review of melt extrusion additive manufacturing processes: I. process design and modeling. *Rapid Prototyping Journal*, 2014.

[29] P. Vischer and R. Clavel. Kinematic calibration of the parallel delta robot. *Robotica*, 1998.

[30] Peter Vischer. *Improving the accuracy of parallel robots*. Phd thesis, Ecole polytechnique federale de Lausanne, 1995/1996.

Chapter 4

Trajectory planning

introduction

A fundamental part of the AM machines is the trajectories generation meant as both the planning than the development of the motion laws for the single machine axis with the purpose to achieve the required manufacturing process. In the Efesto project the study of this part is important both to execute every basic printing operations which require a form of trajectory generation, than to create the customized trajectories required by the specific needs of this technology. The extrusion processes are afflicted by the known problems of overfill and underfill and to guarantee a good printing process it is important to minimize their effects. In the following it is described what it is call the AM digital chain which starting from the object CAD creates the trajectories for the single machine axis. It is explained the two typical problems of AM extrusion processes explaining the needs for the Efesto technology to generate trajectories with specific characteristics. It is proposed an algorithm for the trajectories generation based on the use of Bézier curves to achieve a printing process based on a constant extrusion rate in order to minimize the overfill/underfill problems. An applicative example is carried out on the machine itself.

4.1 AM digital chain

The trajectories development for AM, meant as the process leading to the generation of the motion laws for the actuation systems of the machine, is fundamental to carry out a 3D printing process. A trajectory generation can be divided in 4 parts derived in part from the world of the AM machines [16] and in part from the world of the CNC machines [37] which share several components with the three dimensional printing systems.

These four phases, which are shown in fig.4.1, are the digital representation of the object to print according to a specific CAD format, Computer

Figure 4.1: Workflow of trajectories generation

Aided Design, the slicing algorithm used to slice the object in 2D surfaces which must be overlapped each other, the input code for the AM machine, usually a g-code, and for last the parsing of the input file and the interpolation of the axis trajectories. By acting on only one of these phases, and leaving untouched the others, it is possible to modify the set of trajectories generated during the printing phase of an AM machine. The CAD representation of an object defines its geometric shape at the start; being it a discrete representation of reality it is introduced an approximation error which defines the maximum quality achievable by the AM process. The slicing algorithm defines the printing surface, whose continuous overlapping leads to the final physical object. Usually these surfaces are are planes orthogonal to a printing direction indicated with z, but several studies are going on today searching for more complex printing techniques, on generic surfaces and even depositing material on the void. The g-code, which is born from the necessity to standardize the language of CNC machines, computer numerical control, contains the information codified by the slicing algorithm. The evolution of this language, with the increase amount of informations coded in it, gives the possibility to generate more complex trajectories and dedicated to the 3D printing. The interpolator is the lowest level of this chain and it must take into account the possibility to actual realize the trajectories required for the actuators which will inevitably have some physical limits.

In the following we describe in a more detailed way the 4 phases.

4.1.1 Cad.STL

The standard format for the CAD representation used in the AM field is the STL [16]. This format is born as support of the stereolithography technique and it is often indicated as “Standard Triangulation Language” or “Standard Tessalation Language”, even though it has never been officially recognized by any international organization [19]. The STL requires the description of three dimensional geometric figure through a tasselation process where the surface of a solid is reconstructed through the use of several oriented triangles [38]. Below is given a graphical and informatic representation of what an STL is.

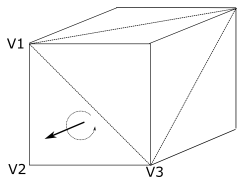

Figure 4.2: STL format

facet normal	-2.555	3.444	5.1111
outer loop			
vertex	0.022	4.155	-1.573
vertex	3.557	2.447	3.44
vertex	-1.247	2.555	4.852
end loop			
end facet			

In fig.4.2 is possible to see the graphical representation of a cube subdivided by triangles in the STL format. For one of the triangles has been indicated the normal vector at the surface and the three triangle vertexes. The orientation of the normal vector is related to the positions of the vertexes since it can be obtained through the use of the right hand rules by connecting the first vertex to the second. Beside the figure is represented the STL syntax describing a generic triangle. It is indicated the normal vector and the three vertexes. In this kind of representation no informations is given about the topology of the triangles which are simply listed in the file. This representation is considered correct, without errors or either said two-manifold, in the moment that some simple conditions apply; every edge union of two vertexes must belong to two triangle at the most, there must be no intersections among triangles and every triangle must have at least one vertex in common with another triangle [38]. This type of representation is prone to several errors in the reconstruction of a 3D surface, in particular in that situations where there is the intersection of two surfaces, in situations of blending surfaces or where there is a surface with an high curvature where the triangle approximation can lead to the formation of undesired holes [38]. It is possible to limit these errors using a tessalation with higher resolutions but it must avoid the collapse of the triangle into a line when one of the three edges become too small. Furthermore some of the errors generated by the tesselation can not be resolved by the use of an higher resolution.

The research of standards suitable for the digital representation of the object is a topic still open today in the AM world and it is of extreme importance for the respect of the geometrical tolerances of the component [42]. In an attempt to improve the gaps of the STL format has been developed in the latest years a new standard, the AMF, Additive Manufacturing File Format [19]. This format expressed in an XML language, extended markup language, has the goals to describe the object independently from the AM process which actually will produce it and to add to the file a series of informations not available in the STL. As regards the geometric description the main innovations brought by this format are two: one is the use of curved triangle and the second one is the use of elements defined constellations. The curved triangle are defined by specifying three vectors in the triangle vertexes or by specifying the edge tangents of the triangle itself. The

use of these elements help to reduce the number of total triangle required to describe curved surfaces and they minimize the approximation error of curved surfaces. The introduction of the element constellation allow to specify the position and orientation of different parts that must be printed and so adding topological informations previously completely absent in the STL format. Beyond these two elements it is possible to find others features aimed to increase the number of informations available related to the object and so aimed to improve the AM processes; for instance it is possible to specify the object colours, materials so defining a unique final product.

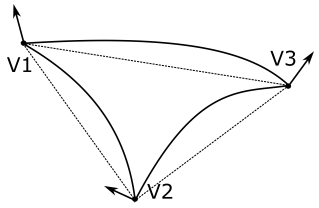

Figure 4.3: Triangle curved using vertex normals

```
<? xml version=1.0 encoding=UTF-8? >
< amf unit=millimiter>
  < object >
    < mesh >
      ...
      < vertices >
        ...
      < /vertices >
      ...
      < triangle >
        ...
      < /triangle >
      ...
    < /mesh >
  < /object >
< /amf >
```

In fig.4.3 there is a representation of a curved triangle in the AMF format whose syntax is represented beside the figure with some of its XML elements.

4.1.2 Slicing

The slicing process is based on the division or slice of a three dimensional object by planes called layer $2.5D$ since their non null thickness [28]. The overlapping of one layer on the other generates the final object. This process today is effectuated by specific software, slicing software, which basically are CAM, computer aided manufacturing, software dedicated to the AM processes [2]. The representation of a 3D object through a sliced model, composed by layer, has some intrinsic difficulties. The main problems to deal within a slicing process during the research for the best layers for the correct object representation are the presence of peaks in the figure, the correct representation of flat area and the staircase effect [1]. In fig.4.4 there is a representation of a cad model before and after a slicing procedure.

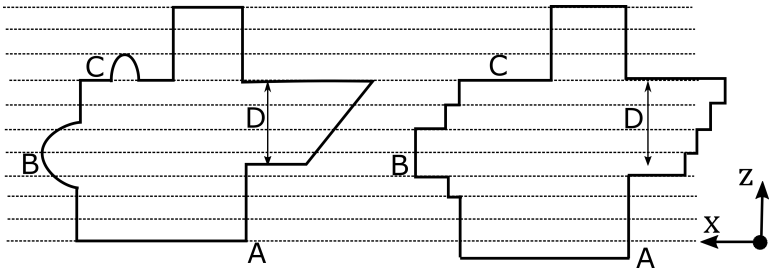

Figure 4.4: Slicing of a cad model

Here are evident, and for illustrative scopes they have been magnified, the main problems that a slicing algorithm has to face. The staircase effect, whose name is pretty much explicative of the problem itself, derives from a discrete representation of continuous surface and it is evident in particular in that object regions where the surface curvature is higher, B. The peaks problem is instead visible in the point C where a feature of the model has been completely omitted by the sliced representation. This happens when some parts of the model have variations, peaks, which are smaller than the layer thickness and so they result to be undetectable. The flat surfaces are the object surfaces parallel to the slicing planes. The main error in this case is the not respect of the dimensional tolerances, D. Here is evident how the relative distance between the two surfaces have been modified, by changing what could be an important feature for the final component. The detection of these surfaces is important also because they are the external surfaces of the object and so they define the surface quality of the object. Many AM technique treat these surfaces in a different way by filling them in a more accurate way than the internal parts of the object [1]. In A is indicate what is the AM technique offset; the first slicing plane must never coincide with the bottom surface of the model otherwise an undesired layer is added to the object.

All these problems can be faced with different approaches aimed to the single cases but in the literature the main development to face the slicing issues has been the adaptive slicing [1, 35, 46]. In [31] the slicing procedures are divided in two groups, the group of the uniform ones and the group of the adaptive ones. In the firsts the layer thickness is kept constant, by leading the slicing algorithm to face all the undesired effects of fig.4.4; here the only way to react is to decrease the layer thickness with a consequent increase of the printing times. In the seconds the layer thickness is variable according to specific logics and parameters in order to optimize some goals of the printed object, for instance printing time and surface quality. In [35] is used an adaptive algorithm to change the layer thickness according to the maximum admissible cusp height of the material in excess or in defect in respect of the object profile. In fig.4.5a is shown the cusp, and it is

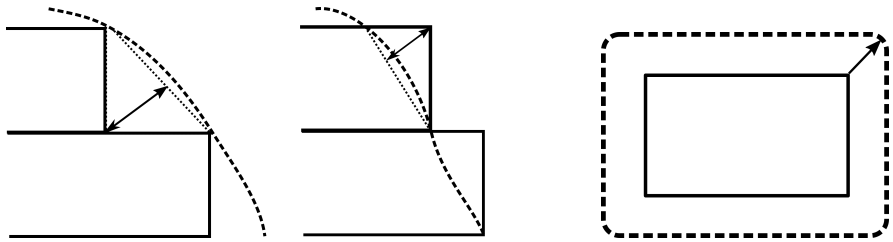

(a) Cusp height **(b)** Contour offset

Figure 4.5: Slicing decision taking

indicated the relative height, during the approximation of a CAD model. The cusp height is an index of the approximation degree effectuated; by keeping constant the layer thickness with higher curvature on the surface we get cusp with bigger heights. To set a limit to this value means to set a limit to the minimum quality acceptable for the reconstruction of the object geometry. The algorithm proposed keeps the cusp height as big as possible inside the limit imposed, in this way is respected the quality required by at the same time optimizing the printing time. The use of the cusp height is a parameter freely chosen to execute an adaptive slicing but other parameters can be considered. For instance in [46] are used the voxel, volume pixel, of the CAD file to determine the layer thickness to apply. Independently from the parameter utilised the approximation of a slicing procedure can be done by excess or by default. In fig.4.5a the best approximation is the one on the left(by default) or the one the right(by excess)? It could be argue that is the one with the minimum cusp height but actually the choice of proceed by excess or by default is AM process dependent [1]. Some AM techniques use superficial and heat treatments after the printing phase which inevitably diminish the material volume; in this case the most logic choice is the one to approximate the model surface by excess. Some decisions of the slicing software are intrinsically tied to the specific AM technique utilised. An other example is given by the contour construction for the different layers, fig.4.5b. The contour generated by the slicing process must be modified in order to compensate the tool utilised fro printing or for any sequent manufacturing process. At this level, differently from the STL or AMF which are constructed regardless of how the piece will actually be made, the slicing software must take under consideration the AM process utilised.

The slicing algorithms have as input file the CAD object, usually as STL. This format introduces a series of errors and issues; to work around the STL defects has been introduced an other important branch of the slicing development, the direct slicing [31]. The direct slicing involves to direct operate the slicing procedure on the CAD model without using the STL file [22]. It is to be notice that the STL too is a CAD format, so the difference of the direct slicing is in using the proprietary format of the CAD

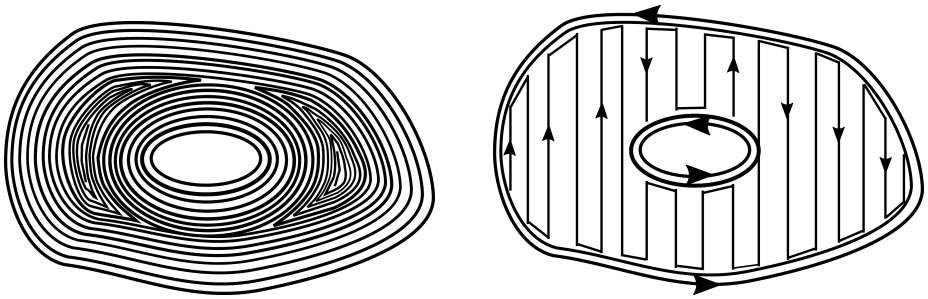

(a) Countour-Parallel tool path **(b)** Direct-Parallel tool path

Figure 4.6: Contours and infill paths

software used to design the object by avoiding the use of an intermediate format which is the STL. Any passages through the original CAD file to the STL involves a loss of informations. This kind of approach can be applied only with the involvement of the CAD software vendors by being their CAD format proprietary and out of any standard [22,45]. This kind of techniques are used even when the CAD file is not generated directly by a CAD software but it is acquired from a reverse engineering operation as from measures effectuated through a CMM, coordinate measure machines [31].

Once are defined the layers where the discretization of the model is effectuated, the slicing software defines the tool paths in order to print the object contours and the internal parts for each layer. In fig.4.6 are shown two possible infill path for one layer. The layers contours are usually separated into internal and external and they are closed paths respectively described counter clockwise and clockwise [40], as shown in fig.4.6b. The importance of separate external from internal contours is in the facility of recognize the areas where to apply an infill path. The contours, which can be repeated more than one time, are scaled according to the necessities of the AM process used to print. The infill path can be evaluated according to different logics. Two possible approaches are shown in fig4.6, where in the left figure the external and internal contours are scaled until the cover the entire area of the layer, whereas in the right figure starting from the same contours, repeated twice, is applied an infill path made of straight lines parallel to a fixed direction. The infill paths applied by the slicing software, more than the layers choice, is related to the specific AM process utilised. Fig.4.6 shows the typical infill paths used in the FDM. In [47] is presented an algorithm for the the generation of infill paths specifically for the SLA. The final output of this work is the generation of an output file for the AM machine, usually the g-code [9]. This files contains the trajectories defined by the slicing algorithm.

The procedure and the concepts here described on the slicing processes are under continuous development. Among the topics most studied there is

the possibility to effectuate slicing procedure along multiple directions [13] or the possibility to effectuate slicing procedure on three dimensional surfaces and not only planes [36]. The concepts at the bases of the slicing software do not change but the geometrical problems and the relative algorithms become more complicated pointing to new applications [30] which could be difficult to realize with the classical slicing techniques.

4.1.3 Gcode

The g-code is an alphanumeric language based on the standard EIA/ISO [37] and it is considered the industrial standard as regards the numerical control machines. Such a standard has been taken from applications like turning and milling and applied to the AM field. The g-code is not an international standard but it is a standard *de facto* whose code can be mainly referred to the norm ISO-6983 [20] but every CNC vendors has its own g-code [37], customized with the add of specific commands. A g-code program is constitute by words, single commands, collected in blocks, lines of code, which describe the movements that the machine must execute and all its auxiliary functions [15]. In fig.4.7 is visible an example of a trajectory generated by a slicing program and on the side the related g-code. The program is divided by lines of code enumerated in sequence. For a complete explanation of all the g-code commands is possible refer to [20]. Here we will explain some of them by focusing on the logic of the program. The heart of the program lies in the G-commands, defined preparatory commands, which specify the point that the machine must reach and the type of interpolation to use. For instance in the third block of the example commands the machine to reach the point of coordinate $X0Y50$, starting from the current position of the machine, with a linear interpolation, $G01$, in the machine workspace, so a straight line. The g-code commands a series of sequential movements by specifying the movement typology and by specifying some parameters as the feed rate, F. A the G-commands can be added others type of instructions as the M-commands, defined miscellaneous functions, which are specific instructions for the machine coded with a unique number and related to the auxiliary functions of the machine itself, as turning-on an heating system. In the example reported is used also the E-command, which is a command usually generated by the slicing software for the FDM machines, which specify the wire length to extrude. By describing the trajectory to follow the g-code do not give any specification about the passage from one G-command to another. It is evident how the trajectory described in the example, sum of straight lines with a constant velocity, is impossible to obtain from a physical point of view. The choice of how interpolate the segments of the trajectory are left to the machine interpolator.

Part Program Example
N01 M140 S60
N02 M104 T0 S200
N03 G01 X0 Y50 F100 E1.2
N04 G02 X50 Y50 I25 J0 F30 E2.0
N05 G01 X50 Y0 F100 E2.87
N06 G01 X10 Y0 F100 E3.2
N07 G01 X0 Y0 F100 E3.45
N08 M104 T0 S0
N09 M140 S0

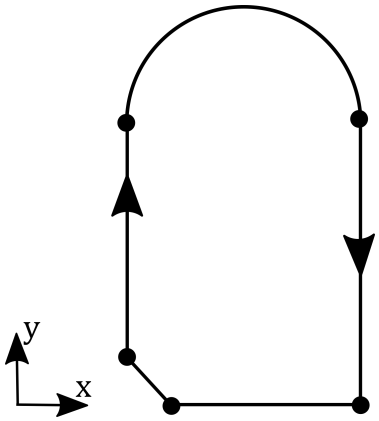

Figure 4.7: G-code example

The intrinsic limits of the g-code has lead to the decision to develop a new standard called STEP-NC, STandard for the Exchange of Product-NC, ended in the norm ISO-14649 and derived from the norm ISO-10303 [18]. The step-nc proposes to substitute to the g-code commands, aimed to specify the movements of the machine tool-centre-point, with instructions which specify the processes to follow according to the concept object-oriented of the WorkingStep. A workingstep is a manufacturing process associated with some process parameters [43]. For instance whereas a g-code gives a circular command to execute a hole in an object, command $G02$, an a step-nc file is simply specified that is desired the creation of a hole in the object in a specified position. It is duty of the machine to translate the workingstep in a trajectory for the single axis. When executing a g-code a machine is blind in respect of what is doing. With the step-nc there is a change in the informations passed to the machine, passing from a logic *how-to-do* of the g-code to a logic *what-to-do* [41]. A file step-nc is constitute by two parts, an header where are listed the general informations of the program, and a data section where are stored all the informations related to the part geometry, the manufacturing processes and the technology to use. The norm ISO-14649, the step-nc, has been created with a specific attention for technology as milling and turning, to which are dedicated specific sections of the norm, but not for the AM. Today a specific section for the AM is under development [21]. The use of this format has been studied and approved in the literature by promoting its use in the AM field [6, 39]. It has to be point out, as described in [6], that the introduction of the step-nc file do not substitute merely the g-code and its logic it drastically change the *digital chain* of the AM processes. The step file, father of the step-nc, are born to contain very different informations about a product and assist the production process during all its life integrating informations coming from the different program as CAD, CAPP, CAM. The use of a step-nc file would

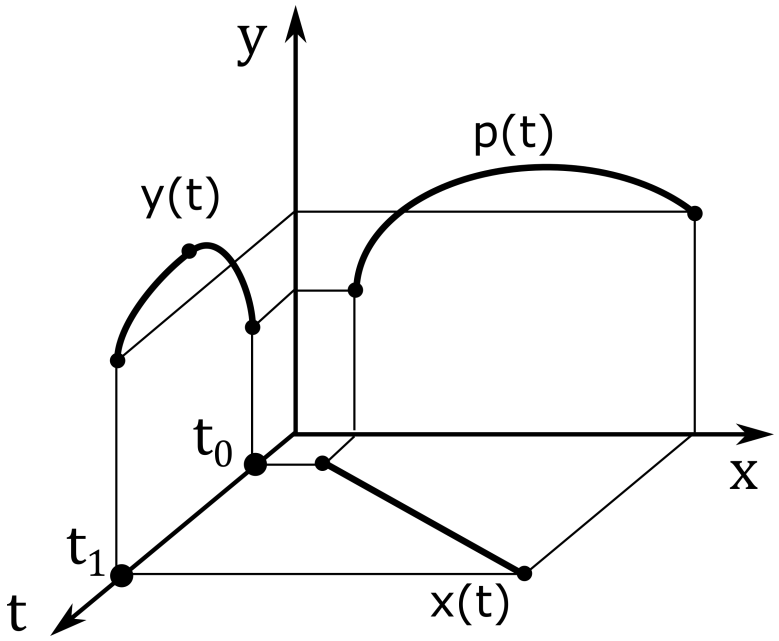

Figure 4.8: Interpolation example

exclude the use of an STL file and of the g-code. In [5] is described how the use of a file step-nc can reduce or eliminate entirely the loss of informations of the digital chain usually used in the AM.

4.1.4 Interpolation

The paths generation for the single machine axis is the lower level of the chain here described in order to create the trajectories for an AM machine. In this sector the AM has largely gleaned from the CNC world where the trajectories development is a topic studied for a long time [26]. The interpolator has the duty to generate such trajectories starting with the parsing of the commands received from the g-code [37]. In fig.4.8 is reported an example of what it has been said. The interpolator generates the single axis trajectories, $x(t)$ and $y(t)$, in order to obtain the desired trajectory in the machine workspace $p(t)$. Every command G of the g-code specify the starting and ending points for the trajectory $p(t)$ and the typology of interpolation desired. The interpolator must add all the middle points required to generate the trajectories $x(t)$ and $y(t)$ by generating their velocity and acceleration profiles and coordinate their motion laws. Here there is one of the ambiguity left by the g-code, which by specifying a constant velocity for the trajectory $p(t)$, the feed rate, leaves a margin of decision to the interpolator on how execute the actual motion laws. Furthermore the g-code, composed by the union of several segments, dictates a trajectory in

the machine workspace that would be impossible to realize. Goal of many interpolators is to minimize the position and velocity errors [3, 23] in order to guarantee the correct execution of the manufacturing process.

The interpolator are divide into two groups, hardware and software interpolator according to how are implemented [37]. The technological evolution in the electronic processors field has pushed the vendors of CNC machine to use more and more the second solution even though still today we can find solution where the hardware approach can have its advantages [12]. Inside the interpolator can be implemented different methods and algorithms in order to accomplish the axis interpolation by aiming to respect different goals, as high precisions or high velocities. The interpolator must take into account the physical limits of the machine given by the limits on forces, torques, velocities and accelerations of the actuators [7]. Among the main methods studied and developed, those based on NURBS curves, Non Uniform Rational Basis-Splines, definitely stand out. In the literature we can find several progresses in their use [3, 12, 23]. The great interest for this kind of curves derives from the fact that the NURBS have found a great utilise in the modern systems of computer graphics thanks to their capacity to describe complex curves and surfaces with a relative small amount of data. Nevertheless the great interest their utilise in the industrial field is still limited [3].

4.2 Overfill and underfill

The correct material deposition for AM extrusion processes can be evaluated through a measure of the material quantity deposited. An incorrect dosage of the material leads to the phenomena of overfill or underfill depending on whether the quantity of material released on time is higher or lower than expected. The underfill and overfill phenomena are very common in the manufacturing process based on the extrusion of material and in the AM fields they have been faced by improving the trajectories generated that are upstream of these phenomena [8, 17, 33, 44]. By focusing on the trajectories generated, the failure to deposit the correct amount of material can be analyzed in two ways; from a point of view purely geometrical, where it is taken into account only of the relative path between printing plate and extrusion system, and from a kinematic point of view where the lack of coordination between the printing velocity and the material flow rate is the cause of the phenomena. The inevitable discretization of a continuous figure through the selective deposition of material through a nozzle leads to the generation of paths where some areas can remain uncovered, underfill, and others where the deposition system has found itself to be more than one time, overfill fig.4.9a. In [44] is pointed out the importance of these effects in order to obtain a god printing quality; it is proposed an algorithm which analyse

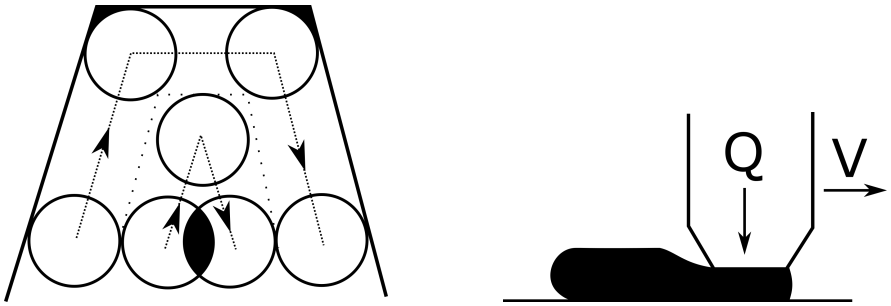

(a) Geometry path

(b) Mismatching between material flow rate, Q, and velocity printing, V

Figure 4.9: Overfill and Underfill

the geometrical path of the machine tool deriving from the slicing process and the underfill and overfill areas are minimized by acting on the relative distance of the material wires deposited, process parameter that is usually kept constant. The lack of coordination between the material flow rate and the printing velocity leads to the same problems derived by having a bad geometrical path, fig.4.9b. In the printing systems the material flow rate is function of the printing velocity, for every g-code commands passed to the machine is specified a printing velocity and the amount of material to extrude, par.4.1.3, kept constant for the entire command. The main problems arises in the passing points from one G-command to another and in the start and stop points. In [8] is pointed out how the interpolation of straight lines in the g-code is one of the causes of the underfill and overfill phenomena; in [8] is proposed an algorithm which consider a constant extrusion rate but it reduces the printing velocity in the passages among two consecutive segments in order to avoid jumps in the velocity and acceleration profiles. In this case the variation of velocity will cause depositioning errors, by being the extrusion rate kept constant, but those errors are kept under a level of acceptability by bringing some benefits in terms of overfill and underfill reduction. Differently in [14] the tangent velocity of the printing trajectories is synchronized with the extrusion rate by keeping constant the ratio between the two ; some improvements are obtained in the curvilinear lines and in the start and stop points. At same time an adaptive control is added to the system to keep constant the temperature of the material. The synchronization of the extrusion system, by considering its extrusion rate and temperature, with the printing velocity leads to the necessity of considerate a dynamic model that for complexity reasons have been excluded in [8]. Such models are dependent from the fluid dynamic properties of the material extruded. In [14] the extrusion dynamic is compared through a constant of proportionality to the dynamic of the mechanical system used to extrude the material so committing some errors by not considering the

delays due to the viscosity of the material. The existence of such delays are pointed out by a Stratasys patent [17], company leader in the FDM sector. In this patent is taken into account during the printing phase a model of the melted material in order to consequently regulate the material flow rate at the entrance of extruder and keep constant the material flow rate out of the nozzle. The model used describes the behaviour of the material flow rate to a step through an exponential trend dependent on a constant τ, a dynamic system of the first order. The constant τ expresses the characteristics of thermal exchange of the material and of the extrusion system. The synchronization between printing velocity and and material flow rate between two printing segments with different velocities requires the use of an extrusion model which takes into account the properties of the material and of the extrusion system.

In the following we propose and develop an algorithm for the trajectories generation based on the Bézier curves starting from the linear segments described by the g-code. To avoid oscillations in material deposition the material flow rate is kept constant all along the trajectory and it is imposed a constant printing velocity. This solution allows to disregard the properties of the material and the development of a thermal and dynamic model of the extrusion system going to reach a constant ratio between speed and flow in most of the trajectory sections. In the context of the Efesto project this will allow to study more materials having the guarantee of a correct extrusion process regardless of the material used.

4.3 Efesto digital chain

The digital chain of the 3D printing are the passages which allow to pass from the idea of a three dimensional object designed on CAD software to the real object. In the Efesto printer this process applied to an print with a constant extrusion rate is composed in the following way:

1. Drawing of the component to be printed using a CAD software and saving the file in an STL format. The SolidWorks and Inventor software are mainly used here.

2. The STL file is utilised to generate a g-code through a slicing software. The open source Slic3r software is mainly used here.

3. The gcode is used as a starting point for generating print trajectories in the robot workspace. MatLab is used here for the reprocessing of the gcode through the algorithms that will be presented later on.

4. The desktop application developed in C# allows to transmit the data created in MatLab to the machine during printing through an online communication.

5. The motion CPU of the system, appropriately programmed, uses the data coming from the PC to generate the trajectories of the individual axes of the machine and print the object.

The use of slicing software allows us to obtain the points, in the print plan $x - y$, which define the contours of the figure and which will be the inputs for the construction of the trajectories in MatLab. Otherwise it would be necessary to develop a slicing algorithm starting from the STL file. Once the points are extracted from the gcode these will be the constraints on the path to follow; these constraints are purely in position, the speed of passage on points, and accelerations, can be set at will.

4.4 Trajectory generation

The problem of constructing a trajectory starting from pre-established points is an interpolation problem that has already been dealt with in the literature, particularly in the world of CNC machines. The use of specific algorithms for the generation of the trajectories depends very much on the type of objective that is set. Kulkarni et al. [27] study the importance of the tool path planning on the resulting stiffness of the printed objects. Jin et al. [24, 25] propose a new path planning algorithm in order to minimize the building time of the part at the same time maintaining a good surface accuracy. In order to overcome deposition problems, related to a new metal based AM technique, Mireles et al. [29] were required to modify the toolpath commands of a pre-existing FDM machine. Rishi [34] has shown how a different feed rate can be used to improve accuracy of the surface or the building time of the internal parts.

For systems based on a constant feed rate, as the Efesto machine, in order to guarantee a uniform material deposition the Direction-Parallel Tool-Path (DP) technique, fig.4.6b, can be used to achieve this goal. Some articles are available in literature proposing DP deposition trajectories using an approach based on lines and parabolas and moving the end-tool with constant feed rate where possible along the trajectory. Thompson [11] shows constant material flow trajectories for straight lines using a constant acceleration to link the velocity for two consecutive lines with different velocities: in this way an absolute velocity error is introduced where the smaller the angle between the two consecutive lines the greater the error. This requires the need to change the material flow during the parabolic segments. Jin [44] suggests a straight lines and parabolas trajectory based entirely on the curvilinear abscissa velocity control. Defining two lines typologies (type I used for lines which intersect the deposition profile, and type II for lines adjacent to the profile boundaries) a different absolute velocity is imposed on the two types: usually velocity I is double velocity II and a constant acceleration profile is used to link the two lines on the curvilinear abscissa. The extruder motion

law is created taking into account the velocity variations of the control parameters. This strategy leads to limited accelerations on active joints during curved paths attaining a good printing velocity. In the field of CNC machining the use of Bézier curves has been exploited in order to obtain continuity on the velocity and acceleration usually not obtainable by the G-Code based on straight lines and the use of G1 commands [10].

We decide to develop an algorithm for the creation a parametric trajectory of the machine TCP, tool-centre-point. The motion law of the printing plate is the equal to the motion law of the linear delta end-effector. The generated trajectories are developed starting from the Bèzier curves, particular case of the NURBS curves which are the same typology of curves with which most of the surfaces are described in computer graphics software to date, including CAD. The goal of these trajectories is to maintain constant the delta linear velocity, and consequently to allow a constant extrusion printing.

4.4.1 Parametric trajectory

To define a trajectory in the cartesian space (XYZ) is necessary to determine a parametrized geometric path

$$\mathbf{p} = \mathbf{p}(u), \qquad u \in [u_{min}, u_{max}] \tag{4.1}$$

where $\mathbf{p}(u)$ is a continuous vector function which describes the path in the robot workspace as function of the independent variable u defined inside a values range [4]. In our case are sufficient three coordinates to describe the linear delta translations.

The vector function so defined it is described by a motion law of type $u = u(t)$ which describes the linear delta TCP motion law.

In order to develop a motion law $u = u(t)$ with a constant velocity, which is the case of our interest, it is necessary to guarantee:

$$\left|\dot{\tilde{\mathbf{p}}}(t)\right| = v_c = costante \tag{4.2}$$

where $\tilde{\mathbf{p}}(t) = (\mathbf{p} \circ u)(t)$, and is derivatives can be evaluated as:

$$\begin{aligned} \dot{\tilde{\mathbf{p}}}(t) &= \frac{d\mathbf{p}}{du}\dot{u}(t) \\ \ddot{\tilde{\mathbf{p}}}(t) &= \frac{d\mathbf{p}}{du}\ddot{u}(t) + \frac{d^2\mathbf{p}}{du^2}\dot{u}^2(t) \\ &... \end{aligned} \tag{4.3}$$

It is not necessary to obtain analytically the function $u(t)$ but its punctual value $u(t_k) = u_k$ can be evaluated for any temporal instant $t_k = kT_s$,

with T_s sampling period. The evaluation of $u_k, k = 0, 1, 2, ...$, is based on the sequent Taylor series:

$$u_{k+1} = u_k + T_s\dot{u}_k + \frac{T_s^2}{2}\ddot{u}_k + o\left(\frac{T_s^n}{n!}u_k^{(n)}\right), \qquad k = 0, 1, 2, ... \tag{4.4}$$

From the eq.4.3 and eq.4.2 is possible to obtain the following conditions:

$$\dot{u}(t) = \frac{v_c}{\left|\frac{d\mathbf{p}}{du}\right|} \tag{4.5}$$

whereas, by deriving again the previous equation with respect to time and developing is obtained:

$$\ddot{u}(t) = -v_c^2 \frac{\frac{d\mathbf{p}^T}{du} \cdot \frac{d^2\mathbf{p}}{du^2}}{\left|\frac{d\mathbf{p}}{du}\right|^4} \tag{4.6}$$

by considering a second order approximation, the value of the variable u at the instant $(k+1)T_s$ can be determined as

$$u_{k+1} = u_k + \frac{v_c T_s}{\left|\frac{d\mathbf{p}}{du}\right|_{u_k}} - \frac{(v_c T_s)^2}{2}\left[\frac{\frac{d\mathbf{p}^T}{du} \cdot \frac{d^2\mathbf{p}}{du^2}}{\left|\frac{d\mathbf{p}}{du}\right|^4}\right]_{u_k} \tag{4.7}$$

As regards the segments of the trajectory with a non null acceleration, start and stop points, we have to modify the evaluation of u_{k+1} as follow:

$$u_{k+1} = u_k + \frac{v_k T_s}{\left|\frac{d\mathbf{p}}{du}\right|_{u_k}} + \frac{T_s^2}{2}\left\{\frac{a_k}{\left|\frac{d\mathbf{p}}{du}\right|_{u_k}} - v_k^2\left[\frac{\frac{d\mathbf{p}^T}{du} \cdot \frac{d^2\mathbf{p}}{du^2}}{\left|\frac{d\mathbf{p}}{du}\right|^4}\right]_{u_k}\right\} \tag{4.8}$$

where $a_k = a(t_k)$ and $v_k = v(t_k)$ are the acceleration and velocity at the instant $t_k = k \cdot T_s$.

4.4.2 Reference system

To evaluate the linear delta motion laws are utilised two reference systems, one fixed to the linear delta platform and and fixed to the Efesto machine frame. The object to be printed is represented in the platform frame and the motion laws are initially evaluated by imaging the platform fixed and the machine nozzle moving. This facilitates the creation of the printing trajectories during the slicing procedures.

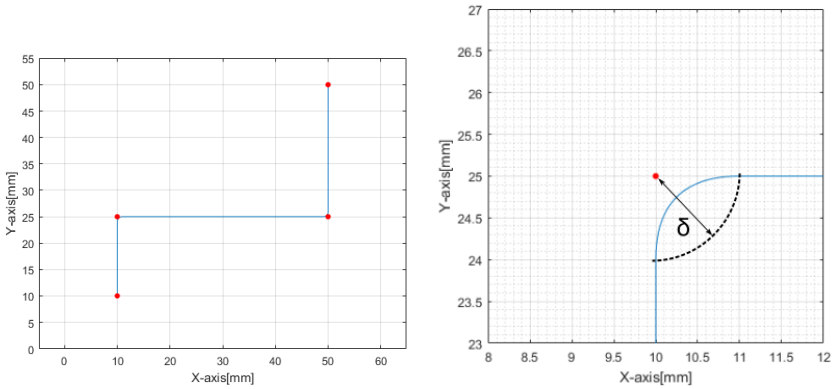

(a) Polygonal trajectory

(b) Junction between two consecutive lines

Figure 4.10: Trajectory example

By considering that in the Efesto printer the extruder is fixed and is the platform to move we have to rewrite the coordinates of a generic point P(x,y,z) from the platform frame $TCP - \hat{x}'\hat{y}'\hat{z}'$ to P(X,Y,Z) in the absolute frame $O - \hat{x}\hat{y}\hat{z}$ by considering the opposite of the TCP displacement expressed by the **p** vector. The following relationship applies:

$$\begin{cases} X = -x \\ Y = -y \\ Z = h_{dep} - z \end{cases} \tag{4.9}$$

where h_{dep} corresponds to the layer thickness of the printing process. At the same way for velocities and accelerations apply:

$$\begin{cases} \dot{X} = -\dot{x} \\ \dot{Y} = -\dot{y} \\ \dot{Z} = -\dot{z} \end{cases} \qquad \begin{cases} \ddot{X} = -\ddot{x} \\ \ddot{Y} = -\ddot{y} \\ \ddot{Z} = -\ddot{z} \end{cases} \tag{4.10}$$

4.4.3 Modification of the g-code

The trajectories generated here starts from the evaluations of the single g-commands which specify every segment of the trajectory by straight lines, since only G1 commands are used, and the relative velocity. Since the will to obtain a printing process with a constant extrusion rate and so a constant velocity along the printing trajectory we need to interpolate the two segments by modifying the trajectory depicted by the g-code. This operation is carried out through the use of second degree Bézier curves. In fig.4.10 is possible to see the modification of a g-code where e trajectory

constitutes by four segments is interpolated by the use of the algorithm here developed. Along a path of this type the linear delta TCP starts with a null velocity and ends with a null velocity; during the entire central path of the trajectory the velocity is kept constant.

4.5 NURBS

The NURBS curves, Non Uniform Rational B-Spline, are born in the '70 from the work of Pierre Bézier and and today they are a standard de facto in the industrial world for the representation, design and exchange of geometrical data [32]. Many international standards utilise them, as the STEP files. The Nurbs curves are expressed by:

$$C(u) = \frac{\sum_{i=0}^{n} N_{i,p}(u) w_i P_i}{\sum_{i=0}^{n} N_{i,p}(u) w_i} \qquad a \leq u \leq b \tag{4.11}$$

where the i-th $N_{i,p}$ is the B-spline of degree p weighted with its value w_i. The values P_i are the curve control points. The Nurbs curve is a parametric curve, where the parameter u can assume the values between a and b; usually these values are set equal to 0 and 1 but this is not mandatory. The B-spline are defined inside what is called knots vector:

$$U = \{\underbrace{a, ..., a}_{\text{p+1}}, u_{p+1}, ..., u_{m-p-1}, \underbrace{b, ..., b}_{\text{p+1}}\} \tag{4.12}$$

The Nurbs curves are so a ratio of a weighted sum of B-Splines. Since the B-splines are the core of these curves we go to show and explain them; for a deeper insight the reader can refer to specialized texts [32]. A B-spline curve is defined starting from the node vector, the degree p of the basic curves which form it and from the control points vector; its definition, very similar to the Nurbs, is:

$$C(u) = \sum_{i=0}^{n} N_{i,p}(u) P_i \qquad a \leq u \leq b \tag{4.13}$$

The B-splines are obtained from sum of the basis functions $N_{i,p}$ so defined:

$$N_{i,0}(u) = \begin{cases} 1 & u_i \leq u \leq u_{i+1} \\ 0 & \text{otherwise} \end{cases} \tag{4.14}$$

$$N_{i,p}(u) = \frac{u - u_i}{u_{i+p} - u_i} N_{i,p-1}(u) + \frac{u_{i+p+1} - u}{u_{i+p+1} - u_{i+1}} N_{i+1,p-1}(u) \tag{4.15}$$

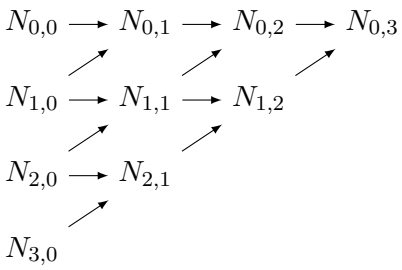

Figure 4.11: Triangular basic Splines scheme

The basis functions are constructed in a recursive way by starting from the ones of zero degree, which can assume only a null or unitary value, to the ones of p degree whose value depends from the basis functions with a lower degree, from the parameter u value and from the knot vector which defines the u_i values. With a reference to fig.4.11 we explain briefly how to evaluate a B-spline in the point $\bar{u}$ starting from e defined knot vector, the use of p basis functions and the control points P_i. In fig.4.11 is represented in a triangular scheme the basis functions from a zero degree, $N_{i,0}$, to a three degree, $N_{i,3}$. Every basis functions depends upon the ones with a lower degrees; for instance the $N_{0,2}$ depends upon the values of $N_{0,1}$ and $N_{1,1}$. The i value indicates the membership interval of the basis functions by referring to the intervals defined by the knots u_i. If we want to evaluate the value of $N_{0,3}(\bar{u})$ we must to calculate all the values of the basis functions on which it depends. It is worth to notice how for each value of u inside the reference interval $a - b$ only one zero degree basis function has a non null value; this means that many of the basis functions on which $N_{0,3}(\bar{u})$ depends have a null value. Different algorithms exist for the iterative calculation of basis functions.

In fig.4.12 are drawn two different B-splines with the same control points P_i but with different degrees, second and third degree. These are plane curves and the control points P re bi-dimensional vectors, $x-y$. By changing the degree of the curve we obtains a different B-spline; the lower is the degree the bigger is the proximity to the control polygon of the B-spline. The control polygon is the polygon defined by the straight lines joining the control points of the system; it is equal to the B-spline with a zero degree. It is important to notice that the control points are not usually the points for which the curve is to be passed; the control points are obtained by solving a system of equations in which the passage of the B-spline is imposed for a series of desired points.

The Bézier curves are a particular case of B-spline, where the parameter u is always defined between 0 and 1 where the knots vector is composed

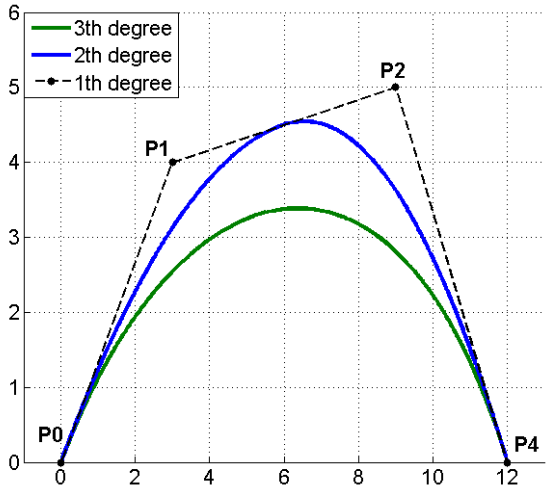

Figure 4.12: Basis spline with fixed control points and different degrees

only by 0 and 1 without middle points.

$$U = \{\underbrace{0, ..., 0}_{\text{p+1}}, \underbrace{1, ..., 1}_{\text{p+1}}\} \tag{4.16}$$

4.5.1 Bézier curves

In order to plan a trajectory with a constant velocity in all its points we implement a parametric curves in the robot workspace. To follow this approach it have been exploited the Bézier curves to generate a parametric path composed by straight lines ans parabolas.

A Bézier curve if degree m is defined as [4]:

$$\mathbf{b}(u) = \sum_{j=0}^{m} B_j^m(u)\mathbf{p}_j, \qquad 0 \leq u \leq 1 \tag{4.17}$$

where the coefficients $\mathbf{p}_j$ are the control points, and the basis functions $B_j^M(u)$ are the Bernstein polynomials defined as:

$$B_j^m(u) = \binom{m}{j} u^j (1-u)^{m-j} \tag{4.18}$$

This expression can be derived from the equations 4.14 and 4.15. The binomial coefficient can be expressed as:

$$\binom{m}{j} = \frac{m!}{j!(m-j)!} \tag{4.19}$$

m										
0	1									
1	1	1								
2	1	2	1							
3	1	3	3	1						
4	1	4	6	4	1					
5	1	5	10	10	5	1				
6	1	6	15	20	15	6	1			
7	1	7	21	35	35	21	7	1		
8	1	8	28	56	70	56	28	8	1	
9	1	9	36	84	126	126	84	36	9	1

Table 4.1: Triangle di Pascal

The binomial coefficient, for $j = 0, 1, ..., m$, gives the shape to the Pascal triangle shown in tab. 4.1 for $m = 1, 2, ..., 9$.

The derivative of a Bézier curve of m degree with respect to the variable u is still a Bézier curve of $m - 1$ degree defined as:

$$\frac{d\mathbf{b}(u)}{du} = m \sum_{i=0}^{m-1} B_i^{m-1}(u)(\mathbf{p}_{i+1} - \mathbf{p_i}) \tag{4.20}$$

It has been used straight lines and parabolas, expressed by Bézier curves of first and second degree, expressed as:

$$\begin{aligned} \mathbf{b}(u) &= (1-u)\mathbf{p}_{j-1}^u + u\mathbf{p}_j^e && straightline \\ \mathbf{b}(u) &= (1-u)^2\mathbf{p}_j^e + 2u(1-u)\mathbf{p}_j + u^2\mathbf{p}_j^u && parabola \end{aligned} \tag{4.21}$$

The complete trajectory is created by the alternation of straight lines and parabolas, each parametrized independently by the parameter u defined between $[0, 1]$. This approach simplifies the writing of the trajectory equations, but complicates the introduction of the motion law along the parametric variable u every times we have to pass from a straight line to a parabola and vice versa.

It is possible to see in fig.4.13 the control points $\mathbf{p}_j$ in the robot workspace which corresponds to the angle points of the trajectory extracted from the g-code. In order to smooth the trajectory defined by two segments and three points, from $\mathbf{p}_{j-1}$ to $\mathbf{p}_{j+1}$, a circle of radius δ centred in the middle point is used to generate the entrance and exit point of the parabola, $\mathbf{p}_j^e$ and $\mathbf{p}_j^u$.

The straight lines will be delimited on one side from the exit point of the previous parabola, $\mathbf{p}_{j-1}^u$, and on the other from the entrance point of the next one $\mathbf{p}_j^e$.

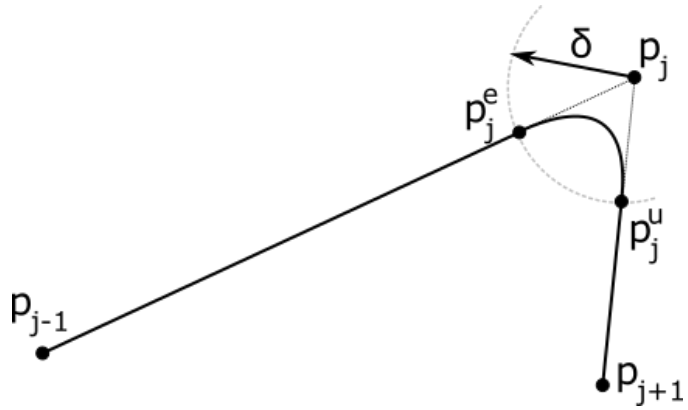

Figure 4.13: Interpolation between two trajectory segments

The derivative of the eq.4.21 with respect to the variable u is evaluated with the formula 4.20, obtaining for the straight lines:

$$\begin{aligned} \frac{d\mathbf{b}}{du} &= -\mathbf{p}_{j-1}^{u} + \mathbf{p}_{j}^{e} \\ \frac{d^2\mathbf{b}}{du^2} &= \mathbf{0} \end{aligned} \tag{4.22}$$

and for the parabolas:

$$\begin{aligned} \frac{d\mathbf{b}}{du} &= -2(1-u)\mathbf{p}_{j}^{e} + [2(1-u) - 2u]\,\mathbf{p}_{j} + 2u\mathbf{p}_{j}^{u} \\ \frac{d^2\mathbf{b}}{du^2} &= 2\mathbf{p}_{j}^{e} - 4\mathbf{p}_{j} + 2\mathbf{p}_{j}^{u} \end{aligned} \tag{4.23}$$

By evaluating for straight lines and parabola $\frac{d\mathbf{b}}{du}$ and $\frac{d^2\mathbf{b}}{du^2}$, by exploiting the equations 4.5 and 4.6 we get $\dot{u}(t)$ and $\ddot{u}(t)$.

It is now possible to evaluate the derivatives with respect to time of the Bézier curves through the use of the equations 4.3, which are for the straight lines:

$$\begin{aligned} \dot{\tilde{\mathbf{b}}}(t) &= \left(-\mathbf{p}_{j-1}^{u} + \mathbf{p}_{j}^{e}\right)\dot{u} \\ \ddot{\tilde{\mathbf{b}}}(t) &= \left(-\mathbf{p}_{j-1}^{u} + \mathbf{p}_{j}^{e}\right)\ddot{u} \end{aligned} \tag{4.24}$$

and for the parabolas:

$$\begin{aligned} \dot{\tilde{\mathbf{b}}}(t) &= -2\,(1-u)\,\dot{u}\mathbf{p}_{j}^{e} + [2\dot{u}\,(1-u) - 2u\dot{u}]\,\mathbf{p}_{j} + 2u\dot{u}\mathbf{p}_{j}^{u} \\ \ddot{\tilde{\mathbf{b}}}(t) &= \left[\dot{u}^2 - 2(1-u)\ddot{u}\right]\mathbf{p}_{j}^{e} + \left[2\ddot{u}(1-u) - 2\dot{u}^2 - 2u\ddot{u}\right]\mathbf{p}_{j} + \left(2\dot{u}^2 + 2u\ddot{u}\right)\mathbf{p}_{j}^{u} \end{aligned} \tag{4.25}$$

It is possible now to generate the motion law of the linear delta TCP by evaluating the discrete values of $u(t)$ for every temporal instant with

a sampling period T_s. The goal is to generate a TPV, trapezoidal profile velocity, motion law for the parameter $u(t)$ in order to satisfy the necessity of constant velocity along the trajectory. For the segments with a constant acceleration is used the eq.4.8, whereas for the central part of the trajectory with a constant velocity is used eq.4.7.

Since the alternation of straight lines and parabolas in the crossing point from the two trajectory segments there will be a velocity variation due to the sampling period used. With reference to fig.4.14 it is possible to see how the last sample of the straight line is unlikely to be the last point of the straight line, $u = 1$, and the first sample of the parabola should be the first point of the parabola, $u = 0$. This choice would not respect the sampling period imposed in the algorithm. We have to guarantee the spatial distance Δb between the last sample of the straight line and the first sample of the parabola by avoiding the case where a minor distance $\Delta s < \Delta b$ is used starting from the point $u = 0$ of each segments. As represented in fig.4.15, by knowing that:

$$\Delta b = v_c \cdot T_s \tag{4.26}$$

$$\Delta r = b_{retta}(u = 1) - b_{retta}(u_f) \tag{4.27}$$

it is necessary to evaluate the variable u_2 carefully to collocate the first sample of the parabolic segment to a distance Δb along the curve evaluated as:

$$\Delta p = \Delta b - \Delta r \tag{4.28}$$

by rewriting opportunely the eq.4.7 for the parabolic segment it is possible to evaluate u_i

$$u_i = \frac{\Delta p}{\left|\frac{d\mathbf{b}}{du}\right|_{u=0}} - \frac{\Delta p^2}{2}\left[\frac{\frac{d\mathbf{b}^T}{du}\cdot\frac{d^2\mathbf{b}}{du^2}}{\left|\frac{d\mathbf{b}}{du}\right|^4}\right]_{u=0} \tag{4.29}$$

The same procedure with the same conventions are followed for the crossing point between the parabola and the straight line:

$$\Delta r = \Delta b - \Delta p \tag{4.30}$$

where

$$\Delta b = v_c \cdot T_s \tag{4.31}$$

whereas for the evaluation of Δb it is necessary to use the formula 4.7 by conveniently substituting

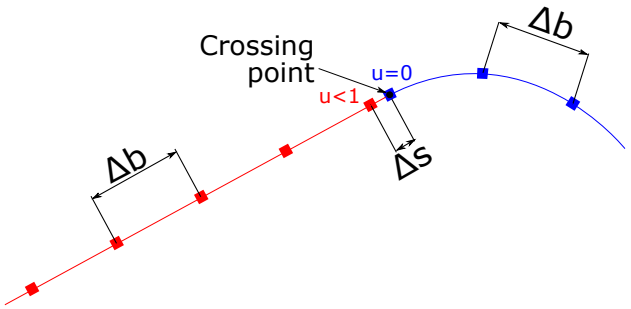

Figure 4.14: Crossing-point

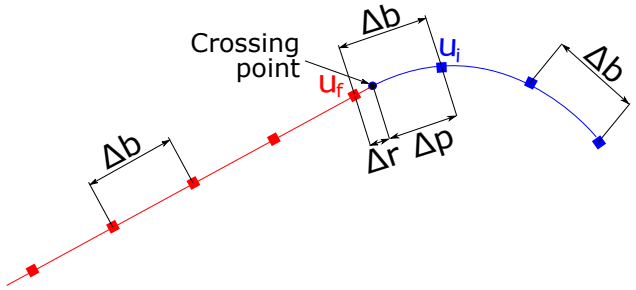

Figure 4.15: Correction of the crossing point

$$\begin{aligned} &u_{k+1} = 1 \\ &u_k = u_f \\ &v_c \cdot T_s = \Delta p \quad \text{unknown variable} \end{aligned} \tag{4.32}$$

by substituting and rewriting, we get a second degree equation with the unknown variable Δp:

$$\frac{1}{2}\left[\frac{\frac{d\mathbf{b}^T}{du}\cdot\frac{d^2\mathbf{b}}{du^2}}{\left|\frac{d\mathbf{b}}{du}\right|^4}\right]_{u_f}\Delta p^2 - \frac{1}{\left|\frac{d\mathbf{b}}{du}\right|_{u_f}}\Delta p + 1 - u_f = 0 \tag{4.33}$$

By resolving with respect to Δp it is possible to evaluate u_i on the straight line by substituting in the eq.4.7:

$$u_i = \frac{\Delta r}{\left|\frac{d\mathbf{b}}{du}\right|_{u=0}} \tag{4.34}$$

Once defined the trajectory in the robot reference system $TCP - \hat{x}'\hat{y}'\hat{z}'$, it is possible to actuate the coordinate change of eq.4.9 and 4.10 by obtaining

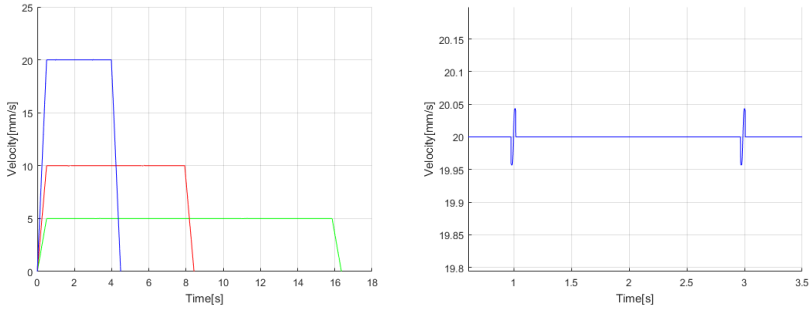

(a) Deposition velocity **(b)** Velocity oscillation

Figure 4.16: Parametric velocity $\dot{u}$

the TCP movement required for the printing process. Through the kinematic equations of the linear delta is possible to obtain the motion laws of the single machine axis.

Example

In this section we show a theoretical example of the use of Bézier curves. The process is carried out starting from a set of N points. The parameter inputs of this algorithm are the velocity to reach, $\dot{u}$ which is kept constant along the central part of the trajectory, and δ, which defines the maximum distance of one point from the trajectory generated, and so can be considered as the maximum error in a production process. Starting from a first point with a null velocity the algorithm takes into account three points at the time, fig.4.13, generating the trajectory until the final point is reached with a null velocity.

In fig.4.10, already used in section 4.4.3, is shown a trajectory generated considering four points highlighted in red. If we look closely it's possible to see how the middle points of the trajectory are not touched by the trajectory itself but the maximum distance of any point from the trajectory is lower than δ. In this way δ can be considered as measure of the process accuracy.

Three different parametric velocity $\dot{u}$ have been set as 5, 10 and 20[mm/s], fig.4.16a. All the velocities have a trapezoidal velocity profile where the maximum velocity reached is equal to the constant velocity, $\dot{u}_c$, that we want to maintain along all the central part of the path. During the central part of the trajectory the velocity can be considered constant with minor oscillations due to the jumps from one straight line to a parabola and vice versa. If we look closely, fig.4.16b, it's possible to see how during the two curves of the path there is a little variation in the parametric velocity $\dot{u}$. For the three velocities tried the percentage variation in the velocity with respect to $\dot{u}_c$ is always smaller than 0.3%,

$\dot{u}_c$[mm/s]	Percentage variation
5	0.14
10	0.27
20	0.22

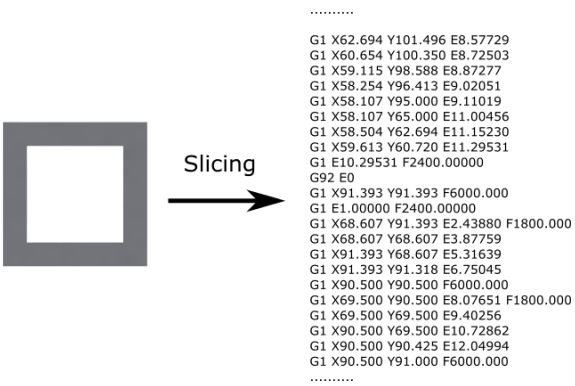

Figure 4.17: Generation of the g-code

4.5.2 Application

In order to demonstrate the applicability of the algorithm developed inside the Efesto machine and its digital chain it is effectuated a printing test.

Starting from the Cad of fig.4.17 it is generated a g-code. From the g-code file are extracted the points which define the figure, in this case a holed square. This points are used as input for the generation trajectory algorithm in MatLab, by creating the trajectory visible in fig.4.18a. It is imposed a printing velocity of 5[mm/s]. The data generated are passed to the machine control system, through the architecture described in the chap.**??**. In fig.4.19 is visible the final object of the printing process. We point out how this is

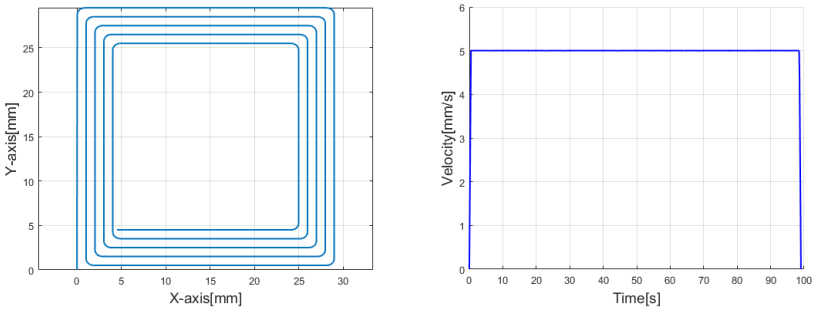

(a) trajectory **(b)** $\dot{u}$

Figure 4.18: Actual trajectory

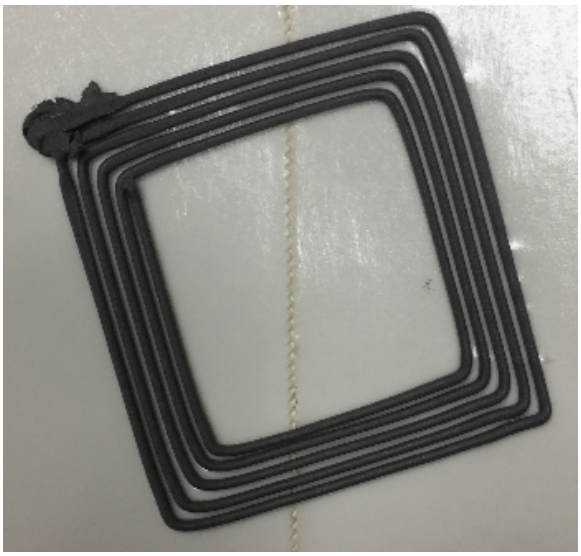

Figure 4.19: Printed object

a printing test finalized to the validation of the algorithm inside the digital chain of the Efesto machine. The result is so considered satisfying since the printing quality depends from many other factors besides the trajectory generated. In chap.5.10 are shown others printed object with the Efesto machine.

4.6 Conclusions

For extrusion-based processes, trajectory planning is essential to avoid overfill and underfill problems generated by an incorrect deposition of material due to a lack of synchronization between the material flow rate and the feed rate of the same. To guarantee the correctness of the process, an algorithm is developed for the generation of the trajectories based on a constant extrusion of material and a constant printing speed. This solution avoids the problems deriving from a poor modelling of the extrusion systems and the materials used. The developed algorithm, based on the use of Bézier curves, has been integrated into the printing chain of the Efesto machine starting from the data of a g-code but is applicable to any series of points specified in the working space of the machine.

bibliography

[1] Dolenc A. and Makela I. Slicing procedures for layered manufacturing techniques. *Computer-Aided Design*, 1994.

[2] C.M. Al and U. Yaman. An automated design and fabrication pipeline for improving the strength of 3d printed artifacts under tensile loading. *AIP Conference Proceedings1960*, 2018.

[3] X. Beudaert, S. Lavernhe, and C. Tournier. Feedrate interpolation with axis jerk constraints on 5-axis nurbs and g1 tool path. *International Journal of Machine Tools and Manufacture*, 2012.

[4] L. Biagiotti and C. Melchiorri. *Trajectory Planning for Automatic Machines and Robots*. Springer, 2008.

[5] R. Bonnard, P. Mognol, and J.Y. Hascoët. A new digital chain for additive manufacturing processes. *Virtual and Physical Prototyping*, 2010.

[6] R. Bonnard, E. Rodriguez, and A. Alvares. An advanced step-nc platform for additive manufacturing. *Research gate*, 2018.

[7] P. Bosetti and E. Bertolazzi. Feed-rate and trajectory optimization for cnc machine tools. *Robotics and Computer-Integrated Manufacturing*, 2014.

[8] A. Bouhal, M.A. Jafari, W.B. Han, and T. Fang. Tracking control and trajectory planning in layered manufacturing applications. *IEEE transactions on industrial electronics*, 1999.

[9] A.C. Brown, D. De Beer, and P. Conradie. Development of a stereolithography(stl) input and computer numerical control(cnc) output algorithm for an entry-level 3-d printer. *South African Journal of Industrial Engineering*, 2014.

[10] B.Sencer, K.Ishizaki, and E.Shamoto. A curvature optimal sharp corner smoothing algorithm for high-speed feed motion generation of nc systems along linear tool paths. *Int.J. of Advanced Manufacturing Technology*, 76:1977–1992, 2015.

[11] B.Thompson and H.S.Yoon. Efficient path planning algorithm for additive manufacturing systems. *IEEE Transactions on Components, Packaging and Manufacturing Technology*, 4:1555–1563, 2014.

[12] J.J. De Santiago-Perez, R.A. Osornio-Rios, R.J. Romero-Troncoso, and L. Morales-Velazquez. Fpga-based hardware cnc interpolator of bezier, splines, b-splines and nurbs curves for industrial applications. *Computers & Industrial Engineering*, 2013.

[13] D. Ding, Z. Pan, D. Cuiuri, H. Li, N. Larkin, and S. van Duin. Automaticmulti-directionslicingalgorithmsforwirebasedadditive manufacturing. *Robotics and Computer-Integrated Manufacturing*, 2015.

[14] D.S. Ertay, A. Yuen, and Y. Altintas. Synchronized material deposition rate control with path velocity on fused filament fabrication machines. *Additive Manufacturing*, 2017.

[15] R.T. Farouki, J. Manjunathaiah, and G.F. Yuan. G codes for the specification of pythagorean-hodograph tool paths and associated feedrate functions on open-architecture cnc machines. *International Journal of Machine Tools & Manufacture*, 1999.

[16] I. Gibson, D.W. Rosen, and B. Stucker. *Additive Manufacturing Technologies. Rapid Prototyping to direct digital manufacturing.* Springer, 2010.

[17] Stratasys Inc. Melt flow compensation in an extrusion apparatus, 2003. US-patent 6,547,995, inventor: James W. Comb.

[18] Iso14649-industrial automation systems and integration — physical device control — data model for computerizednumerical controllers —. https://bsol.bsigroup.com/. 2010.

[19] Iso52915-specification for additive manufacturing file format(amf) version 1.2. https://bsol.bsigroup.com/. 2017.

[20] Iso6983-automation systems and integration-numerical control of machines—program format and definitions of address words. https://bsol.bsigroup.com/. 2009.

[21] International organization for standardization. https://www.iso.org/standard/72194.html. accessed:06-2018.

[22] R. Jamieson and H. Hacker. Direct slicing of cad models for rapid prototyping. *Rapid Prototyping Journal*, 1995.

[23] Z. Jia, J. Ma, D. Song, F. Wang, and W. Liu. A review of contouring-error reduction method in multi-axis cnc machining. *International Journal of Machine Tools and Manufacture*, 2017.

[24] G.Q. Jin, W.D. Li, and L.Gao. An adaptive process planning approach of rapid prototyping and manufacturing. *Robotics and Computer-IntegratedManufacturing*, 2013.

[25] G.Q. Jin, W.D. Li, C.F. Tsai, and L. Wang. Adaptive tool-path generation of rapid prototyping for complex product models. *Journal of Manufacturing Systems*, 2011.

[26] Y. Koren. Control of machine tools. *Journal of Manufacturing Science and Engineering*, 1997.

[27] P. Kulkarni and D. Dutta. Deposition strategies and resulting part stiffnesses in fused deposition modeling. *Journal of Manufacturing Science and Engineering*, 1999.

[28] P. Kulkarni, A. Marsan, and D. Dutta. A review of process planning techniques in layered manufacturing. *Rapid Prototyping Journal*, 2000.

[29] Jorge Mireles, David Espalin, David Roberson, Bob Zinniel, Francisco Medina, and Ryan Wicker. Fused deposition modeling of metals. *23rd Annual International Solid Freeform Fabrication Symposium - An Additive Manufacturing Conference*, 2012.

[30] Mx3d website. http://mx3d.com/. accessed:06-2018.

[31] P.M. Pandey, N.V. Reddy, and S.G. Dhande. Slicing procedures in layered manufacturing:a review. *Rapid Prototyping Journal*, 2003.

[32] L. Piegl and W. Tiller. *The Nurbs book*. Springer, 1995.

[33] F. Prša, J. Irlinger and T.C. Lueth. Algorithm for detecting and solving the problem of under-filled pointed ends based on 3d printing plastic droplet generation. In *ASME 2014 International Mechanical Engineering Congress and Exposition*, volume 2A:Advanced Manufacturing. -, 2014.

[34] Omkar Rishi. Feed rate effects in freeform filament extrusion, 2012/2013.

[35] E. Sabourin, S.A. Houser, and J.H. Bøhn. Adaptive slicing using stepwise uniform refinement. *Rapid Prototyping Journal*, 1996.

[36] S. Singamneni, O. Diegel, B. Huang, I. Gibson, and R. Chowdhury. Curved layer fused deposition modeling. *Research Gate*, 2010.

[37] S.H. Suh, S.K. Kang, D.H. Chung, and I. Stroud. *Theory and Design of CNC Systems*. Springer, 2008.

[38] Matyasi Gy. Szilvasi-Nagy M. Analysis of stl files. *Mathematical and computer modelling*, 2003.

[39] J. Um, M. Rauch, J.Y. Hascoët, and I. Stroud. Step-nc compliant process planning of additive manufacturing: remanufacturing. *International Journal Advanced of Manufacturing Technology*, 2017.

[40] N. Volpato, A. Franzoni, D.C. Luvizon, and J.M. Schramm. Identifying the directions of a set of 2d contours for additive manufacturing process planning. *International Journal of Advenced Manufacturing Technology*, 2013.

[41] H. Wang, X. Xu, and J. Des Tedford. An adaptable cnc system based on step-nc and function blocks. *International Journal of Production Research*, 2007.

[42] J. Xiao, N. Anwer, A. Durupt, J. Le Duigou, and B. Eynard. Information exchange standards for design, tolerancing and additive manufacturing: a research review. *International Journal on Interactive Design and Manufacturing*, 2017.

[43] X.W. Xu. Realization of step-nc enabled machining. *Robotics and Computer-Integrated Manufacturing*, 2005.

[44] Y.A.Jin, Y.He, and J.Z.Fu W.F.Gan Z.W. Lin. Optimization of tool-path generation for material extrusion-based additive manufacturing technology. *Additive Manufacturing*, 1:32–47, 2014.

[45] Z. Zhao and Z. Luc. Adaptive direct slicing of the solid model for rapid prototyping. *International Journal of Production Research*, 2000.

[46] X. Zheng, K. Cheng, X. Zhou, J. Lin, and X. Jing. An adaptive direct slicing method based on tilted voxel of two-photon polymerization. *The International Journal of Advanced Manufacturing Technology*, 2018.

[47] C. Zhou. A direct tool path planning algorithm for line scanning based stereolithography. *Journal of Manufacturing Science and Engineering*, 2014.

Chapter 5

Industry 4.0

introduction

One of the main promoters of AM is industry 4.0 whose main idea is the digital representation of the production processes with a total integration of the industries in a manufacturing network. The AM machines, which are considered in the shop floor as CNC machines, must be integrated with their digital chain in the industrial environments. In order to do that is very important the understanding of the evolution that is going on inside the production sites where the use of the cyber-physical systems is becoming mainstream. These systems, born in the embedded world, acquire a new meaning in industry 4.0 and their concepts are going to influence the design of industrial machines. This chapter presents and analyses the main concepts of the new industrial paradigm in order to understand if and what are the changes required for industrial machines in the near future, including AM machines. It is possible to distinguish the main features of a CPS in the industry 4.0 context, the need to evolve the industrial machines to have specific features which are fundamental in the new industrial context. This critical analysis will lead to the integration of the digital flow of information in a 3D printer such as the Efesto machine inside the production environments.

5.1 Efesto digital chain

In fig.5.1 is shown the digital flow of data in a 3D printer as the Efesto machine. AM machines are considered a key technology in the near future of manufacturing industry and it wonders how to integrate them inside the industrial architecture. In the block scheme is indicated for each part a possible information/data that can be pulled out. From the initial CAD file, usually an STL, to the several measure obtainable along the process. Here a distinction can be made from the first two block, CAD and CAM,

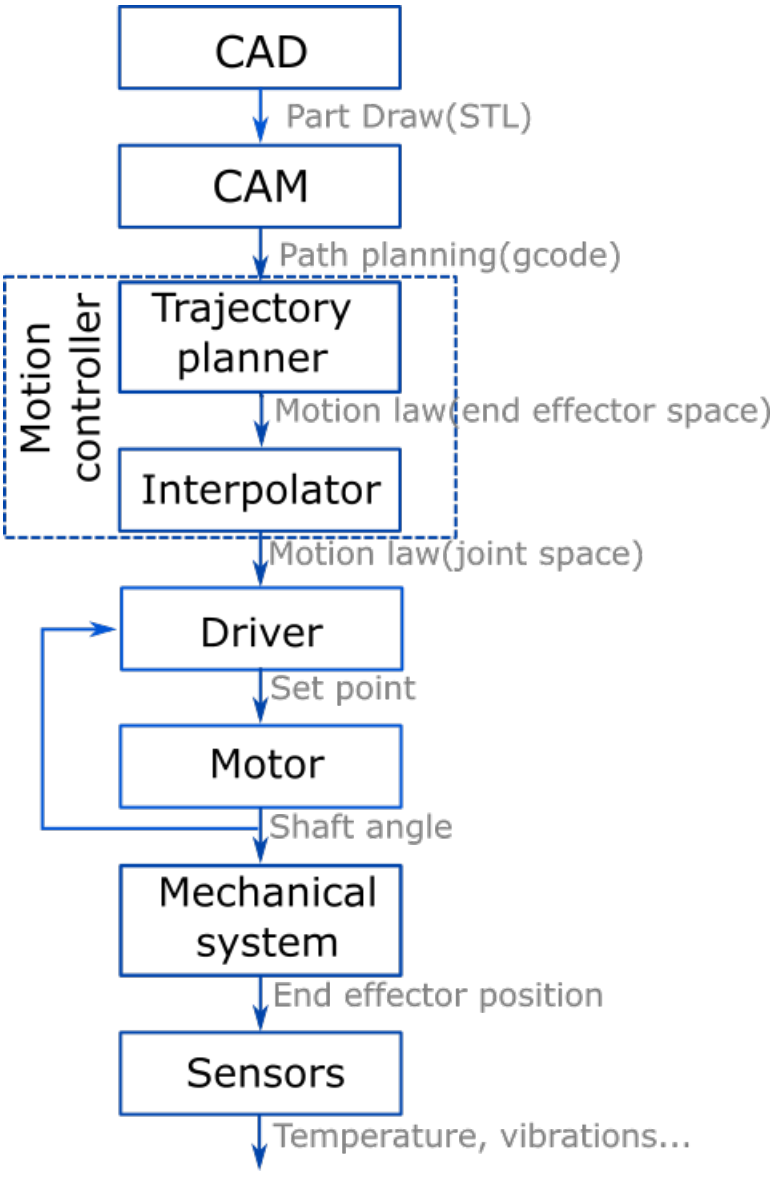

Figure 5.1: AM digital chain

which are software usually not integrated inside the AM machines but which are fundamental to provide some input files for the printing process, and the all other block which are specific components of the machine. The information/data indicated from one block to another are a possible choice in that particular point of the chain but other options are possible. For instance after the motor block could be extracted the motor current instead of the shaft angle. With the advent of an industry increasingly linked to the digital world, the use of each of the information in this flow can be useful for improving production.

In the following is a carried out an analysis the new industrial paradigm that has grown in recent years and its core components called Cyber Physical systems. This will lead to the to the integration of the presented scheme inside an industrial architecture. A theoretical example of its use is done on the Efesto machine in order to explain its usefulness. We want to point out how the communications concepts derived from this chapter have been utilised in the design phase of this machine expressed in chap.2. To improve the fluency of this work the topics related to industry 4.0 even though they have influenced this work in other points are concentrated in this chapter.

5.2 A new industrial paradigm

The industrial evolution has recently encountered a new industrial paradigm often called industry 4.0. This new paradigm involves different aspects of the industrial world, from a management point of view to a technical one [1]. It is not always clear what is going to change and how, and that's why we can find many explanations about it and many researches related to it. In [53] it is discussed the evolution of the production systems from the second industrial revolution until today focusing on the use of the internet of things and the relationship with customers. In [27] the research is focused on the union from the physical and the digital world by proposing a 5 levels architecture for cyber-physical systems. [24] gives an explanation of this paradigm based on a list of social, economic, political changes and technological innovations. These different approaches to the subject depends on the different fields of study of the single scholars.

From the point of view of an industrial machines designer the focus is on how to design the cyber-physical systems, CPSs, that industry 4.0 indicates as the basic bricks of the new production systems; their design varies according to how these systems are conceived and we can find different examples of CPS in the literature. In [13] is described the design of an Unmanned Ground Vehicle, UGV, through a design process derived from the V-model of the mechatronic. The authors refer to their UGV as a CPS. The vehicle is controlled from a remote user, and this is the only kind of communication with the outside world. In [27] is proposed a model for the

development of CPSs inside industrial environments. Here the concept of CPS is expressed through a pyramidal software architecture whose hardware is the physical machine , the lowest layer from which are received the data needed to the extraction of informations required to different levels of the industrial production; the design process is focused on the communication capabilities of the system which is supposed to live inside a more interactive environment. The two systems in [13] and [27] are not the same even though they are reported with the same name. As the description of industry 4.0 concepts is strictly related to the scholars fields of study, the design of a CPS is strictly related to the environment of the designer. In [40], consequently to an analysis on the use of CPSs inside production environments, is claimed how many concepts and researches at the base of industry 4.0 are not new but they are based on the work in several different fields of the last 20 years, so it must be paid a lot of attention on the environment in which these technologies are developed. In order to understand the concept of cyber-physical system is important to understand the environment they live in. Concepts as machine to machine communication, M2M, or integration in a communication network are not new from a technical point of view, but if they are seen integrated in a general vision of a different way of make business they assume a new value. The industrial machines design can not be separated from the context of their application since their evolution is pulled by the evolution of the business management.

The concept of CPS is not univoque as it is not clear how they fit in the new production environments; anyhow their development, in particular the development of cyber-physical additive manufacturing systems is considered crucial to the new industrial paradigm [11].

5.3 Birth of term

Starting from 2011 is born a new term *industry 4.0* launched at the Hannover fair, term promoted by the German govern which supported a working group made of academical parties as acatech, the german academy for science and engineer, and industrial partners [1]. This action starts from an organic vision of the new industrial era in which Germany, one of the industrial automation world leaders, proposes itself as a guide by promoting a possible evolution. We can trace the origin of this initiative to the 2005 when it is founded the Technologie-Initiative SmartFactory KL from 7 industrial and research partners with the aim to develop the industry of the future [44]. A first prototype is released in the 2008 based on the development of microeletronics components, communication technology, smart devices and based on concepts of flexibility, self-organizing and user-oriented so realizing to the industrial level the vision of a distributed intelligence as depicted by Mark Weiser [8, 49]. Following this initiative many others have

tried to define what will be the industrial evolution. In the USA is born the term *industrial internet* promoted by the IIC, industrial internet consortium, association founded by Cisco, General Electric, AT&T and IBM in order to define the development of the industrial communication standards. The two organizations have made official in the march 2016 an agreement for the future development of the industry [17]. All these initiatives have captured the attention of many other countries which have started their own plans for the development of their industry; among the many we cite as example the China initiatives termed *internet plus* [33] and *Made in China 2025* [29]. Many studies followed trying to understand what is this new industrial vision and which are the consequences that will bring; a study was conducted for the european parlament by the economic and science department [45] with a main focus on the the possible future scenarios lead by this change. Beyond the different names that is possible to give and are born related to this topic they all have some in common; the future scenario of the industrial world. We will focus on the German plan *industry 4.0* which has been the first, to the best of our knowledge to have been introduced referring to an organic vision of the next industry.

5.4 Industry 4.0

On many discussions related to industry 4.0 this is presented as follow-up of the previous three industrial revolutions. Trying to understand what makes an industrial change an industrial revolution can help to understand why this is a revolution too.

The economist Jeremy Rifkin claims how an industrial revolution is always accompanied by a new couple communication/energy [41]. The ensemble of new communication forms and new energy sources may be the push to major social and economical changes. According to Rifkin the steam power and the printing are the basis of the first industrial revolution instead the electrical communications and the energy based on the oil are the basis of the second one. New forms of energy and communication allow to shrink time and space by connecting people and markets and so promoting new form of business. Beyond the socio-historic analysis what emerges from the Rifkin's point of view is how technological improvements had allowed some strong social and economical changes; in the industrial world these technological changes has led to new ways of production, both from a practical perspective than from a conceptual one. In the first three industrial revolutions, fig.5.2, we have passed from a mass production to a production more concerned with the cost and quality of product, business change, thanks to the transition from steam power to electrical energy and to the introduction of automation, technological change, [1].

The changes promoted by industry 4.0 are many and they touch different

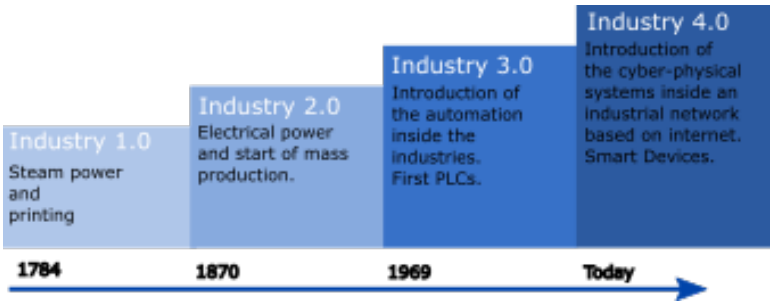

Figure 5.2: Industrial revolutions

aspects of the industrial world. We can start from the milestone technologies of this revolution in order to touch the different changes that it will bring in the industries. The main actors of industry 4.0 are two:

- internet
- CPS(cyber physical system)

These two technologies implies a new way of information exchange, both internally and externally to the industry, and a new way to conceive the automatic systems. The definition of a CPS could have different expressions, for this reason in the later we will clarify the meaning of this term and its importance inside this context. The term internet is a very broad definition but it allows to sum the progress in the ICT, information and communication technology, sector and the born of the *smart objects* which is leading to have at our disposal an amount of data bigger and bigger, from a quantity point of view, thanks to the objects connected to the net. In this way is arise the concept of IoT, internet of things, which is based upon the availability of data coming from the smart objects. The analysis of these data, Big data, is driving to an increasing amount of informations available in times more and more little.

The innovative idea of industry 4.0 relies on exploiting these data and these communication systems in order to create an industrial network where everything is connected and is represented by a digital copy, digital twin. This will allow to create an efficient and flexible production system capable to respond to the quick changes of the market which is more and more concerned by customization of products and reduced lead times. Fig.5.3 shows a representation of industry 4.0 where the central core consist of Big Data stored in a cloud platform. Today the amount of data available for any kind of analysis are so much that make use the word Big. Data come from the industries shop floors, data about machines, warehouses, state of products and production, thanks to a complete digitalization of any industrial components. Products are represented as alone components in the

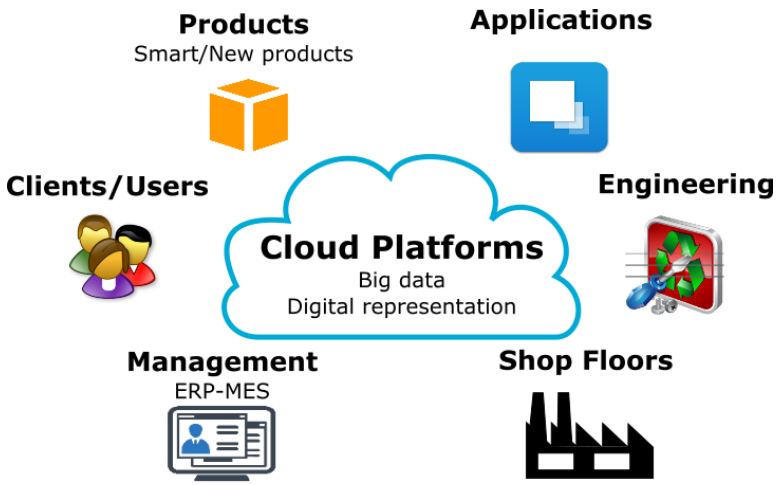

Figure 5.3: Digital Market

picture, this outlines the vision of smart products always traceable during all their lifecycle. Giving the possibility to have access to these data it's possible to provide management solutions, engineering services, or any kind of possible application from anywhere to anyone. The main problems which immediately arise are:

Interoperability of data Data collect from different machines of different vendors and different industries must be easily usable; protocol standardization and an ontology integration for data is needed.

Security An industrial network raises issues related to cyber attacks that must be addressed.

A digital replica of the real world implies the possibility to save time and investments exploiting simulation on the digital world diminishing for instance the construction of prototypes or adjustments of the supply chain for new products. Main goals of industry 4.0 are to achieve a new horizontal integration through a network based on factories, suppliers, customers, and products connected together through cloud platforms; end-to-end digital integration of engineering across the entire value chain; a new form of vertical integration inside single companies [1].

5.5 Traditional CPS

The CPS is one of the milestone technologies of industry 4.0 and so it is important to have a clear and well defined conception of it. In the state of art we can find different definitions of what a CPS is; in the following we will search for the origin of the term, explain it according to the vision of the

embedded systems and mechatronic world and we will picture it according to the industry 4.0 definition.

The term itself has origin from Helen Gill in the 2006 at the National Science Foundation in the USA as described by Lee et al. [26]. Gill uses this term to describe the integration between computation and physical processes inside the context of the embedded systems. Lee traces the origin of the name to many decades before during the second world war to Norbert Wiener which used the term cybernetics to describe the union of different control systems through a main communication network. According to Lee the *Cyber-Physical Systems (CPS) are integrations of computation with physical processes. Embedded computers and networks monitor and control the physical processes, usually with feedback loops where physical processes affect computations and vice versa* [25]. It is important to point out how in the vision of Lee a CPS is the integration and not the union of control systems, network and physical part. It is not enough to join the three things to have a CPS but it is necessary to face the problem by changing the engineering design of the different parts which are mutually influenced by each other. The physical part of a CPS can be a mechanical part, a chemical or biological process until to consider a human being [26]. The computational part is constituted by two or more computational systems connected in a network, they interact with the physical part through sensors and actuators. In fig.5.4 is shown the design of a typical CPS, [26]. These systems are usually described through hybrid models through the use of differential equations, ODEs, for the physical parts, and finite state models, FSM, for the computational part. The entire design phase of these components try to integrate the different parts which their are made of. Natural approach to this problem has always been to divide a complex project in smaller an simpler parts by hoping that their optimum design will lead as close as to the possible optimum design of the entire system. The development of design technology, particularly of CAx software, allowed to integrate different design phase, once divided, in a more complex process but which is today manageable. The study about CPS design has grown a lot in the latest years since it was acknowledged the necessity for an holistic design of these systems. In the development of the embedded systems, from which the CPSs are derived, Helen Gill, founder of the term, points out how there is need for these components of a repeatable discipline based on scientific foundations ed equipped with production methods efficient and reliable [14]. This design development is partially come out from the development of the mechatronic systems, in fact mechatronic systems are often considered the physical part of a CPS [13].

Mechatronic is considered an integrative discipline mainly of the fields of mechanic, electronic and control [18]. Mechatronic has introduced the effort to integrate these disciplines inside itself in a design process which was no longer divided in separated phases but based on an holistic approach of the

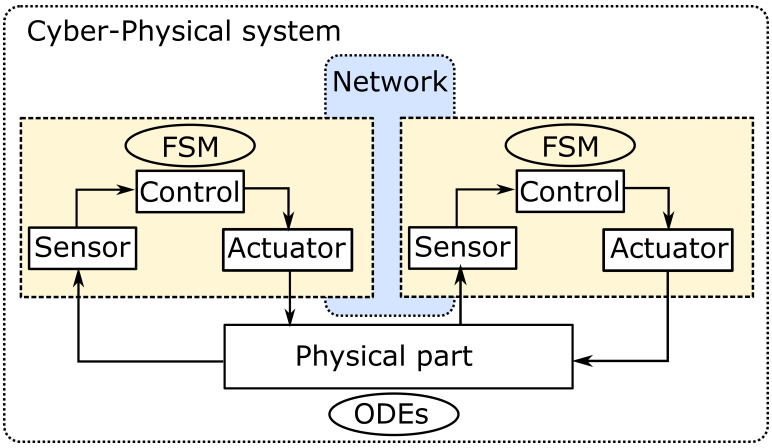

Figure 5.4: Design of a typical CPS

component design where the interaction among the different subsystems was considered from the beginning. A mechatronic system has two main actors to interact with, a user from whom it usually expects inputs or to whom give outputs, and the environment which is considered as a source of disturbances to isolate and eliminate [19], so it is conceived as a closed system with the aim to accomplish a task independently from the outside world.The design of a CPS starting from a mechatronic one will bring with it these concepts and the outcome will be different from the one of a CPS born from the embedded systems world as shown by the design mentioned in the initial part of this chapter [13]. Guerineau et al. [15] make an interesting study on the differences between a CPS and a mechatronic system. Actually from the outcome of this study we see that there are many similarities between the two. CPSs comes from the IT and embedded systems world and so they have a major informatic background which has encountered the necessity to have a physical equivalent in the real world, differently of mechatronic systems which come from a science field where the hardware was prevalent at the beginning. The two worlds are sliding one inside the other pushed by industry 4.0 which has taken to extreme the concept by making the couple real-virtual something of indivisible.

In the context of industry 4.0 we can find a reference to CPSs, which are defined as a convergence between physical and virtual world, in the milestone report of the German movement for the new industry [1]. More detailed is the description given by the academic party of industry 4.0, the acatech, which speak about them as systems based on embedded software capable to have access on physical data and capable to influence the physical processes through sensors and actuators; they must be able to interact both with the physical and the digital world, they must be connected to a global network with the possibility to retrieve informations and obtain services,

with the possibility to interact with a human being [2]. In this context the CPSs are a set of physical part, electronic hardware, and software which are connected through a network. They are able to accomplish specific tasks independently and to communicate with the external environment in order to accomplish different tasks. In order to give a practical example a CPS could be a simple sensors capable to provide on the network a measure thanks to an internet connection, otherwise it could be an entire industry which provides a production service of specific goods and whose production is always visible to a management level. The concept of CPS inside industry 4.0 is not the same as presented by Lee, here it is given a lot of attention to the capacity of the CPS to communicate with an outside world, instead in the description coming from the embedded world, fig.5.4, the concept of network is something internal to the CPS itself. Inside industry 4.0 any component with a digital representation and the possibility to communicate with the outside world is a CPS, no matter how its internal design is. Even though the acatech arises the problem of the integration among the different disciplines on which the CPSs rely upon [2] it is normal that in an initial stage of industry 4.0 a simple union of physical and digital part leads to the synthesize of a CPS. With time, as pointed out by Lee, it will be necessary the development of design discipline for these components.

5.5.1 RAMI model

In order to define a common development of CPSs inside the industrial sector it has been defined by a working group of the industry 4.0 platform a Reference Architecture Model for Industry 4.0, RAMI [48]. This model aims to specify a reference standard for the IT infrastructure upon which every CPS should be developed inside the industry; the problem of standardization became more and more important inside a totally connected world. The explanation of this model will lead to a better understanding of what a CPS is for industry 4.0 and what they can do inside an industrial network.

This three-dimensional model is an extension and an adaptation of the Smart Grid Architecture Model(SGAM). Looking at fig.5.5 is possible to see how this IT superstructure is described along three axis and it is referred to generic objects that in [48] are labelled as components. The vertical axis is divided by levels, everyone describing a specific aspect of the component; the two horizontals describe the component along all its life cycle, according to the standard IEC 62890, and according to its collocation on a business level, with the definitions extracted by the standard IEC 62264 and extended with the levels Product at the bottom and Connected World on the top. In the description of the component on the life cycle axis a distinction is made between type and instance. Type is a component during its design and testing phase; instance are all the components produced based on the same type. The different vertical layers contains all the informations, divided

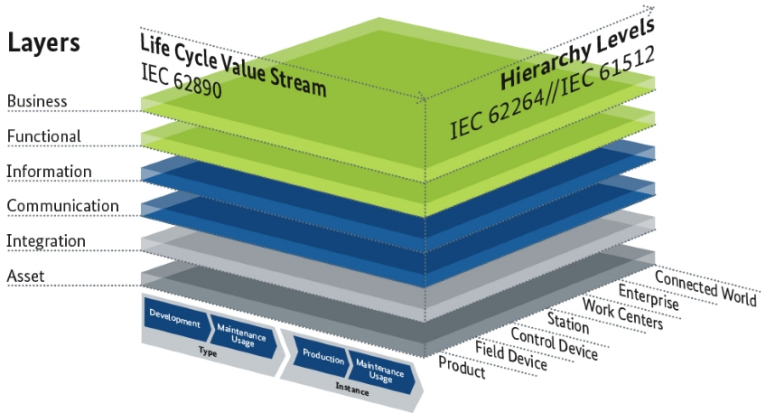

Figure 5.5: RAMI model

by fields, relative to the component ; this approach is needed in order to simplify the organization of an extended amount of data of different nature. This organization allows to simplify the union of two or more components and it allows to nest one inside the other; one component can be composed by two or more components, everyone with the same overall architecture. This kind of division must be intended according to an IT logic for which every layer is an IT layer which can exchange data only with the adjacent ones. We give a brief explanation of the role of each layer taken from [48]:

asset layer Here we have the physical part of the component, it could be a worker or a machine as well.

integration layer It manages the connection between the real world and the digital one by allowing to gather data from the physical part of the component.

comunication layer It describes the communication protocols and the mechanisms for the communication among components by ensuring the interoperability of data

information layer It is concerned with the preprocessing of data gathered from the asset in order to guarantee their integrity.

functional layer It describes the functions and services put at disposal from the component. To this level it happens the actual integration between components.

business layer It ensures the integration of the available functions according to the business models to which the component is subject to.

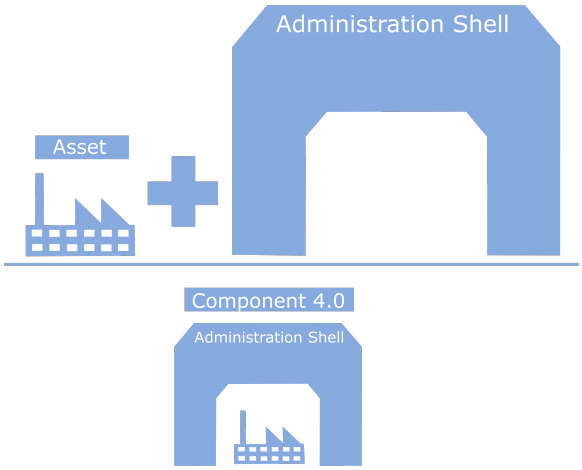

Figure 5.6: Administration shell

According to this model every component inside an industry, in the moment it acquires an IT architecture as the one described, can become a component 4.0 which is defined as specific case of a cyber-physical system [48]. Once again we find out how CPSs which come from the embedded system world are tied to the idea of a network inside the CPS itself instead a component 4.0 does not need to have a specific inside network but it must be able to communicate with an external one in order to share data the functions/services they are capable of. The IT architecture put upon a component is called from this model *Administration shell* [48]. As shown in fig.5.6 every asset of the company can become a component 4.0 with the add of the administration shell. We are talking as already mentioned of human personnel, machines and even software in this context. This is an another big difference with typical CPSs. A designer of a typical CPS is concerned with a physical part which in some order is always material at end; in industry 4.0 a physical part is anything can accomplish a task and provide it to the network. According to this concept a CAD software too which provides a drawing service can be a component 4.0. A component with its administration shell become a component 4.0 or CPS which provides its functions to the network according to a service oriented logic.

As an example of component 4.0 let's consider a sensor. This is a field device in the component hierarchy and it is a type during its design phase and an instance when it is actually produced. We point out that the sensor keeps to be a type through its technical designs, which describe it and that are update through modifications and improvements, and it is an instance to the production site where it is actually used. The physical sensor, the asset, provides to the industrial network its services at the functional layer which acts thanks to the availability of data guaranteed by the underlying IT layers, the whole integrated in the value stream of the firm through the business

layer. If the sensor is a temperature sensor the business layer guarantees that the sensor is integrated in the production process, for instance in order to start or stop a specific manufacturing phase. If the sensor is nested inside a machine the business layer guarantees that its services are integrated in the process provide by the machine itself. If now we enlarge our vision to an entire production site, which would be the ensemble of many components 4.0, we see how this is an enterprise in the hierarchy level and it would be type through its design and instance as an actual physical industry. The industry have the duty to produce a specific set of goods by providing a production service guaranteed by its physical layer which acts based on the functions recall on that site which is integrated in the company value stream through its business layer.

5.6 Business models

The technological evolution described so far is linked to the business evolution of the industry. The digital dimension of industry 4.0 leads to new possibilities of horizontal integration, meant as the interactions among industries, suppliers and customers, and so by leading to new ways of business. These new business models are based on the possibility to access a great amount of data in a faster and faster way and to a complete digitalization of the real world. The industries in the form of CPSs connected to an industrial network provide to third parties a set of services according to a service oriented architecture, SOA [1,48]. In the industrial world the concept of SOA is arise from the field of the business IT in the attempt to create an IT support for company managers giving them an assistance for a fast rearrangement of the production in order to follow rapid business changes in the companies themselves. Bieberstein et al. [5] defines the SOA as *a framework for integrating business processes and supporting IT infrastructure as secure, standardized components—services—that can be reused and combined to address changing business priorities.* This concept is directly transferable to the CPS whose functions can be reused and recombined to create new and different value streams. One of the main problem related to the actual implementation of this concept is the different perspective of a service from a technical point of view and a managerial one. Perrey et al. [36] point out very well the difference between them. On the business side a service is something for whom a client is dispose to pay, for a technician a service is something to implement independently from how it is actually realized. The concept of SOA is born to conciliate the business necessities of a company with the IT functions or services needed by the several departments of a company by integrating them in a centralized IT platform. The utopia of SOA lies on ensuring an IT platform which provides services from a business point of view, abstracting from how they are actually realized, which can be recombined to form new

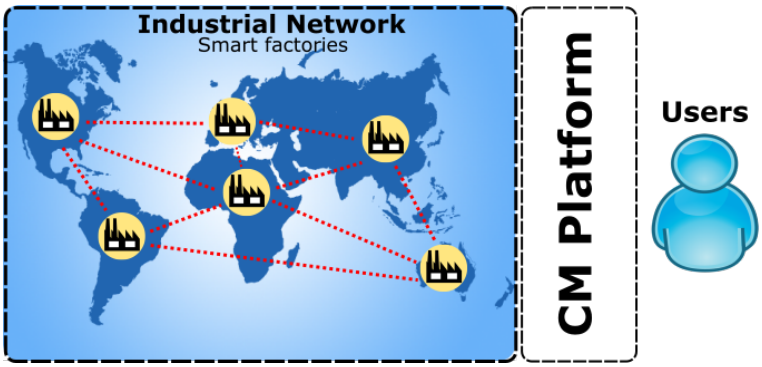

Figure 5.7: Cloud Manufacturing

ones on demand [36]. Industry 4.0 exports this concept enlarging it to every component 4.0 under the form of CPSs providing services; these services can be called and recombined thanks to the IT architecture of the CPSs and their business layer which defines their utilise. Un industrial network which connects thousands of industries allows to have an infinite number of value streams considering all the possible combinations given by the CPSs connected in the network.

One of the main implications in terms of new business model is the so called *Cloud Manufacturing*, CM. This concept derives from the cloud computing idea as explained by Xu [52], and it can be described as *manufacturing resources provided as a service over the internet*. In the same way as computing resources are made accessible on cloud platforms, for instance for very heavy engineering analysis as FEM, Finite Element Method, or CFD, Computational Fluid Dynamics, the same thing can happen for the production resources as the production sites conceived as CPS. The sharing of production resources for a product manufacturing is what is a virtual enterprise described by Camarinha-Matos et al. [9] as *a temporary alliance of enterprises that come together to share skills or core competencies and resources in order to better respond to business opportunities, and whose cooperation is supported by computer networks*. At the time which this definition was given, 1999, the implementation of such idea was far away from the possibilities of the modern technologies. The evolution of the ICT and automation world has led to the progress of the advanced manufacturing by resulting in the CM [46]. The CM platforms have many analogies with the CPS platforms defined in [1]. Liu et al. [28] by executing a comparison between the industry 4.0 and CM and their respective platforms conclude as one could turn into the other. CM is focused on the IT problem of connecting customers, with their personal requests, with the services they require. Industry 4.0 is focused on connecting the industries in an only one production network. The two things are complementary.

In fig.5.7 is represented the link between users and an industrial network

made by several firms. You can find three main actors in cloud manufacturing:

Clients They can use Platform to research a suitable solution for their products.

Cloud Manufacturing Platforms They respond to client orders forming a new supply chain for every specific product. Platforms base their decision on data made available by industries. A firm can not have the right machines, know how or production availability to respond to the request.

Manufacturers Industry 4.0 enables companies to make available Big Data and digital representations of CPSs. Platforms run simulations on a completely virtual replica of the factory in order to evaluate the formation of the supply chain for a specific product.

Of course such a structure arise many questions about security of data, quality of products and services released by different firms, coordination of such a system, how to share profits in a peer to peer system, exchange of standard files and many others.

There are some implementations of cloud manufacturing already existing listed by Wu et al. [50]. In this first stage are born websites, platforms, which simply connect designers with manufacturers. Examples are Quirky [39] and Shapeways [43]. These websites allow designers, or anybody has an idea, to manufacture their creation. Quirky submits the idea to a community and if there is a good response a prototype is built and proposed to a company for production. Any revenue is shared according to Quirky rules. Shapeways instead allows to produce the part using mainly 3D printers; materials of the product can be picked by the designer which can set a price and sell the product over the internet or make a production order with a specific ship. MFG.com [30] is a website which provides customers, engineers and designers, with the suitable supplier according to the drawings given to the website. MFG.com collects suppliers from 50 states from all over the world. Even though these are step forwards to CM what is missing in these solutions is the forming of a real dynamic supply chain; customers are linked to single suppliers and manufacturers but industries gathered in the platform do not collaborate among them.

5.7 Industrial architecture

In order to achieve a flexible and customized production, industry 4.0 needs to change the internal organization of the production systems. In this part we are going to focus on the vertical integration of a company.

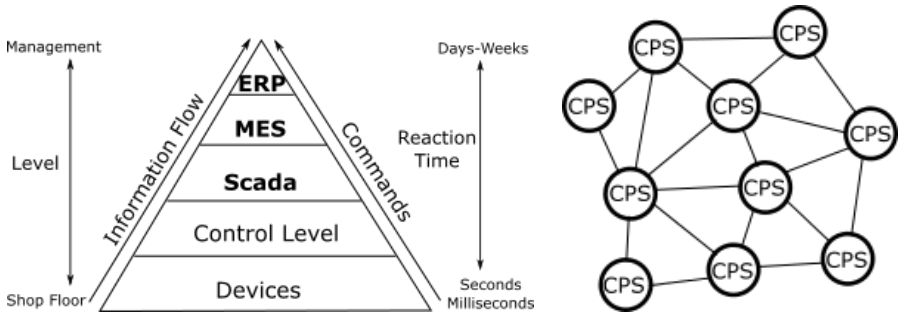

(a) ISA-95 model **(b)** Distributed control

Figure 5.8: Transformation of the industrial architecture

From the advent of the IT in the industrial field many software components are born to support the several departments of a company, starting from the design software CAD/CAM, for design and production support, to software for the company management which implemented logic as MRP I, material requirements planning, or MRP II, manufacturing requirement planning. The production of a company was divided among its different departments everyone supported by its own IT structure; for this reason between the '70 and the '80 has grown the concept of CIM(computer integrated manufacturing) with the purpose of a seamless integration among the different actors of a firm and the several IT structures which supported them, all to achieve a higher quality of products and reduced costs and lead times. CIM promoted a new industrial paradigm whose success relied in the centralization of the informations which were shared among the different firm departments [47]. The development of CIM was accompanied by the development of the aforementioned software. Particularly at the beginning of the '90 were born two software packages called ERP, enterprise resource planning, and MES, manufacturing execution system. The first one is related to the gathering of all those software related the the company management and they are basically an evolution of the aforementioned software for MRP I and II, [34]. The second one is derived from the necessity to connect the management level of a firm with its production sites [20]. During this continuous evolution became necessary to standardise the industrial architecture in order to integrate components of different natures. In this way is born one of the most well-known standard in the industrial field, the ISA-95 [7], fig.5.8a.

This standard represents a firm according to a pyramidal architecture in which the informations flows from the bottom to the top, and the commands vice versa, from the shop floor to the management level. This vision abstracts two different concepts; one is the definition of the responsibilities inside the firm, the other is the definition of the mutual interfaces among the

IT components born during the years. On the top of the pyramid we find the ERP systems that nowadays are very broad packages which accomplish many management tasks for different departments, from the management of the material to the management of the employees [38]. Right underneath we find the MES systems which have the task to manage the production according to the decisions and the plans developed in the upper levels, they have to gather the data from the production processes and pass them to the ERP in order to allow it to take fast and correct management decisions. By going down to the bottom of the pyramid we encounter the SCADA, supervisory controls and data acquisition, systems which actually gather the data from the actual production components, so directly from lower systems as PLCs, CNC machines or other devices put in operations.

Through the introduction of the CPSs this architecture is going to drastically change from a pyramidal concept, where the tasks are well defined and separated, to a distributed system where every CPS has a certain degree of intelligence and autonomy and participate to the value stream of the production process by providing its functions [31]. This assertion is usually represented by a set of CPSs connected one to the other, fig.5.8b. Their collaboration is focused on the production process, every CPSs participate to those tasks once relegated to ERP and MES systems. Even these latter will become CPSs by providing their software skills in the internal network of the firm. For instance if a machine acquires the autonomy to ask the change of a tool without the intervention of a MES, or if it can ask to an operator the loading of a new component to machine, these are a simple but effective demonstrations of a redistributions of the duties. The redistributions of duties and the active participation of all CPSs, machines, employees and software, inside the company leads to a distributed control. The flexibility of the system is guaranteed by the functions provided by every CPSs which are seen from the management level as services which can be recombined as needed. The natural consequence of this architecture is the *smart factory*.

5.7.1 Smart Factory

Consequence of the CPSs and of the evolution in the ICT and industrial automation fields is the smart factory. A smart factory is the productive heart of the industry 4.0 where it actually takes place the production process based on the concepts of flexibility, modularity and customization.

An example of smart factory is given by Zuehlke [55] in the description of a bench test created in Kaiserslautern with the participation of different industrial partners. A smart factory must embraces the concepts of modularity and high customization of the product. The modularity is given by the CPSs and their autonomy. A CPS can be an AGV, automated guided vehicle, an automated warehouse, a CNC machine or the workers integrated in the system through different forms of HMI, human machine interface.

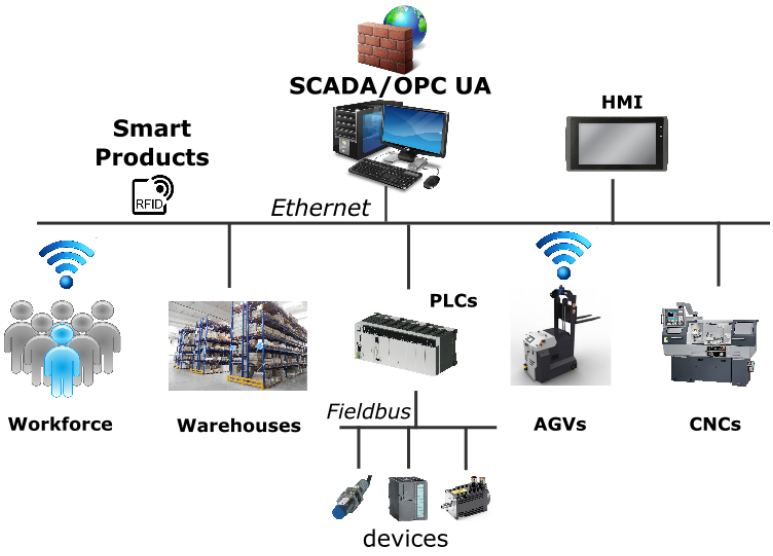

Figure 5.9: Smart Factory

The possibility of product customization is a direct consequence of the flexibility and modularity given by the CPSs capable to respond in real time to a continuous variation of the production demand. The smart factories must born from the current production sites through a gradual evolution and the introduction of new technologies and systems. It is possible to find in the literature examples of use of some specific technologies for smart factories, particularly in the

field of communication and product traceability.

Industrial Ethernet It is necessary a standard on the different communication layers. As physical layer the ethernet seems to be the most obvious solution due to its wide spread. Sauter at al. [42] propose an hybrid architecture based on a main cable ethernet backbone and several wireless access points. This could be a solution for the connection of the CPSs inside the shop floor.

OPC UA is a communication protocol capable to run on ethernet and it has been very used in the last years [16]. Even though is not official it seems to be considered a de facto standard for industry 4.0. The development of a standard communication protocol is fundamental for the integration of components coming from different vendors.

RFID tags and readers are used for the traceability of products and so for a better production management. Zhong et al. [54] propose the use of tags on single products or pallets and the use of readers on machines, automated warehouses and workers, in order to create a smart logistic

environment. There is also the possibility to leave the tag on product all along its life cycle turn it into a smart product.

In fig.5.9 is shown a possible example of a smart factory architecture. This architecture can seems conflicting with the one represented in fig.5.8b but it actually shows how the concepts of industry 4.0 are repeatable in the context of traditional shop floor. The all components of the factory are connected in a main network through wired or wireless communication systems. Every components provide some functionalities to the production system as all CPSs should do. The architecture of future must growth from the old version and that's why in this representation a central system which recollects all the data from the other parts of the factory is maintained. Innovation can be introduced with equipments more and more autonomous, connected to the system and which provide their operations according to a SOA concept. Discharge of responsibilities leads from a hierarchy system to a distributed one.

Industrial machines

The development of industrial machines toward the industry of the future will require the implementation of new functionalities by the designers of the same. An interesting analysis is made by Xu [51]on the functional development of the CNC machines. Xu analyses the evolution of the CNC machines from their entrance in the shop floors in the '70 until today at the industry 4.0 time. The conclusions of this analysis is that in the next future these machines must embrace new concepts of:

self-awareness Capacity to understand their duty inside the system and how to carry out it

self-maintenance Capacity to evaluate their health status and so to reveal the necessity of maintenance and repair operations

self-optimization Capacity to evaluate their job in order to promote its improvement

Even if Xu focuses its analysis on CNC machines its deductions can be easily extended to other machines usually utilised in industrial implants as AGVs or automated warehouses. These concepts in the design process are embodied through the functions that the components can accomplish. When a CNC machine provides a machining operation through a function on the shop floor network, it basically defines its role in the system, self-awareness. The capability to require a maintenance procedure or to provide an evaluation of its job through an analysis of its status express a self-maintenance and self-optimization ability.

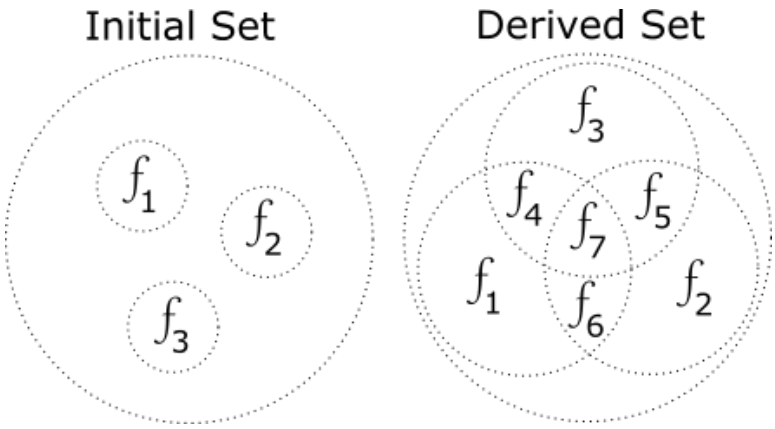

Figure 5.10: CPS 4.0 as a set of functions

To the characteristics listed by Xu we add the concept of modularity, fundamental in a flexible industry. The concept of modularity in industrial machines is reached through the machine processes combined with their communication skills. Consider three machines that can do three different jobs, f_1, f_2 and f_3 and a product that needs all three to be realized. A production management system, MES, is able to autonomously organize the production plan when it detects the three machines in the company network and recognizes the three available processes. If we consider the three processes as functions available on the net we can easily imagine how these can be combined as desired to create more complex ones, fig. 5.10. Every time we add a machine to the system, we add a function to the initial set of available processes; the number of possible combinations grows exponentially. The sharing of functionalities in order to accomplish a task is well expressed by Mosterman et al. [32]. Mosterman describes a pick and place system built in order to move some simple coloured blocks along a line on specific spots. Every block is a smart device capable to ask for a specific pick and place plan; for instance a block can ask to the system to be moved two spots on the right of its actual position. The pick and place machine manages the requests of the blocks according to a specific logic. The whole system is the ensemble of the capabilities of its subsystems; the capacity of the blocks to make a request and the capacity of the pick and place machine to manage and deliver them.

WorkForce

Even though from a conceptual point of view the workforce integrated in the production system as CPS does not involve great differences with the other components of the system, we feel obliged to do a little separate treatment on what will be some consequences for the people who will work in the

industry of the future.

Staff integration is essential for the success of the vision 4.0. In the recent past the attempt to reach a complete industrial automation has failed in many sectors in the face of the impossibility of completely automating the various production phases, making it clear that the elimination of the human component was not only impossible, at least today, but also counter productive. This gave birth to a new topic concerning human-machine collaboration. The main themes in this regard are those related to the use of collaborative robots and augmented reality systems, AR, along with the more classic interaction systems that are generally called HMI, human machine interface.

The concept of augmented reality exists since well before Industry 4.0 and it is defined as the integration of virtual reality with the real one [4]. In virtual reality, the real world is replaced by virtual reality, instead in AR we have the composition of the real world with the virtual one. The AR has possible applications in different sectors besides the industrial one in which it can be used in different phases of the operator's work. A typical example of augmented reality in industry 4.0 is the use of optical see-trough glasses to instruct and guide an operator during his tasks. An example of this type of use is given by Paelke [35] and Kolberg et al. [22]. Paelke describes a demonstration in which an operator, following the images that are in real time superimposed on his vision of reality, is guided step by step in the assembly of a component, on which parts he must choose and how to mount them. A similar description is made by Kolberg that promotes the use of these systems for flexible productions in which the operator can easily customize the product following the instructions received through the glasses and which can be updated very quickly between one product and another ; in addition, Kolberg emphasizes the integration of operators within the company's CPSs through appropriate human-machine interfaces.

The use of collaborative robots, cobots, arises from the need to combine the strength of the machines with the flexibility of the man [37]. Cobots are those robots designed for an direct interaction with a man contrary to the most classic robots usually designated to work in isolated cells mainly for safety reasons. In particular this solution has been used in the assembling field [6, 10, 23], rather than in the manufacturing processes, where the great variety of products required by the increasingly customized production and the presence of difficult-to-automate tasks makes the presence of the man fundamental. In industry 4.0, collaboration between man and machine is essential to achieve the required production flexibility [3]; collaborative robots must be able to work with humans without endangering or injuring them in any way [21]. The operator within the smart factory seen as CPS must be able to interact with the other components of the factory and it is therefore necessary to develop interfaces for human-machine communication, HMI. Usually this interaction occurs through a screen with a special GUI inter-

face, but different ways of communication can be established. For example, Christiernin et al. [12] studies the use of a kinetic camera for an operator-machine interaction.

The change proposed by industry 4.0 will therefore require the development of new skills by operators. According to the study carried out for the department of economics and science of the EU [45] the workers of industry 4.0 must have excellent communication skills, be able to develop their work more autonomously, all together with new skills mainly in the IT field. In 2020 it is expected a lack of people suitable to work in a complex environment such as that of industry 4.0 of approximately 825,000 specialists [45] and that is why it is important to develop dedicated development programs, internally and externally to companies. Many concerns then arise on the possibility of job losses as on the possibility of worst job guarantees with the formation of the so-called "click and cloud workers" and in terms of work quality with phenomena of alienation and sensation of control loss due to the virtual environment in which they work [45].

As a personal thought, we want to conclude this paragraph by underlining how the technological developments promoted by industry 4.0 must take into account the social impacts that are created, first of all with regard to the quality of the work.

5.8 CPS 4.0

As a result of the analysis of the concept of CPS and of the changes brought by industry 4.0 we give the definition of what we call CPS 4.0, a point of meeting between the classical definition of CPS and their use made inside industry 4.0.

A CPS 4.0 is a system capable of active/passive communications externally to the system itself, whose inner nature is totally generic, from a mechatronic system to another CPS, from a pure software to a human being, and whose maximum level of abstraction is given by the services/functions which is capable to provide and receive.

Independently from the name chosen the concepts expressed by this definition embraces the main features for the development of the new industry. The capacity to communicate in an at priori unknown environment in order to guarantee the availability of informations in faster, more efficient and more meaningful ways is the feature that most of all will influence the CPSs which make available in a interconnected net their services in order to make possible a production characterized by high flexibility and modularity.

Table 5.1 summarizes the final comparison of this study highlighting the differences from the classical meaning of CPS to the one considered

Table 5.1: Features of classical CPSs and CPSs 4.0

CPS	Classical	4.0
	Internal Network	External Network
	Physical part necessary	Physical Part optional
	Saving on energy and space	Focus on services provided
		Modularity

by industry 4.0. Notice that Industry 4.0, borrows the name CPS from the embedded system field, but changes the meaning. Given the idea of an industry network made of CPSs the internal nature of the latters is of interest only for the designers not for who utilise or organize them. With that it is not mean to diminish the value or the importance of the design phase of these components but we want to highlight the level of abstraction needed to a management level that is given by the functions that the CPSs provide. For industry 4.0 everything can be a CPS as long it has an IT superstructure, as the one represented by the RAMI model, in the form of an administration shell or the like but it is not given any specification on the design process of these components. The same action inside a shop floor can be accomplished by a mechanical machine than a person, it wouldn't have any meaning to compare the design of the first with the management of the second. Some services can be supplied by software which do not have a physical counterpart as in the classical definition of CPS, but they exist and they offer several services inside a company. According to the specific case of CPS 4.0 we can face different thematics but these one are to a lower level than the one of the services provided. The abstraction brought by the services provided by CPSs 4.0 is independent from how that services are actually implemented and it brings with it the modularity needed by a flexible production.

Referring at fig.5.11 is possible to see how a CPS 4.0 is conceived through its functions, an internal part the whole connected to an external network. In the picture are represented simultaneously multiple situations that we can find inside a CPS 4.0 which can be internally made of a mechatronic system, or a software, or a human being with some sort of HMI, or there can be other CPSs nested inside it. The distinction between functions provided and functions required is based on the idea of what the component can do a what can ask in order to do that. They have a communication ability which could be active or passive. A passive communication is the one for example provided by RFID tags where are stored the informations related to the object.

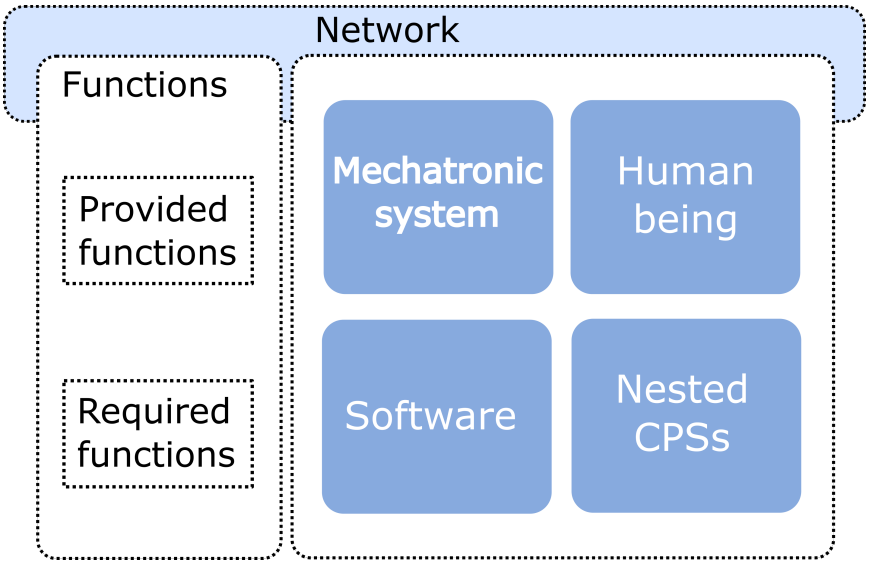

Figure 5.11: Conceptual design of a CPS 4.0

5.9 Integration of AM data flow

If we take again the scheme of fig. 5.1 we can now re-contextualize it within the framework of industry 4.0 and in the perspective of an integrated CPS within the industrial context. In fig.5.12 we see the flow of data related to the AM machine integrated with the typical software of a company, some of which have been already described in par.5.7 as part of the ISA-95 standard, others have been added in this scheme since they came later in common use in these environments. These are the PDM, product data management, and the PLM, product lyfecicle management, which have tried to fill the gap between the management software and those software more closely related to design and industrial production, CAD/CAM. In the middle of the two worlds given by the data flow of an AM machine, in blue, and by the data collection and management programs, in green, it is inserted the digital version of the machine, digital twin, and the cloud, meant as a point of collection and connection between the various parts of the system. The digital twin has been split in two parts to underline how the representation of reality given by physical-mathematical models can be used both to foresee what will happen, through offline simulations, than what happens through a real-time representation based on data measured directly on the machine. In the case of a 3D printer, the path generated by the CAM and described by the gcode can be used to simulate the production of the piece before it takes place; the data collected by the motors can be used to see what is actually done by the machine and compare the result with the simulation done at priori to verify the goodness of the model proposed by the digital

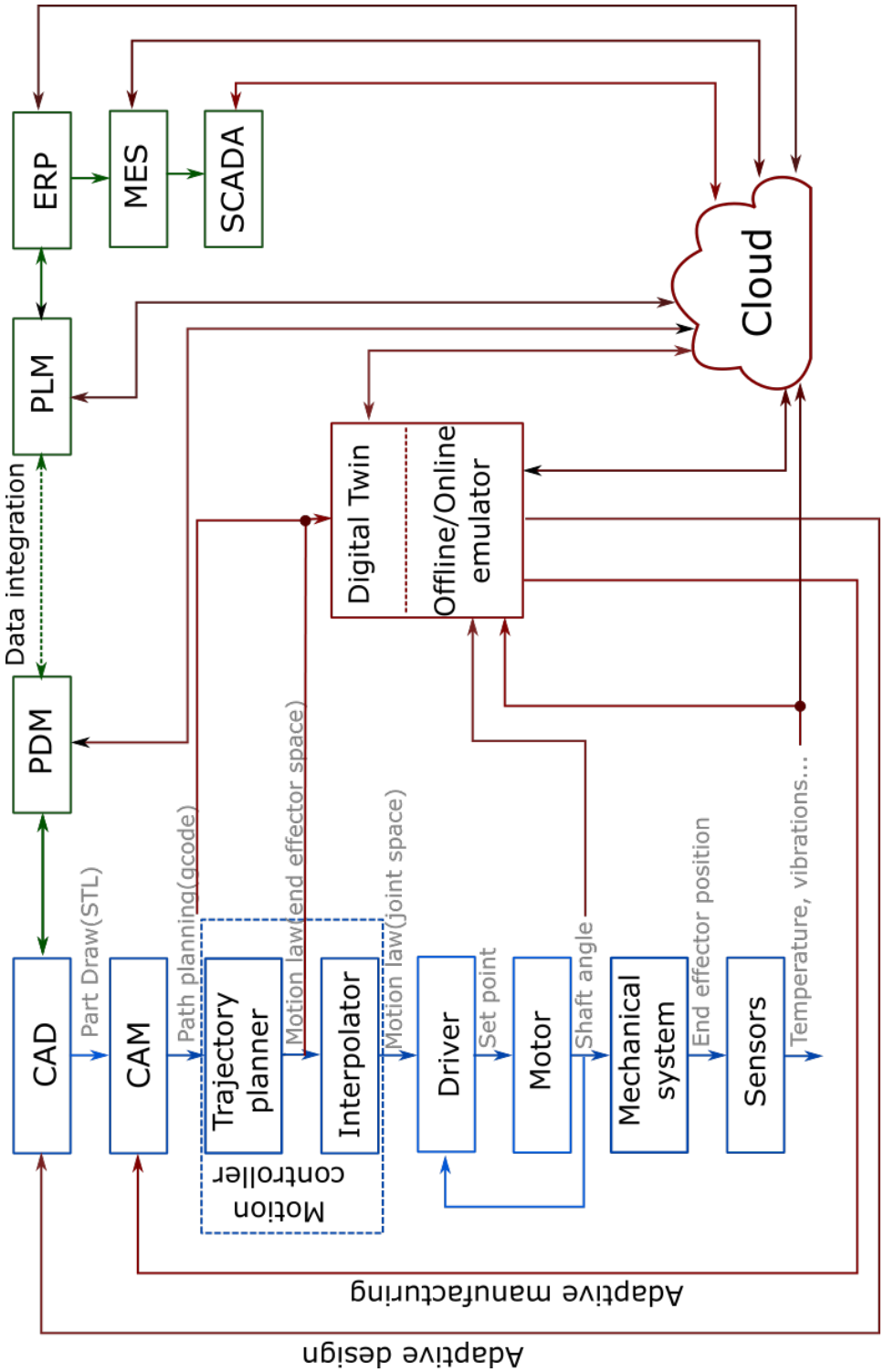

Figure 5.12: AM integrated inside a industry 4.0 factory

twin or the goodness of the machine. The figure highlights two main feedbacks starting from the digital twin and directed towards the CAD/CAM software; respectively linked one to the theme of adaptive manufacturing and one to that of active design. The data related to the simulations and/or emulations of the AM machine allow to study and optimize the production going to work or on how the component was designed, CAD, or on how the component was produced, CAM. The digital twin interacts indirectly with the management and data collection programs through the cloud, closing the production control loops, MES, for the management of controlled maintenance and/or materials, ERP, as for the connection of operators to the machine.

The introduction of AM machines as CPS capable of communicating within the company system close the communication and control loops with the management and data collection software through their digital twin and the presence of a reference cloud. As shown in the figure, the data collected by the machine through the available sensors are not necessarily addressed to the digital twin, but can be collected directly in the cloud to be exploited by the company's software, or by third parties who are granted access to such data, realizing the interconnection between companies, suppliers and customers envisaged by industry 4.0.

5.9.1 Adaptive manufacturing example

The integration of AM machines as depicted in fig.5.12 can be directly applied to the Efesto machine. It is here proposed an adaptive manufacturing example based on a real problem observed on the Efesto machine.

In fig.5.13 two graphs are visible relative to a trajectory performed by one of the three delta linear motors during the printing of a component. The position, Q, and the velocity, $\dot{Q}$, are represented, and for each of the two the planned trajectory and the one actually performed by the motor are shown. It is quite evident how after an initial part where the two curves, both in position and in speed, go hand in hand, there is an evident gap between the two. The direct consequence of an error of this type is a poor execution of the printing process which had obviously been planned differently. The reason for this error is due to the stepwise discretization of the velocity profile. The control system of the printer, and more precisely the drivers of the motors, are able to follow any law of motion through velocity steps. A good choice of the discretization level allows to approximate a continuous variation of the velocity in general without particular problems. In the specific case, an anomaly has occurred which involves, in some points, as seen in the graph in position, the apparent stop of the motor which starts again with a delay compared to the expected trajectory. If we go to zoom in on one of the points where the error happens, in the velocity graph, we realize how this phenomenon happens when the speed of execution near the

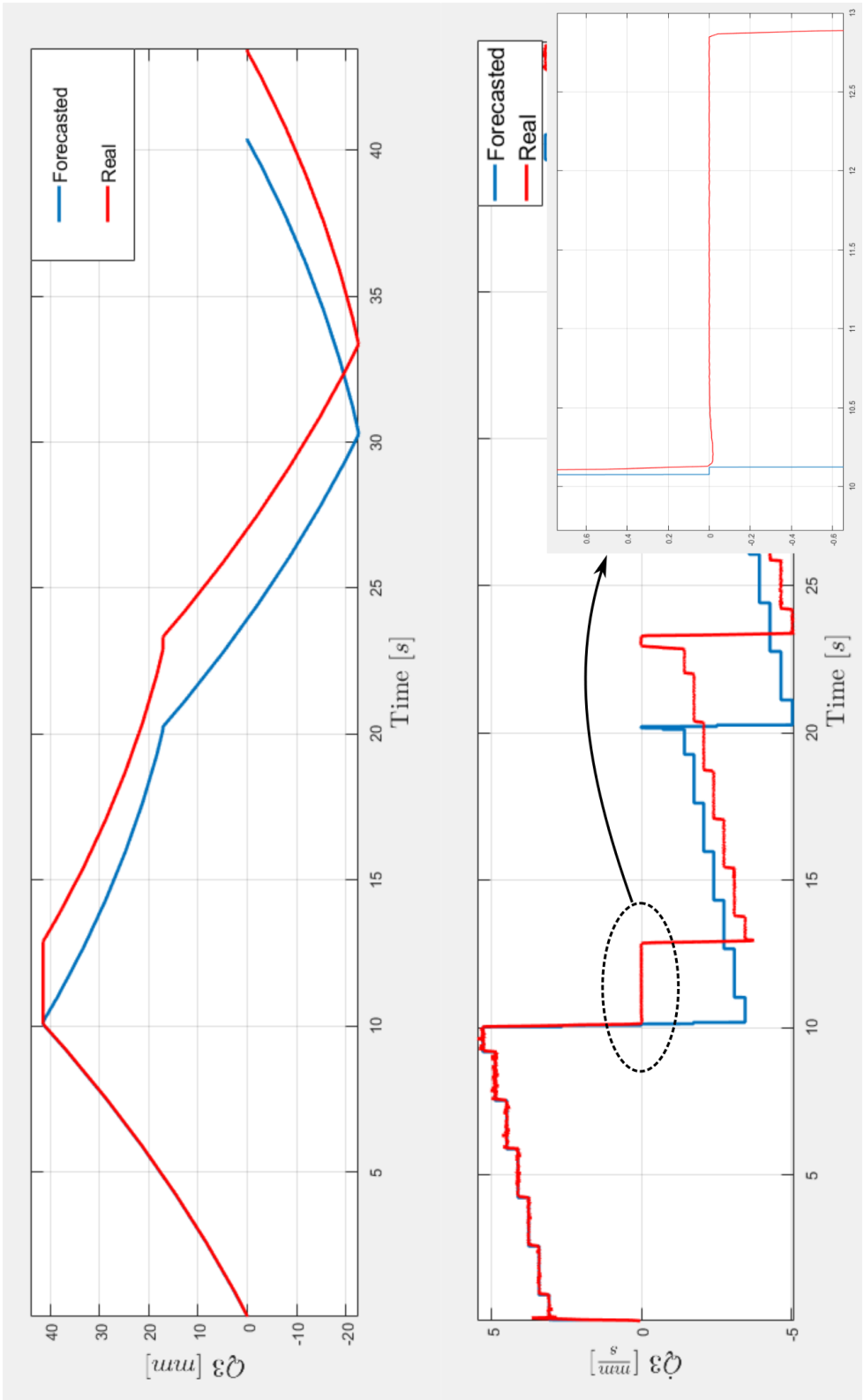

Figure 5.13: Forecast and real motion law on a Efesto motor

zero was foreseen for the motor. Even though from the graph might appear that the commanded velocity, in blue, has a null value in reality and it is simply very small. In an attempt to execute this command, an error occurs on the part of the motor controller, the driver, which causes the motor to run at a very low speed for a longer time than the programmed one. [1].

The resolution of this problem required time and efforts, but more importantly it was only detected retrospectively on the controls carried out manually on the trajectories effectuated by the motors during some tests. The integration of the machine within a scheme such as the one proposed in fig.5.12 would allow to automate the process that was done here manually going to avoid problems like the one presented and maybe discovering new ones. This integration for the above-mentioned case can take place as follows:

- During the printing process are measured the motors positions and velocities
- Such curves are compared with the theoretical curve generated by the interpolator for the motors.
- When a difference is detected the problem can be immediately reported to the CAM closing a control loop on the product manufacturing process
- The planning of the trajectory can be modified for the future production of the product.

This example of adaptive manufacturing on the one hand demonstrates the potential of an industrial machine, and in particular of an AM machine, integrated within the computer system of a production plant, on the other shows how there is certainly a lot to do when having to equip the industrial machines of systems able to supply an ever increasing quantity of data, to have models of the machines always more detailed, and to develop more and more sophisticated algorithms able to act according to the problems detected.

5.10 Conclusions

In this chapter has been presented a critical analysis of the industry 4.0 concepts in particularly on the meaning of the cyber-physical systems. This analysis started from the need to integrate AM systems and their digital part within the digital systems of production sites. An integration scheme

[1] We do not go into detail to explain the causes of the phenomenon related to the driver control logic since it is not essential to the message that we want to transmit

is proposed for AM machines within production contexts, underlining the possibility of working in the direction of adaptive design and manufacturing. In addition, the data collected by the machine can be exploited by other company software or through simulations/emulations of a digital twin of the machine or directly from a data collection cloud. A theoretical example carried out on the Efesto machine shows the possibility of a fast detection of manufacturing problems with the chance to correct them with a feedback on the issue itself.

bibliography

[1] Working Group Industry 4.0. Final report of the industrie 4.0 working group. securing the future of german manufacturing industry recommendations for implementing the strategic initiative industrie 4.0, 2013.

[2] Acatech. Cyber-physical systems. driving force for innovation in mobility, health, energy and production, 2011.

[3] R.E. Andersena, E.B. Hansena, D. Cernya, S. Madsena, B. Pulendralingama, S. Bøghb, and D. Chrysostomoub. Integration of a skill-based collaborative mobile robot in a smart cyber-physical environment. *27th International Conference on Flexible Automation and Intelligent Manufacturing*, 2017.

[4] R.T. Azuma. A survey of augmented reality. *Presence: Teleoperators and virtual environments*, 6, 1997.

[5] N. Bieberstein, S. Bose, M. Fiammante, K. Jones, and R. Shah. *Service-Oriented Architecture Compass: Business Value, Planning, and Enterprise Roadmap*. FT Press, 2005.

[6] H. Bley, G. Reinhart, G. Seliger, M. Bernardi, and T. Korne. Appropriate human involvement in assembly and disassembly. *CIRP annals - manufacturing technology*, 53, 2004.

[7] D. Brandl. Business to manufacturing (b2m) collaboration between business and manufacturing using isa-95. *REE, Revue de l'Electicite e de l'Electronique*, 2002.

[8] K. Breiner, D. Görlich, O. Maschino, G. Meixner, and D. Zühlke. Runtime adaptation of a universal user interface for ambient intelligent production environments. In *Human-Computer Interaction. Interacting in Various Application Domains*. Springer, 2009.

[9] L.M. Camarinha-Matos and H. Afsarmanesh. The virtual enterprise concept. In *Infrastructures for virtual enterprises- Networking Industrial Enterpriseses*. Springer, 1999.

[10] A. Cherubini, R. Passama, A. Crosnier, A. Lasnier, and P. Fraisse. Collaborative manufacturing with physical human–robot interaction. *Robotics and computer-integrated manufacturing*, 40, 2016.

[11] S.R. Chhetri, S. Faezi, and M.A. Faruque. Information leakage-aware computer-aided cyber-physical manufacturing. *IEEE transactions on information forensics and security*, 13, 2018.

[12] L.G. Christiernin and S. Augustsson. Interacting with industrial robots: A motion-based interface. *Proceedings of the Workshop on Advanced Visual Interfaces AVI*, 2016.

[13] L. Escobar, N. Carvajal, J. Naranjo, A. Ibarra, C. Villacís, M. Zambrano, and F. Galárraga. Design and implementation of complex systems using mechatronics and cyber-physical systems approaches. *International Conference on Mechatronics and Automation*, 2017.

[14] H. Gill. Challenges for critical embedded systems. *Proceedings of the 10th IEEE International Workshop on Object-Oriented Real-Time Dependable Systems*, 2005.

[15] B. Guérineau, M. Bricogne, A. Durupt, and Rivest L. Mechatronics vs. cyber physical systems: towards a conceptual framework for a suitable design methodology. *17th International Conference on Research and Education in Mechatronics, REM*, 2016.

[16] X. Hong and W. Jianhua. Using standard components in automation industry: A study on opc specification. *Computer standards and interfaces*, 28, 2006.

[17] Industry 4.0 platform. https://www.plattform-i40.de/I40/Redaktion/EN/News/Actual/2016/2016-05-20-IIC.html. Accessed: 2017-11-09.

[18] R. Isermann. Modeling and design methodology for mechatronic systems. *Transactions on Mechatronics*, 1996.

[19] K. Janschek. *Mechatronik Systems Design: methods, models, concepts*. Springer, 2012.

[20] J. Kletti. *Manufacturing Execution Systems – MES*. Springer, 2007.

[21] P.J. Koch, M.K. van Amstel, P. Debska, M.A. Thormann, A.J. Tetzlaff, and D. Bøghb, S.and Chrysostomou. A skill-based robot co-worker for

industrial maintenance tasks. *27th International Conference on Flexible Automation and Intelligent Manufacturing*, 2017.

[22] D. Kolberg and D. Zulhke. Lean automation enabled by industry 4.0 technologies. *IFAC proceeding volumes*, 48, 2015.

[23] J. Kruger, T.K. Lien, and A. Verl. Cooperation of human and machines in assembly lines. *CIRP annals - manufacturing technology*, 58, 2009.

[24] H. Lasi, P. Fettke, H.G. Kemper, T. Feld, and M. Hoffmann. Industry 4.0. *Business & Information Systems Engineering*, 2014.

[25] E.A. Lee. Cyber physical systems: Design challenges. *11th IEEE Symposium on Object Oriented Real-Time Distributed Computing*, 2008.

[26] E.A. Lee and S.A. Seshia. *Introduction to embedded systems: A cyber-physical systems approach.* MIT Press, 2017.

[27] J. Lee, B. Bagheri, and H. Kao. A cyber-physical systems architecture for industry 4.0-based manufacturing systems. *Manufacturing letters*, 2015.

[28] Y. Liu and X. Xu. Industry 4.0 and cloud manufacturing: A comparative analysis. *Journal of Manufacturing Science and Engineering, Transactions of the ASME*, 2017.

[29] Made in china 2025. http://english.gov.cn/2016special/madeinchina2025/. Accessed: 2018-02-18.

[30] MFG, 2016.

[31] L. Monostoria. Cyber-physical production systems: Roots, expectations and r&d challenges. *Proceedings of the 47th CIRP Conference on Manufacturing Systems*, 2014.

[32] P.J. Mosterman and J. Zander. Industry 4.0 as a cyber-physical system study. *Software and Systems Modeling*, 15, 2016.

[33] Premier of the State Council of China. Proceedings of the 3rd session of the 12th national people's congress, 2015.

[34] Blevins P. Enterprise resource planning (erp) - an executive perspective. *Annual International Conference Proceedings - American Production and Inventory Control Society*, 1994.

[35] V. Paelke. Augmented reality in the smart factory: Supporting workers in an industry 4.0. environment. *International Conference on Emerging Technologies and Factory Automation*, 2014.

[36] R. Perrey and M. Lycett. Service-oriented architecture. *Applications and the Internet Workshops*, 2003.

[37] M. Peshkin and J.E. Colgate. Cobots. *Industrial Robot*, 26, 1999.

[38] C.A. Ptak. *ERP Theory and Applications for Integrating the Supply Chain.* St. Lucie Press, 2004.

[39] Quirky, 2016.

[40] L. Ribeiro and M. Bjorkman. Transitioning from standard automation solutions to cyber-physical production systems: An assessment of critical conceptual and technical challenges. *IEEE systems journal*, 2017.

[41] J. Rifkin. *The third industrial revolution.* Palgrave Macmillan, 2011.

[42] T. Sauter, J. Jasperneite, and L. Lo Bello. Towards new hybrid networks for industrial automation. *Conference on Emerging Technologies and Factory Automation*, 2009.

[43] Shapeways, 2016.

[44] Smart factory kl. http://smartfactory.de/en. Accessed: 2017-21-09.

[45] J. Smith, S. Kreutzer, C. Moeller, and M Carlberg. Industry 4.0. study for the itre committee, 2016.

[46] SF. Tao, Y. Cheng, L. Zhang, and A.Y.C. Nee. Advanced manufacturing systems: socialization characteristics and trends. *J.of Intelligent Manufacturing*, 2015.

[47] V. Thomson and U. Graefe. Cim-a manufacturing paradigm. *International Journal of Computer Integrated Manufacturing*, 1989.

[48] VDI/VDE and ZVEI. Status report reference architecture model industrie 4.0, rami4.0, 2015.

[49] M. Weiser. The computer for the 21st century. *Scientific American*, 265, 1991.

[50] D. Wu, M.J. Greer, D.W. Rosen, and D. Schaefer. Cloud manufacturing: Strategic vision and state of the art. *Journal of manufacturing systems*, 32, 2013.

[51] Xu X. Machine tool 4.0 for the new era of manufacturing. *Int.J. of Advanced Manufacturing Technology*, 2017.

[52] X. Xu. From cloud computing to cloud manufacturing. *Robotics and Computer-Integrated Manufacturing*, 28, 2012.

[53] K.E. Yin, Y. Stecke and D. Li. The evolution of production systems from industry 2.0 through industry 4.0. *International Journal of Production Research*, 2017.

[54] R.Y. Zhong, S. Lan, C. Xu, Q. Dai, and G.Q. Huang. Visualization of rfid-enabled shopfloor logistics big data in cloud manufacturing. *International Journal of advanced manufacturing technology*, 2015.

[55] D. Zuehlke. Smartfactory-towards a factory of things. *annual reviews in control*, 34, 2015.

Photobook

One of the main goal of this work has always been to allow the development of a new 3D printing technique within the manufacturing world of Additive Manufacturing. Although in this work we have dealt with the development of the machine from a mechanical, control and flow of information point of view, from the STL file to the printed object, we can not but dedicate a small window to those that have been the uses of the machine. This chapter shows a series of annotated photos of the objects produced by the Efesto printer. We would like to thank the researchers, assignees and experts who, by working on the technology of the machine, allowed the printing of these components.

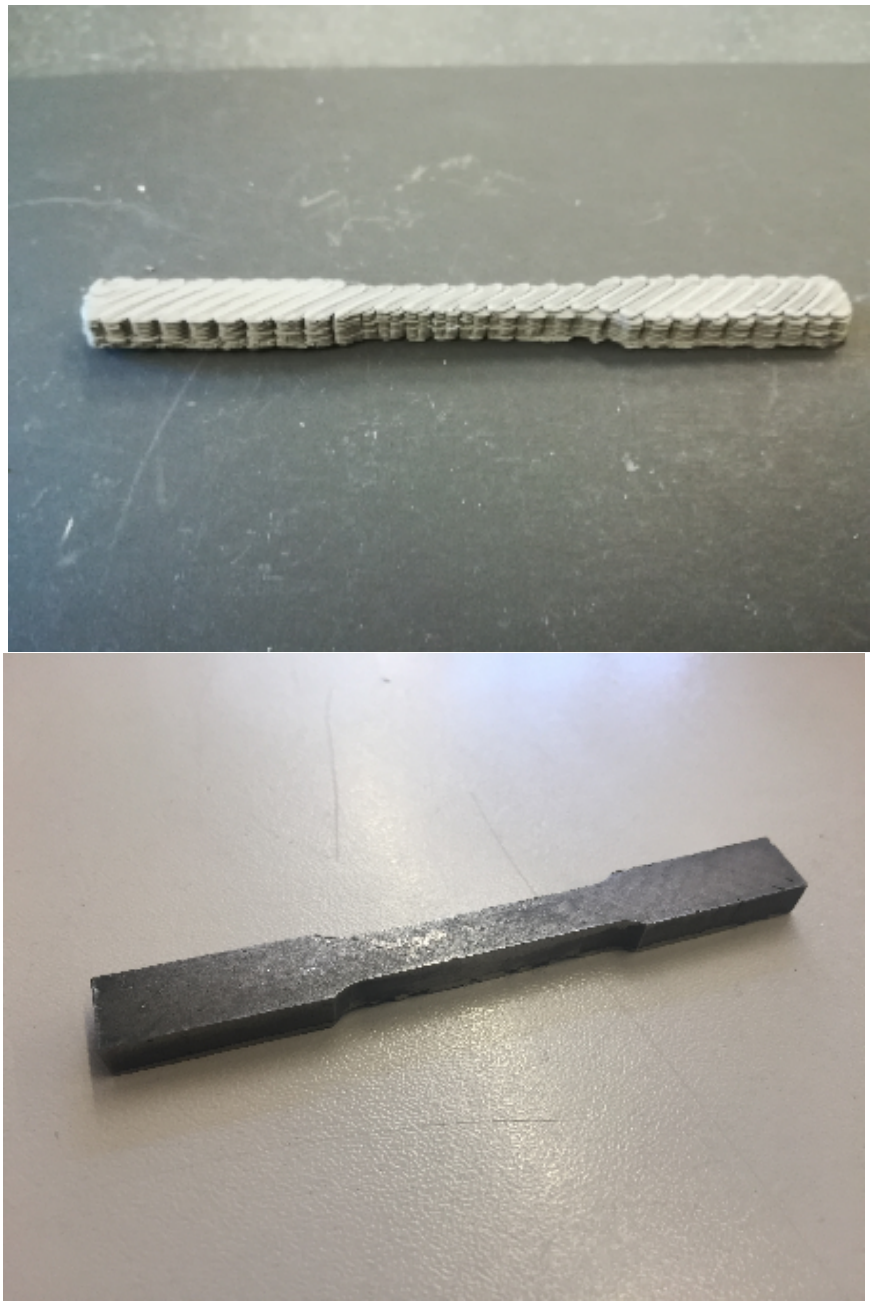

Print of a steel specimen for tensile tests. The specimen is moulded, sintered and finished to machine tools before being subjected to tensile tests.

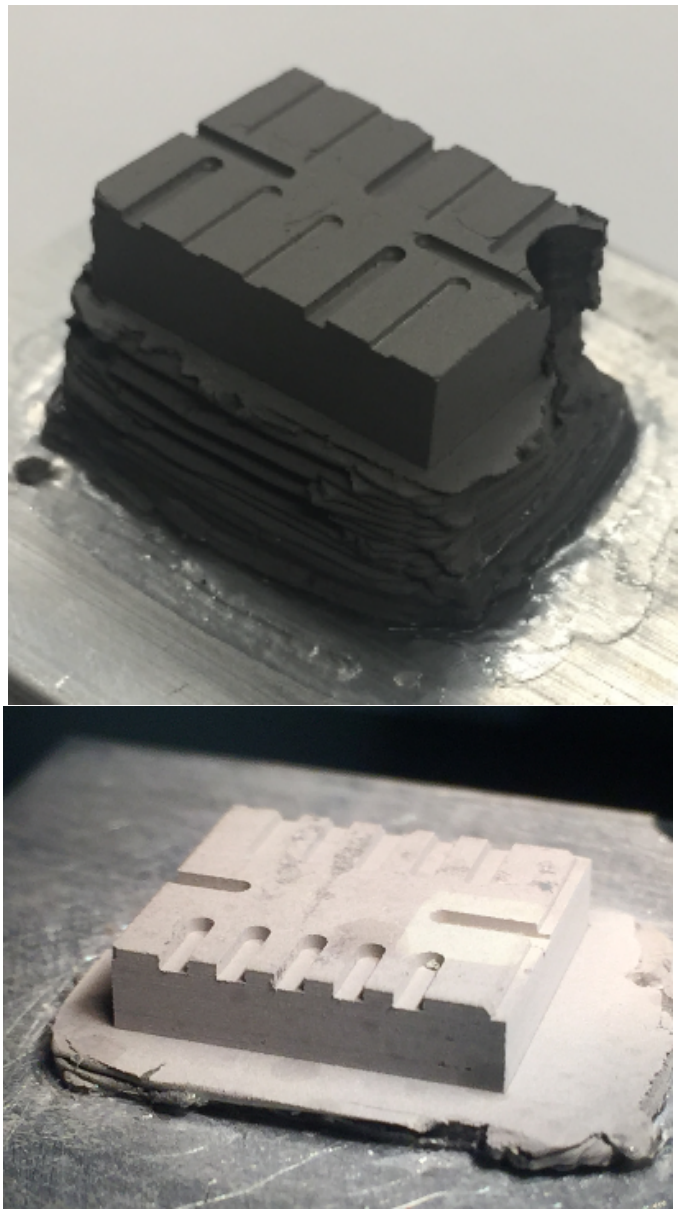

Test of hybrid manufacturing on green parts. Two printed parts, steel and alumina, are machined right after the printing phase by milling, before the debinding and sintering phases.

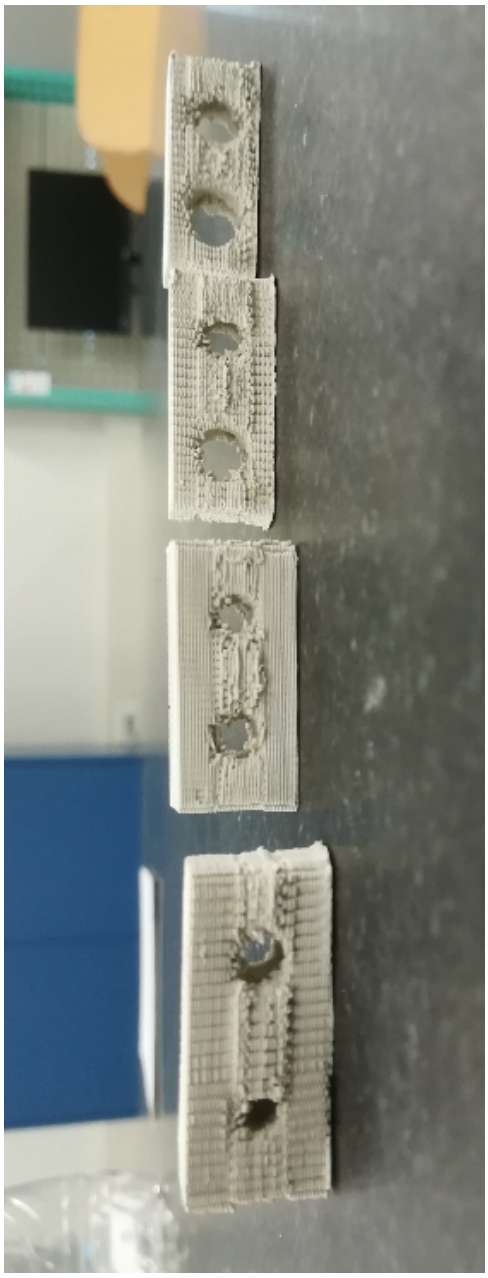

Prints for the study of through holes. Alumina.

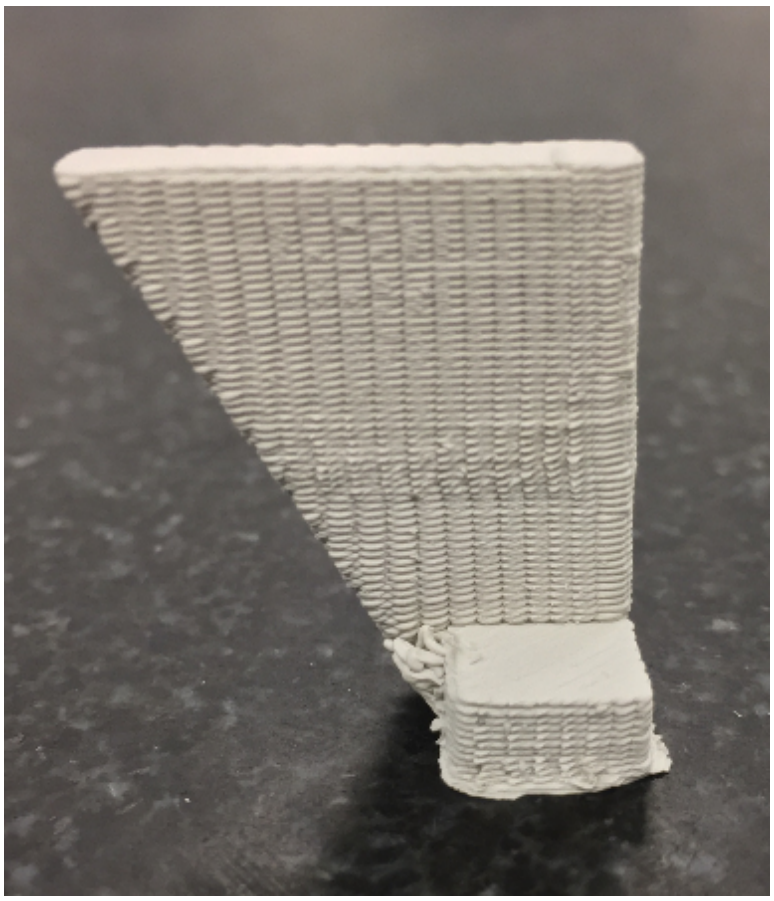

Print for the study of hanging structures. Alumina.

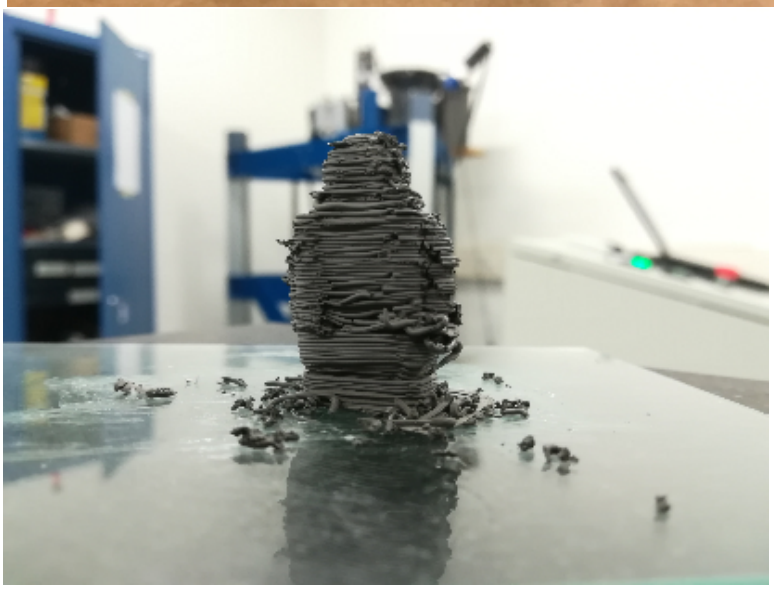

Prints of small robots. Steel and alumina.

Sintered parts, cut and polished for a study of porosity.

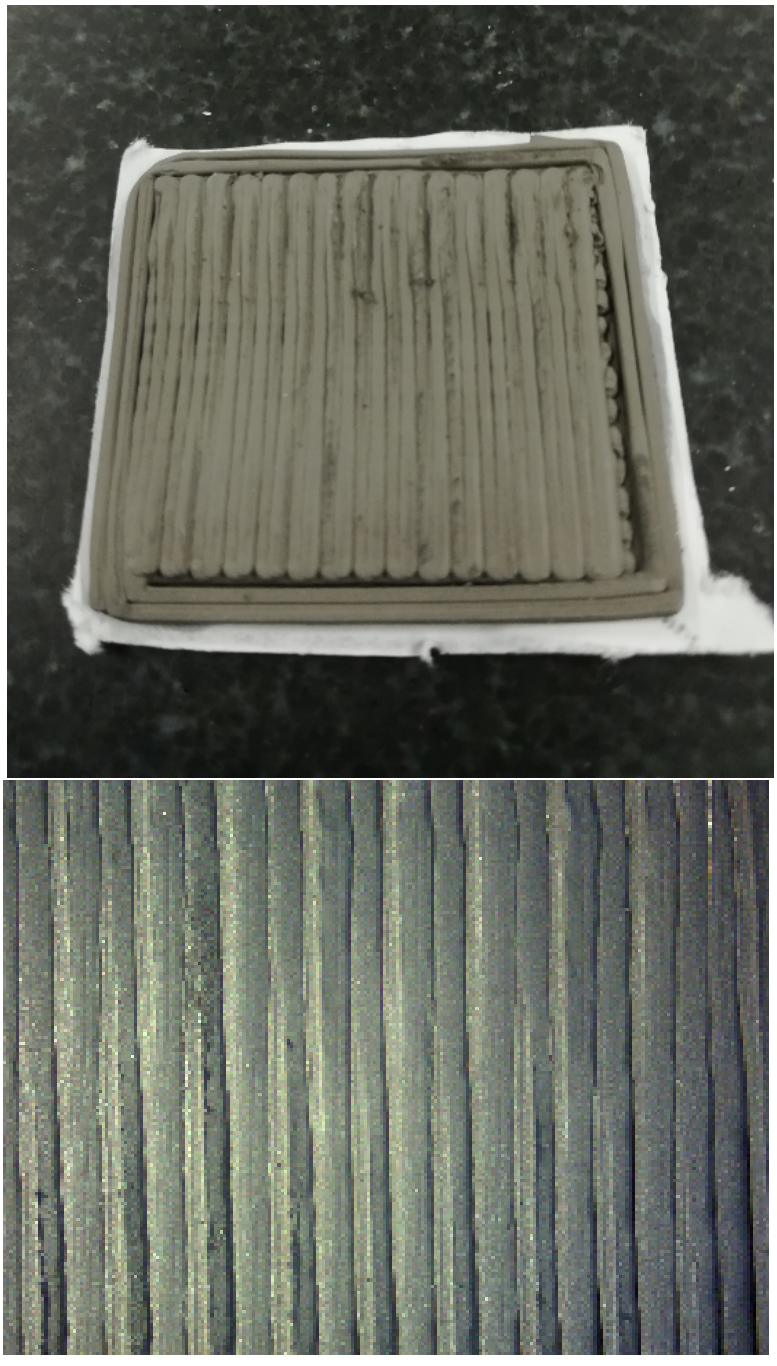

Printing sample for the study of the process parameters.

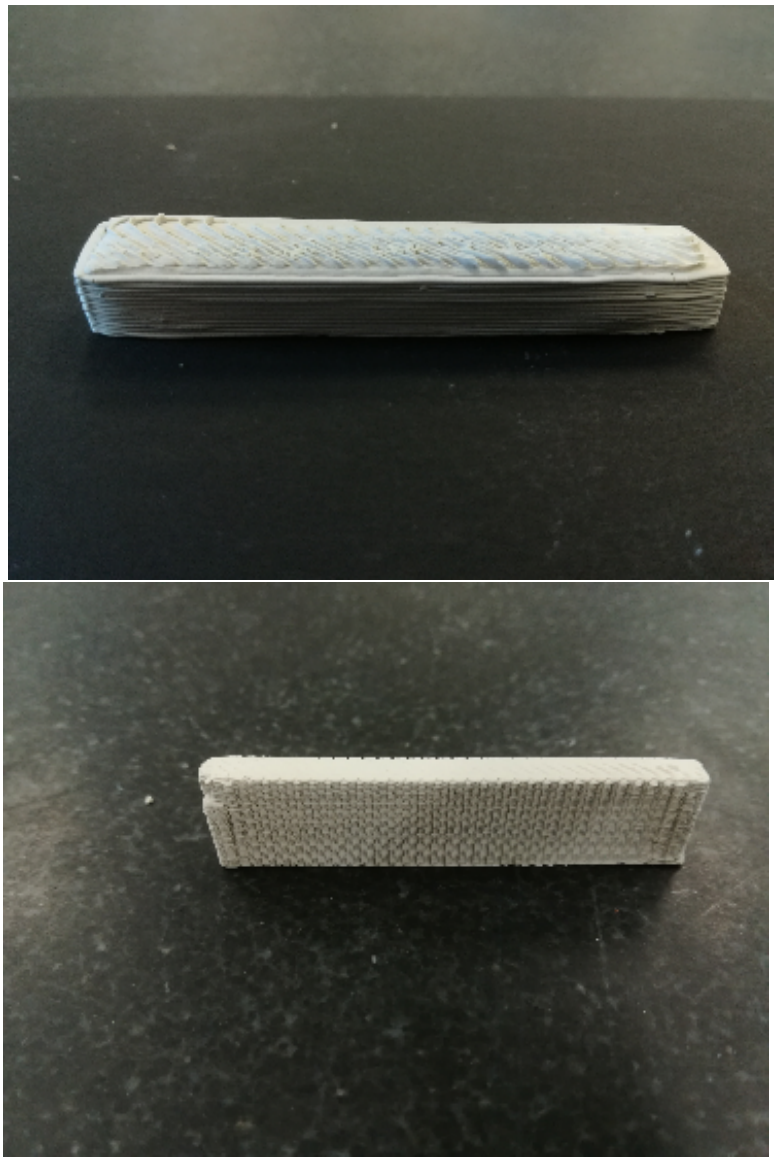

Printing samples for the study of alumina behaviour.

Conclusions

With this thesis work we have participated in the development of a new technology whose possible industrial and social benefits have been widely proven in the literature. Specifically it has been designed and developed a prototype for an innovative process of Additive Manufacturing based on the extrusion of a metallic or ceramic feedstock according to the technological process of Metal Injection Moulding for the production of functional parts.

This work leaves:

1. An innovative and tailored designing solution for a specific AM process through the use of a mechatronic approach.
2. A stochastic method for the evaluation of the probability success of a calibration process for robots applied in extrusion-based additive manufacturing techniques with a specific solution for the linear delta. The creation of success maps based on a stochastic method that allow to evaluate how to set the different calibration steps in order to maximize the success of the technological process.
3. An algorithm for trajectories generations for a printing process with constant extrusion rate in order to minimize the problems of overfill and underfill.
4. A critical analysis of industry 4.0 with particular attention to the CPSs in order to integrate the AM machines and their data within the industrial environments.

In addition to the points listed above distributed throughout work, starting from the first chapter, we leave a profound knowledge of AM technology for extrusion, both from the point of view of the technology itself, limits and process parameters, than from a point view of the digital chain necessary for the implementation of a 3D printing process.

Publications

Here are listed the scientific publications carried out during the PhD period, 2015-2018. The articles are divided by year, indicating the title, authors and

the main publication informations.

2018 *A simplified approach to the calibration of extrusion based AM systems*, Sbaglia L., Giberti H., Castelli K., In proceedings IFIT2018

The Cyber-Physical Systems within the industry 4.0 framework, Sbaglia L., Giberti H., Silvestri M., In proceedings IFIT2018

R*apid production of hollow SS316 profiles by extrusion based additive manufacturing*, Rane K., Cataldo S., Parenti P., Sbaglia L. et al., AIP Conference Proceedings, doi:10.1063/1.5035006

A robotic design for a MIM based technology, Giberti H., Sbaglia L., Mechanisms and Machine Science, Volume 49, pages 565-572, doi:10.1007/978-3-319-61276-8_59

2017 *Mechatronic design for an extrusion-based additive manufacturing machine*, Giberti H., Sbaglia L., Silvestri M., Machines, Volume 5, Issue 4, doi:10.3390/machines5040029

A path planning algorithm for industrial processes under velocity constraints with an application to additive manufacturing, Giberti H., Sbaglia L., Urgo M., Journal of Manufacturing Systems, Volume 43, pages 160-167, doi:10.1016/j.jmsy.2017.03.003

Trajectories generation with constant extrusion rate for experimentations on am techniques and extrusion based technologies, Giberti H., Sbaglia L., Parabiaghi M., Mechanisms and Machine Science, Volume 47, pages 153-160, doi:10.1007/978-3-319-48375-7_17

2016 *Kinematic synthesis of a new 3D printing solution*, Giberti H., Fiore E., Sbaglia L., MATEC Web of Conferences, Volume 45, doi:10.1051/matecconf/20164504013

APPENDIX A

Hints of robotics

This appendix gives some brief references to concepts of kinematics and robotics. For a deeper further informations we refer the reader to specialized texts [1].

A.1 Serial and parallel robots

The term *robot* has un undefined origin and its meaning can be interpreted in different ways. Limited to industrial applications we mean a multi-purpose manipulator, with three or more axes, programmable and subjected to automatic commands. Axes means the degrees of mobility of the joints of the robot that can be of the rotary or translation type. The main parts that compose it are therefore:

- mechanical structure(manipulator)
- power supply
- control system

The kinematic of a robot is defined by its set of kinematic constraints divided in passive and active constraints. The active joints are the joints whose motion is controlled, as for instance electric motors, instead the passive joints motion is a consequence of the active joints ones. The number of active joints defines the robot degree of freedom, Dofs. The active joints can be redundant, this is clear when they are more than six. The position, $x - y - z$, and the orientation, $\theta - \phi - \psi$, of a robot defines its pose. The pose of a robot is specified on one of its rigid bodies called end-effector; usually the end-effector is a part of the robot of particular interest, for instance the hand of a pick-and-place robot. The end-effector pose is specified in a respect of a specific point called tool-centre-point,

[1] As the book *Robotica Industriale*, Giovanni Legnani, CEA 2003

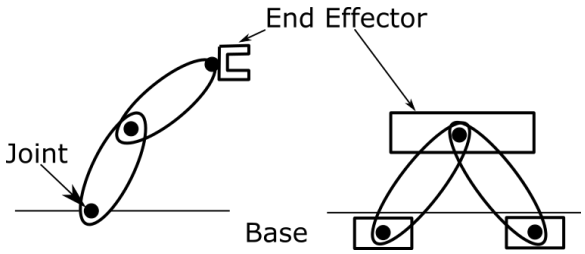

Figure A.1: Open and close kinematic chain

TCP. The end-effector pose is defined in relationship with the positions of the active joints. It is defined usually two spaces for a robot:

Joint space Its the space defined by the values of the active joints.

Workspace Its the space defined by the values of the end-effector pose.

The workspace defines the positions and orientations that can be assumed by the robot.
I robot possono in base alla loro struttura meccanica possono essere divisi in due grandi gruppi:

- Serial robots
- Parallel robots

The serial robots are constitute by rigid bodies connected through active and passive joints in order to form an open kinematic chain, inversely the parallel robot can form closed kinematic chain. A man consequence for this it is that for a serial robot any set of values in the joints space leads to a robot pose, the same is not true for a parallel robot where the values of the active joints must be chosen carefully in order to not damage the system. It is possible to have hybrid solution between parallel and serial robot where at the same time exist closed and open chain. In fi.A.1there is a schematic example of an open chain, on the left, and of a closed chain, on the right. Starting from a body defined base for a parallel robot is possible to arrive to the end-effector and come back to the base without passing twice on the same body. It is evident from the figure how the same is not possible from a serial robot. We talk of *full parallel robot* when the degree of freedom of the robot are equal to its number closed kinematic chains. This solution is very common and leads to a robot with an active joint for each kinematic chain.

A.2 Forward and inverse kinematics

The analysis of a robot starts from its kinematic. It is important to define the kinematic relationship between the actuated joints, q_i, and the end-effector coordinates, x_i.

$$\begin{cases} x_1 = f_1(Q) \\ x_2 = f_2(Q) \\ \cdots \\ x_i = f_i(Q) \\ \cdots \\ x_n = f_n(Q) \end{cases} \qquad \begin{aligned} X &= F(Q) \\ Q &= [q_1, q_2, \cdots, q_j, \cdots, q_m]^T \\ X &= [x_1, x_2, \cdots, x_i, \cdots, x_n]^T \end{aligned} \tag{A.1}$$

The knowledge of the functions f_i allows to pass from Q to X and vice versa. In the first case we talk about forward kinematics, in the second case of inverse kinematic. From a mathematical view point the two kind of equations are the inverse of the other. In practice the different is very important because usually for serial robots is very easy the solution of the first, forward equation, since there is a unique solution $\bar{X}$ given a $\bar{Q}$, but multiple solutions can exist for the inverse equations. For parallel robots instead the solution of the forward kinematic equations is more complicated than the inverse kinematic equations. Deriving the kinematic equations with respect to time it is possible to obtain a velocity relationship:

$$\dot{X} = [J(Q)]\dot{Q} \qquad\qquad J(Q) = \frac{dX}{dQ} \tag{A.2}$$

The matrix $[J(Q)]$ is named Jacobian matrix of the system. It is the set of the derivatives of f with respect to the variables q. In addition to establishing the link between velocities, the Jacobian matrix expresses the link between the forces (or torques) applied to the end-effector and those applied to the active joints. By differentiating the relation A.1 we obtain:

$$\delta X = [J]\delta Q \tag{A.3}$$

Let's consider the virtual work of the system, δL, this must be null for every possible displacement:

$$\delta L = \delta X^T f_e + \delta Q^T f_g \tag{A.4}$$

where f_e are the forces applied to the end-effector and f_g are the ones applied on the active joints. By replacing to δX its expression in A.3:

$$\delta L = \delta Q^T([J]^T f_e + f_g) = 0 \tag{A.5}$$

Since the relationship must apply for each infinitesimal displacement δQ it must apply:

$$[J]^T f_e + f_g = 0 \tag{A.6}$$

And so:

$$f_g = -[J]^T f_e \tag{A.7}$$

It must be considered how this analysis holds in a static evaluation of the robot. It is not considered any dynamic force or the own weight of the structure. It is called kinetostatic analysis.

A.3 Force and velocity transmission factors

From eq.A.2 and A.7 is possible to evaluate the velocity and forces required to the actuators according to the velocities and forces applied to the robot in every single pose. It is possible to construct the manipulability ellipsoids. If we impose that the vector norm of Q is:

$$||\dot{Q}||_2 = \dot{Q}^T\dot{Q} < 1 \tag{A.8}$$

The choice of the euclidean norm is arbitrary as the value 1 which is used as a reference value. It must apply then:

$$\dot{X}^T([J]^{-1})^T[J]^{-1}\dot{X} < 1 \tag{A.9}$$

This last expression is the velocity manipulability ellipsoid, fig.A.2.
Same considerations can be done starting from eq.A.7 by obtaining a force manipulability ellipsoid.
The same operations can be executed starting from the workspace with a uniform space $\dot{X}$ and f_e and transform them in joints space through the use of $[J]^{-1}$ and $[J]^T$. It can be noticed the minus sign in the eq.A.7. The sign can be changed in order to consider the forces applied from the constraints on the end-effector instead of the than the external forces, $f_C = -f_e$.

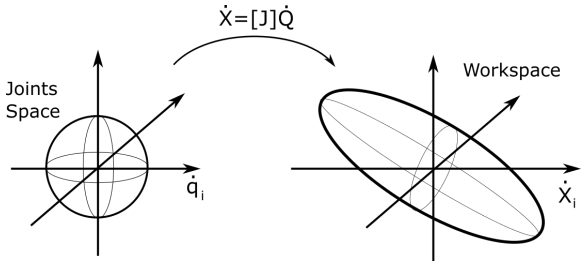

Figure A.2: Velocity manipulability ellipsoid

$$\tau_v = ||\dot{Q}||_\infty = ||[J]^{-1}\dot{X}||_\infty \leq ||[J]^{-1}||_\infty ||\dot{X}||_\infty \tag{A.10}$$

$$\tau_f = ||f_g||_\infty = ||[J]^T f_C||_\infty \leq ||[J]^T||_\infty ||f_C||_\infty \tag{A.11}$$

The inequalities written holds for any norm applicable on vectors, not only for the infinity norm used in this case. The infinite norm of a vector coincides with its largest element in absolute value while the infinite norm of a matrix coincides with the maximum among the sums of the absolute values of each single row.

$$||X||_\infty = \max_{1\leq i\leq n} |x_i| \qquad ||J||_\infty = \max_{1\leq i\leq n} \sum_{j=1}^{n} |a_{ij}| \tag{A.12}$$

In this way it was possible to define the velocity and force transmission factors, τ_v and τf. By imposing that the norm of vectors $\dot{X}$ and f_C is unitary, this in the case of the infinity norm means that the greatest velocity and force applied to the end-effector is not larger than one, the transmission factors are linked to the Jacobian of the system. Low transmission factors in a specific pose of the robot indicates that for unitary velocities and forces on the end-effector the velocities and forces on the active joints remain contained according to a proportionality value expressed by τ_v and τ_f .

$$\dot{Q}_{i,max} = \tau_v \qquad f_{g,max} = \tau_f \tag{A.13}$$

A.4 Singular configurations

The singular configurations of a robot are those whose Jacobian determinant or its inverse assume a null value:

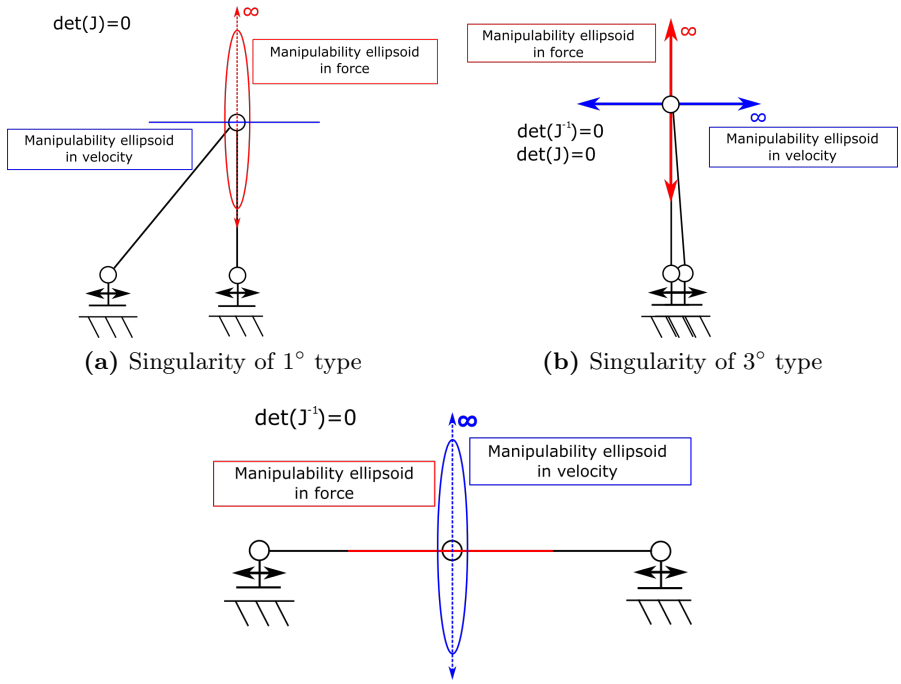

(a) Singularity of 1° type

(b) Singularity of 3° type

(c) Singularity of 2° type

Figure A.3: Configurazioni Singolari

$$det([J]) = 0 \quad \Leftrightarrow \quad det([J]^{-1}) = \infty \tag{A.14}$$

$$det([J]^{-1}) = 0 \quad \Leftrightarrow \quad det([J]) = \infty \tag{A.15}$$

This fact corresponds to having ellipsoids of manipulability in velocity or force that have degenerated, so that one or more axes of the ellipse become infinite. From a physical point of view this means that in that particular pose the robot can bring infinite forces and velocities on the end-effector along certain directions. This is not a good thing and it is evident from the three typical cases of singularity shown in figure A.3. In the moment which the Jacobian determinant becomes null it is possible for the structure to bear an infinite load along the a specific direction since the load its is discharged on the ground. This lead on a loss of mobility in the same direction . If the inverse Jacobian determinant becomes null we have the opposite situation, it is possible to transmit infinite velocity but it si not possible to bear any load. There is a duality between the two situations called the kinetostatic duality. The poses where it is possible to bear infinite load we have a loss of control on the velocity and vice versa. There can be some cases where both determinants can assume a null value. The length of the semi-axes of the ellipsoids is related to the reciprocal of

singular values, σ_j of the Jacobian:

$$\frac{1}{\sigma_j(J^{-1})} = \frac{1}{\sqrt{\lambda_j((JJ^T)^{-1})}} \tag{A.16}$$

The singular values are related to the eigenvalues of the matrix according to the relation described by eq.A.16. It seems evident that to avoid singular positions one must have singular values that do not tend to zero. The eq.A.16 refers to the singular values of the inverse Jacobian and therefore to the relationships on the velocities between active joints and workspace. The same considerations can be made on the transposed Jacobian and then on the ellipsoid of manipulability in force. Being the proximity of a robot to its singular configurations detectable through the ellipsoids of manipulability we can see how these are also linked to the transmission factors. In singular configurations these tend to assume infinite values; along the directions in which infinite loads are possible, high velocity transmission factor will be obtained, vice versa along directions with infinite velocity it will be obtained big force transmission factors.

APPENDIX B

Agile eye

In this appendix are shown the kinematic studies and a concept design of the agile eye. The data retrieved have been used to correctly size the linear delta and to predispose the Efesto printer to have 5 Dofs.

B.1 Kinematics

The agile eye is a parallel kinematic robot capable to execute until 3 Dofs. In the configuration here studied the robot has been adapted with the use of two kinematic chains in order to accomplish two rotations, yaw and pitch. In fig.B.1 is shown the robot where the rigid bodies from the motors to the platform have been labelled as link-ith. The robot has two kinematic chains not identical; one is composed by the only link-1, the other from the remaining links. The link-1 is directly connected to the motor-1, M1, which rotates around the axis-1, and a revolute joint is interconnected betwee the link-1 and the platform. Similar structure, but with one more link, is the second kinematic chain. The robot architecture is composed by the kinematic chains $\bar{R}R$ and $\bar{R}RR$, where the first joints of the kinematic chains are the active ones. The core of this kinematic is based on the fact that all revolute joints axis are intersected in one point, the robot TCP which became the rotation centre of the system. The configuration shown in fig.B.1 is not the only one possible but it 's the one followed in this study. This configuration allows to have the motors in the same plane of the initial position of the platform; this will facilitate the mount of the agile eye on the linear delta. For the kinematic resolution of the agile eye it is possible to start form the literature where its kinematic

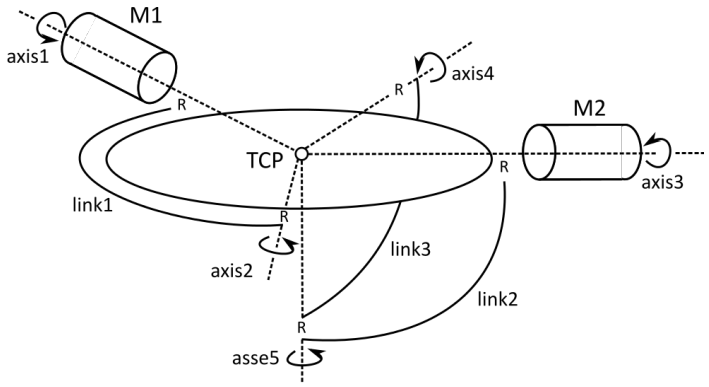

Figure B.1: Scheme of the agile eye with 2 DoFs

with 3Dofs is explained [1] [2]. Starting from this solutions it has been resolved the forward and inverse kinematic equations.

With the inverse kinematic equations we set the relationships between the platform rotations, pitch and yaw indicated with α and β, and the motor rotations θ_1 and θ_2. We use the pose matrix method to solve the problem. The pose matrices describe the relative position between two rigid bodies. In order to solve a kinematic chain is possible associate a fixed frame and describe the relative displacements between two consecutive body through a pose matrix. Given a body 0 and a body 1 the pose matrix describing the relative position of 1 with respect to 0 is labelled as M_{01}. In fig.B.2 is represented the kinematic solution for the agile eye. It is pretty evident how one kinematic chain has a very simple solution; the rotation θ_1 of motor-1 is always equal to the platform angle α. The other kinematic chain is resolved through the use of 5 frames, enumerated in the figure. A fixed frame in the TCP, 0; a frame 1 positioned in the motor-2 position and fixed to the ground and a second frame in the same position but fixed with the motor rotation; a frame 3 describing the relative rotation between link 2 and 3, and a frame 4 describing the relative rotation between link 3 and platform; in the end a frame 5 that is fixed on the platform and that in the initial position is overlapping frame 0. The unknown variable inside this closed kinematic chain are the three rotations of the revolute joints; θ_2, motor rotation, γ between link-2 and link-3, ψ between link-3 and platform. We solve the inverse kinematic of the robot with this kinematic chain by imposing its equality with a matrix describing the robot rotations α and β. First of all we write the matrix $M_{\alpha\beta}$ basin its rotation on

[1] Gosselin C.M. and Hamel J.F., *The agile eye: a high-performance three-degree-of-freedom camera-orienting device*, 1994, International Conference on robotics and automation

[2] Palmieri G. at al., *Design and testing of a spherical parallel mini manipulator*, 2014, IEEE

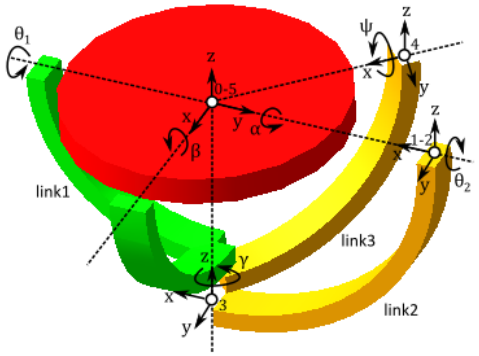

Figure B.2: Model of Agile Eye

nautical angles. The terms $c\alpha$ and $s\alpha$ mean for $\cos\alpha$ and $sin\alpha$.

$$\mathbf{M}_{\alpha\beta} = \begin{bmatrix} c\alpha & s\alpha s\beta & s\alpha c\beta & 0 \\ 0 & c\beta & -s\beta & 0 \\ -s\alpha & c\alpha s\beta & c\alpha c\beta & 0 \\ 0 & 0 & 0 & 1 \end{bmatrix} \tag{B.1}$$

In the following are reported the five matrix M_{i-i+1}. It is possible to notice the recursive use of the terms $s45°$ and $cs45°$ which describe the relative initial position between link-2 and link-3. This is an arbitrary choice derived from some considerations explained in the later. The term R indicates the radius of the links which are quarter of a circle. Even though the links will have a different radius in the construction of the robot the kinematic solution does not change.

$$\mathbf{M_{01}} = \begin{bmatrix} -c90 & s90 & 0 & 0 \\ -s90 & -c90 & 0 & R \\ 0 & 0 & 1 & 0 \\ 0 & 0 & 0 & 1 \end{bmatrix} \tag{B.2}$$

$$\mathbf{M_{12}} = \begin{bmatrix} 1 & 0 & 0 & 0 \\ 0 & c\theta_2 & -s\theta_2 & 0 \\ 0 & s\theta_2 & c\theta_2 & 0 \\ 0 & 0 & 0 & 1 \end{bmatrix} \tag{B.3}$$

$$\mathbf{M_{23}} = \begin{bmatrix} c\gamma & -s\gamma & 0 & R \\ s\gamma & c\gamma & 0 & 0 \\ 0 & 0 & 1 & -R \\ 0 & 0 & 0 & 1 \end{bmatrix} \tag{B.4}$$

$$\mathbf{M_{34}} = \begin{bmatrix} c45 & -c\psi s45 & s\psi s45 & -Rc45 \\ s45 & c\psi c45 & -s\psi c45 & -Rs45 \\ 0 & s\psi & c\psi & R \\ 0 & 0 & 0 & 1 \end{bmatrix} \tag{B.5}$$

$$\mathbf{M_{45}} = \begin{bmatrix} c45 & -s45 & 0 & R \\ s45 & c45 & 0 & 0 \\ 0 & 0 & 1 & 0 \\ 0 & 0 & 0 & 1 \end{bmatrix} \tag{B.6}$$

By multiplying such matrices we get the final matrix which connect the fixed frame on the ground with the frame fixed on the platform.

$$\mathbf{M_{05}} = \begin{bmatrix} c\theta_2 cs^2[sm+cp] - s\theta_2 s\psi cs & -c\theta_2 cs^2[cm+sp] - s\theta_2 s\psi cs & c\theta_2 cs[s\gamma s\psi - c\gamma s\psi] - s\theta_2 c\psi & 0 \\ -cs^2 cm + cs^2 sp & cs^2[-sm+cp] & -cs[c\gamma s\psi + s\gamma s\psi] & 0 \\ s\theta_2 cs^2[sm+cp] + c\theta_2 s\psi cs & -s\theta_2 cs^2[cm+sp] + c\theta_2 s\psi cs & s\theta_2 cs[s\gamma s\psi - c\gamma s\psi] + c\theta_2 c\psi & 0 \\ 0 & 0 & 0 & 1 \end{bmatrix} \tag{B.7}$$

where the term cs indicates the sine or cosine of 45°, the terms cp, cm, sp, sm indicate respectively $c\gamma(1+c\psi)$, $c\gamma(1-c\psi)$, $s\gamma(1+c\psi)$ e $s\gamma(1-c\psi)$. If we impose the equality between the 3x3 matrix obtained from the first three rows and columns of $\mathbf{M_{05}}$ with the elements in the same position of $\mathbf{M}_{\alpha\beta}$ we get 9 scalar non linear equations. To solve the problem and relate θ_2 with α and βwe can use the 4 equations in position (1,1),(3,1),(1,2) and (3,2).

$$c\alpha = c\theta_2 cs^2[sm+cp] - s\theta_2 s\psi cs \tag{B.8}$$

$$-s\alpha = s\theta_2 cs^2[sm+cp] + c\theta_2 s\psi cs \tag{B.9}$$

$$s\alpha s\beta = -c\theta_2 cs^2[cm+sp] - s\theta_2 s\psi cs \tag{B.10}$$

$$c\alpha s\beta = -s\theta_2 cs^2[cm+sp] + c\theta_2 s\psi cs \tag{B.11}$$

By isolating the term $[sm+cp]$ from eq.B.8 and B.9, and the term $[cm+sp]$ from eq.B.10 and B.11 we get:

$$\frac{c\alpha + s\theta_2 s\psi cs}{c\theta_2} = \frac{-s\alpha - c\theta_2 s\psi cs}{s\theta_2} \tag{B.12}$$

$$\frac{s\alpha s\beta + s\theta_2 s\psi cs}{c\theta_2} = \frac{c\alpha s\beta - c\theta_2 s\psi cs}{s\theta_2} \tag{B.13}$$

$$\tag{B.14}$$

By isolating the term $s\psi cs$ we get the final equation:

$$\theta_2 = \arctan\left(\frac{s\alpha - c\alpha s\beta}{s\alpha s\beta - c\alpha}\right) \tag{B.15}$$

It can be notice that when β is equal to zero θ_2 is equal to α. The motor rotations differ only when it is desired a robot pose with a non null β. The inverse kinematic equations are:

$$\begin{cases} \theta_1 = \alpha \\ \theta_2 = \arctan\left(\frac{s\alpha - c\alpha s\beta}{s\alpha s\beta - c\alpha}\right) \end{cases} \tag{B.16}$$

The inverse of such equations are the forward kinematic equations:

$$\begin{cases} \alpha = \theta_1 \\ \beta = \arcsin \frac{s\alpha + c\alpha tan\theta_2}{tan\theta_2 s\alpha + c\alpha} \end{cases} \tag{B.17}$$

B.1.1 Velocity analysis

From the inverse kinematic equations and deriving them with respect to the time we get the inverse Jacobian:

$$\begin{Bmatrix} \dot{\theta_1} \\ \dot{\theta_2} \end{Bmatrix} = \begin{bmatrix} 1 & 0 \\ \frac{s\beta^2 - 1}{1 + s\beta^2 - 4s\alpha c\alpha s\beta} & \frac{c\beta^2(c\alpha^2 - s\alpha^2)}{1 + s\beta^2 - 4s\alpha c\alpha s\beta} \end{bmatrix} \begin{Bmatrix} \dot{\alpha} \\ \dot{\beta} \end{Bmatrix} \tag{B.18}$$

$$\dot{\mathbf{\Theta}} = [J]^{-1}\mathbf{W} \tag{B.19}$$

It is possible to retrieve the direct Jacobian by deriving the forward kinematic equations where they hold:

$$\mathbf{W} = [J]\dot{\mathbf{\Theta}} \tag{B.20}$$

$$[J] = \begin{bmatrix} 1 & 0 \\ \frac{1 - \tan\theta_2^2}{\sqrt{\tan\theta_2^2(s\theta_1^2 - c\theta_1^2) + c\theta_1^2 - s\theta_1^2}(\tan\theta_2 s\theta_1 + c\theta_1)^2} & \frac{c\theta_1^2 - s\theta_1^2}{c\theta_2^2\sqrt{\tan\theta_2^2(s\theta_1^2 - c\theta_1^2) + c\theta_1^2 - s\theta_1^2}(\tan\theta_2 s\theta_1 + c\theta_1)^2} \end{bmatrix} \tag{B.21}$$

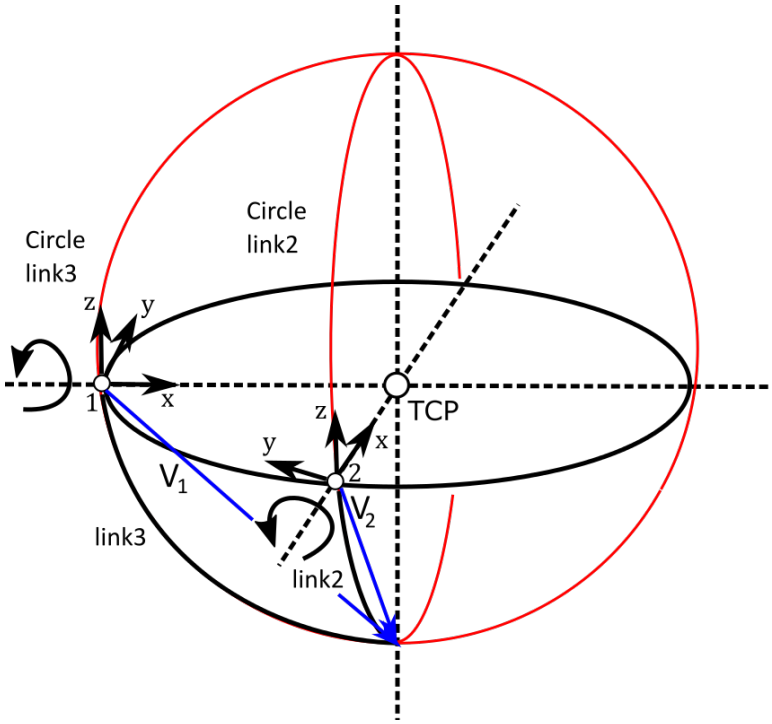

Figure B.3: Geometrical approach

B.1.2 Geometrical approach

Even though the pose matrices use has lead us to the solution of the kinematic problem, inverse and forward, we want to show another possible approach based on the system geometry to solve the inverse kinematic problem. The unknown relationship is still the one between the platform pose and the second motor rotation. Looking at fig.B.3 is possible to notice how fixed the platform position the links 2 and 3 can only rotate around the revolute joints axis passing through the TCP. Their rotations describe respectively two circles, centred in the TCP, with at least two intersection points. The solution depends upon the mounting choice of the links. We can so write the vector equation:

$$P_1 + [R_1]V_1^{'} = P_2 + [R_2]V_2^{'} \tag{B.22}$$

The meaning of such equation is better understandable from fig.B.4. Vectors P_1 and P_2 are vectors of fixed length and they define the position of two frames, 1 and 2. The frame 1 is fixed on the ground instead the frame 2 is fixed on the platform. The vectors $V_1^{'}$ and $V_2^{'}$ are expressed in such frames and they are reported in absolute frame thanks to the matrices $[R_1]$ and $[R_2]$. The vector equation is written with respect to this

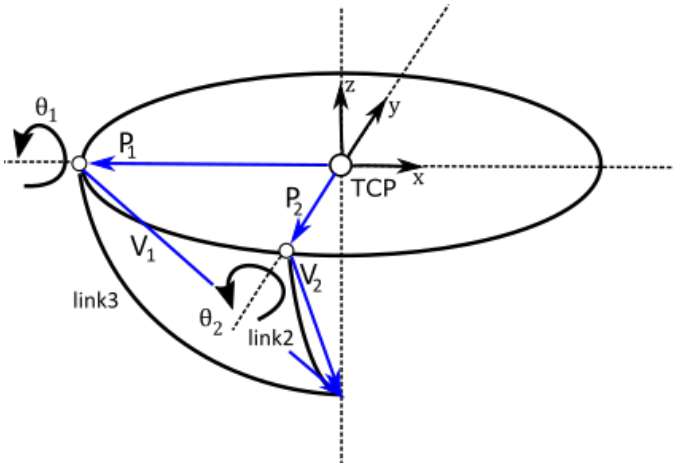

Figure B.4: Vectorial scheme of the geometrical approach

absolute frame positioned in the TCP. The use of the frames 1 and 2 allows to write the vectors V_1 and V_2 as:

$$V_1^{'} = \begin{Bmatrix} V_{1x} \\ \rho_1 \cos\theta_1 \\ \rho_1 \sin\theta_1 \end{Bmatrix} \qquad V_2^{'} = \begin{Bmatrix} V_{2x} \\ \rho_2 \cos\theta_2 \\ \rho_2 \sin\theta_2 \end{Bmatrix} \tag{B.23}$$

The two vectors are completely defined by the angles θ_1 and θ_2. These two angles define the vector rotations around their respective axis. The angle θ_2 coincides with th motor-2 rotation. The term θ_1 expresses the rotation of link-3 with respect to the platform. The vectors V_1 and V_2 have a fixed module. The matrices $[R_1]$ and $[R_2]$ are defined by the unit vectors of the frames 1 and 2 expressed in the absolute reference system. This terms are known once is fixed the platform pose.

$$[R_1] = [\hat{x_1}, \hat{y_1}, \hat{z_1}] \qquad [R_2] = [\hat{x_2}, \hat{y_2}, \hat{z_2}] \tag{B.24}$$

The vector eq.B.22 express the scalar equations:

$$\begin{cases} P_{1x} + \hat{x}_{1x}V_{1x} + \hat{y}_{1x}\rho_1 c\theta_1 + \hat{z}_{1x}\rho_1 s\theta_1 = P_{2x} + \hat{x}_{2x}V_{2x} + \hat{y}_{2x}\rho_2 c\theta_2 + \hat{z}_{2x}\rho_2 s\theta_2 \\ P_{1y} + \hat{x}_{1y}V_{1y} + \hat{y}_{1y}\rho_1 c\theta_1 + \hat{z}_{1y}\rho_1 s\theta_1 = P_{2y} + \hat{x}_{2y}V_{2y} + \hat{y}_{2y}\rho_2 c\theta_2 + \hat{z}_{2y}\rho_2 s\theta_2 \\ P_{1z} + \hat{x}_{1z}V_{1z} + \hat{y}_{1z}\rho_1 c\theta_1 + \hat{z}_{1z}\rho_1 s\theta_1 = P_{2z} + \hat{x}_{2z}V_{2z} + \hat{y}_{2z}\rho_2 c\theta_2 + \hat{z}_{2z}\rho_2 s\theta_2 \end{cases} \tag{B.25}$$

By substitution we get a non linear equation with the unique unknown variable θ_2.

$$a \sin\theta_2 + b \cos\theta_2 = c \tag{B.26}$$

The term a, b and c are constant. The solution to the equation can be found applying the following substitutions:

$$t = tan(\frac{\theta_2}{2}) \qquad \sin\theta_2 = \frac{2t}{1+t^2} \qquad \cos\theta_2 = \frac{1-t^2}{1+t^2} \tag{B.27}$$

For the parameter t:

$$t_{1,2} = \frac{b \pm \sqrt{b^2 + a^2 - c^2}}{c + a} \tag{B.28}$$

The rotation θ_2:

$$\theta_{1,2} = 2\arctan(t_{1,2}) \tag{B.29}$$

The choice between one solution or the other depends on how the agile eye is mounted. The angles α and β are not directly expressed in this equations but they defines the values of the vectors $P1$ and $P2$.
Since here are not explicit the relationship between α, β and θ_1, θ_2 we can evaluate the Jacobian matrix in a numerical way since it always apply:

$$[J]^{-1} = \begin{bmatrix} \frac{d\theta_1}{d\alpha} & \frac{d\theta_1}{d\beta} \\ \frac{d\theta_2}{d\alpha} & \frac{d\theta_2}{d\beta} \end{bmatrix} \tag{B.30}$$

B.1.3 Synthesis

For the agile eye synthesis the goal is to reach the desired rotations by avoiding the interferences among the links and by obtaining a final architecture that facilitate the mounting of the agile eye on the linear delta. In order to achieve these goals the following choices are taken:

- concentric links
- motors position on a same plane
- motors position opposed
- minimization of the transmission factors

The robot links are considered to be concentric. This avoid any possibility of collision during the robot rotations. The motors are placed on a same plane, coincident with the initial plane of the agile eye platform, and in an opposite position, fig.B.5. This solution facilitate the integrability of the agile eye with the linear delta and balance the weight of the two motors.

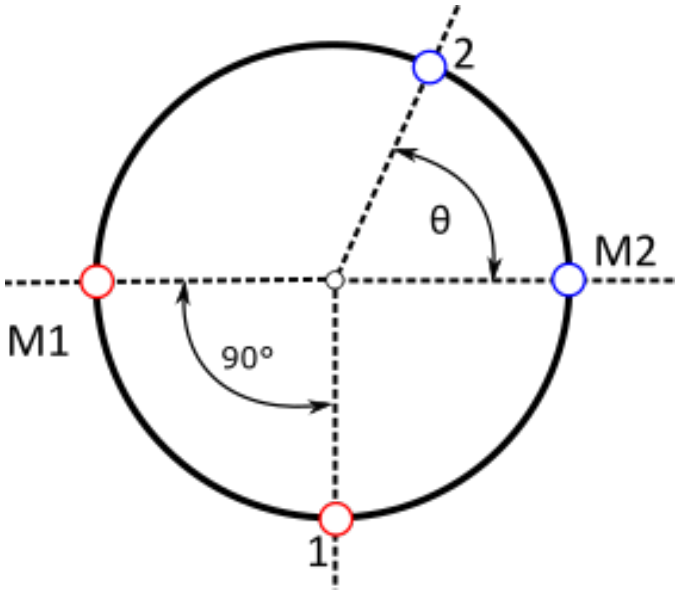

Figure B.5: Position of the Agile Eye motors

Table B.1: Force transmition factor for the motor 2 with different θ

θ	τ_f	τ_v
30°	3.04	1.47
45°	3.12	1.49
60°	3.86	1.35
90°	-	-
120°	3.86	1.35
135°	3.12	1.49
150°	3.04	1.47

The last point aims to verify that the motors required for the system are not oversized. This would increase the weight on the linear delta. In order to minimize the transmission factors of the kinematic chain of motor-2 the connecting point, 1, of link-1 to the platform is fixed, instead the point 2 has been varied according to the angle θ. In table B.1 is possible to see how the velocity and force transmission factors change by changing the angle θ.

It is possible to notice how the lowest velocity transmission factor is get near the value $\theta = 90°$, instead the minimum for the force transmission factor is for $\theta = 0$ and $\theta = 180$. These values are impossible to reach since they are singular configurations of the agile eye. The value $\theta = 45°$ is considered to be a good choice to keep low transmission factors and remain away from the singular configurations of the system.

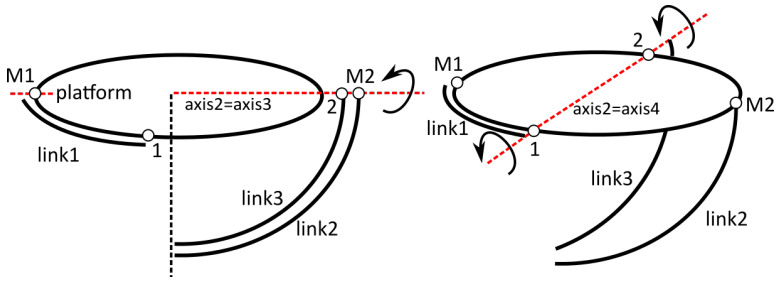

Figure B.6: Singular configurations of the agile eye

Singular configurations

It is important to define the singular configurations of the robot. Give the configuration of the agile eye we have two possible singular configurations. With reference to fig.B.5 is possible to see how is possible to reach a position where the link-2 and 3 are perfectly aligned. This result in a loss of control for the system since the motor-2 could rotate together with link-2 and link-3 without any movement from the agile eye platform. Another possibility is when the revolute axis of the joints between link-1 and platform and link-3 and platform are aligned. In this case the platform is free to rotate around these axis without no rotations of the motors. Anyway this second possibility happens only for an incorrect mounting of the robot.

B.2 Concept design

For the agile eye must be defined the overall dimensions in order to correctly size the platform moved by the linear delta. In order to do that it is defined a concept design of the agile eye according to the configuration studied in the previous sections. In fig.B.7 is possible to see a constructive solution where the motors are set in an opposite position, one respect to the other. The revolute joints are represented by simple pivots. In fig.B.7b is shown the robot in a rotated pose. It is important that during the printing process the object which is manufactured on the agile eye platform does not hit the external structure such as the motors. This can be verified visually by rotating the platform inside the required rotations ranges of $\pm 45°$. In the figure are used for the two motors two Harmonic Drive. These motors are very small and they encapsulate the reduction system; the choice of such motors would limit weight and size of the agile eye.

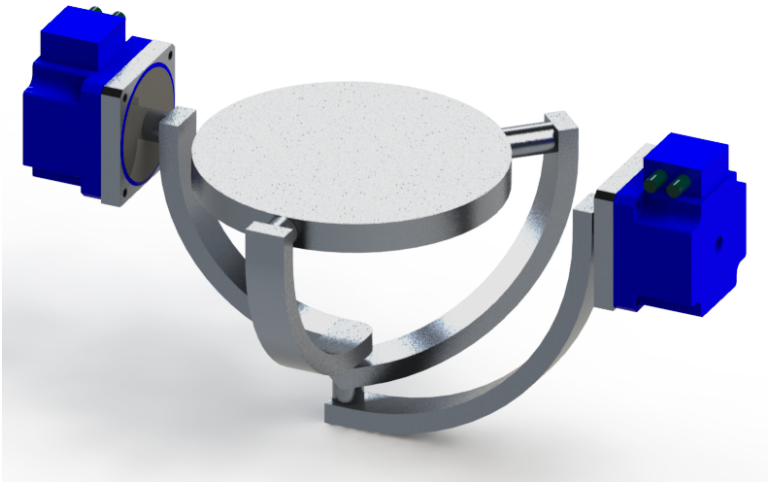

(a)

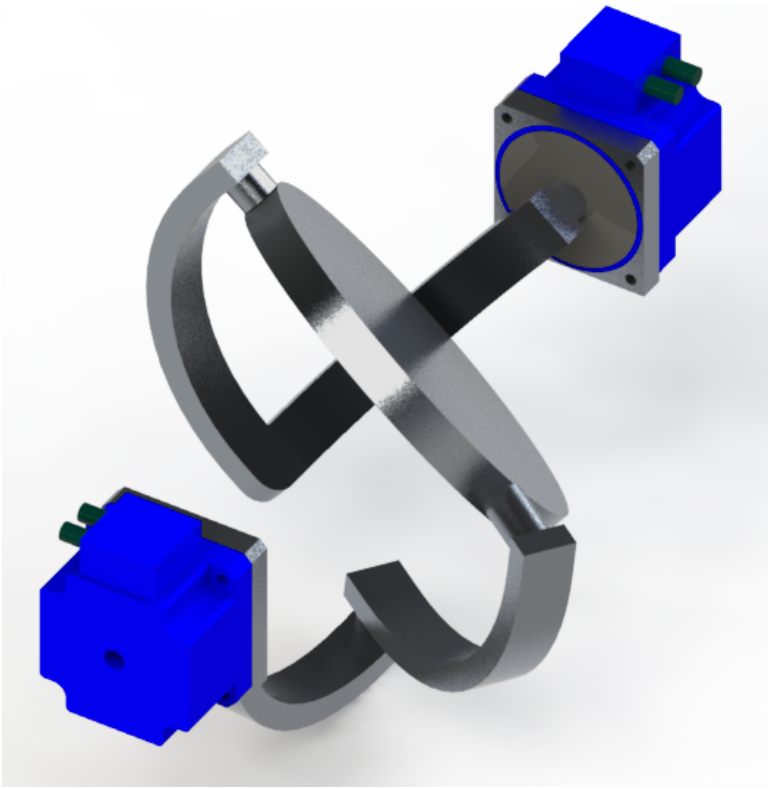

(b)

Figure B.7: Agile Eye concept design